

Statistical mechanics of disordered systems: spins, spheres and machines

Hajime Yoshino^{1,2}

¹*Cybermedia Center, Osaka University, Toyonaka, Osaka 560-0043, Japan*

²*Graduate School of Science, Osaka University, Toyonaka, Osaka 560-0043, Japan**

(Dated: today)

In this lecture note, we discuss physics of glasses and related problems from a theoretical perspective based on solvable mean-field models of spins, machines and spheres. The standard theoretical tools for glassy systems, in particular the replica method, which were originally developed for systems with strong quenched disorder such as spinglasse, can be applied to glassy systems without quenched disorder. In this note we discuss p -spin ferromagnetic Ising model in the supercooled paramagnetic phase, deep neural network and hard-spheres in large dimensional limit. (This is a working note. Any comments are welcome. Please do not redistribute too much.)

* yoshino.hajime.cmc@osaka-u.ac.jp

CONTENTS

I	Introduction	7
I. Basic phenomenology of glasses		7
II. Related problems in computer science : constraint satisfaction problems and statistical inferences		7
A. Constraint satisfaction problems		7
B. Statistical Inference		8
1. Bayes formula		8
2. Teacher-student setting		9
3. Mutual information		9
4. Bayes optimal case: Nishimori condition		10
5. Various estimators		10
III. Models		10
A. Generalized p -spin models on a dense graph		10
1. Graphical representation		10
2. Dense tree-like graphs		11
3. Dense graphs with layers		12
4. Disorder-free models		12
5. Models with weak/strong quenched disorder		13
B. Conventional p -spin mean-field spinglass models with disordered global coupling		13
C. M -component vectorial p -spin models with a generic potential		15
D. Planting		17
1. Simple setting 1 a)		17
2. Simple setting 1b): Inverse Ising model		17
3. Simple setting 2 : error correcting code		17
4. Vectorial version		19
5. Examples: with some references		19
E. Exactly solvable <i>vectorial</i> CSPs and inference problems		19
1. Vectorial constraint satisfaction problems		19
2. Vectorial inference problems		20
F. Perceptron		20
1. Random inputs/outputs : a constraint satisfaction problem		21
2. Teacher-student scenario : a statistical inference problem		21
G. Spheres in large dimensional limit		22
 II <i>p</i> -spin models on a dense graph		 23
IV. Warming up: ferromagnetism		23
A. Basic phenomenology of ferromagnetism		23
B. Generic strategy		24
1. The order parameter, conjugated field		24
2. Legendre transform		24
3. 1st step of the recipe		25
4. Plefka expansion		26
5. Higher order terms		27
6. Cumulant expansion		27
C. Ising p -spin ferromagnetic model		27
1. Derivation of the free-energy function and the equation of states		27
2. 2nd order transition: $p = 2$ case		29
3. 1st order transition: $p > 2$ case		31
D. Scalar spherical p -spin ferromagnetic model		31

V.	Simplest glass model : random energy model (REM)	33
A.	Random energy levels in the $p = \infty$ ferromagnetic Ising model	33
B.	Analysis of REM	34
1.	Thermodynamics	34
2.	Fluctuations below T_K	36
C.	Stability against crystallization	36
D.	Shuffling of energy levels induced by random pinning fields	37
VI.	Replicated spin system	39
A.	Basic phenomenology	39
1.	Ergodicity breaking	40
2.	Replica symmetry breaking	40
3.	How the ϵ -coupling can be realized?	41
4.	Thermodynamics : $n \rightarrow 0$	42
5.	Distribution of “random” free-energy	42
6.	Parisi’s ansatz	43
B.	Free-energy functional	43
1.	Order parameter, symmetry breaking field and Legendre transforms	43
2.	Plefka expansion	46
3.	Cumulant expansion	47
C.	Scalar p -spin models	47
1.	Entropic part of the free-energy	47
2.	Interaction part of the free-energy	49
3.	Total free-energy, variational equation and the Hessian matrix	50
4.	Models with quenched disorder	52
D.	M -component vectorial p -spin models with a generic potential	52
1.	Entropic part of the free-energy	53
2.	Interaction part of the free-energy	53
3.	Total free-energy	54
E.	Density functional approach	54
VII.	Replica symmetric (RS) solution	55
A.	Scalar Ising p -spin model	55
1.	RS solution	55
2.	SK model : $p = 2$ Ising	57
3.	Random Energy Model (RSM) : $p = \infty$ Ising	57
B.	Scalar spherical p -spin model	58
C.	Vectorial p -spin models	59
1.	RS solution	59
2.	hardcore potential	60
3.	hardcore $p = 1$ model: Perceptron	61
VIII.	Glass transitions with one step replica symmetry breaking (1RSB)	63
A.	Scalar Ising p -spin models	63
1.	1RSB solution	63
2.	$p = \infty$ Ising model	65
B.	Distribution of overlap $P(q)$	66
C.	Systems with many metastable states	67
D.	Complexity	68
E.	$2 < p < \infty$ Ising model	69
1.	Search for solutions	69
2.	Dynamical transition	69
3.	Complexity	70
4.	Gardner transition	70
F.	Disentangling hierarchy of responses	70
G.	Scalar spherical p -spin model	73

IX.	State following: Franz-Parisi potential	74
A.	The idea of glass state following	74
B.	p -spin Ising case	74
1.	Simplest ansatz	74
C.	p -spin spherical case	77
1.	Basics	77
2.	Temperature perturbation	78
D.	Teacher-student setting: statistical inference of planted configuration	79
1.	Planted p -spin	80
2.	Shannon's bound	83
3.	Perceptron learning	84
X.	Further replica symmetry breakings	88
A.	Hierarchical energy landscape and responses with $2, 3, \dots, k$ RSB	88
B.	Overlap distribution function $P(q)$ and the order parameter function $q(x)$	89
C.	p -spin Ising model	90
1.	Free-energy of k -RSB ansatz	90
2.	Variational equations	92
3.	Stability	93
4.	Continuous RSB: $k \rightarrow \infty$ limit	94
5.	Analysis of k -RSB solution: $p = 2$ case (SK model)	96
D.	Vectorial p -spin models with soft/hardcore potential	96
1.	k -RSB ansatz and $k \rightarrow \infty$ limit	97
2.	Analysis of k -RSB solution	97
3.	Marginal stability	97
4.	Jamming	98
XI.	Cavity approach	99
A.	Belief Propagation(BP) equations	99
B.	relaxed-BP equations	100
C.	Approximate Message Passing (AMP) or TAP equations	101
D.	State Evolution	102
XII.	Dynamical mean-field theory	103
A.	Model	103
B.	MSR generating functional	103
C.	Dynamical order parameters and the effective Langevin equation	104
D.	Self-consistent equations of the correlation and response functions	107
E.	Equilibrium dynamics	108
F.	Out-of-equilibrium dynamics	110
III	Spheres in large dimensional limit	112
XIII.	Replicated liquid	112
A.	Replicated system of spheres	112
B.	Derivation of the free-energy in $d \rightarrow \infty$ limit	113
C.	Variational equation and Hessian matrix	117
D.	Radial distribution function $g(r)$ or the effective potential	118
E.	Compression and Decompression	118
F.	Shear	119
1.	Simple shear	119
2.	Metastable states under shear	120
3.	Replicas under shear	121
G.	Parisi's ansatz	123
H.	1RSB ansatz	123
1.	Free-energy	123
2.	Effective potential	124

3. Complexity	124
4. Variational equation	125
5. Pressure	125
6. Shear-modulus	125
I. k -RSB ansatz and $k \rightarrow \infty$ limit	126
1. Free-energy	126
2. Variational equations	127
3. Effective potential	128
4. Pressure	128
5. Shear-modulus	128
6. Stability of k -RSB	129
7. Continuous RSB: $k \rightarrow \infty$ limit	130
J. Glass state following	131
1. General setting	132
2. Simplest ansatz	132
3. Reference system	133
4. Student system	133
5. Pressure and shear-stress	133
6. Gardner transition	134
XIV. Hard sphere glass	135
A. 1RSB ansatz ($k = 1$)	135
1. Dynamical transition	135
2. Jamming	135
3. Kauzmann transition	137
4. Gardner transition	138
B. k -RSB ansatz and $k \rightarrow \infty$	138
C. Jamming	138
1. Scaling analysis of the full RSB solution approaching jamming	138
2. Physical consequences	140
D. Glass State following	141
1. Glass equation of states, stress-strain curves	141
2. Jamming and shear-jamming	141
Acknowledgments	142
IV Appendix	143
A. Some useful formula	143
B. Some useful formula for RS	143
C. Some useful formula for state following	144
D. Some useful formulae	144
E. Recursion formula for $g(m_i, h)$ and $f(m_i, h)$	146
1. k -RSB	146
F. Recursion formula for $P_{i,j}(h, h')$	146
1. k -RSB	146
G. Asymptotic behaviour of the error function	147
H. Clustering property	148

I.	Properties of low lying states in the glass phase of the random energy model	149
1.	Distribution of energy gaps	149
2.	Two level system	149
J.	Gaussian integrals	150
K.	Eigen values of the Hessian matrix	150
L.	Some explicit computations of higher order terms in the Plefka expansion	150
M.	Langevin dynamics	151
1.	From Langevin equation to Fokker-Planck equation	151
2.	Fluctuation dissipation theorems: 1st and 2nd	151
3.	MSR generating functional	152
a.	Reminder: functional, functional derivatives and functional integrals (path-integrals)	152
b.	Discretization of the Langevin dynamics	153
c.	Martin-Siggia-Rose (MSR) generating functional	153
d.	Correlated noise	154
e.	Some useful identities	155
	References	155

Part I

Introduction

I. BASIC PHENOMENOLOGY OF GLASSES

Reviews and books: SpinglassTheoryAndBeyond[1], Binder-Yong [2], Mydosh [3], Taniguchi-Kawamura [4], Pedestrian1 [5], Pedestrian2 [6], Biroli-Berthier[7], Mézard-Montanari[8], Nishimori[9], Krzakala-Zdeborová[10], Huang[11], Parisi-Urbani-Zamponi[12]

- spin-glasses (with quenched disorder) $p = 2$
- structural glass: supercooling, glass transition
- optimization problems, inference problems, machine learning

Spin-glass transitions without quenched disorder have been observed in some geometrically frustrated magnets including pyrochlore compounds. For recent theoretical analysis see [13, 14].

Theoretical perspective:

- mean-field theory / beyond mean-field (perturbative RG, droplet, RFOT, ...)
- Is mean-field theory useful in practice? - jamming $d_u = 2$? (lucky), glass state following (1st principle theory of amorphous solids), problems on tree like graphs (mean-field works by definition)

II. RELATED PROBLEMS IN COMPUTER SCIENCE : CONSTRAINT SATISFACTION PROBLEMS AND STATISTICAL INFERENCE

A. Constraint satisfaction problems

In constraint satisfaction problems (CSP) we have variables that are forced to satisfy a certain number of constraints, such as the magic square: a square array of numbers, usually positive integers, is called a magic square if the sums of the numbers in each row, each column, and both main diagonals are the same (Wikipedia).

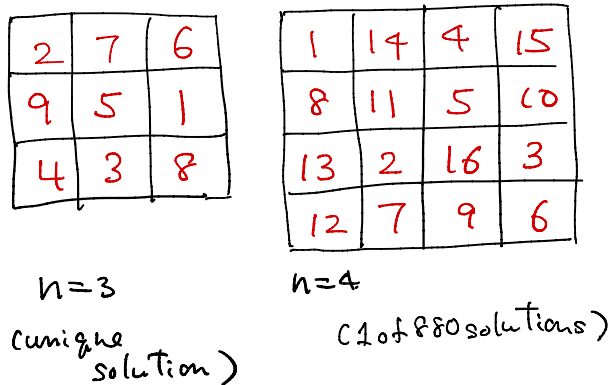


FIG. 1. Examples of magic squares of size $n \times n$

The family of problems known as boolean satisfiability (SAT) problems, such as the K -SAT problem, are well known in computer science. One considers N boolean variables which are forced to satisfy M constraints expressed by boolean functions. Generic boolean functions may be considered as *random* boolean functions.

From the point of view of the statistical mechanics of disordered systems, we are interested in the ensemble of solutions (or SAT states) for a given CSP. We ask how many solutions exist for a given CSP. Naturally, we expect that the number of solutions decreases with increasing the number of constraints M . We also ask how the solutions are connected in the solution space. Clustering of the solutions can be regarded as a glass transition (See Fig. 2).

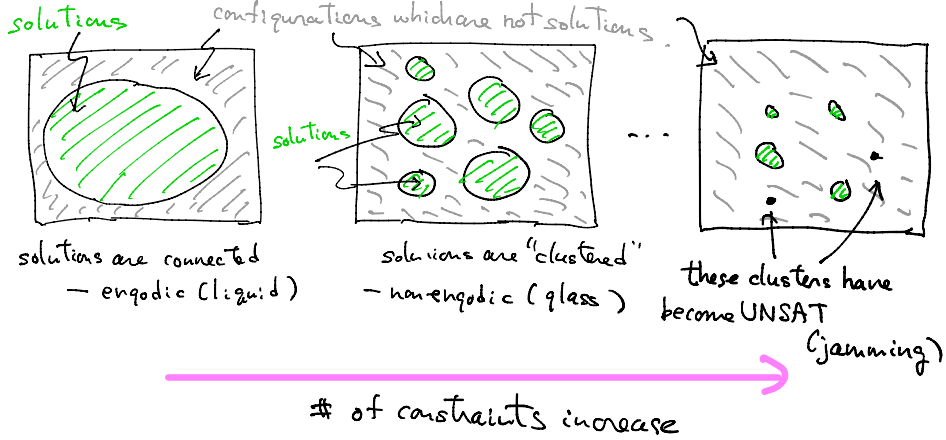


FIG. 2. A simple schematic picture of the solution space of a constraint satisfaction problem.

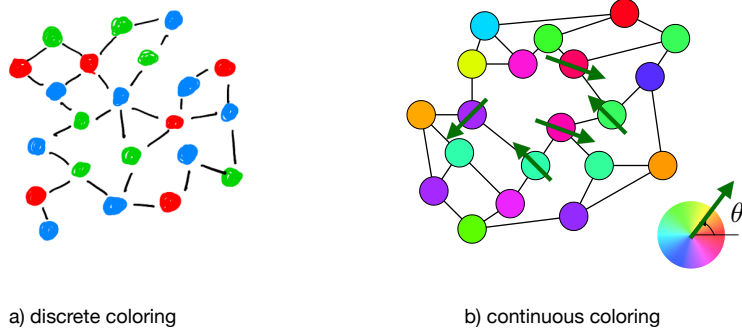


FIG. 3. Coloring of graphs. a) a discrete coloring with $q = 3$ colors and b) a continuous coloring (took from [15]). The color angle $0 \leq \theta < 2\pi$, as in the standard HSV color map, can be represented by a XY spin, i.e. a vector with $M = 2$ component (green arrow). The example shown here is a solution to the requirement that color angle on adjacent vertexes must be greater than or equal to $2\pi/3$.

Increasing the number of constraints M , the clusters become smaller. At a certain point, the size of a cluster becomes 0, i. e. UNSAT transition means complete loss of SAT states. This can be regarded as jamming.

Yet another good example is coloring. Given a graph, one has to put colors such that adjacent nodes have different colors. In Fig. 3 we show the cases of the standard discrete coloring and a continuous variant. In discrete coloring, one is allowed to use a finite number of colors like red, blue, and green. Discrete coloring of random graphs has been studied extensively in the context of statistical mechanics of disordered systems [8, 16]. One can naturally consider continuous versions such as circular coloring of graphs or periodic scheduling [17]. In such continuous coloring one considers 'color angle' $0 < \theta < 2\pi$ on the vertexes of a given graph such that angles on adjacent vertexes are sufficiently separated from each other (See Fig. 3).

B. Statistical Inference

1. Bayes formula

The probability distribution $P(A, B)$ of two quantities A, B can be related to conditional probability distributions $P(A|B)$ and $P(B|A)$ as

$$P(A, B) = P(A|B)P(B) = P(B|A)P(A) \quad (\text{II.1})$$

This yields the Bayes formula

$$\underbrace{P(A|B)}_{\text{posterior probability}} = \underbrace{P(B|A)}_{\text{likelihood}} \underbrace{P(A)}_{\text{prior probability}} \frac{1}{\underbrace{\sum_A P(B|A)P(A)}_{\text{evidence (just normalization const.)}}} \quad (\text{II.2})$$

2. Teacher-student setting

To explain statistical inference based on the Bayes formula, it is very convenient and instructive to use the teacher-student scenario[10].

- **Teacher** generates a *ground truth* A^* using a *prior* distribution $P(A)$. It generates a *data* B whose distribution is given by the *likelihood* $P(B|A)$. It gives B to the student.
- **Student** tries to infer the ground truth A^* from the data B using the Bayes formula Eq. (II.2): it generates an estimate A using a Boltzmann distribution, with $\beta = 1$,

$$P(A|B) = \frac{1}{Z_\beta} e^{-\beta H(A|B)} \quad (\text{II.3})$$

$$H(A|B) = -\ln P(B|A) - \ln P(A) \quad (\text{II.4})$$

$$Z_\beta = P(B) = \int dA e^{-\beta H(A|B)} \quad (\text{II.5})$$

Let us introduce two kinds of averages.

- Average over 'data'

$$[\dots] = \int dB P(B) \dots = \int dB dA^* P(B|A^*) P(A^*) \dots \quad (\text{II.6})$$

- Expectation by students with fixed data 'B'

$$\langle \dots \rangle_{\text{student}} = \int dA P(A|B) \dots = \frac{1}{P(B)} \int dA P(B|A) P(A) \dots = \frac{1}{\int dA P(B|A) P(A)} \int dA P(B|A) P(A) \dots \quad (\text{II.7})$$

where we used the Bayes theorem.

3. Mutual information

It is interesting to consider the mutual information

$$\begin{aligned} I(A; B) &= \int dA dB P(A, B) \log \frac{P(A, B)}{P(A)P(B)} \\ &= \int dA dB P(A, B) \log \frac{P(A|B)}{P(A)} \\ &= \int dB P(B) \underbrace{\int dA P(A|B) \log \frac{P(A|B)}{P(A)}}_{D_{\text{KL}}(P(A|B)||P(A))} \\ &= \left[\left\langle \log \frac{P(A|B)}{P(A)} \right\rangle \right] \end{aligned} \quad (\text{II.8})$$

Here $D_{\text{KL}}(P(X)||Q(X))$ is the KullbackLeibler (KL) divergence which is a measure of the 'distance' between two probability distributions $P(X)$ and $Q(X)$. In other words the mutual information $I(A, B)$ quantifies the change of the strength of belief of the student on teacher's A due to the observation of the 'data' B .

4. Bayes optimal case: Nishimori condition

In the formulation described above, it is assumed that the student knows teacher's prior $P(A)$ and teacher's likelihood $P(B|A)$. This is a somewhat idealized situation called as *Bayes optimal*. In this case the following useful relation holds [10, 18], which is related to the Nishimori line Eq. (III.42) in the spinglass problem [9, 19].

Let us consider two students 1 and 2 and a function $f(A_1, A_2)$. Its expectation value is

$$\begin{aligned} \llbracket \langle f(A_1, A_2) \rangle_{\text{student } 1,2} \rrbracket &= \int dA_1 dA_2 dB P(A_1|B) P(A_2|B) P(B) f(A_1, A_2) \\ &= \int dA_1 dA_2 dB P(A_1|B) P(B|A_2) P(A_2) f(A_1, A_2) \end{aligned} \quad (\text{II.9})$$

where we used the Bayes formula. On the other hand we can consider

$$\llbracket \langle f(A_1, A^*) \rangle_{\text{student } 1} \rrbracket = \int dA_1 dA^* dB P(A_1|B) P(B|A^*) P(A^*) f(A_1, A^*) \quad (\text{II.10})$$

Clearly we observe

$$\llbracket \langle f(A_1, A_2) \rangle_{\text{student } 1,2} \rrbracket = \llbracket \langle f(A_1, A^*) \rangle_{\text{student } 1} \rrbracket \quad (\text{II.11})$$

5. Various estimators

More precisely, there are some possibilities to generate a specific estimate \hat{A} .

- The so called MMSE (minimum mean-squared error) estimator gives an estimate by

$$\hat{A} = \sum_A P(A|B) A \quad (\text{II.12})$$

which minimizes the mean-squared error

$$\text{MSE} = \sum_A P(A|B) (A - \hat{A})^2 \quad (\text{II.13})$$

Here $\beta = 1$. (Check that $(\partial/\partial \hat{A}) \text{MSE} = 0$ with Eq. (II.12)).

- On the other hand, the so called MAP (maximum a posteriori estimator) gives

$$\hat{A} = \operatorname{argmax}_A P(A|B) \quad (\text{II.14})$$

which maximizes the posterior distribution. In other words it considers $\beta = \infty$.

To evaluate the quality of the inference, we wish to quantify to what extent A^* and A produced by the posterior distribution function $P(A|B)$ are similar.

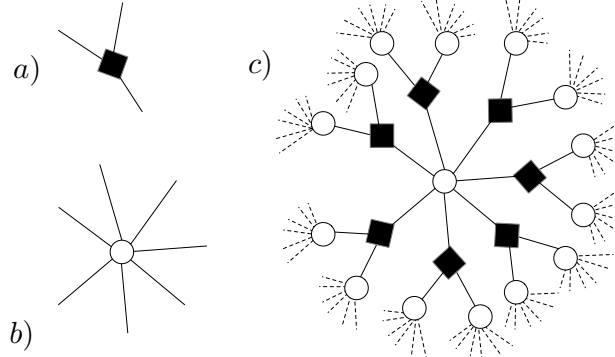
III. MODELS

A. Generalized p -spin models on a dense graph

1. Graphical representation

We consider graphs with N variable nodes $i = 1, 2, \dots, N$ and N_{\blacksquare} factor nodes $\blacksquare = 1, 2, \dots, N_{\blacksquare}$. Each factor node, represented as \blacksquare in Fig. 4 a), has p arms and each variable node, represented as \circlearrowleft in Fig. 4 a), has c arms. The arms of factor nodes are joined with arms of different variable nodes. This means,

$$N_{\blacksquare} p = N c \quad (\text{III.1})$$

FIG. 4. a graph with $p = 3$ and $c = 7$

or

$$\frac{N_{\blacksquare}}{N} = \frac{c}{p} = \frac{c}{\alpha} \gamma \quad \gamma = \frac{\alpha}{p} \quad (\text{III.2})$$

Here we introduced some additional (unnecessary) parameters α and γ . (These will help us later to make connections with vectorial models which will be introduced in sec III C.)

Let us consider a system of spins S_i ($i = 1, 2, \dots, N$) which are sitting on the variable nodes. We suppose that the equilibrium probability distribution is given by,

$$P(S_1, S_2, \dots, S_N) = \frac{1}{Z} \prod_{\blacksquare=1}^{N_{\blacksquare}} \psi_{\blacksquare}(\{S_i\}_{i \in \partial \blacksquare}) \prod_{i=1}^N \phi_i(S_i) \quad (\text{III.3})$$

where

$$Z = \left(\prod_{i=1}^N \text{Tr}_{S_i} \right) \prod_{\blacksquare=1}^{N_{\blacksquare}} \psi_{\blacksquare}(\{S_i\}_{i \in \partial \blacksquare}) \prod_{i=1}^N \phi_i(S_i) \quad (\text{III.4})$$

is the partition function. Here Tr_{S_i} means to take a summation over all possible values of S_i (e.g. in the case of Ising spins $\text{Tr}_{S_i} = \sum_{S_i=-1}^1$). Here $\partial \blacksquare$ means p variable nodes connected to \blacksquare . We can view Eq. (III.3) as the Boltzmann distribution of a system with Hamiltonian,

$$-\beta H = \sum_{\blacksquare=1}^{N_{\blacksquare}} \ln \psi_{\blacksquare}(\{S_i\}_{i \in \partial \blacksquare}) + \sum_{i=1}^N \phi_i(S_i) \quad (\text{III.5})$$

at an inverse temperature β .

- $\psi_{\blacksquare}(\{S_i\}_{i \in \partial \blacksquare})$ represents an interaction associate with factor node \blacksquare . We will consider the cases that it is a function of p -body product $\prod_{i \in \partial \blacksquare} S_i$. (see below)
- $\phi_i(S_i)$ represents a 'bias' associated with a variable node i . For example, $\ln \phi_i(S_i) = -\beta h_i S_i$ due to a local field h_i .

2. Dense tree-like graphs

We consider 'dense graphs' with the following properties,

- We wish to work with graphs which are locally tree-like such that effects of closed loops can be neglected.
- We wish to work with graphs with large number of connectivity c .

Globally connected graphs have large connectivity $c = O(N^{p-1})$ (see Eq. (III.14)) but it has many loops. On the other hand, sparse random graphs are locally tree-like. On a tree, the number of variable nodes at distance l from a given variable node scales as $N(l) \sim (c(p-1))^l$. This implies typical loop length in a random graph of size N is $L_{\text{loop}} \propto \ln N / \ln(c(p-1))$. Thus we can consider *intermediately dense* random graph with connectivity $1 \ll c \ll N$ and consider $c \rightarrow \infty$ limit after $N \rightarrow \infty$ limit.

Such intermediately dense graph may be constructed also deterministically (Rizzo-Cavaliere-Yoshino, in progress).

Technically the dense limit $c \rightarrow \infty$ greatly simplifies the theoretical analysis which one can see in the cumulant expansions of the interaction part of the free-energy (see for example Eq. (IV.34)) or the dynamical action (see Eq. (XII.24)).

3. Dense graphs with layers

It is also interesting to consider dense graphs with the layered geometry such as those used in feed-forward neural networks. For instance consider a network of width N and depth L as shown in Fig. 5 : there are N nodes $i = 1, 2, \dots, N$ in each layer $l = 0, 1, 2, \dots, L$. Suppose that each node in l -th layer is connected to $c/2$ factor nodes located between the l -th and $l-1$ -th layer and the other $c/2$ factor nodes located between the l -th and $l+1$ -th layer. Then by considering $1 \ll c \ll N$, we obtain a $1 + \infty$ dimensional system with dense inter-layer couplings where the effects of loops can be neglected. This construction is useful, for instance, to develop mean-field theories for deep neural networks [20].

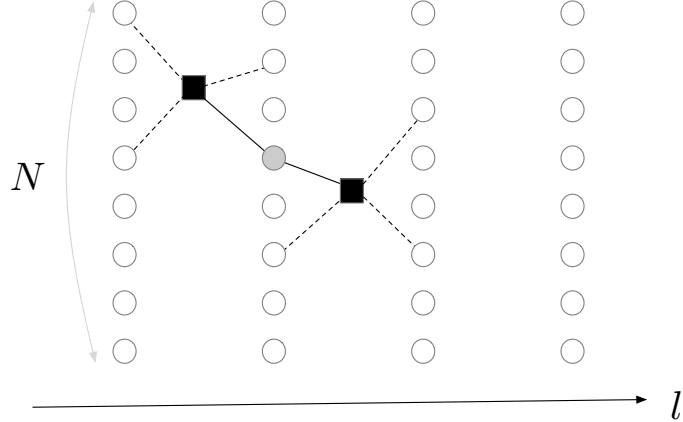


FIG. 5. a graph in a layered geometry with $p = 4$ and $c = 2$

4. Disorder-free models

We have spins on the variable nodes $i = 1, 2, \dots, N$. Here we consider scalar spins. More specifically we consider

- Ising spin:

$$S_i = \pm 1 \quad i = 1, 2, \dots, N \quad (\text{III.6})$$

- scalar-spherical spin :

$$\sum_{i=1}^N S_i^2 = N \quad (\text{III.7})$$

We consider Hamiltonians of the form,

$$H = -\frac{J}{\sqrt{c/\alpha}} \sum_{\blacksquare} \underbrace{\prod_{j \in \partial \blacksquare} S_j}_{p-\text{body}} \quad (\text{III.8})$$

Note that the standard choice is different: change the coupling constant in Eq. (III.8) as $J \rightarrow J/\sqrt{c/\alpha}$. The latter is natural to study the ferromagnetic phase as the energy in the ferromagnetic phase becomes $O(N)$ (see Eq. (III.1)) with such a choice. However, as we will see, the present, non-standard choice becomes convenient for us to study the glassy phases in the disorder-free limit.[15]

5. Models with weak/strong quenched disorder

In this lecture we will show that, as long as mean-field models are concerned, the disorder-free models exhibit glassy phases [15]. But it is also useful to discuss connections with more traditional spinglass models with quenched disorder, like the Edwards-Anderson model [21]. With the strong enough quenched disorder, the crystalline phase become completely suppressed. In the view of glass physics this is convenient because one can forget about the crystalline phase. See Fig. 6.

The role of quenched disorder is also interesting in the context of (random) constraint satisfaction problems, statistical inferences, optimization problems,...

A model with strong quench disorder can be introduced by modifying the p-body spin product in Eq. (III.8) as,

$$\prod_{j \in \partial \blacksquare} S_j \rightarrow \xi \blacksquare \prod_{j \in \partial \blacksquare} S_j \quad (\text{III.9})$$

where $\xi \blacksquare$'s are quenched random variables which are independent from each other and follow a Gaussian distribution with zero mean and unit variance, i. e.

$$\overline{\xi \blacksquare}^\xi = 0 \quad (\overline{\xi \blacksquare})^{2\xi} = 1. \quad (\text{III.10})$$

We can also construct an intermediately disordered model by

$$\prod_{j \in \partial \blacksquare} S_j \rightarrow \eta \blacksquare \prod_{j \in \partial \blacksquare} S_j \quad \eta \blacksquare = \frac{\lambda}{\sqrt{c/\alpha}} + \sqrt{1 - \left(\frac{\lambda}{\sqrt{c/\alpha}}\right)^2} \xi \blacksquare \quad 0 \leq \frac{\lambda}{\sqrt{c/\alpha}} \leq 1 \quad (\text{III.11})$$

Note that $\overline{\eta \blacksquare}^\xi = \lambda/\sqrt{c/\alpha}$ while

$$(\overline{\eta \blacksquare})^{2\xi} = 1 \quad (\text{III.12})$$

holds independently of λ .

- Note that our disorder-free model Eq. (III.8) corresponds to $\frac{\lambda}{\sqrt{c/\alpha}} = 1$. This choice is convenient to study the glassy phases in the disorder-free limit. As we see later in sec. VI C 4 (see also sec. 3.3 of [15]), the effect of self-generated randomness and quenched disorder add together. By employing the parametrization given by Eq. (III.11), which ensures $(\overline{\eta \blacksquare})^{2\xi} = 1$ (see Eq. (III.12)) the resultant glass transition temperature becomes independent of λ .
- With this choice, one has to note that the ferromagnetic phase emerge at very high temperatures of $O(\sqrt{c})$. As we will see later $p > 2$ models allow meta-stable super-cooled paramagnetic phase at any temperatures and the strength of the ferromagnetic bias λ . Consequently we will find glass transitions up to the disorder-free-limit.
- We will see in the next section sec. III B that this parameterization is very similar to the standard parameterization used in the Edwards-Anderson model ($p = 2$) [21] and its extension to $p > 2$ models.

B. Conventional p -spin mean-field spinglass models with disordered global coupling

In the conventional p -spin mean-field spinglass models with global couplings, we have

$$N \blacksquare = N(N-1) \cdots (N-p+1)/p! \sim N^p/p! \quad (\text{III.13})$$

interactions. Then the relation Eq. (III.1) implies

$$c = N^{p-1}/(p-1)! \quad (\text{III.14})$$

The Hamiltonian is

$$H = - \sum_{1 \leq i_1 < i_2 \dots < i_p \leq N} J_{i_1, i_2, \dots, i_p} s_{i_1} s_{i_2} \cdots s_{i_p} \quad (\text{III.15})$$

where the couplings J_{i_1, i_2, \dots, i_p} 's are independent and identically distributed (IID) random variables which follows a Gaussian distribution with a ferromagnetic $J_0 > 0$ bias,

$$P(J_{i_1, i_2, \dots, i_p}) = \frac{e^{-\frac{(J_{i_1, i_2, \dots, i_p} - \Lambda J_0)^2}{2\Delta^2 J^2}}}{\sqrt{2\pi\Delta^2 J^2}} \quad \Delta = \sqrt{\frac{p!}{2N^{p-1}}} \quad \Lambda = \frac{1}{N^{p-1}} \quad (\text{III.16})$$

The above model can also be expressed as

$$H = -J \sum_{\blacksquare} \frac{\eta_{\blacksquare}}{\sqrt{c/\alpha}} \prod_{\substack{j \in \blacksquare \\ p\text{-body}}} s_j . \quad (\text{III.17})$$

with

$$\eta_{\blacksquare} = \frac{\lambda}{\sqrt{c/\alpha}} + \xi_{\blacksquare} \quad \alpha = \frac{p}{2} \quad \lambda = \frac{2}{p!} \frac{J_0}{J} \quad (\text{III.18})$$

with ξ defined in the same way as Eq. (III.10). From Eq. (III.2) we see $\gamma = \alpha/p = 1/2$ in this conventional model. Note also that $\overline{\eta_{\blacksquare}}^{\xi} = \lambda/\sqrt{c/\alpha}$ while

$$\overline{\eta_{\blacksquare}}^{\xi} = 1 + (\lambda/\sqrt{c/\alpha})^2 \quad (\text{III.19})$$

Comparing this conventional model Eq. (III.18) with our intermediately disordered model Eq. (III.11), we find that they are very similar except for the following points.

- One difference is that we consider dense limit $c \rightarrow \infty$ after $N \rightarrow \infty$ limit while $c \propto N^{p-1}$ in the conventional 'globally coupled model' Eq. (III.14). In this sense our dense model is less dense compared with the globally coupled model.
- Comparing Eq. (III.18) with Eq. (III.11) or Eq. (III.12) with Eq. (III.19), we find there is a slight difference of order $(\lambda/\sqrt{c/\alpha})^2$.
 - The difference is related to the fact in the conventional parametrization there is no genuine disorder-free limit while our parametrization allows disorder-free in the limit $\lambda/\sqrt{c/\alpha} \rightarrow 1$.
 - Otherwise, this is just a small difference which disappear in the dense limit $c \rightarrow \infty$ so that one would not expect to much changes of the physics. Our disorder-free limit is essentially equivalent to the region of $\lambda = J_0/J \sim O(\sqrt{c/\alpha}) \xrightarrow[c \rightarrow \infty]{} \infty$ in Fig. 6 obtained by the conventional globally coupled model.

In Fig 6 we show the known phase diagrams of the standard $p = 2$ (SK model) [22] and $p = 3$ Ising spinglass models with the global coupling. Note that the same phase diagrams should be obtained also by the model on the dense graph (with the quenched disorder Eq. (III.11)) in the dense limit $c \rightarrow \infty$. The phases are characterized by the Edwards-Anderson spinglass order parameter,

$$q = \frac{1}{N} \sum_{i=1}^N \langle S_i \rangle^2, \quad (\text{III.20})$$

and the ferromagnetic order parameter (magnetization),

$$m = \frac{1}{N} \sum_{i=1}^N \langle S_i \rangle. \quad (\text{III.21})$$

Along the Nishimori line [19] these become identical $m = q$ (see Eq. (IX.34)).

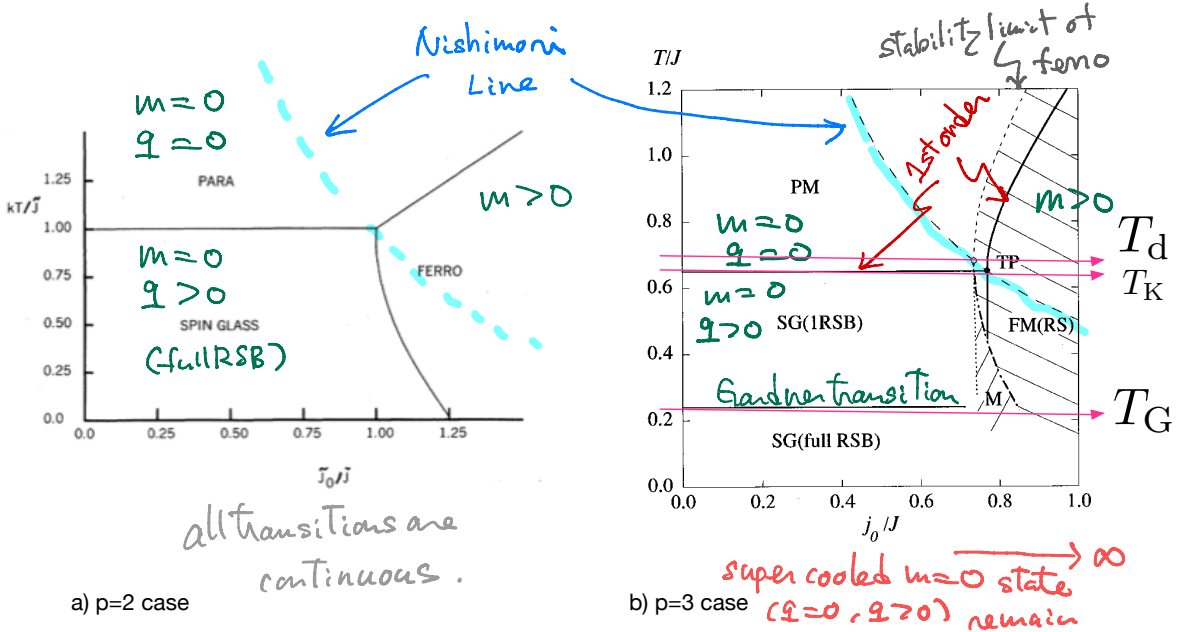


FIG. 6. Phase diagrams of mean-field Ising p -spin spin glass models with global coupling Eq. (III.18) where J represents the strength of the quenched disorder and j_0 represents the strength of ferromagnetic bias. a) SK model ($p = 2$) (taken from [22]). In this case quenched disorder is inevitable to study glassy phases. b) $p = 3$ model (taken from [23]). Importantly, in the case $p > 2$, the $m = 0$ state remains as a supercooled liquid (paramagnetic phase) when the true equilibrium state is the ferromagnetic one (See Fig. 12 b)). The glass transition (and the Gardner transition) can take place within the *supercooled paramagnetic phase* at the same temperature independent of the strength of the ferromagnetic bias up to the limit $j_0/J \rightarrow \infty$. We essentially obtain the same phase diagram also by our model Eq. (III.8) for which the horizontal axis j_0/J is replaced by $p!\lambda/2$. The parameter λ connects the fully disordered system $\lambda = 0$ and disorder-free system $\lambda = \sqrt{c/\alpha} \xrightarrow{c \rightarrow \infty} \infty$ (see Eq. (III.11)). In our model the vertical axis is still T/J but this J is *not* the strength of quenched disorder but the basic energy scale which do not vanish in the disorder-free limit $\lambda = \infty$. The difference of the two models is related to the slight difference of the models at order $(\lambda/\sqrt{c/\alpha})^2$ mentioned above. We take into account that the effect of self-generated randomness, which has not been considered in conventional literatures, which add on top of quenched disorder. With the parametrization given by Eq. (III.11) the effective randomness becomes independent of λ so that glass transition temperature becomes independent of λ (see sec. VI C 4 (see also sec. 3.3 of [15]).

C. M -component vectorial p -spin models with a generic potential

Here we discuss a family of vectorial spin models introduced in [15] which are useful to model strongly non-linear interactions between spins, such as the hard-core interaction. In these models we have spins which are M -component vectorial variables which are normalized as,

$$\sum_{\mu=1}^M (S_i^{\mu})^2 = M \quad (\text{III.22})$$

We can consider (i) Ising spins $\sum_{\mu=1}^M = \pm 1$ or (ii) continuous spins which meet the normalization Eq. (III.22).

For the graph, we consider graphs with connectivity $c = \alpha M$. We will consider the limit $M \rightarrow \infty$ with fixed α . Thus we have,

$$N_{\blacksquare} = (c/p)N = \gamma NM \quad \gamma = \frac{\alpha}{p} \quad (\text{III.23})$$

Similarly to sec III A, we consider dense, locally tree-like graphs.

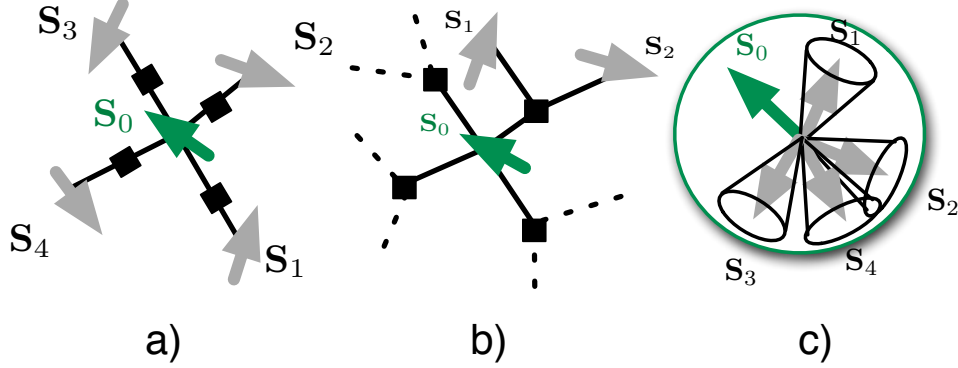


FIG. 7. A schematic figure of the vector model. Panel a) is for the cases of $p = 2$ and b) is for the case of $p = 3$ -body interaction on a graph with connectivity $c = 4$. Vectorial spins with M components, in this example $M = 3$ (Heisenberg spins), are put on the vertexes of a lattice or a graph as shown in the left panel a). The filled square represents the interaction nodes each of which connects a set of p spins on the vertexes (variable nodes) interacting with each other. For the hardcore potential given by Eq. (III.26) the spin \mathbf{S}_0 in panel c) is excluded from the cones around each of the neighboring spins $\mathbf{S}_1, \mathbf{S}_2, \mathbf{S}_3$. (Note that, for instance, \mathbf{S}_2 and \mathbf{S}_4 can overlap if they are not directly connected by a link). The size of the cones grows with decreasing the parameter δ . Thus the excluding volume effect becomes larger by decreasing δ or increasing the connectivity c . (Taken from [15])

The Hamiltonian is given by,

$$H[\{S\}] = \sum_{\blacksquare} v(r_{\blacksquare}) \quad r_{\blacksquare} = \frac{1}{\sqrt{M}} \sum_{\mu=1}^M \prod_{j \in \partial \blacksquare} S_j^\mu \quad (\text{III.24})$$

For the potential, we consider the following potentials in this lecture,

- Linear potential (ferromagnetic model)

$$v(x) = -Jx \quad (\text{III.25})$$

In this case we naturally find [15] all the phenomena found in the scalar p -spin models.

- Hardcore potential

$$e^{-\beta v(x)} = \theta(\delta - x) \quad (\text{III.26})$$

This is relevant to study the solution space of a class of continuous constraint satisfaction problems [15] and related inference problems which we discuss in III E.

- Soft-core potential

$$V(x) = \epsilon x^2 \theta(-x) \quad (\text{III.27})$$

This potential becomes hardcore in the limit $\epsilon \rightarrow \infty$.

Similarly to the scalar model, we can consider models with strong quenched disorder,

$$\prod_{j \in \partial \blacksquare} S_j^\mu \rightarrow \xi_{\blacksquare}^\mu \prod_{j \in \partial \blacksquare} S_j^\mu \quad (\text{III.28})$$

where ξ_{\blacksquare} 's are quenched random variables which are independent from each other and follow a Gaussian distribution with zero mean and unit variance, i. e. $\overline{\xi_{\blacksquare}} = 0$, $\overline{\xi_{\blacksquare}^2} = 1$.

We can also consider systems intermediately disordered system

$$\frac{\lambda}{\sqrt{M}} \xi_{\blacksquare} \rightarrow \eta_{\blacksquare} = \frac{\lambda}{\sqrt{M}} + \sqrt{1 - \left(\frac{\lambda}{\sqrt{M}} \right)^2} \xi_{\blacksquare} \quad 0 \leq \frac{\lambda}{\sqrt{M}} \leq 1 \quad (\text{III.29})$$

D. Planting

1. Simple setting 1 a)

- Teacher: The teacher has the spin configurations S_i^* ($i = 1, 2, \dots, N$), which is the ground truth. The teacher generates a data, which is a p -spin Hamiltonian H_J on a dense graph which we discussed previously in sec IIIA 5, with the probability,

$$P(J|S^*)P(S^*) = e^{-\beta H_J(S^*)} \quad (\text{III.30})$$

at temperature T . Here J represents symbolically the complete set of parameters which specify the Hamiltonian + graph. The Hamiltonian $H_J(S)$ is defined adding some constant to endure the normalization $\sum_J e^{-\beta H_J(S)} = P(S)$.

- Student: The student receives the p -spin Hamiltonian + graph from the teacher. It is also informed of the temperature T the teacher used to create the Hamiltonian. The task of the student is try to infer the actual spin configuration S^* of the teacher using the Bayes formulaEq. (II.2),

$$P(S|J) = \frac{P(J|S)P(S)}{\sum_S P(J|S)P(S)} = \frac{e^{-\beta H_J(S)}}{\sum_S e^{-\beta H_J(S)}} \quad (\text{III.31})$$

Thus the student can use the Hamiltonian + graph to generate an estimate \hat{S} using the Hamiltonian at temperature T . Here the student knows everything about the teacher except for the spin configuration itself. This is a *Bayes optimal* situation[10, 18].

2. Simple setting 1b): Inverse Ising model

- Teacher: The teacher has a p -spin Hamiltonian H_J with disordered coupling J on a dense graph which we discussed previously in sec IIIA 5. The disordered coupling J^* parametrized by ξ_{\blacksquare}^* ($\blacksquare = 1, 2, \dots, N_{\blacksquare}$) is the ground truth.

The teacher generates a data S_i^μ ($i = 1, 2, \dots, N$) ($\mu = 1, 2, \dots, M$) with the probability,

$$P(S|J^*)P(J^*) = e^{-\beta \sum_{\mu=1}^M H_J(S^\mu)} \quad (\text{III.32})$$

at temperature T . $H_J(S)$ is defined adding some constant to endure the normalization $\sum_J e^{-\beta H_J(S)} = P(S)$.

- Student: The student receives the the data S_i^μ ($i = 1, 2, \dots, N$) ($\mu = 1, 2, \dots, M$). It is also informed of the temperature T the teacher used to create the data. The task of the student is try to infer the ctual teacher's couplings J^* using the Bayes formulaEq. (II.2),

$$P(J|S) = \frac{P(S|J)P(J)}{\sum_J P(S|J)P(J)} = \frac{e^{-\beta H_J(S)}}{\sum_J e^{-\beta H_J(S)}} \quad (\text{III.33})$$

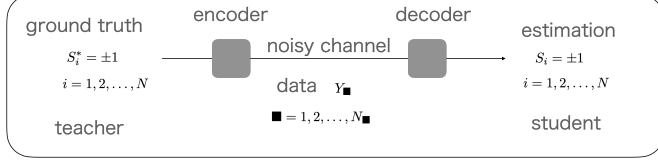
Thus the student can use the Hamiltonian + graph to generate an estimate \hat{J} using the Hamiltonian at temperature T . Here the student knows everything about the teacher except for the actual values of the coupling. This is also a *Bayes optimal* situation[10, 18].

3. Simple setting 2 : error correcting code

The following is known as an error correcting code problem called as Sourlas code [24].

- Teacher: The teacher has the spin configurations S_i^* . It creates a data, which consists of the following elements,

$$Y_{\blacksquare} = \frac{\Lambda^*}{\sqrt{c/\alpha}} \prod_{i \in \partial_{\blacksquare}} \underbrace{S_i^* + w_{\blacksquare}^*}_{\text{p-body}} \quad (\blacksquare = 1, 2, \dots, N_{\blacksquare}) \quad (\text{III.34})$$



We assume the graph created here has the property discussed previously (locally tree-like dense graph). Here w_{\blacksquare}^* is a noise which follows a distribution $W(w)$. Then we have,

$$P(Y_{\blacksquare}|S^*)P(S^*) = W\left(Y_{\blacksquare} - \frac{\Lambda}{\sqrt{c/\alpha}} \prod_{i \in \partial \blacksquare} S_i^*\right) P(S^*) \quad (\text{III.35})$$

For simplicity we assume a flat prior distribution $P(S^*) = \text{const.}$

- Student: The student is given the set of data Y_{\blacksquare} ($\blacksquare = 1, 2, \dots, N_{\blacksquare}$) and the graph. It also knows the function $W(\cdot)$, the parameter Λ and $P(S) = \text{const.}$ Then it tries to infer the teachers spin configurations S_i^* using the Bayes formula Eq. (II.2),

$$\begin{aligned} P(S|Y) &= \frac{P(Y|S)P(S)}{\sum_S P(Y|S)P(S)} = \frac{e^{-\beta H(S)}}{\sum_S e^{-\beta H(S)}} \\ -\beta H(S) &= -\beta \sum_{\blacksquare} v \left(Y_{\blacksquare} - \frac{\Lambda}{\sqrt{c/\alpha}} \prod_{i \in \partial \blacksquare} S_i \right) \quad -\beta v(x) = \ln W(x) \end{aligned} \quad (\text{III.36})$$

Thus the student can use the Hamiltonian $H(S)$ to generate an estimate \tilde{S} . Again, the student knows everything about the teacher except for the spin configuration itself: *Bayes optimal*.

Example - For example let us consider the case of Ising spins $S_i = \pm 1$ and take the Gaussian distribution for the noise,

$$W(x) = \frac{e^{-\frac{x^2}{2\Delta^2}}}{\sqrt{2\pi\Delta^2}} \quad (\text{III.37})$$

Then we find

$$\begin{aligned} -\beta v \left(Y_{\blacksquare} - \frac{\Lambda}{\sqrt{c/\alpha}} \prod_{i \in \partial \blacksquare} S_i \right) &= \frac{1}{\Delta^2} \frac{\Lambda}{\sqrt{c/\alpha}} Y_{\blacksquare} \prod_{i \in \partial \blacksquare} S_i - \frac{Y_{\blacksquare}^2}{2\Delta^2} - \frac{1}{2\Delta^2} \frac{\Lambda^2}{c/\alpha} \\ &= \frac{\Lambda/\Delta}{\sqrt{c/\alpha}} \left(\frac{\Lambda^*/\Delta}{\sqrt{c/\alpha}} + \frac{\tilde{w}_{\blacksquare}}{\Delta} \right) \prod_{i \in \partial \blacksquare} \tilde{S}_i + \dots \end{aligned} \quad (\text{III.38})$$

the \dots represent irrelevant constant terms which do not contain S_i . Here we introduced,

$$\tilde{S}_i = S_i^* S_i \quad \tilde{w}_{\blacksquare} = \left(\prod_{i \in \partial \blacksquare} S_i^* \right) w_{\blacksquare} \quad (\text{III.39})$$

Note that \tilde{S}_i take Ising values and \tilde{w}_{\blacksquare} follows the same Gaussian distribution as w_{\blacksquare} . Thus we essentially recovered the spinglass model Eq. (III.11) or Eq. (III.18). For instance, in the case of global coupling Eq. (III.16), we find the following correspondence,

$$\begin{aligned} \beta J &\rightarrow \frac{\Lambda}{\Delta} \\ \lambda &\rightarrow \frac{\Lambda^*}{\Delta} \end{aligned} \quad (\text{III.40})$$

Note that Λ/Δ means just the signal-to-noise (S/N) ratio. In the Bayes optimal case we have

$$\Lambda = \Lambda^* \quad (\text{III.41})$$

which is equivalent to

$$\beta J = \lambda \quad (\text{III.42})$$

The latter is the so called Nishimori line [9, 19] where the inference becomes Bayes optimal [18] and the identity $m = q$ holds (See Fig. 6).

Interestingly, due to the gauge transformation Eq. (III.39), the magnetization Eq. (III.21),

$$m = \frac{1}{N} \sum_{i=1}^N \tilde{S}_i = \frac{1}{N} \sum_{i=1}^N S_i^* S_i \quad (\text{III.43})$$

can be understood as the overlap of the inferred spin configurations with respect to the ground truth S^* . Thus inferences are expected to be successful in the ferromagnetic phase $m > 0$. Along the Nishimori line (Bayes optimal inference), the ferromagnetic phase is found in the regime of large enough S/N ratio $\lambda = (2/p!)J_0/J$ (see Eq. (III.18)), which makes sense.

4. Vectorial version

We can naturally consider vectorial inference problems using the vectorial p -spin models introduced in sec. III C : inference of S_i^μ with $(i = 1, 2, \dots, N)$ and $(\mu = 1, 2, \dots, M)$.

5. Examples: with some references

1. Error correcting codes (Sourlas [24], Kabashima-Saad [25]): $p = 2, 3, \dots, \infty$. If one uses scalar model with dense coupling $c \gg 1$ (including global coupling $c \propto N^p$), the transmission rate (number of bits/number of codes) becomes $R = N/N_\blacksquare = p/c \rightarrow 0$ as $c \rightarrow \infty$. This problem is solved using the sparse coupling [25]). The vectorial version (Yokoi-Nagasawa-Obuchi-Yoshino) (see below) also realizes finite transmission rate $R = NM/N_\blacksquare = p/\alpha = 1/\gamma$.
2. Inference of discrete coloring (Krzakala-Zdeborova[26]): $p = 2$
3. Linear estimation : $p = 1$ with ξ_\blacksquare
 - Perceptron learning (Gardner-Derrida [27]) (ξ_\blacksquare : random input/outputs)
 - CDMA multiuser-detection (Kabashima[28], Tanaka[29]) (ξ_\blacksquare : spreading code)
 - Compressed sensing (Candes-Tao-Donoho[30], Kabashima-Wadayama-Tanaka [31]) (ξ_\blacksquare : random matrix)
4. Spiked tensor estimation (generalization of principle component analysis (PCA) $p = 2$)

E. Exactly solvable vectorial CSPs and inference problems

1. Vectorial constraint satisfaction problems

In sec. II A we mentioned some constraint satisfaction problems (CSP). Here we introduce a family of CSPs of vectorial variables which can be solved exactly by the replica approach [15]. It is a system of large- M component vectorial p -spin model on dense graphs of connectivity $c = \alpha M$ introduced in sec III C with non-linear potentials like the hardcore potential Eq. (III.26) or the soft-core potential Eq. (III.27). We can also include some quenched disorder (see Eq. (III.29)).

- $p = 1$ case: as we see below in sec. III F, it is actually equivalent to the perceptron problem.
- $p = 2$ case: it can be regarded as a generalized version of the continuous coloring discussed in sec. II A. The hardcore potential Eq. (III.26) induces a kind of excluded volume effect in the spin space similarly to the hardcore potential for hard-spheres which induces excluded volume effect in the real space (See Fig. 7 c)). The parameter δ in Eq. (III.26) controls the threshold on the inner product of vectorial spins on adjacent nodes. Smaller δ forces the two spins to be separated more in the spin space. Thus it plays the role similar to the diameter of the hard-spheres.

2. Vectorial inference problems

Naturally there are related inference problems of vectorial variables based on $p \geq 2$ models (S. Yokoi, master thesis, Osaka Univ, 2018) (Nagasawa-Yokoi-Obuchi-Yoshino, work in progress). This amount to consider problems such as vectorial error correcting codes, generalization of the linear estimation ($p = 1$) inference problems (CDMA multi-user detection, Perceptron learning, Compressed sensing,...) listed in sec III D 5 to non-linear estimations $p \geq 2$.

F. Perceptron

Let us consider a single perceptron, which has the simplest activation function,

$$S_0 = \text{sgn} \left(\sum_{i=1}^N \frac{J_i}{\sqrt{N}} S_i \right) \quad (\text{III.44})$$

Here $S_i = \pm 1$ ($i = 0, 1, \dots, N$) represent the activity of neurons. A machine is characterized by a set of weights J_i ($i = 1, 2, \dots, N$) which take continuous values subjected to a spherical constraint

$$\sum_{i=1}^N J_i^2 = N \quad (\text{III.45})$$

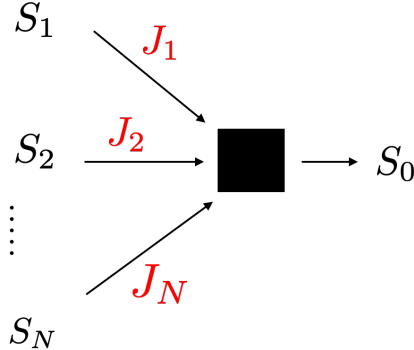


FIG. 8. Single perceptron

We consider M sets of input/output configurations

$$S_i^\mu = \pm 1 \quad i = 0, 1, \dots, N \quad \mu = 1, 2, \dots, M \quad (\text{III.46})$$

and ask how many different realization of machines is possible, which meet this set of constraints. The volume of the design phase space[32, 33] is called as Gardner volume[32, 33]¹,

$$V_G[\{S\}] = \int \prod_{i=1}^N dJ_i \delta \left(\sum_{i=1}^N J_i^2 - N \right) \prod_{\mu=1}^M \theta(r^\mu) \quad r^\mu = S_0^\mu \sum_{i=1}^N \frac{J_i}{\sqrt{N}} S_i^\mu - \kappa \quad (\text{III.47})$$

The parameter κ is 0 in the original problem. An important parameter is

$$\alpha_{\text{perceptron}} = \frac{M}{N} \quad (\text{III.48})$$

¹ See the portrait of E. Gardner written by B. Derrida, I. J. R. Atchison and D. J. Wallace

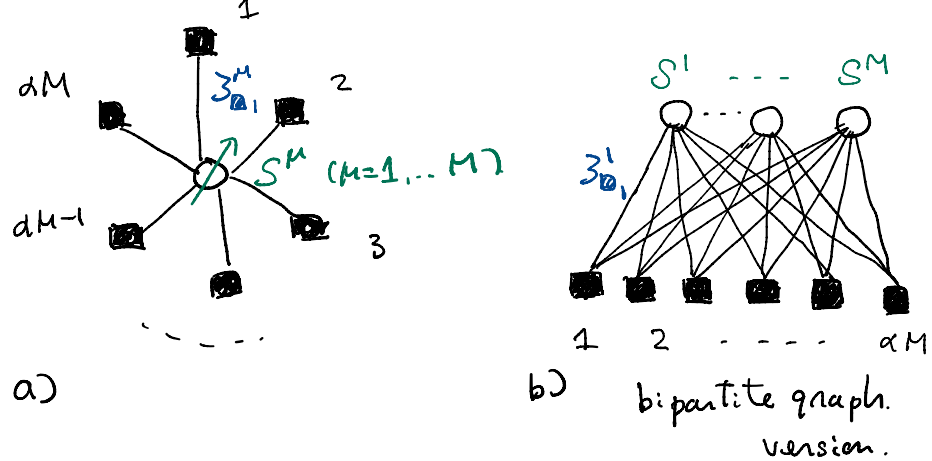


FIG. 9. Single perceptron as $p = 1$ vectorial spin model: a) our representation b) (more common) representation by a bipartite graph

This is the same as the partition function of a vectorial $p = 1$ spin model with $N = 1$ spin with M components Eq. (III.24) with quenched disorder Eq. (III.28) and the hardcore potential Eq. (III.26),

$$H[\{S\}] = \sum_{\blacksquare=1}^{N_\blacksquare} v(r_\blacksquare) \quad r_\blacksquare = \frac{1}{\sqrt{M}} \sum_{\mu=1}^M \xi_\blacksquare^\mu S^\mu \quad e^{-\beta v(x)} = \theta(\delta - x) \quad (\text{III.49})$$

but with the following translations

$$i \rightarrow \mu \quad N \rightarrow M \quad J_i \rightarrow S^\mu \quad (\text{III.50})$$

$$\mu \rightarrow \blacksquare \quad M \rightarrow N_\blacksquare = M\alpha \quad S_0^\mu S_i^\mu \rightarrow -\xi_\blacksquare^\mu \quad (\text{III.51})$$

$$\alpha_{\text{perceptron}} = \frac{M}{N} \rightarrow \alpha = \frac{c}{M} \quad (\text{III.52})$$

$$\kappa \rightarrow -\delta \quad (\text{III.53})$$

In the 1st equation we used Eq. (III.23) with $p = 1$ and $N = 1$.

1. Random inputs/outputs : a constraint satisfaction problem

One important problem is the analysis in the case the input/outputs are random [32, 33]. This amount to study the statistical mechanics of the $p = 1$ spin model with the Hardcore potential and the quenched disorder ξ_\blacksquare^μ . This is the 'simplest' random constraint satisfaction problem of continuous variables. One is interested, for instance, how the solution space becomes clustered by increasing the number of constraints. This is exactly a problem of glass transitions. Another interesting problem is what is the limit of storage. This is exactly the 'simplest' jamming [34].

2. Teacher-student scenario : a statistical inference problem

In the above setting the machine is just memorizing random data (noise). More meaningful scheme of learning can be formulated by the teacher-student scenario discussed in sec. ???. We will discuss it in sec. IX D 3.

G. Spheres in large dimensional limit

We consider a simple system of N particles of mass m in d -dimensional space, with 2-body interactions,

$$H = \sum_{i=1}^N \frac{|\mathbf{p}_i|^2}{2m} + \sum_{i < j} v(r_{ij}) \quad r_{ij} = |\mathbf{x}_i - \mathbf{x}_j|$$

where \mathbf{x}_i ($i = 1, 2, \dots, N$) are d -dimensional vectors which represent the positions of the particles and \mathbf{p}_i 's are their momenta.

The free-energy of the system is given by

$$-\beta F = \ln Z \quad (\text{III.54})$$

with the partition function

$$Z = Z^{\text{id}} \int \prod_{i=1}^N \frac{d^d x_i}{V} \prod_{i < j} (1 + f(r_{ij})) \quad Z^{\text{id}} = \frac{V^d}{N!} \left(\int_{-\infty}^{\infty} dp e^{-\beta \frac{p^2}{2m}} \right)^{Nd} = \frac{(V/\lambda_{\text{th}}^d)^N}{N!} \quad (\text{III.55})$$

where Z^{id} is the partition function of the ideal gas, and $f(r)$ is the Mayer function

$$f(r) = e^{-\beta v(r)} - 1 \quad (\text{III.56})$$

and $\lambda_{\text{th}} = h/\sqrt{2\pi mk_B T}$ is the de Broglie wave length.

Expansion of the free-energy in power series of the Mayer function converges in liquids [35]. We can naturally decompose the free-energy into the ideal gas part, which is purely entropic, and the excessive part due to interactions,

$$F = F^{\text{id}} + F^{\text{ex}} \quad (\text{III.57})$$

where the ideal gas part is obtained as,

$$-\beta F^{\text{id}} = \rho V [1 - \ln(\rho \lambda_{\text{th}}^d)] \quad (\text{III.58})$$

with the number density $\rho = N/V$ and the volume of the container V . The excessive part due to interactions reads,

$$\begin{aligned} -\beta F^{\text{ex}} &= \frac{1}{2!} \sum_{ij} \int \frac{d^d x_i}{V} \int \frac{d^d x_j}{V} f(\mathbf{x}_i - \mathbf{x}_j) \\ &\quad + \frac{1}{3!} \sum_{i,j,k} \int \frac{d^d x_i}{V} \int \frac{d^d x_j}{V} \int \frac{d^d x_k}{V} f(\mathbf{x}_i - \mathbf{x}_j) f(\mathbf{x}_j - \mathbf{x}_k) f(\mathbf{x}_k - \mathbf{x}_i) + \dots \end{aligned} \quad (\text{III.59})$$

A very important quantity is the radial distribution function $g(r)$ [35],

$$\left\langle \frac{1}{N} \sum_{i \neq j} \delta(\mathbf{r} - (\mathbf{r}_i - \mathbf{r}_j)) \right\rangle = \rho g(r) \quad (\text{III.60})$$

where we assumed rotational symmetry. A useful identity is [35],

$$\frac{\delta(-\beta F^{\text{ex}})/N}{\delta(-\beta v(r))} = \frac{1}{2} \rho (d\Omega_d) r^{d-1} g(r) \quad (\text{III.61})$$

where Ω_d is the volume of d -dimensional unit sphere.

[**After legendre transform**] It is possible to show that in large dimensional limit $d \rightarrow \infty$, the Mayer expansion of a class of system including hardspheres, terminates at the 1st Mayer correction because higher order terms become exponentially small in d (see sec 2.3 of [12]).

$$\begin{aligned} -\beta F_1^{\text{ex}}/N &= \frac{1}{2} \sum_{i \neq 1} \int \frac{d^d x_i}{V} f(|\mathbf{x}_i - \mathbf{x}_1|) \\ &= \frac{1}{2} \rho (d\Omega_d) \int_0^\infty dr r^{d-1} f(r) \end{aligned} \quad (\text{III.62})$$

Then we immediately find $g(r) = e^{-\beta v(r)}$ in this case.

Part II

p -spin models on a dense graph

IV. WARMING UP: FERROMAGNETISM

A. Basic phenomenology of ferromagnetism

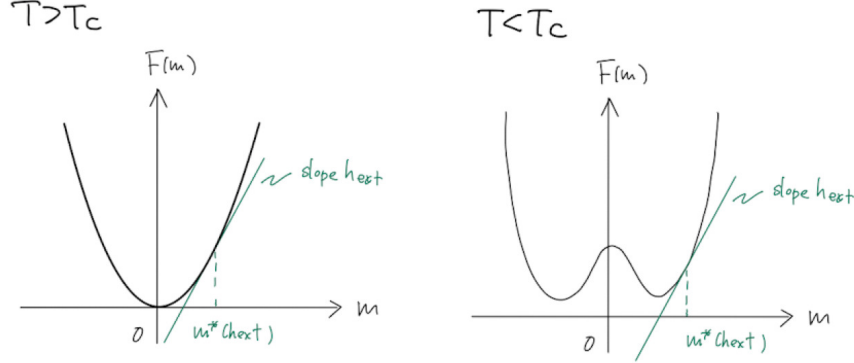


FIG. 10. Landau free-energy (see Fig. IV.2). Here $a > 0$ (left) $a < 0$ (right) and with $b > 0$ corresponding to the usual ferromagnetic Ising model (with $p = 2$) at a temperature T above and below the critical temperature T_c respectively.

Here we discuss ferromagnetic phase transitions. The aim is to introduce our basic strategies to analyze phase transitions which we also use for glassy systems later.

The phenomenology of ferromagnetism is well known. The order parameter is the magnetization m . The conjugated field is the external magnetic field h_{ext} . If the system without h_{ext} is symmetric under global reflection $m \rightarrow -m$, h_{ext} breaks the symmetry. We are interested with the order parameter, called as spontaneous magnetization m_s , defined as,

$$m_s = \lim_{h_{\text{ext}} \rightarrow 0^+} \lim_{N \rightarrow \infty} m(h_{\text{ext}}), \quad (\text{IV.1})$$

Here N is the size of the system (number of spins). This reflects 'spontaneous symmetry breaking'. In the paramagnetic phase the two limits can be interchanged $\lim_{h \rightarrow 0} \lim_{N \rightarrow \infty} m(h) = \lim_{N \rightarrow \infty} \lim_{h \rightarrow 0} m(h) = 0$. But in the ferromagnetic phase the two limits do not commute: while $\lim_{N \rightarrow \infty} \lim_{h \rightarrow 0} m(h) = 0$, $\lim_{h \rightarrow 0^+} \lim_{N \rightarrow \infty} m(h) > 0$ (and $\lim_{h \rightarrow 0^-} \lim_{N \rightarrow \infty} m(h) < 0$).

The Landau theory for the ferromagnetism give qualitative (mean-field) picture for the emergence of the ferromagnetic phase characterized by $|m_s| > 0$. Within the Landau theory we assume that the free-energy $F(m)$ of the system constrained to take a given magnetization m take the following form (see Fig. 10),

$$\frac{-\beta F(m)}{N} = am^2 + bm^4 + \dots \quad (\text{IV.2})$$

Then the free-energy $G(h_{\text{ext}})$ in the presence of an external field h_{ext} can be expressed as,

$$e^{-\beta G(h_{\text{ext}})} = \int dm e^{Nh_{\text{ext}}m - \beta F(m)} = e^{Nh_{\text{ext}}m^*(h_{\text{ext}}) - \beta F(m^*(h_{\text{ext}}))} \quad (\text{IV.3})$$

where $m^*(h_{\text{ext}})$ is the saddle point for the integration which is determined by,

$$h_{\text{ext}} = \frac{1}{N} \left. \frac{\partial -\beta F(m)}{\partial m} \right|_{m=m^*(h_{\text{ext}})} \quad (\text{IV.4})$$

in the thermodynamic limit $N \rightarrow \infty$. Thus the order parameter m_s Eq. (IV.1) can be obtained as $m_s = m^*(0)$.

We will discuss in the following how to derive the free-energy $F(m)$ (and also $G(h)$) within a solvable (mean-field) microscopic model.

B. Generic strategy

1. The order parameter, conjugated field

Suppose that we have a system of spins S_i ($i = 1, 2, \dots, N$) with a Hamiltonian $H[\{S_i\}]$. Let us introduce an additional term due to a coupling to a magnetic field h ,

$$-\beta H[\{S_i\}] \rightarrow -\beta H[\{S_i\}] + h \sum_{i=1}^N S_i \quad (\text{IV.5})$$

The free-energy of the system is,

$$-\beta G(h) = \ln \left(\prod_{i=1}^N \text{Tr}_{S_i} \right) e^{-\beta H[\{S_i\}] + h \sum_{i=1}^N S_i} \quad (\text{IV.6})$$

from which we can evaluate the magnetization as,

$$m(h) = \frac{1}{N} \sum_{i=1}^N \langle S_i \rangle_h = \frac{1}{N} \frac{\partial(-\beta G(h))}{\partial h}. \quad (\text{IV.7})$$

In the following, the system we consider may or may not be invariant under global spin reversion $S_i \rightarrow -S_i$ for $\forall i$. If it is symmetric, h breaks the symmetry explicitly.

If the system has ferromagnetism, we are interested with the order parameter defined as,

$$\lim_{h \rightarrow 0} \lim_{N \rightarrow \infty} m(h) \quad (\text{IV.8})$$

In the paramagnetic phase the two limits can be interchanged $\lim_{h \rightarrow 0} \lim_{N \rightarrow \infty} m(h) = \lim_{N \rightarrow \infty} \lim_{h \rightarrow 0} m(h) = 0$. But in the ferromagnetic phase the two limits do not commute: while $\lim_{N \rightarrow \infty} \lim_{h \rightarrow 0} m(h) = 0$, $\lim_{h \rightarrow 0^+} \lim_{N \rightarrow \infty} m(h) > 0$ (and $\lim_{h \rightarrow 0^-} \lim_{N \rightarrow \infty} m(h) < 0$).

2. Legendre transform

Let us define a Legendre transform,

$$-\beta F(m) = -\beta G(h^*) - Nh^* m \quad (\text{IV.9})$$

where $h^* = h^*(m)$ is determined by

$$m = \frac{1}{N} \frac{\partial(-\beta G(h))}{\partial h} \Big|_{h=h^*(m)} = \frac{1}{N} \sum_{i=1}^N \langle S_i \rangle_{h=h^*(m)} \quad (\text{IV.10})$$

Note that the linear susceptibility can be obtained as

$$\chi = \frac{\partial m}{\partial h} = \frac{1}{N} \frac{\partial^2(-\beta G(h))}{\partial h^2} \Big|_{h=h^*(m)} = \frac{1}{N} \sum_{i,j=1}^N [\langle S_i S_j \rangle - \langle S_i \rangle \langle S_j \rangle] \quad (\text{IV.11})$$

The inverse Legendre transform is defined as,

$$-\beta G(h) = -\beta F(m^*) + N h m^* \quad (\text{IV.12})$$

where $m^* = m^*(h)$ is determined by²

$$-h = \frac{1}{N} \frac{\partial(-\beta F(m))}{\partial m} \Big|_{m=m^*(h)} \quad (\text{IV.13})$$

² From Eq. (IV.9), $\partial_m(-\beta F(m)) = -Nh^* + (\partial h^*/\partial m) \underbrace{\partial_{h^*}(-\beta G(h^*) - Nh^* m)}_0 = -Nh^*$ where we used Eq. (IV.10).

Corresponding to the susceptibility Eq. (IV.11), we find,

$$\chi^{-1} = \frac{\partial h}{\partial m} = \frac{1}{N} \frac{\partial^2(\beta F(m))}{\partial^2 m} \Big|_{m=m^*(h)} \quad (\text{IV.14})$$

3. 1st step of the recipe

The Legendre transform and its inverse discussed above can be implemented as follows. We start from an identity,

$$1 = N \int dm \delta(Nm - \sum_{i=1}^N S_i) = N \int dm \int_{-i\infty}^{i\infty} \frac{dh}{2\pi i} e^{-Nm h} \prod_{i=1}^N e^{hS_i} \quad (\text{IV.15})$$

where we used an integral representation of the delta function

$$\delta(x) = \int_{-i\infty}^{i\infty} \frac{dk}{2\pi i} e^{-kx} \quad (\text{IV.16})$$

We can analyze the partition function of the system under external magnetic field h_{ext} as follows,

$$\begin{aligned} Z(h_{\text{ext}}) &= \prod_{i=1}^N \text{Tr}_{S_i} e^{-\beta H + h_{\text{ext}} \sum_{i=1}^N S_i} = N \int dm \int_{-i\infty}^{i\infty} \frac{dh}{2\pi i} e^{-Nm h} \prod_{i=1}^N \left(\text{Tr}_{S_i} e^{(h+h_{\text{ext}})S_i} \right) e^{-\beta H} \\ &= N \int dm e^{Nh_{\text{ext}} m} \int_{h_{\text{ext}}-i\infty}^{h_{\text{ext}}+i\infty} \frac{dh}{2\pi i} e^{-Nm h} e^{-\beta G_0(h)} \langle e^{-\beta H} \rangle_{h,0} \\ &= N \int dm e^{Nh_{\text{ext}} m} \int_{h_{\text{ext}}-i\infty}^{h_{\text{ext}}+i\infty} \frac{dh}{2\pi i} e^{-Nm h} e^{-\beta G(h)} = N \int dm e^{Nh_{\text{ext}} m} e^{-\beta F(m)} \\ &= e^{Nh_{\text{ext}} m^*(h_{\text{ext}}) - \beta F(m^*(h_{\text{ext}}))} \end{aligned} \quad (\text{IV.17})$$

In the 3rd equation we introduced

$$-\beta G_0(h) = N \ln \text{Tr}_S e^{hS} \quad (\text{IV.18})$$

and an averaging defined by a non-interacting system,

$$\langle \dots \rangle_{h,0} = \frac{\prod_{i=1}^N \text{Tr}_{S_i} e^{hS_i} \dots}{\prod_{i=1}^N \text{Tr}_{S_i} e^{hS_i}} \quad (\text{IV.19})$$

The subscript $\langle \dots \rangle_{h,0}$ is meant to emphasize that the interaction is absent in this averaging. Note that in this averaging different spins are mutually indecent from each other. For instance we have,

$$\langle S_i S_j \rangle_{h,0} = \langle S_i \rangle_{h,0} \langle S_j \rangle_{h,0} \quad i \neq j \quad (\text{IV.20})$$

In the 4th equation we introduced

$$-\beta G(h) = -\beta G_0(h) + \ln \langle e^{-\beta H} \rangle_h. \quad (\text{IV.21})$$

The integration over h is done by the saddle point method assuming $N \gg 1$. Note that the saddle point method works if the susceptibility χ Eq. (IV.11) is positive (semi-)definite at around the saddle point h^* .³ In the 5th equation we performed the integration over m again by the saddle point method and used the Legendre transform Eq. (IV.9),

$$-\beta F(m) = -\beta G(h^*(m)) - N h^*(m)m \quad (\text{IV.22})$$

³ The integration variable may be changed to $t = i(h - h^*)$ around the saddle point h^* which presumably lies on the real h axis. Then along the t axis around $t = 0$ we find $(-\beta G)(h) - (-\beta G)(h^*) = (1/2)(-\beta G'')(h)(h - h^*)^2 = -(1/2)N\chi t^2 \leq 0$ as long as $\chi \geq 0$.

with $h^*(m)$ determined by Eq. (IV.10),

$$m = \frac{1}{N} \frac{\partial(-\beta G(h))}{\partial h} \Big|_{h=h^*(m)} = \frac{1}{N} \sum_{i=1}^N \langle S_i \rangle_{h=h^*(m)} \quad (\text{IV.23})$$

or

$$m = \langle S_i \rangle_{h=h^*(m)} \quad \forall i \quad (\text{IV.24})$$

since all spins are equivalent. Let us emphasize that here $\langle \dots \rangle_h$ is the averaging *in the presence of the interactions* so that it is different from $\langle \dots \rangle_{h,0}$ defined in Eq. (IV.19). The integration over m by the saddle point method works if the inverse of the susceptibility χ^{-1} Eq. (IV.14) is positive (semi-)definite at around the saddle point m^* . Here m^* is defined by Eq. (IV.13) with $h = h_{\text{ext}}$.

4. Plefka expansion

Now our task is to compute the free-energy $F(m)$ defined in Eq. (IV.9). To this end, we will follow the idea of Plefka expansion [36]. The computations presented in the following sections follow this strategy.

Suppose that the effect of the interactions between the spins S_i ($i = 1, 2, \dots, N$) can be treated perturbatively which enable the following decompositions,

$$F = F_0 + \lambda F_1 + \frac{\lambda^2}{2} F_2 \dots \quad G = G_0 + \lambda G_1 + \frac{\lambda^2}{2} G_2 + \dots \quad h = h_0 + \lambda h_1 + \frac{\lambda^2}{2} h_2 + \dots \quad (\text{IV.25})$$

Here the quantities with suffix 0 represent those which are present in the absence of interactions (like the ideal gas free-energy) and those with suffix 1, 2, ... represent those due to interactions. Here we omitted the higher-order terms. The parameter λ , which is introduced as a bookkeeping device to organize a perturbation theory, is put back to $\lambda = 1$ in the end.

The Legendre transform Eq. (IV.9) becomes, at $O(\lambda^0)$,

$$-\beta F_0(m) = -\beta G_0(h_0^*) - Nh_0^* m \quad (\text{IV.26})$$

where h_0^* is defined such that,

$$\frac{1}{N} \frac{\partial}{\partial h} (-\beta G_0(h)) \Big|_{h=h_0^*(m)} = m = \frac{1}{N} \sum_{i=1}^N \langle S_i \rangle_{h=h_0^*(m)}. \quad (\text{IV.27})$$

The latter implies

$$\langle S_i \rangle_{h=h_0^*(m)} = m \quad \forall i \quad (\text{IV.28})$$

Since all spins are equivalent in the averaging Eq. (IV.19).

Then at $O(\lambda)$ we find,

$$-\beta F_1(m) = -\beta G_1(h_0^*(m)) + \frac{\partial}{\partial h} (-\beta G_0(h)) \Big|_{h=h_0^*(m)} h_1^* - Nh_1^* m = -\beta G_1(h_0^*(m)) \quad (\text{IV.29})$$

In the 2nd equation we used Eq. (IV.27). Minimization of the free-energy $F(m)$ (see Eq. (IV.13) with $h = 0$) implies $h_0^* = -\lambda h_1^*$ up to this order.

If higher order terms $O(\lambda^2)$ in the expansion Eq. (VI.46) vanish (which happens in our cases as we see below), the treatment described above become exact resulting in a free-energy function $F(m)$, bringing back back $\lambda = 1$,

$$-\beta F(m) = -\beta F_0(m) - \beta F_1(m) = -\beta G_0(h_0^*(m)) - Nh_0^*(m)m - \beta G_1(h_0^*(m)) \quad (\text{IV.30})$$

with $h_0^*(m)$ determined by Eq. (IV.27). We call $F_0(m)$ as the entropic part of the free-energy and $F_1(m)$ as the interaction part of the free-energy.

5. Higher order terms

At 2nd order we find

$$\begin{aligned} -F_2(m) &= -G_2(h_0^*) - 2G'_1(h_0^*)h_1^* - G'_0(h_0^*)h_2^* - G''_0(h_0^*)(h_1^*)^2 - Nh_2^*m \\ &= -G_2(h_0^*) - 2G'_1(h_0^*)h_1^* - G''_0(h_0^*)(h_1^*)^2 \\ &= -G_2(h_0^*) + \frac{(G'_1(h_0^*))^2}{G''_0(h_0^*)} \end{aligned} \quad (\text{IV.31})$$

The 2nd line is due to Eq. (IV.27). To derive the last line we used,

$$h_1^* = -\frac{G'_1(h_0^*)}{G''_0(h_0^*)} \quad (\text{IV.32})$$

which is obtained as follows. First we expand Eq. (IV.10) as,

$$-Nm = G'(h)|_{h=h^*} = G'_0(h_0^*) + \lambda(G'_1(h_0^*) + G''_0(h_0^*)h_1^*) + O(\lambda^2). \quad (\text{IV.33})$$

Then using Eq. (IV.27) in the last equation we obtain Eq. (IV.32).

6. Cumulant expansion

The effect of interactions in the free-energy $G(h)$ Eq. (IV.21) can be analyzed by the cumulant expansion,

$$\ln\langle e^{-\lambda\beta H}\rangle_{h,0} = \lambda\langle(-\beta H)\rangle_{h,0} + \frac{\lambda^2}{2} \left(\langle(\beta H)^2\rangle_{h,0} - \langle(\beta H)\rangle_{h,0}^2 \right) + \dots \quad (\text{IV.34})$$

Here the averaging $\langle \dots \rangle_{h,0}$ is the averaging in the absence of the interactions (see Eq. (IV.19)). Remember that the spins are independent from each other in the evaluation of $\langle \dots \rangle_{h,0}$ Eq. (IV.19). This procedure will allow us to obtain the Plefka expansion of the free-energy $G(h)$ as $G(h) = G_0(h) + \lambda G_1 h + \frac{\lambda^2}{2} G_2(h) + \dots$. Subsequently we construct the free-energy $F(m)$ as described above.

Luckily, we will see that in our mean-field ferromagnetic model, the expansion stops at the 1st order: the higher order terms become negligible in dense limit $c \rightarrow \infty$ (or $M \rightarrow \infty$ in vectorial version [15])). In this case the simple prescription described above will work.

C. Ising p -spin ferromagnetic model

Here let us consider specifically the ferromagnetic p -spin model Eq. (III.8),

$$H = -\frac{J}{\sqrt{c/\alpha}} \sum_{\blacksquare} \underbrace{\prod_{j \in \partial \blacksquare} S_j}_{p-\text{body}} \quad (\text{IV.35})$$

with Ising spins $S_i = \pm 1$. To study the ferromagnetic phase it is convenient to rescale the energy introducing J_0 such that,

$$J = \frac{J_0}{\sqrt{c/\alpha}} \quad (\text{IV.36})$$

1. Derivation of the free-energy function and the equation of states

For the Ising model we easily find,

$$-\beta G_0(h) = N \ln 2 \cosh(h) \quad (\text{IV.37})$$

from which we find $h_0^*(m)$ defined by Eq. (IV.27),

$$m = \tanh(h_0^*(m)) \quad (\text{IV.38})$$

Thus we find the entropic part of the free-energy as,

$$-\beta F_0(m)/N = \ln 2 \cosh(h) - mh \quad h = \tanh^{-1}(m) \quad (\text{IV.39})$$

Next we examine the cumulants Eq. (IV.34). The 1st cumulant is obtained as,

$$\lambda \langle (-\beta H) \rangle_{h,0} = (\beta J) \frac{1}{\sqrt{c/\alpha}} \sum_{\blacksquare} \left\langle \prod_{j \in \partial \blacksquare} S_j \right\rangle_{h,0} = \lambda (\beta J) \frac{1}{\sqrt{c/\alpha}} N_{\blacksquare} m^p = N \lambda \gamma(\beta J_0) m^p \quad (\text{IV.40})$$

Here we used the fact that spins are independent from each other in the evaluation of $\langle \dots \rangle_{h,0}$ Eq. (IV.19). Finally we used Eq. (III.2) which implies $N_{\blacksquare} = N \gamma(c/\alpha)$ and J_0 defined in Eq. (IV.36). This is the only contribution to $G_1(h)$.

Let us consider higher order terms. The 2nd cumulant which contributes to $G_2(h)$ reads as,

$$\lambda^2 \langle (-\beta H)^2 \rangle_{h,0} - \langle (-\beta H) \rangle_{h,0}^2 = \lambda^2 \frac{(\beta J)^2}{c/\alpha} \sum_{\blacksquare_1, \blacksquare_2} \left[\left\langle \prod_{k \in \partial \blacksquare_1} \prod_{l \in \partial \blacksquare_2} S_k S_l \right\rangle_{h,0} - \left\langle \prod_{k \in \partial \blacksquare_1} S_k \right\rangle_{h,0} \left\langle \prod_{l \in \partial \blacksquare_2} S_l \right\rangle_{h,0} \right] \quad (\text{IV.41})$$

We can summarize the contributions to higher order cumulants as follows.

- One contribution is due to terms with $\blacksquare_1 = \blacksquare_2 = \dots$. For instance at the 2nd order we have,

$$\lambda^2 \frac{(\beta J)^2}{c/\alpha} \sum_{\blacksquare_1, \blacksquare_2} \left\{ \delta_{\blacksquare_1, \blacksquare_2} \left[\langle S^2 \rangle_{h,0}^p - \langle S \rangle_{h,0}^{2p} \right] \right\} = \lambda^2 \frac{1}{c/\alpha} (\beta J_0)^2 N \gamma(1 - m^{2p}) \quad (\text{IV.42})$$

This contributes to $G_2(h)$. However it is smaller than the 1st cumulant by a factor of $O(1/c/\alpha)$ so that it can be neglected in the dense limit $c \rightarrow \infty$. One can easily see that analogous terms which appear in higher order cumulants and contribute to $G_3(h), G_4(h), \dots$ (which are not associated with loops discussed below) vanish more rapidly than Eq. (IV.41) in the dense limit $c \rightarrow \infty$.

- Another contribution into $G_2(h)$ is due to a connected diagram in which one spin is shared by two factor nodes. However it becomes eliminated in $F(m)$: one can check that its contribution in $F_2(m) = -G_2(h_0^*) + \frac{(G'_1(h_0^*))^2}{G''_o(h_0^*)}$ (see Eq. (IV.31)) vanishes because of the 2nd term. (see Fig. 52 in appendix L). This reflects a generic property of this kind of Legendre transformations which leave only one line irreducible or 1PI (one particle irreducible) diagrams, i. e. diagrams which consist of 'closed loops' (diagrams which cannot be disconnected by cutting one line) (see Chap 6.5 of [37] for a proof).
- Finally let us recall that our graphs are locally tree-like so that the closed loops mentioned above can be neglected (see sec. III A). It means contribution by loop diagrams in $F_2(m), F_3(m), F_4(m) \dots$ are absent in our case. For example, consider a loop diagram shown in Fig 11 which is for $p = 2$ model. It involves 3 interactions so that it carries a factor $(\beta J/(c/\alpha))^3$ and potentially relevant for $F_3(m)$. For a given node 0 (out of N possible nodes), there are c choices for i connected to 0 and $c - 1$ choices for j , different from i , connected to 0.
 - If the loop is part of a random graph with connectivity c , the probability that an arbitrary chosen remaining (unconnected) arm of i is connected to one of the remaining arm of j is $\sim (c - 1)/N$. Then the over-all contribution of this type of diagram is $(J/(c/\alpha))^3 \times c(c - 1) \times (c - 1)/N \sim J^3/N$ which vanishes in the limit $N \rightarrow \infty$. More generally the contribution of a diagram with l loops in a random graph will scale as c^k/N^l (with k being a certain exponent) which vanish in $N \rightarrow \infty$ limit.
 - If the graph is the globally coupled one, i and j are connected with probability 1. Then the over-all contribution of this type of diagram is $(J/(c/\alpha))^3 \times c(c - 1) \sim J^3/c$ where $c \propto N^{p-1}$. Thus the contribution still vanishes limit $N \rightarrow \infty$ because the coupling is sufficiently weak.

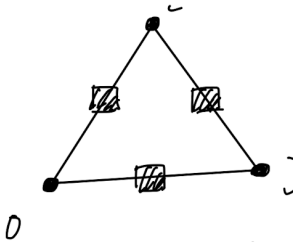


FIG. 11. A loop connecting 3 spins in $p = 2$ model

Thus we find the interaction part of the free-energy as,

$$-\beta F_1(m)/N = -\beta G_1(h_0^*(m))/N = \gamma(\beta J_0)m^p. \quad (\text{IV.43})$$

in the dense limit $c \rightarrow \infty$. This means the Plefka expansion stops at the 1st order in the present model.

To summarize we find the free-energy function as,

$$-\lim_{N \rightarrow \infty} \beta F(m)/N = -m \tanh^{-1}(m) + \ln 2 \cosh(\tanh^{-1}(m)) + \gamma(\beta J_0)m^p. \quad (\text{IV.44})$$

In the presence of an external field h_{ext} , the saddle point equation Eq. (IV.13) becomes

$$m = \tanh(Am^{p-1} + h_{\text{ext}}) \quad A = p\gamma(\beta J_0) \quad (\text{IV.45})$$

The stability of the solutions can be examined by,

$$\frac{1}{N} \frac{d^2 \beta F(m)}{dm^2} = \frac{1}{1-m^2} - p(p-1)\gamma(\beta J_0)m^{p-2} \quad (\text{IV.46})$$

which must be positive.

2. 2nd order transition: $p = 2$ case

Here we focus on the $p = 2$ case. The cases with $p > 2$ will be discussed in next.

For $h_{\text{ext}} = 0$, we find the paramagnetic solution $m = 0$ of Eq. (IV.45) always exists. However from Eq. (IV.46) we find it becomes unstable at low temperatures such that

$$1 - A < 0 \quad (\text{IV.47})$$

or

$$A > A_c \quad (\text{IV.48})$$

where A_c is a critical point defined by

$$A_c = 1. \quad (\text{IV.49})$$

In the case $p = 2$ the equation of state Eq. (IV.45) can be expanded in power series of m as,

$$m = \tanh(Am) = Am - \frac{A^3}{3}m^3 + \dots \quad (\text{IV.50})$$

We find the $|m| > 0$ solution,

$$m = \pm \sqrt{3(A - A_c)} \quad A > A_c, \quad (\text{IV.51})$$

which emerges continuously at the critical point found above. Clearly this indicates a 2nd order phase transition to the phases with broken symmetry. From Eq. (IV.46) we find, the paramagnetic solution $m = 0$ is stable only for $A < A_c$.

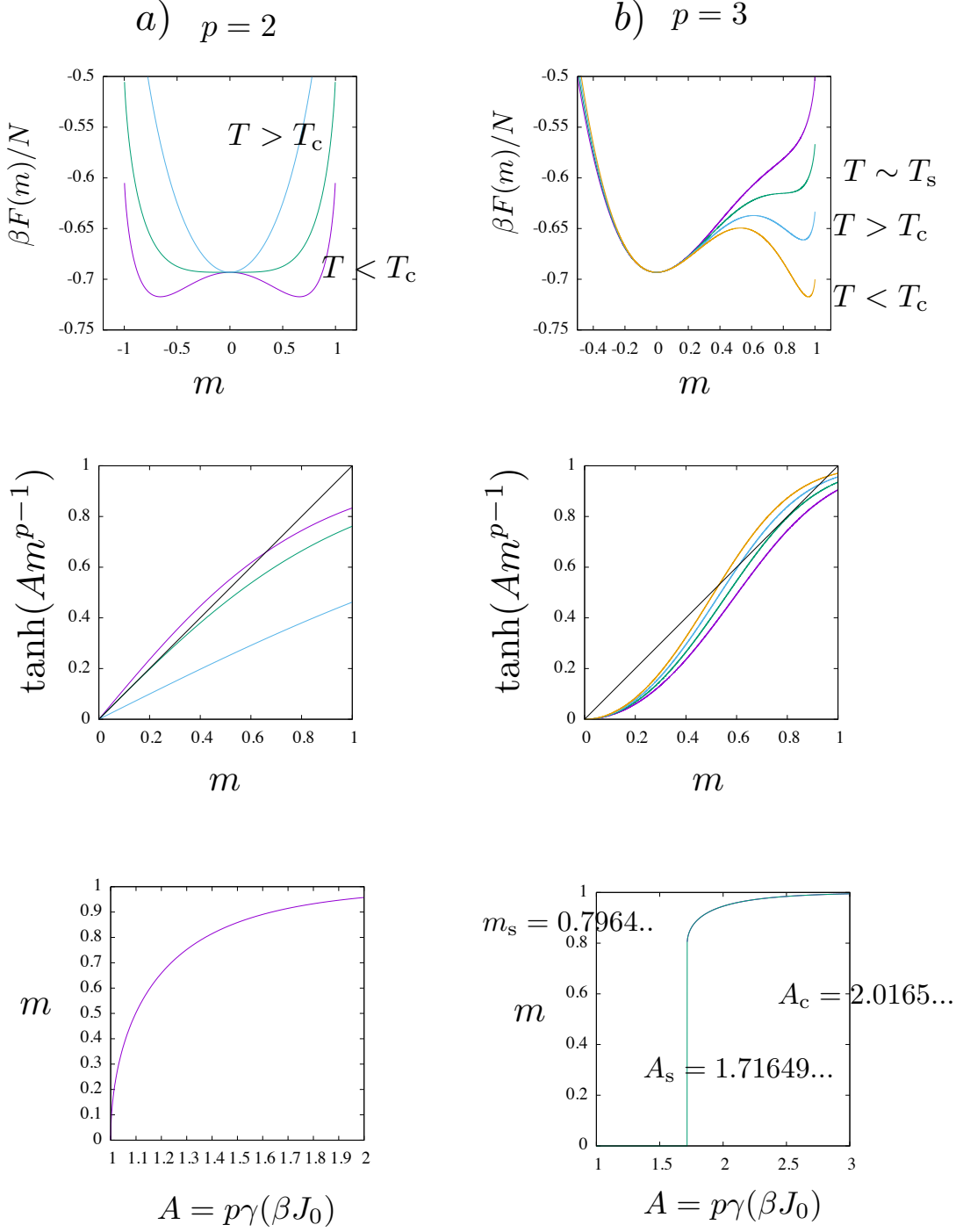


FIG. 12. Free-energy function and equation of state of the p -spin ferromagnets. In the case $p > 2$, the $m = 0$ solution (paramagnetic phase) remains as a metastable state down to $T = 0$ ($A = \infty$). In this $m = 0$ sector, we will look for glassy phases later. Contrarily, in the case $p = 2$, the $m = 0$ solution becomes unstable below the ferromagnetic transition temperature T_c . In this case we are forced to introduce strong quenched disorder to eliminate the ferromagnetic phase so that glass transitions become possible. (Note: this is the situation with the linear-potential Eq. (III.25). With non-linear potentials like the hardcore potential, Eq. (III.26) glassy phases can emerge even with $p = 2$ [15].)

In the presence of the external field h_{ext} we find,

$$m = Am + h_{\text{ext}} - \frac{A^3}{3}m^3 + \dots \quad (\text{IV.52})$$

which implies

$$m \sim \chi h \quad \chi = \frac{1}{(A_c - A)^\gamma} \quad \gamma = 1 \quad (\text{IV.53})$$

in the paramagnetic phase $A < A_c$. The linear susceptibility diverges approaching A_c with the critical exponent $\gamma = 1$. At the critical point $A = A_c$, one finds,

$$m \propto h_{\text{ext}}^{1/\delta} \quad \delta = 3 \quad (\text{IV.54})$$

with the critical exponent $\delta = 3$.

3. 1st order transition: $p > 2$ case

In the case $p > 2$ the paramagnetic solution $m = 0$, which always verifies the equation of state Eq. (IV.45), is always (meta) stable as can be seen from Eq. (IV.46). The situation is very different from the case $p = 2$. This means absence of the Kirkwood instability (instability toward crystallization) in this model. We will look for glassy states in this regime.

The ferromagnetic solution $|m| > 0$ emerges by a 1st order transition at A_c . The ferromagnetic solution has a spinodal point $A_s (< A_c)$ at which it disappears. Right at the spinodal point $A = A_s$, the $m > 0$ solution satisfies,

$$1 = \frac{d}{dm} \tanh(Am^{p-1}) = (1 - \tanh^2(Am^{p-1}))(p-1)Am^{p-2} = (1 - m^2)(p-1)Am^{p-2} \quad (\text{IV.55})$$

which means the stability condition Eq. (IV.46) is just marginally satisfied.

In the limit $p \rightarrow \infty$, we find only $m = 0$ and $m = 1$ are possible and they verify the saddle point equation at any finite temperatures because $A \rightarrow \infty$ as $p \rightarrow \infty$ and both of them are (meta) stable.⁴ The free-energy of the paramagnetic state $m = 0$ and the ferromagnetic state are found as

$$-\beta F(0)/N = \ln 2 \quad -\beta F(1)/N = \gamma(\beta J_0) \quad (\text{IV.56})$$

Thus the 1st order transition takes place at $\beta_c J_0 = \ln 2/\gamma$.

D. Scalar spherical p -spin ferromagnetic model

Now we consider again the ferromagnetic p -spin model Eq. (III.8) but with scalar spherical spins Eq. (III.7) normalized such that $\sum_{i=1}^N S_i^2 = N$.

In this case we have

$$\begin{aligned} \prod_{i=1}^N \text{Tr}_{S_i} \dots &= \int \prod_{i=1}^N dS_i \delta \left(N - \sum_{i=1}^N S_i^2 \right) \dots = \int \prod_{i=1}^N dS_i N \int_{-i\infty}^{i\infty} \frac{d\Lambda}{2\pi i} e^{\Lambda(N - \sum_{i=1}^N S_i^2)} \dots \\ &= N \int_{-i\infty}^{i\infty} \frac{d\Lambda}{2\pi i} e^{\Lambda N} \prod_{i=1}^N \left[\int dS_i e^{-\Lambda S_i^2 + h S_i} \right] \dots \end{aligned} \quad (\text{IV.57})$$

so that we find

$$\begin{aligned} -\beta N G_0(h) &= \ln N \int_{-i\infty}^{i\infty} \frac{d\Lambda}{2\pi i} e^{\Lambda N} \left[\int dS e^{-\Lambda S^2 + h S} \right]^N = \ln N \int_{-i\infty}^{i\infty} \frac{d\Lambda}{2\pi i} \exp \left[\frac{h^2}{4\Lambda} - \frac{1}{2} \ln \frac{\Lambda}{\pi} + \Lambda \right]^N \\ &\simeq N \left[\frac{h^2}{4\Lambda_*} - \frac{1}{2} \ln \frac{\Lambda_*}{\pi} + \Lambda_* \right] \end{aligned} \quad (\text{IV.58})$$

⁴ Concerning the ferromagnetic solution, we have $m \sim 1 - 2e^{-Am^{p-1}}$. Then we find $d^2 F(m)/dm^2 \sim 4e^{2A} \rightarrow +\infty$ as $A \rightarrow \infty$.

where we dropped sub-leading terms. The Gaussian integration over S is performed assuming $\text{Re}(\Lambda) > 0$ along the integration path of λ . The integration over Λ is performed by saddle point method with the saddle point $\Lambda_* = \Lambda_*(h)$ given by

$$0 = -\frac{h^2}{4\Lambda_*^2} - \frac{1}{2\Lambda_*} + 1 \quad \text{or} \quad \Lambda_* = \frac{1 + \sqrt{1 + h^2}}{2} \quad (\text{IV.59})$$

In the latter we choose the solution with $\Lambda_* > 0$. On the other hand, $h_0^*(m)$ defined by Eq. (IV.27) is obtained as

$$m = \frac{\int dS S e^{-\Lambda_* S^2 + h_0^* S}}{\int dS e^{-\Lambda_* S^2 + h_0^* S}} = \frac{h_0^*}{2\Lambda_*^2} \quad (\text{IV.60})$$

Thus we find the entropic part of the free-energy as,

$$-\beta F_0(m)/N = -\beta G_0(h_0^*) - h_0^* m = \frac{1}{2} + \frac{1}{2} \ln(2\pi(1 - m^2)) \quad (\text{IV.61})$$

Apparently the interaction part of the free-energy is the same as the Ising case. Thus we obtain the free-energy as,

$$-\lim_{N \rightarrow \infty} \beta F(m)/N = \frac{1}{2} + \frac{1}{2} \ln(2\pi(1 - m^2)) + \gamma(\beta J_0)m^p. \quad (\text{IV.62})$$

In the presence of an external field h_{ext} , the saddle point equation Eq. (IV.13) becomes,

$$0 = m \left(-\frac{1}{1 - m^2} + \beta p \gamma(\beta J_0) m^{p-2} \right) + h_{\text{ext}} \quad (\text{IV.63})$$

The stability of the solutions can be examined by,

$$\frac{1}{N} \frac{d^2 \beta F(m)}{dm^2} = \frac{1 + m^2}{1 - m^2} - p(p - 1)\gamma(\beta J_0)m^{p-2} \quad (\text{IV.64})$$

which must be positive.

The behaviour of the system is qualitatively the same as the Ising case: 1) 2nd order phase transition in $p = 2$ case and 2) 1st order phase transitions for $p > 2$. In particular we note that the supercooled paramagnetic phase $m = 0$ remains (meta)stable at all temperatures.

V. SIMPLEST GLASS MODEL : RANDOM ENERGY MODEL (REM)

A. Random energy levels in the $p = \infty$ ferromagnetic Ising model

Here we show that the spectrum energy of the ferromagnetic Ising p -spin model Eq. (III.8) with the *dense coupling* is that of the random energy model (REM)[38]. Here we perform the same kind of analysis as done by Derrida [38] for the p -spin Ising *spin-glass model with strong quenched disorder* (see sec. III A) but on the purely ferromagnetic model.

First let us examine the distribution function of the energy among different configurations. As shown below, it is found to be a Gaussian distribution.

$$\begin{aligned} P(E) &= \left\langle \delta \left(E + \frac{J}{\sqrt{c/\alpha}} \sum_{\blacksquare} \prod_{j \in \partial \blacksquare} S_j \right) \right\rangle_S = \int \frac{d\kappa}{2\pi} e^{i\kappa E} \left\langle e^{i\kappa \frac{J}{\sqrt{c/\alpha}} \sum_{\blacksquare} \prod_{j \in \partial \blacksquare} S_j} \right\rangle_S \\ &= \int \frac{d\kappa}{2\pi} e^{i\kappa E - \frac{\kappa^2}{2} \gamma J^2 N} = \frac{e^{-\frac{E^2}{2\gamma N J^2}}}{\sqrt{2\pi\gamma N J^2}} \end{aligned} \quad (\text{V.1})$$

where we introduced

$$\langle \dots \rangle_S = \frac{\prod_{i=1}^N \sum_{S_i=\pm 1} \dots}{2^N} \quad (\text{V.2})$$

To derive the above result we evaluated the cumulant expansion,

$$\begin{aligned} \ln \left\langle e^{i\kappa \frac{J}{\sqrt{c/\alpha}} \sum_{\blacksquare} \prod_{j \in \partial \blacksquare} S_j} \right\rangle_S &= i\kappa \sum_{\blacksquare} \frac{J}{\sqrt{c/\alpha}} \left\langle \prod_{j \in \partial \blacksquare} S_j \right\rangle_S - \frac{\kappa^2}{2} \frac{J^2}{c/\alpha} \sum_{\blacksquare_1, \blacksquare_2} \left\langle \prod_{j \in \partial \blacksquare_1} \prod_{k \in \partial \blacksquare_2} S_j S_k \right\rangle_S^c \\ &\quad + \frac{\kappa^4}{3!} \frac{J^3}{(c/\alpha)^{3/2}} \sum_{\blacksquare_1, \blacksquare_2, \blacksquare_3} \left\langle \prod_{j_1 \in \partial \blacksquare_1} \prod_{j_2 \in \partial \blacksquare_2} \prod_{j_3 \in \partial \blacksquare_3} S_{j_1} S_{j_2} S_{j_3} \right\rangle_S^c + \dots \\ &= -\frac{\kappa^2}{2} \frac{J^2}{c/\alpha} \sum_{\blacksquare_1, \blacksquare_2} \delta_{\blacksquare_1, \blacksquare_2} + \frac{\kappa^4}{4!} \frac{J^4}{(c/\alpha)^2} \sum_{\blacksquare_1, \blacksquare_2, \blacksquare_3, \blacksquare_4} \delta_{\blacksquare_1, \blacksquare_2} \delta_{\blacksquare_2, \blacksquare_3} \delta_{\blacksquare_3, \blacksquare_4} + \dots \\ &= -\frac{\kappa^2}{2} \gamma J^2 N + \frac{\kappa^4}{4!} \gamma J^4 \frac{N}{c/\alpha} + \dots + \dots + \text{“loop corrections”} \end{aligned} \quad (\text{V.3})$$

where $\langle \dots \rangle^c$ represents a connected correlation function, e.g.

$$\left\langle \prod_{j_1 \in \partial \blacksquare_1} \prod_{j_2 \in \partial \blacksquare_2} S_{j_1} S_{j_2} \right\rangle_S^c = \left\langle \prod_{j_1 \in \partial \blacksquare_1} \prod_{j_2 \in \partial \blacksquare_2} S_{j_1} S_{j_2} \right\rangle_S - \left\langle \prod_{j_1 \in \partial \blacksquare_1} S_{j_1} \right\rangle_S \left\langle \prod_{j_2 \in \partial \blacksquare_2} S_{j_2} \right\rangle_S \quad (\text{V.4})$$

Here we used $N_{\blacksquare} = \gamma N(c/\alpha)$ (see Eq. (III.2)).

Remaining possible contributions to the expansion are those associated with loops. *Here it is crucial to recall that our graphs are locally tree-like and closed loops can be neglected.* (see sec. III A). For example, Fig. 11 shows a loop for $p = 2$ model which consists of 3 interactions so that it carries a factor $(J/\sqrt{c/\alpha})^3$. For a given node 0 (out of N possible nodes), there are c choices for i connected to 0 and $c - 1$ choices for j , different from i , connected to 0.

- If the loop is part of a random graph, the probability that an arbitrary chosen remaining (unconnected) arm of i is connected to one of the remaining arm of j is $\sim (c - 1)/N$. Then the over-all contribution of this type of diagram is $(J/\sqrt{c/\alpha})^3 \times c(c - 1) \times (c - 1)/N \sim J^3 c^{3/2}/N$ which vanishes in the limit $N \rightarrow \infty$. More generally the contribution of a diagram with l loops in a random graph will scale as c^k/N^l , with k being a certain integer, which vanish in $N \rightarrow \infty$ limit. (In a $p = 2$ system with finite N spins, the maximum length of a single loop L_{\max} is estimated as $(c - 1)^{L_{\max}} \sim N$. Such a loop will make a contribution of order $c^k/N \sim \sqrt{N}/N \sim 1/\sqrt{N}$ which vanishes in $N \rightarrow \infty$.)
- If the graph is the globally coupled one, i and j are connected with probability 1. Then the over-all contribution of this type of diagram is $(J/\sqrt{c/\alpha})^3 \times c(c - 1) \sim J^3 c^{1/2}$ where $c \propto N^{p-1}$. Thus the contribution cannot be neglected. Globally coupled ferromagnetic model is quite different in this respect.

- Consider the conventional globally coupled mean-field spin-glass model discussed in sec. III B. If ξ_{\square} 's follow the Gaussian distribution Eq. (III.10), then averaging over ξ_{\square} 's higher order cumulants disappear. This is the analysis done by Derrida [38]. [Q] For the case of $\pm J$?

One can do the exactly same analysis for p-spin *spin-glass* model (with strong quenched disorder) with global coupling (see III B) and find exactly the same result. Note that in the original paper [38] which considered the p-spin spin-glass model with the global coupling the *energy fluctuation of a fixed spin configuration $\{S_i\}$ among different realization of the quenched disorder $P(E)$* was studied. It turned out that the energy distribution do not depend on the choice of the spin configuration $\{S_i\}$. The resultant energy distribution is formally the same as the one obtained above.

Next let us examine the distribution of the energies E_1 and E_2 associated with two different states (S_1, S_2, \dots, S_N) and $(S'_1, S'_2, \dots, S'_N)$ which have mutual overlap $q = (1/N) \sum_{i=1}^N S_i S'_i$. Suppose that we choose S_1 arbitrarily. Then construct S_2 by flipping some fraction of S_1 (following some, say deterministic, rule) such that their mutual overlap is q .

[Exercise]

$$P(E_1, E_2; q) \xrightarrow{p \rightarrow \infty} P(E_1)P(E_2) \quad \text{for} \quad 0 \leq |q| < 1 \quad (\text{V.5})$$

holds.

Similarly it is easy to find,

$$P(q) = \langle \langle \delta(Nq - \sum_{i=1}^N S_i S'_i) \rangle \rangle_{S'} \xrightarrow{N \rightarrow \infty} \delta(q) \quad \text{for} \quad 0 \leq |q| < 1 \quad (\text{V.6})$$

(Hint: Appendix H)

[Exercise] Show also that simultaneous distribution of the energy and magnetization $M = \sum_{i=1}^N S_i$ is

$$P(E, M) = \frac{e^{-\frac{E^2}{2\gamma N J^2}}}{\sqrt{2\pi\gamma N J^2}} \frac{e^{-\frac{M^2}{2N}}}{\sqrt{2\pi N}} \quad (\text{V.7})$$

B. Analysis of REM

In the random energy model (REM), the energies $E_\alpha = NJe_\alpha$ associated with the microscopic states $\alpha = 1, 2, \dots, 2^N$ are drawn from the Gaussian distribution,

$$P(E) = \frac{1}{\sqrt{2\gamma\pi N J^2}} e^{-\frac{E^2}{2\gamma N J^2}} \quad (\text{V.8})$$

independently from each other. Introducing dimension-less energy $e_\alpha = E_\alpha/(NJ)$ we find its distribution as

$$p(e) = \frac{1}{\sqrt{2\gamma\pi N}} e^{-\frac{Ne^2}{2\gamma}} \quad (\text{V.9})$$

1. Thermodynamics

The partition function of REM is obtained as,

$$Z = \sum_{\alpha=1}^{2^N} e^{-N\beta J e_\alpha} = \int de e^{N(\Sigma(e) - (\beta J)e)} \sim e^{N(\Sigma(e^*) - (\beta J)e^*)} \quad (\text{V.10})$$

thus we find

$$-\beta F/N = \ln Z = \Sigma(e^*) - (\beta J)e^* \quad (\text{V.11})$$

where we introduced the entropy (per spin), which is called as structural entropy of complexity in glass physics,

$$\Sigma(e) = \frac{1}{N} \ln \sum_{\alpha} \delta(e - e_{\alpha}) = \frac{1}{N} \ln (2^N p(e)) \sim \ln 2 - \frac{e^2}{2\gamma} \quad (\text{V.12})$$

We find the complexity is positive in the range $e_{\min} < e < e_{\max}$ with

$$e_{\min} = -\sqrt{2\gamma \ln 2} \quad e_{\max} = \sqrt{2\gamma \ln 2} \quad (\text{V.13})$$

The saddle point e^* is given by,

$$\beta J = \left. \frac{d\Sigma(e)}{de} \right|_{e=e^*(T)} = -\frac{e^*(T)}{\gamma} \quad (\text{V.14})$$

which yields,

$$e^*(T) = -\gamma\beta J. \quad (\text{V.15})$$

We find a critical temperature T_K such that

$$e^*(T_K) = e_{\min} = -\sqrt{2\gamma \ln 2} \quad (\text{V.16})$$

or

$$k_B T_K = J \sqrt{\frac{\gamma}{2 \ln 2}} \quad (\text{V.17})$$

at which the complexity vanishes

$$\Sigma(e^*(T_K)) = 0 \quad (\text{V.18})$$

The free-energy is obtained for $T > T_K$ as

$$-\beta F/N = \ln 2 - \frac{e(T)^2}{2\gamma} - (\beta J)e(T) = \ln 2 + \frac{\gamma}{2}(\beta J)^2 \quad (\text{V.19})$$

and for $T < T_K$,

$$-\beta F/N = -\beta J e_{\min}. \quad (\text{V.20})$$

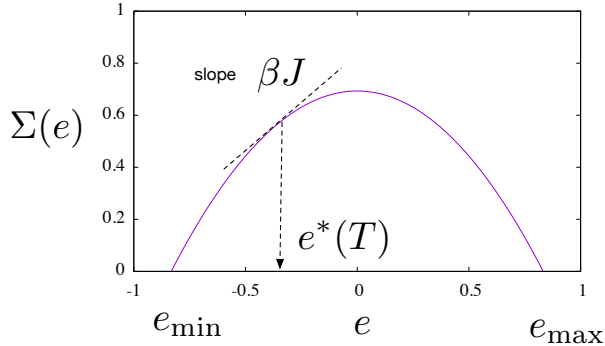
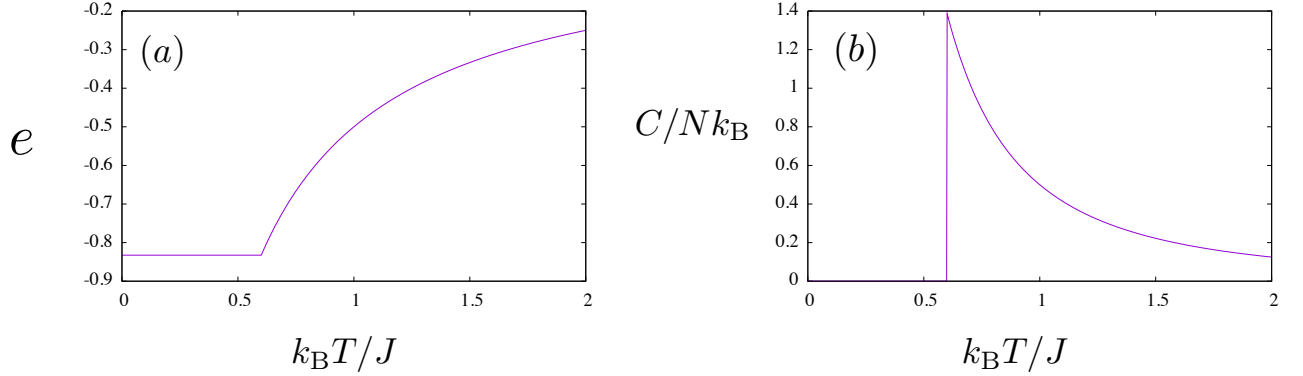


FIG. 13. Complexity of REM ($\gamma = 1/2$)

We can also study thermodynamics of the system in the presence of uniform external magnetic field. In the presence of external magnetic field h , the energy of α th state becomes

$$E_{\alpha} \rightarrow E_{\alpha} - hM_{\alpha} \quad (\text{V.21})$$

FIG. 14. Thermodynamics of REM ($\gamma = 1/2$)

where M_α is the magnetization. To study the thermodynamics of the system it is convenient to introduce a *generalized complexity* [39, 40] as follows. From the simultaneous distribution Eq. (V.7) of the energy and magnetization, we find that the magnetization M_α follows a Gaussian distribution which is decoupled with the energy. Introducing $m_\alpha = M_\alpha/N$, one can naturally define generalized complexity $\Sigma(e, m)$ [39, 40] which is obtained as,

$$\Sigma(e, m) = \ln 2 - \frac{e^2}{2\gamma} - \frac{m^2}{2}. \quad (\text{V.22})$$

Here e refers to the dimension-less energy (per spin) due to the ferromagnetic interaction.

[Exercize] Study magnetic response of the system above and below T_K .

2. Fluctuations below T_K

In the random energy model, the energies $E_\alpha = NJe_\alpha$ associated with the microscopic states $\alpha = 1, 2, \dots, 2^N$ are drawn from the Gaussian distribution Eq. (V.8) independently from each other. As the result the distribution of the energy in the system can be expressed using the complexity $\Sigma(e)$. Let us focus on the distribution of the low lying states. We find the distribution of the shifted energy

$$\hat{E} = NJ(e - e_{\min}) \quad (\text{V.23})$$

as

$$p(\hat{E}) = e^{N\Sigma(e)} \simeq A(\kappa)e^{\kappa\hat{E}} \quad (\text{V.24})$$

with

$$\kappa = -\frac{e_{\min}}{\gamma J} = \frac{1}{k_B T_K} = \beta_K, \quad (\text{V.25})$$

which follows from Eq. (V.17) and $A(\kappa)$ being a normalization constant. Thus concerning the low lying states, we can assume that their energy follows the exponential distribution [41].

[Note: the energy levels of the system Eq. (III.8) with the Ising spins $S_i = \pm 1$ are discretized if the connectivity c is finite. Only in the $c \rightarrow \infty$ limit, it becomes continuous.]

Using this, we can perform low temperature expansion to study the behavior of the system in the glass phase $T < T_K$. See appendix sec. I.

C. Stability against crystallization

So far we considered realization of a glass phase in the super-cooled paramagnetic phase $m = 0$. Let us discuss here possible instability of the paramagnetic phase toward ferromagnetism (crystallization) $m > 0$. As we discussed

in sec. IV C 3, the paramagnetic $m = 0$ solution remains locally stable (meta-stable) down to 0 temperature. But what about the possibility of some activated processes by which the system escapes the $m = 0$ state and reach the ferromagnetic state? The time τ needed for such an activated process will be

$$\tau = \tau_0 e^{\beta \Delta F} \quad (\text{V.26})$$

where ΔF is the energy barrier. In present the model, which is a mean-field model, the energy barrier for an activation process from the $m = 0$ state to the ferromagnetic state $m > 0$ is given by,

$$\beta \Delta F = \beta F(m_{\max}) - \beta F(0) \quad (\text{V.27})$$

where m_{\max} is the magnetization where the free-energy function $F(m)$ (see Eq. (IV.44)) becomes locally maximum between the $m = 0$ and $m > 0$ minima (see Fig. 12 b) top panel). As such, the magnetization m_{\max} has to obey the saddle point equation Eq. (IV.45). This corresponds to the lower $m > 0$ crossing point between the strait line and the $\tanh(Am^{p-1})$ curve shown in Fig. 12 b) central panel).

Let us recall that the natural energy scale for the ferromagnetism J_0 is related to that for the glass J as $J_0 = \sqrt{c/\alpha}J$ (see Eq. (IV.36)). In other words, working at the natural temperatures for the glass $\beta J \sim O(1)$ means working at extremely low temperatures for the ferromagnetism $\beta J_0 = \sqrt{c/\alpha}\beta J \gg 1$ in the dense limit $c \rightarrow \infty$. At such low temperatures m_{\max} becomes very small. For very small m , the saddle point equation Eq. (IV.45) becomes simplified as,

$$m = Am^{p-1} + O(m^{3(p-1)}) \quad (\text{V.28})$$

from which we find

$$m_{\max} \simeq A^{-1/(p-2)} \quad A = p\gamma(\beta J_0) \quad (\text{V.29})$$

On the other hand, Eq. (IV.44) can be expanded as

$$-\beta F(m) = \ln 2 - \frac{1}{2}m^2 + O(m^4) \quad (\text{V.30})$$

so that we obtain, assuming $\beta J = O(1)$,

$$\beta \Delta F \simeq \frac{N}{2}m_{\max}^2 \sim Nc^{-\frac{1}{p-2}} \quad (\text{V.31})$$

From the above result we realize that we can indeed prohibit the activated process by taking $N \rightarrow \infty$ limit *before* $c \rightarrow \infty$ limit. However in the case of the global coupling $c \sim O(N^{p-1})$ (see Eq. (III.14)) we find $\beta \Delta F \propto N^{-\frac{1}{p-2}}$ so that the energy barrier vanishes! This means we cannot realize the desired super-cooled paramagnetic phase with the global coupling.

D. Shuffling of energy levels induced by random pinning fields

Here let us discuss effects of random pinning fields. We consider the ferromagnetic p -spin model Eq. (III.8),

$$H = -\frac{J}{\sqrt{c/\alpha}} \sum_{\blacksquare} \underbrace{\prod_{j \in \partial \blacksquare} S_j}_{p\text{-body}} - \sum_{i=1}^N h_i S_i \quad (\text{V.32})$$

Here h_i is a quenched random pinning fields with a Gaussian distribution of zero mean and variance,

$$\overline{h_i}^h = 0 \quad \overline{h_i h_j}^h = 2\epsilon\delta_{ij}. \quad (\text{V.33})$$

Here $\overline{\dots}^h$ represents the average over different realizations of the quenched random field.

We find the energy distribution Eq. (V.1) becomes modified as,

$$\overline{P(E)}^h = \frac{e^{-\frac{E^2}{2N(\gamma J^2 + 2\epsilon)}}}{\sqrt{2\pi N(\gamma J^2 + 2\epsilon)}} \quad (\text{V.34})$$

We see that the effect of the pinning is just some increase of the variance of the state-to-state energy fluctuation. Similarly we find again Eq. (V.5) in the $p \rightarrow \infty$ limit,

$$\overline{P(E_1, E_2, q)}^h \xrightarrow{p \rightarrow \infty} \overline{P(E_1)}^h \overline{P(E_2)}^h \quad \text{for} \quad 0 \leq |q| < 1 \quad (\text{V.35})$$

The above observations suggests the random pinning field do not change the basic thermodynamic properties of the unperturbed disorder-free system. We emphasize that REM is realized in the absence of the random pinning field. However the following observations suggest interesting consequences of radom pinning.

- **Static chaos effect:** the radom pinning field will induce crossings of the low lying states discussed in (see [VB 2](#) and appendix sec. [I](#)) leading to complete reshuffling of the low lysing states in $N/N(\epsilon) \rightarrow \infty$ limit with $N(\epsilon) \propto 1/\epsilon^2$ [39, 40] for arbitraly small but finite strength of the pinning field ϵ at low temperatures $0 < T < T_K$. Consder two systems a and b which are subjected to different realizations of the pinning fields h_i^a and h_i^b $i = 1, 2, \dots, N$ which are uncorrelated. Because of the reshuffling menthioned above, the low lying states of the two systems become totally uncorrelated in $N/N(\epsilon) \rightarrow \infty$ limit for arbitraly small ϵ . Thus $N \rightarrow \infty$ limit and $\epsilon \rightarrow 0$ limit do not commute below T_K .
- **Sample-to-sample fluctuation:** Thus different realizations of the pinning field will result in totally different glasses in $N/N(\epsilon) \rightarrow \infty$ limit for arbitraly small ϵ . In this limit, one may be interested to consider glass-to-glass or sample-to-sample fluctuations of thermodynamic quantities.
 - See sec [VIA 3](#) and sec [VIA 5](#) for related discussions.
 - Addition of weak queched randomness in the interaction Eq. ([III.11](#)) will induce similar effect (chaos effect and sample-to-sample fluctuations).
 - Actually even *uniform* external field h will induce level crossings, i.e. static chaos effect. Using the generalized complexity Eq. ([V.22](#)) one can analyze the static chaos effect [39, 40]. There one finds $N(h) \sim 1/h^2$.
 - In the case of the glasses of spheres (see [III](#)), one can consider *shear* (see [XIII F](#)) as a natural protocol to induce shuffling of the states [42, 43] much as done by the external magnetic field h in the spin system.

VI. REPLICATED SPIN SYSTEM

A. Basic phenomenology

We may imagine a putative free-energy landscape of glassy systems as Fig. 15F with multiple local minima. The horizontal axis is labeled as 'configurational space' which is somewhat obscure (the real configurational space is extremely high dimensional space). Later we will see a concrete example: such glassy states emerge in the supercooled paramagnetic state of the p -spin ferromagnetic model with $p > 2$ [15, 44]. Indeed we have already found the random energy model (REM) in $p \rightarrow \infty$ limit. One can also add quenched disorder. With strong enough quenched disorder, one can realize glassy states also with $p = 2$, i. e. the Edwards-Anderson spinglass model including the SK model.

How can we detect that the free-energy landscape has multiple local minima? The counter part is that of crystalline state which is unique, up to some degeneracies due to global symmetries, as shown in Fig. 10. In sharp contrast to such crystalline states, there may be no simple ways to describe the real space configurations of the system in the local minima. The system would look just as disordered as a typical configuration in the liquid state.

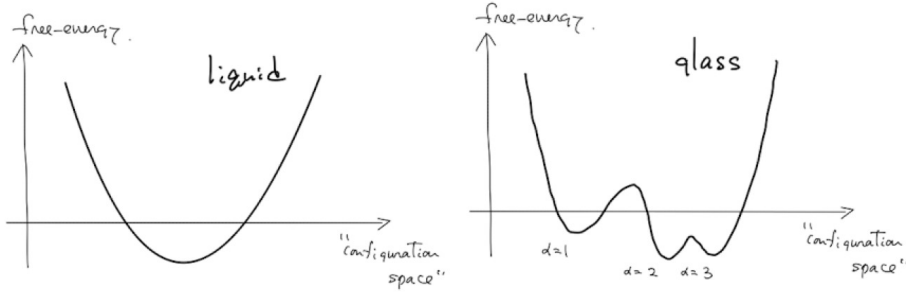


FIG. 15. Schematic free-energy landscape of a glassy system

The powerful theoretical tool is replicas, copies of the same system. For simplicity, suppose that we have a generic system which consists of N degrees of freedom $\{S\} = (S_1, S_2, \dots, S_N)$ whose Hamiltonian is $H[\{S\}]$, which can be with/without the quenched disorder. Let us introduce n replicas $a = 1, 2, \dots, n$ and a replicated Hamiltonian,

$$-\beta H_n[\hat{\epsilon}] = -\beta \sum_{a=1}^n H[\{S_i^a\}] + \sum_{a < b} \epsilon_{ab} \sum_{i=1}^N S_i^a S_i^b. \quad (\text{VI.1})$$

Here we introduced the 2nd term on the r.h.s. which represents an artificial attractive coupling $\epsilon_{ab} > 0$ between replicas. The field ϵ_{ab} explicitly breaks the replica symmetry, i.e. the permutation symmetry of replica index. This allows us to evaluate the overlap between the replicas,

$$q_{ab} = \frac{1}{N} \sum_{i=1}^N \langle S_i^a S_i^b \rangle_\epsilon \quad (\text{VI.2})$$

We are interested with,

$$\lim_{\hat{\epsilon} \rightarrow 0} \lim_{N \rightarrow \infty} q_{ab} \quad (\text{VI.3})$$

and consider that this is the glass order parameter of the system. This is the idea of explicit replica symmetry breaking (RSB) by Parisi and Virasoro [45]. Similarly to the magnetic field h for magnetization in ferromagnetic systems, the field ϵ_{ab} is conjugated to the glass order parameter q_{ab} .

This field ϵ_{ab} have the following two major roles to detect the presence of multiple free-energy minima as shown in Fig. 15.

- Detection of ergodicity breaking
- Detection of replica symmetry (or permutation symmetry) breaking

1. Ergodicity breaking

For simplicity, let us assume the simplest (replica symmetric) form

$$\epsilon_{ab} = \epsilon \quad a \neq b. \quad (\text{VI.4})$$

in the following. With an attractive coupling $\epsilon > 0$ we may be able to force the two replicas a and b to stay in the same metastable state. By taking the thermodynamic limit $N \rightarrow \infty$, the barriers separating the minima may diverge, i.e. ergodicity breaking. Then by switching off the attractive coupling $\epsilon \rightarrow 0^+$, the two replica may remain stuck in the same metastable state. This should happen in a glassy phase. In this case we will find,

$$q_{\text{EA}} = \lim_{\epsilon \rightarrow 0} \lim_{N \rightarrow \infty} q_{ab} > 0. \quad (\text{VI.5})$$

This is the so called Edwards-Anderson (EA) order parameter [21]. On the other hand, in the liquid phase, the barriers separating the minima should remain finite even by taking $N \rightarrow \infty$. Then by sending $\epsilon \rightarrow 0^+$, the two replica will restart to explore the phase space freely moving away from each other. Typical configurations in different minima have zero-mutual overlap so that we will observe $\lim_{\epsilon \rightarrow 0} \lim_{N \rightarrow \infty} q_{ab} = 0$ in this case. Thus the two limits $\lim_{\epsilon \rightarrow 0}$ and $\lim_{N \rightarrow \infty}$ commute in the liquid phase but do not commute in the glass phase reflecting the ergodicity breaking.

The original idea of S. Edwards and P. W. Anderson [21], to detect the *ergodicity breaking* is to consider the long-time limit of the spin auto-correlation function $C(t)$,

$$q_{\text{EA}} = \lim_{t \rightarrow \infty} C(t) = \frac{1}{N} \sum_{i=1}^N \langle s_i \rangle^2 \quad (\text{VI.6})$$

with

$$C(t) \equiv \frac{1}{N} \sum_{i=1}^N \langle S_i(0) S_i(t) \rangle = \frac{1}{N} \sum_{i=1}^N \langle (S_i(0) - \langle S_i \rangle)(S_i(t) - \langle S_i \rangle) \rangle + \frac{1}{N} \sum_{i=1}^N \langle s_i \rangle^2 \quad (\text{VI.7})$$

Here we assume that the configuration of the system at $t = 0$ is an equilibrium configuration and $\langle \dots \rangle$ represents the average over different realizations such equilibrium configurations. Note that thermal fluctuations in equilibrium decorrelate in the large time limit $\langle (S_i(0) - \langle S_i \rangle)(S_i(t) - \langle S_i \rangle) \rangle \xrightarrow{t \rightarrow \infty} 0$. In the liquid phase the auto-correlation function decays down to 0 after finite relaxation time. The latter diverges at the glass transition (if present) leading to $q_{\text{EA}} > 0$. Thus the EA order parameter detects the ergodicity breaking. In the glassy phase the average $\langle \dots \rangle$ means to take average over thermal fluctuations within a metastable state so that the two definitions (interpretations) of the EA order parameter Eq. (VI.5) and Eq. (VI.6) become the same.

A useful feature of the EA order parameter is that one does not need to know how to characterize the configuration of systems in the free-energy minima. This is much different from the usual crystalline order parameter, such as the ferromagnetic order parameter, which is defined as a projection of the configuration of the system onto a target crystalline configuration, which one needs to know in advance. On the other hand, this means that an ergodicity breaking detected by the EA order parameter do not necessarily mean a glass transition. Indeed even a ferromagnet exhibits an ergodicity breaking: the free-energy barrier separating the two minima in Fig. 10 diverges in $N \rightarrow \infty$ limit.

Finally let us note that in some cases like the p -spin models with $p = 2, 4, 6, \dots$ the system is symmetric under global 'spin flip' $s_i \rightarrow -s_i$ for $\forall i$, the perturbation Eq. (VI.1) breaks this symmetry. One observes that the system is no longer invariant under global flip in *single* replica, say a , $x_i^a \rightarrow -x_i^a$ for $\forall i$. It is the case even with the simplest (replica symmetric) perturbation Eq. (VI.4). In this respect, the role played by the field ϵ is like the magnetic field conjugated to the magnetization which is the order parameter for ferromagnets.

2. Replica symmetry breaking

In the absence of the ϵ -coupling term, the system given by the Hamiltonian Eq. (VI.1) is fully symmetric under permutations of the indices $a = 1, 2, \dots, n$. This is the replica symmetry. Now switching on some ϵ_{ab} we can break this symmetry. As one can imagine this will have interesting results if the free-energy landscape have multiple local minima. For instance the matrix $\hat{\epsilon}$ of the form in Fig. 16 with $\epsilon > 0$ can bring the two replicas 2 and 3 closer to each other and the other two replicas 1 and 4 closer to each other, creating two groups of replicas. Because there are no couplings between the two groups, they may sit on different free-energy minima. And the two groups may remain

sitting distinct minima even after switching off the field $\epsilon \rightarrow 0$ if the free-energy landscape actually consists of multiple minima as in Fig. 15. This is the replica symmetry breaking (RSB). On the other hand, if there is only single minimum, the groups will merge restoring back the replica symmetry.

$$\mathcal{E}_{ab} = \begin{matrix} & \begin{matrix} 1 & 2 & 3 & 4 \end{matrix} \\ \begin{matrix} 1 \\ 2 \\ 3 \\ 4 \end{matrix} & \begin{matrix} \epsilon & & & \\ & 0 & & \epsilon \\ & \epsilon & & \\ & & \epsilon & \end{matrix} \end{matrix}$$

FIG. 16. An epsilon coupling matrix which breaks the replica symmetry. Matrix elements are zero except for the 4 elements with $\epsilon > 0$.

Note that the RSB automatically also means an ergodicity breaking, but of a more complicated version involving the hierarchical organization of relaxations [46–50].

3. How the ϵ -coupling can be realized?

In the theoretical formulation, we introduced conveniently the field ϵ_{ab} as Eq. (VI.1). But we have to ask ourselves what plays the role of the somewhat fictitious field in reality. The perturbations like Eq. (VI.1) can be introduced by considering 'random pinning fields' [45, 51].

The replicated system Eq. (VI.1) can be realized by considering 'pinning field' as the following.

$$-\beta H_n[\hat{\epsilon}] = -\beta \sum_{a=1}^n H[\{S_i^a\}] + \sum_a \sum_{i=1}^N h_i^a S_i^a \quad (\text{VI.8})$$

Where h_i^a is a Gaussian random pinning field with zero mean and variance

$$\overline{h_i^a h_j^b} = 2\epsilon_{ab}\delta_{ij} \quad (\text{VI.9})$$

where \dots represents the average over realizations of the pinning field.

Now let us consider the partition function of the replicated system averaged over the pinning field,

$$\begin{aligned} \overline{Z_n}[\hat{\epsilon}] &= \prod_a \prod_i \text{Tr}_{S_i^a} \overline{e^{-\beta H_n}} = \prod_a \prod_i \text{Tr}_{S_i^a} e^{-\beta \sum_a H[\{S_i^a\}]} \overline{e^{\sum_a \sum_i h_i^a S_i^a}} \\ &= \prod_a \prod_i \text{Tr}_{S_i^a} e^{-\beta \sum_a H[\{S_i^a\}] + \sum_i \sum_{a,b} \epsilon_{ab} S_i^a S_i^b} \end{aligned} \quad (\text{VI.10})$$

Now what does it mean to take 'an average over the random pinning field'?

- A physical interpretation is that it means to take an average over different independent realizations of glasses starting from the liquid state. If the ergodicity breaking (sec. VIA 1) take place, different initial condition will result in different glasses. This is what the replica symmetry breaking means. The random pinning field mimics the role of different initial conditions in experiments and computer simulations. Note that this is analogous to the usual interpretation of the the symmetry breaking field h for the ferromagnet (see sec. IVB): random initial condition will have magnetization of order $1/\sqrt{N}$ which may be polarized positively or negatively which selects one among the two possible ferromagnetic state related by global reflection as the final state.
- In the context of machine learning, the role of symmetry breaking field may be played by 1) choices of boundary conditions (inputs/outputs data) 2) choices of initial condition for learning.
- **Todo** Replica symmetry breaking: ϵ_{ab} can break the replica symmetry. But the analysis is done in $n \rightarrow 0$ limit. Is it possible to realize a certain 'real' replica approach which enable to detect the RSB?

4. Thermodynamics : $n \rightarrow 0$

So far, the number of replicas n was an arbitrary integer $n = 1, 2, 3, \dots$. But physically we would be interested with the thermodynamic free-energy of a *single* system,

$$-\beta F = \ln Z. \quad (\text{VI.11})$$

How can we compute this? We can use the following trick. Assuming that we can make analytic continuation of n to real values we can write,

$$\ln Z = \partial_n Z^n|_{n=0} \quad (\text{VI.12})$$

In order for this to work we have to obtain the replicated partition function Z^n as an analytic function of n . On the other hand we have the partition function of replicated system Eq. (VI.10) averaged over the pinning field. Now we assume that the free-energy F is a self-averaging quantity in the sense that the limit $\lim_{N \rightarrow \infty} F/N$ is unique irrespective the realizations of the pinning field so that we can write,

$$\frac{-\beta F}{N} = \lim_{\hat{\epsilon} \rightarrow 0} \frac{1}{N} \partial_n \overline{Z}_n[\hat{\epsilon}] \Big|_{n=0} \quad (\text{VI.13})$$

where $\overline{Z}_n[\hat{\epsilon}]$ is the replicated partition function averaged over the pinning field Eq. (VI.10).

5. Distribution of "random" free-energy

Here we discuss distribution of free-energy of differently created glasses [52, 53]. For us, there are two possibilities to create 'different' glasses:

- Different realization of the quenched disorder ξ_{\blacksquare} (see sec. III A 5)
- No quenched disorder but different cooling or quenching from the liquid state. In our view this can be modeled theoretically in statistical mechanics in terms of infinitesimal random pinning field of strength ϵ which is switched off $\epsilon \rightarrow 0$ after $N \rightarrow \infty$. (See sec. VIA 3)

Consider an ensemble of 'glasses' $i = 1, 2, \dots, K$ with free-energy Nf_i . Let us define 'disorder average' as,

$$\overline{\dots} = \lim_{K \rightarrow \infty} \frac{1}{K} \sum_{i=1}^K \dots. \quad (\text{VI.14})$$

and introduced the 'rate-function' (large deviation function) for the large deviation of the free-energy ,

$$R(f) = \lim_{N \rightarrow \infty} \frac{1}{N} \ln \frac{1}{K} \sum_{i=1}^K \delta(f - f_i) \quad (\text{VI.15})$$

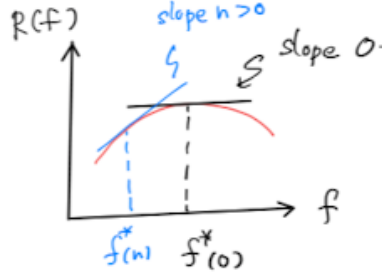


FIG. 17. Large deviation function of the random free-energy

Now let us consider

$$-\beta n \psi_n \equiv \frac{1}{N} \ln \overline{Z}^n \quad \overline{Z}^n = \lim_{K \rightarrow \infty} \frac{1}{K} \sum_{i=1}^K Z_i^n \quad Z_i = e^{-N\beta f_i} \quad (\text{VI.16})$$

where n is a real number. We show below that $-\beta n\psi_n$ is the Legendre transform of the large deviation function $R(f)$. Indeed we find,

$$\overline{Z^n} = \int df e^{N(R(f) - \beta nf)} = e^{N(R(f^*) - \beta nf^*(n))} \quad (\text{VI.17})$$

where $f^*(n)$ is defined as

$$\frac{\partial R(f)}{\partial f} \Big|_{f=f^*(n)} = \beta n. \quad (\text{VI.18})$$

which means

$$-\beta n\psi_n = -\beta nf^*(n) + R(f^*(n)) \quad (\text{VI.19})$$

Taking ∂_n we find

$$f^*(n) = \partial_n(n\psi_n) = -\frac{1}{\beta N} \partial_n \ln \overline{Z^n} \quad (\text{VI.20})$$

while

$$R(f^*) = n^2 \partial_n \beta \psi_n \quad (\text{VI.21})$$

Thus we can compute the function $R(f)$ from $\frac{1}{N} \ln \overline{Z^n}$.

Assuming that $R(f)$ is concaved upward as in Fig. 17, Eq. (VI.17) implies that $\overline{Z^n}$ is dominated by 'typical free-energy' if $n = 0$. Instead it would be dominated by atypical free-energy if $n \neq 0$. In this way we can understand better significance of the famous formula for the 'typical' free-energy,

$$f^*(0) = \lim_{n \rightarrow 0} \partial_n(n\psi_n) = -\lim_{n \rightarrow 0} \partial_n \frac{1}{\beta N} \ln \underbrace{\overline{Z^n}}_{1+(\overline{Z^n}-1)+\dots} = -\frac{1}{\beta N} \lim_{n \rightarrow 0} \partial_n \overline{Z^n} = -\frac{1}{\beta N} \overline{\ln Z} \quad (\text{VI.22})$$

6. Parisi's ansatz

In the following we look for the following form of order parameter proposed by G. Parisi [54],

$$q_{ab} = \sum_{i=0}^{k+1} q_i (I_{ab}^{m_i} - I_{ab}^{m_{i+1}}) = \sum_{i=1}^{k+1} (q_i - q_{i-1}) I_{ab}^{m_i} + q_0 \quad (\text{VI.23})$$

where I_{ab}^m is a generalized ('fat') Identity matrix of size $n \times n$ composed of blocks of size $m \times m$. Here we assumed $q_{k+1} = 1$ and $I_{ab}^{m_{k+2}} = 0$.

The hierarchical structure of the order parameter q_{ab} Eq. (VI.23) assumed in the Parisi's ansatz imply the same hierarchical structure in the symmetry breaking field ϵ_{ab} .

Note that a family of equivalent saddle points other than the one Eq. (VI.23) can be obtained just by making permutations of the replica indices. All of them take exactly the same value of the free-energy functional $f[\hat{q}^*]$ so that if we take a sum over all of them, the replica (permutation) symmetry is restored. Choosing one out of them, like the one parameterized as Eq. (VI.23), means to break the replica symmetry. Physically we justify this by saying that it is realized as a spontaneous symmetry breaking, like the ferromagnetic phase transition of Ising model. The coupling parameter ϵ_{ab} discussed previously can be regarded as the symmetry breaking field.

In the limit $n \rightarrow 0$, we obtain a function $q(x)$ as shown in panel d) of Fig. 18. As we will see, the order parameter functions encode characteristics of the complex free-energy landscape [1].

B. Free-energy functional

1. Order parameter, symmetry breaking field and Legendre transforms

For simplicity, suppose that we have a generic system which consists of N degrees of freedom $\{S\} = (S_1, S_2, \dots, S_N)$ whose Hamiltonian is $H[\{S\}]$, which can be with/without the quenched disorder. Let us introduce n replicas $a =$

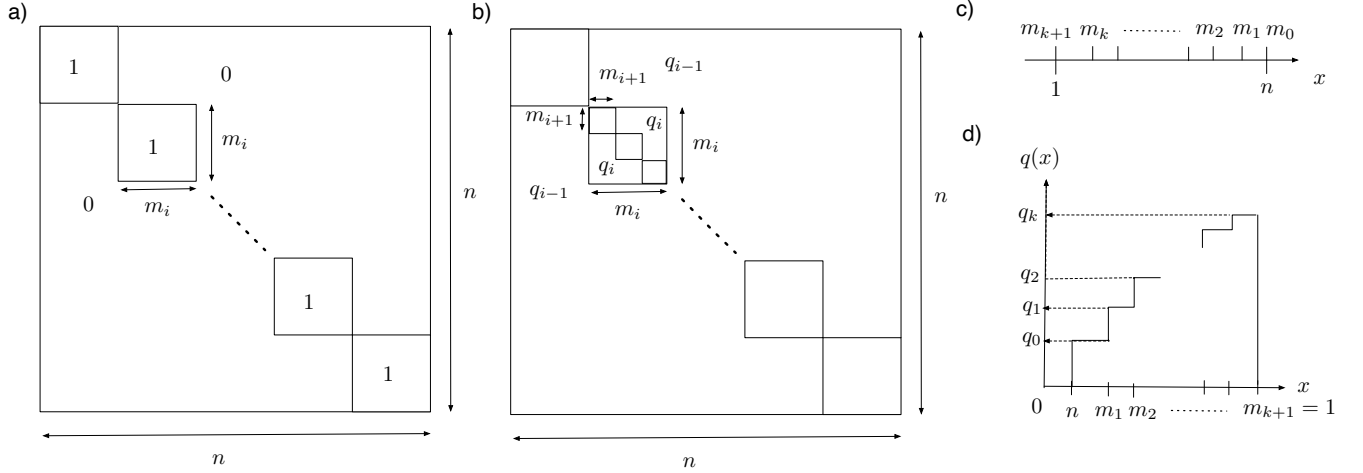


FIG. 18. Parisi's matrix

$1, 2, \dots, n$ and a replicated Hamiltonian, as Eq. (VI.1) which reads,

$$-\beta H_n[\hat{\epsilon}] = -\beta \sum_{a=1}^n H[\{S_i^a\}] + \sum_{a < b} \epsilon_{ab} \sum_{i=1}^N S_i^a S_i^b. \quad (\text{VI.24})$$

Here we introduced the 2nd term on the r.h.s. which represents an artificial attractive coupling $\epsilon_{ab} > 0$ between replicas. The field ϵ_{ab} explicitly breaks the replica symmetry, i.e. the permutation symmetry of replica index.

The free-energy of the replicated system can be defined as,

$$-\beta G_n[\hat{\epsilon}] = \ln \prod_{a=1}^n \prod_{i=1}^N \text{Tr}_{S_i^a} e^{-\beta H_n[\hat{\epsilon}].} \quad (\text{VI.25})$$

This allows us to evaluate the overlap between the replicas,

$$q_{ab} = \frac{1}{N} \sum_{i=1}^N \langle S_i^a S_i^b \rangle_\epsilon = \frac{1}{N} \frac{\partial(-\beta G_n)[\hat{\epsilon}]}{\partial \epsilon_{ab}} \quad (\text{VI.26})$$

We are interested with,

$$\lim_{\hat{\epsilon} \rightarrow 0} \lim_{N \rightarrow \infty} q_{ab} \quad (\text{VI.27})$$

One can define a 'glass' susceptibility,

$$\chi_{ab,cd} \equiv \frac{1}{N} \frac{\partial}{\partial \epsilon_{ab} \partial \epsilon_{cd}} (-\beta G)[\hat{\epsilon}] = \frac{\partial q_{ab}}{\partial \epsilon_{cd}} = \frac{1}{N} \sum_{i,j=1}^N \left[\langle S_i^a S_i^b S_j^c S_j^d \rangle_\epsilon - \langle S_i^a S_i^b \rangle_\epsilon \langle S_j^c S_j^d \rangle_\epsilon \right] \quad (\text{VI.28})$$

Instability toward spontaneous replica symmetry breaking may accompany divergence of the glass susceptibility at $\epsilon = 0$.

Let us then consider the Legendre transform of the free-energy,

$$-\beta F_n[\hat{q}] = -\beta G_n[\hat{\epsilon}^*] - N \sum_{a < b} \epsilon_{ab}^* q_{ab} \quad (\text{VI.29})$$

where $\hat{\epsilon}^* = \hat{\epsilon}^*[\hat{q}]$ is defined by Eq. (VI.26),

$$q_{ab} = \frac{1}{N} \sum_{i=1}^N \langle S_i^a S_i^b \rangle_\epsilon = \frac{1}{N} \frac{\partial(-\beta G_n)[\hat{\epsilon}]}{\partial \epsilon_{ab}}. \quad (\text{VI.30})$$

The inverse of the Legendre transform is,

$$-\beta G_n[\hat{\epsilon}] = -\beta F_n[\hat{q}^*] + N \sum_{a < b} \epsilon_{ab} q_{ab}^* \quad (\text{VI.31})$$

where $\hat{q}^* = \hat{q}^*[\hat{\epsilon}]$ is defined such that,

$$-\epsilon_{ab} = \frac{1}{N} \left. \frac{\partial}{\partial q_{ab}} (-\beta F_n[\hat{q}]) \right|_{\hat{q}=\hat{q}^*[\hat{\epsilon}]} \quad (\text{VI.32})$$

The last expression tells us that the order parameter of our interest, which detects the spontaneous RSB Eq. (VI.3), can be obtained by minimizing the free-energy $F[\hat{q}]$ which yields $\epsilon_{ab} = 0$. Related to Eq. (VI.28) is the Hessian matrix,

$$M_{a \neq b, c \neq d} \equiv \left. \frac{1}{N} \frac{\partial^2}{\partial q_{a < b} \partial q_{c < d}} (\beta F_n[\hat{q}]) \right|_{\hat{q}} = (\chi^{-1})_{ab,cd} \quad (\text{VI.33})$$

The divergence of the glass susceptibility Eq. (VI.28) imply vanishing of the eigen value(s) of the Hessian matrix [55]. Thermodynamic stability implies $\chi_{ab,cd} < \infty$ or positive (semi-)definiteness of the eigenvalues of the Hessian matrix.

Now similarly to Eq. (IV.15) we start from an identity,

$$1 = \int_{-\infty}^{\infty} \int_{-i\infty}^{i\infty} \prod_{a < b} \left(\frac{N}{2\pi i} \right) dq_{ab} d\epsilon_{ab} e^{N \sum_{a < b} \epsilon_{ab} (N^{-1} \sum_i^N (S_i)^a (S_i)^b - q_{ab})} \quad (\text{VI.34})$$

$$\begin{aligned} \overline{Z_n}[\epsilon^{\text{ext}}] &= \prod_{a=1}^n \prod_{i=1}^N \text{Tr}_{S_i^a} e^{-\beta \sum_{a=1}^n H[S_i^a] + \sum_{a < b} \epsilon_{ab}^{\text{ext}} \sum_{i=1}^N S_i^a S_i^b} \\ &= \prod_{a < b} N \int dq_{ab} \int_{-i\infty}^{i\infty} \prod_{a < b} \frac{d\epsilon_{ab}}{2\pi i} e^{-N \sum_{a < b} \epsilon_{ab} q_{ab}} \prod_{i=1}^N \left(\prod_{a=1}^n \text{Tr}_{S_i^a} e^{\sum_{a < b} (\epsilon_{ab}^{\text{ext}} + \epsilon_{ab}) S_i^a S_i^b} \right) e^{-\beta \sum_{a=1}^n H[\{S_i^a\}]} \\ &= \prod_{a < b} N \int dq_{ab} e^{N \sum_{a < b} \epsilon_{ab}^{\text{ext}} q_{ab}} \int_{\epsilon_{ab}^{\text{ext}} - i\infty}^{\epsilon_{ab}^{\text{ext}} + i\infty} \frac{d\epsilon_{ab}}{2\pi i} e^{-N \sum_{a < b} \epsilon_{ab} q_{ab}} e^{-\beta G_{n,0}(\hat{\epsilon})} \langle e^{-\beta \sum_{a=1}^n H[\{S_i^a\}]} \rangle_{\epsilon,0} \\ &= \prod_{a < b} N \int dq_{ab} e^{N \sum_{a < b} \epsilon_{ab}^{\text{ext}} q_{ab}} \int_{\epsilon_{ab}^{\text{ext}} - i\infty}^{\epsilon_{ab}^{\text{ext}} + i\infty} \frac{d\epsilon_{ab}}{2\pi i} e^{-N \sum_{a < b} \epsilon_{ab} q_{ab}} e^{-\beta G(\hat{\epsilon})} \\ &= \prod_{a < b} \int N dq_{ab} e^{N \sum_{a < b} \epsilon_{ab}^{\text{ext}} q_{ab} - \beta F(\hat{q})} = e^{N \sum_{a < b} \epsilon_{ab}^{\text{ext}} q_{ab}^* - \beta F(\hat{q}^*)} \end{aligned} \quad (\text{VI.35})$$

In the 3rd equation we introduced

$$-\beta G_{n,0}(\hat{\epsilon}) = N \ln \prod_{c=1}^n \text{Tr}_{S_c} e^{\sum_{a < b} \epsilon_{ab} S_i^a S_i^b} \quad (\text{VI.36})$$

and

$$\langle \dots \rangle_{\epsilon,0} = \frac{\prod_{c=1}^n \prod_{i=1}^N \text{Tr}_{S_i^c} e^{\sum_{a < b} \epsilon_{ab} S_i^a S_i^b} \dots}{\prod_{c=1}^n \prod_{i=1}^N \text{Tr}_{S_i^c} e^{\sum_{a < b} \epsilon_{ab} S_i^a S_i^b}} \quad (\text{VI.37})$$

The subscript $\langle \dots \rangle_{\epsilon,0}$ is meant to emphasize that the interaction is absent in this averaging. Obviously odd moments of the spins vanish by symmetry,

$$\langle S_i^a \rangle_{\epsilon,0} = 0 \quad \langle S_i^a S_i^b S_i^c \rangle_{\epsilon,0} = 0 \dots \quad (\text{VI.38})$$

Note that in this averaging different spins are mutually indecent from each other. For instance we have,

$$\langle S_i^a S_i^b S_j^c S_j^d \rangle_{\epsilon,0} = \langle S_i^a S_i^b \rangle_{\epsilon,0} \langle S_j^c S_j^d \rangle_{\epsilon,0} \quad i \neq j \quad (\text{VI.39})$$

In the 4th equation we introduced

$$-\beta G_n(\hat{\epsilon}) = -\beta G_{n,0}(\hat{\epsilon}) + \ln \langle e^{-\beta H} \rangle_{\epsilon,0}. \quad (\text{VI.40})$$

The integration over $\hat{\epsilon}$ can be done by the saddle point method assuming $N \gg 1$. Note that the saddle point method works if the glass susceptibility matrix $\chi_{ab,cd}$ Eq. (VI.28) is positive (semi-)definite at around the saddle point $\hat{\epsilon}^*$. Here $\hat{\epsilon} = \hat{\epsilon}^*(\hat{q})$ is defined by Eq. (VI.26). In the 5th equation we performed the integration over \hat{q} again by the saddle point method and used the Legendre transform Eq. (VI.29),

$$-\beta F_n(\hat{q}) = -\beta G_n(\hat{\epsilon}^*(\hat{q})) - N \sum_{a < b} \epsilon_{ab}^*(\hat{q}) q_{ab} \quad (\text{VI.41})$$

where $\hat{\epsilon}^* = \hat{\epsilon}^*[\hat{q}]$ is defined by,

$$q_{ab} = \frac{1}{N} \sum_{i=1}^N \langle S_i^a S_i^b \rangle_{\epsilon,0} = \frac{1}{N} \frac{\partial(-\beta G_n)[\hat{\epsilon}]}{\partial \epsilon_{ab}} \quad (\text{VI.42})$$

or

$$q_{ab} = \langle S_i^a S_i^b \rangle_{\epsilon} \quad \forall i \quad (\text{VI.43})$$

since all spins are equivalent in the averaging. Let us emphasize that here $\langle \dots \rangle_{\epsilon}$ is the averaging *in the presence of the interactions* so that it is different from $\langle \dots \rangle_{\epsilon,0}$ defined in Eq. (VI.37). The integration over \hat{q} works if the inverse of the glass susceptibility or the Hessian matrix $M_{a \neq b, c \neq d}$ Eq. (VI.33) is positive (semi-)definite at around the saddle point \hat{q}^* . Here \hat{q}^* is defined by Eq. (VI.32) with $\hat{\epsilon} = 0$.

Finally the thermodynamic free-energy F Eq. (VI.13) is obtained as,

$$\frac{-\beta F}{N} = \lim_{\hat{\epsilon}^{\text{ext}} \rightarrow 0} \frac{1}{N} \partial_n \overline{Z}_n[\hat{\epsilon}^{\text{ext}}] \Big|_{n=0} = \frac{1}{N} \partial_n e^{-\beta F_n[\hat{q}^*]} \Big|_{n=0} \quad (\text{VI.44})$$

which implies

$$F/N = f[\hat{q}^*] \quad f[\hat{q}] = \partial_n F_n[\hat{q}] \Big|_{n=0}/N \quad (\text{VI.45})$$

2. Plefka expansion

Now our task is to compute the free-energy $F[\hat{q}]$ defined in Eq. (VI.29). To this end, we will follow the same idea of Plefka expansion [36] we used for the ferromagnet in sec. IVB 4. The computations presented in the following sections follow this strategy.

Suppose that the effect of the interactions between the dynamical variables S_i ($i = 1, 2, \dots, N$) can be treated perturbatively which enable the following decompositions,

$$F_n = F_{n,0} + \lambda F_{n,1} + \frac{\lambda^2}{2} F_{n,2} + \dots \quad G_n = G_{n,0} + \lambda G_{n,1} + \frac{\lambda^2}{2} G_{n,2} + \dots \quad \epsilon_{ab} = (\epsilon_0)_{ab} + \lambda (\epsilon_1)_{ab} + \frac{\lambda^2}{2} (\epsilon_2)_{ab} \dots \quad (\text{VI.46})$$

Here the quantities with suffix 0 represent those which are present in the absence of interactions (like the ideal gas free-energy) and those with suffix 1, 2, ... represent those due to interactions. Here we omitted the higher-order terms. The parameter λ , which is introduced to organize a perturbation theory, is put back to $\lambda = 1$ in the end.

The Legendre transform Eq. (VI.29) becomes, at $O(\lambda^0)$,

$$-\beta F_{n,0}[\hat{q}] = -\beta G_{n,0}[\hat{\epsilon}_0^*] - N \sum_{a < b} (\epsilon_0^*)_{ab} q_{ab} \quad (\text{VI.47})$$

where $(\epsilon_0^*)_{ab}$ is defined such that,

$$q_{ab} = \frac{1}{N} \frac{\partial}{\partial \epsilon_{ab}} (-\beta G_{n,0}[\hat{\epsilon}]) \Big|_{\hat{\epsilon}=\hat{\epsilon}_0^*[\hat{q}]} \quad (a \neq b) \quad (\text{VI.48})$$

The latter implies

$$\langle S_i^a S_i^b \rangle_{\epsilon=\epsilon_0^*[\hat{q}]} = q_{ab} \quad \forall i \quad (\text{VI.49})$$

Since all spins are equivalent in the averaging.

Then at $O(\lambda)$ we find,

$$\begin{aligned} -\beta F_{n,1}[\hat{q}] &= -\beta G_{n,1}[\hat{\epsilon}_0^*[\hat{q}]] + \sum_{a < b} \frac{\partial}{\partial \epsilon_{ab}} (-\beta G_{n,0}[\hat{\epsilon}]) \Big|_{\hat{\epsilon}=\hat{\epsilon}_0^*[\hat{q}]} (\epsilon_1^*)_{ab} - N \sum_{a < b} (\epsilon_1^*)_{ab} q_{ab} \\ &= -\beta G_{n,1}[\hat{\epsilon}_0^*[\hat{q}]] \end{aligned} \quad (\text{VI.50})$$

In the 2nd equation we used Eq. (VI.48). Minimization of the free-energy $F[\hat{q}]$ (see Eq. (VI.32)) implies $(\epsilon_0^*)_{ab} = -\lambda(\epsilon_1^*)_{ab}$ up to this order.

Higher order terms $O(\lambda)^2$ can be considered similarly to the case of ferromagnet discussed in sec. IV B 5. If such higher order terms vanish (which is the case in the mean-field models we study), similarly to Eq. (IV.30) we found in sec. IV B 4, we can bring back $\lambda = 1$ and obtain,

$$F_n[\hat{q}] = -\beta F_{n,0}[\hat{q}] - \beta F_{n,1}[\hat{q}] = -\beta G_{n,0}[\hat{\epsilon}^*] - N \sum_{a < b} \epsilon_{ab}^* q_{ab} - \beta G_{n,1}[\hat{\epsilon}^*] \quad (\text{VI.51})$$

where $\hat{\epsilon}^* = \hat{\epsilon}^*[\hat{q}]$ is determined by Eq. (VI.48). We will refer to $F_0[\hat{q}]$ as the entropic part of the free-energy and $F_1[\hat{q}]$ as the interaction part of the free-energy.

3. Cumulant expansion

The effect of interaction in the free-energy $G(\hat{\epsilon})$ Eq. (VI.40) can be evaluated using the cumulant expansion much as done for the ferromagnetic case (see sec. IV B 6). This will allow us to obtain the Plefka expansion of the free-energy $G(\hat{\epsilon})$ as $G(\hat{\epsilon}) = G_0(\hat{\epsilon}) + \lambda G_1 \hat{\epsilon} + \frac{\lambda^2}{2} G_2(\hat{\epsilon}) + \dots$. Then we can construct the free-energy $F(\hat{q})$ can be constructed as described above.

C. Scalar p -spin models

Here let us consider specifically the p -spin ferromagnetic model

$$H = -\frac{J}{\sqrt{c/\alpha}} \sum_{\blacksquare} \underbrace{\prod_{j \in \partial \blacksquare} S_j}_{p\text{-body}} \quad (\text{VI.52})$$

with Ising spins $S_i = \pm 1$ or spherical spins $\sum_{i=1}^N S_i^2 = 1$.

1. Entropic part of the free-energy

Let us find the entropic part of the free-energy. To this end we have to evaluate

$$-\beta G_0[\hat{\epsilon}]/N = \ln \text{Tr}_S e^{\sum_{a < b} \epsilon_{ab} S^a S^b} \quad (\text{VI.53})$$

- Ising

$$\begin{aligned} \prod_{a=1}^n \sum_{S_a=\pm 1} e^{\sum_{a < b} \epsilon_{ab} S^a S^b} &= \prod_{a=1}^n \sum_{S_a=\pm 1} e^{\sum_{a < b} \epsilon_{ab} \frac{\partial^2}{\partial h_a \partial h_b}} e^{\sum_{c=1}^n h_c S^c} \Big|_{h=0} \\ &= e^{\sum_{a < b} \epsilon_{ab} \frac{\partial^2}{\partial h_a \partial h_b}} \prod_{c=1}^n 2 \cosh(h_c) \Big|_{h=0} \end{aligned} \quad (\text{VI.54})$$

Thus we find,

$$\begin{aligned}
-\beta G_{n,0}[\hat{\epsilon}] / N &= \ln e^{\sum_{a < b} \epsilon_{ab} \frac{\partial^2}{\partial h_a \partial h_b}} \prod_{c=1}^n 2 \cosh(h_c) \Big|_{h=0} \\
&= \ln e^{\frac{1}{2} \sum_{a \neq b} \epsilon_{ab} \frac{\partial^2}{\partial h_a \partial h_b}} \prod_{c=1}^n 2 \cosh(h_c) \Big|_{h=0} \\
&= \ln e^{\frac{1}{2} \sum_{a,b} \epsilon_{ab} \frac{\partial^2}{\partial h_a \partial h_b} - \frac{1}{2} \sum_a \epsilon_{aa} \frac{\partial^2}{\partial h_a^2}} \prod_{c=1}^n 2 \cosh(h_c) \Big|_{h=0} \\
&= -\frac{1}{2} \sum_{a=1}^n \epsilon_{aa} + \ln e^{\frac{1}{2} \sum_{a,b} \epsilon_{ab} \frac{\partial^2}{\partial h_a \partial h_b}} \prod_{c=1}^n 2 \cosh(h_c) \Big|_{h=0}
\end{aligned} \tag{VI.55}$$

Here we introduced ϵ_{aa} for convenience, whose value is arbitrary. Then we find,

$$\begin{aligned}
-\beta F_{n,0}[\hat{q}] / N &= -\beta G_{n,0}[\hat{\epsilon}_0^*] / N = -\frac{1}{2} \sum_{a \neq b} (\epsilon_0^*)_{ab} q_{ab} + \ln e^{\frac{1}{2} \sum_{a \neq b} (\epsilon_0^*)_{ab} \frac{\partial^2}{\partial h_a \partial h_b}} \prod_{c=1}^n 2 \cosh(h_c) \Big|_{h=0} \\
&= -\frac{1}{2} \sum_{a,b=1}^n (\epsilon_0^*)_{ab} q_{ab} + \ln e^{\frac{1}{2} \sum_{a,b} (\epsilon_0^*)_{ab} \frac{\partial^2}{\partial h_a \partial h_b}} \prod_{c=1}^n 2 \cosh(h_c) \Big|_{h=0}
\end{aligned} \tag{VI.56}$$

In the last equation we introduced $q_{aa} = 1$. Here $(\epsilon_0^*)_{ab} = (\epsilon_0^*)_{ab}[\hat{q}]$ is determined by Eq. (VI.48) (or Eq. (VI.49)), which becomes,

$$q_{ab} = \frac{e^{\frac{1}{2} \sum_{c,d} (\epsilon_0^*)_{ab} \frac{\partial^2}{\partial h_c \partial h_d}} \left(\prod_{e=1}^n 2 \cosh(h_e) \right) \tanh(h_a) \tanh(h_b) \Big|_{h=0}}{e^{\frac{1}{2} \sum_{c,d} (\epsilon_0^*)_{cd} \frac{\partial^2}{\partial h_c \partial h_d}} \prod_{e=1}^n 2 \cosh(h_e) \Big|_{h=0}} \quad (a \neq b) \tag{VI.57}$$

- Spherical model

In the spherical model, the trace over the spins can be expressed as,

$$\begin{aligned}
\prod_{i=1}^N \text{Tr}_{S_i} &= \int_{-\infty}^{\infty} \prod_{i=1}^N dS_i \delta \left(\sum_{i=1}^N S_i^2 - N \right) \\
&= \int_{-\infty}^{\infty} \prod_{i=1}^N dS_i N \int_{-\infty}^{\infty} \frac{d\lambda}{2\pi i} e^{\lambda(\sum_{i=1}^N (S_i)^2) - N}
\end{aligned} \tag{VI.58}$$

Then we can write

$$\begin{aligned}
&\left(\prod_{i=1}^N \prod_{c=1}^n \text{Tr}_{S_i^c} \right) e^{\sum_{a < b} \sum_{i=1}^N \epsilon_{ab} S_i^a S_i^b} \\
&= \left(\prod_{c=1}^n \prod_{i=1}^N \int_{-\infty}^{\infty} dS_i^c \right) \prod_{c=1}^n \left\{ N \int_{-i\infty}^{i\infty} \frac{d\lambda_c}{2\pi i} e^{\lambda_c(\sum_{i=1}^N (S_i^c)^2) - N} \right\} e^{\sum_{a < b} \sum_{i=1}^N \epsilon_{ab} S_i^a S_i^b} \\
&= \prod_{c=1}^n \left\{ N \int_{-i\infty}^{i\infty} \frac{d(\epsilon_{cc}/2)}{2\pi i} e^{-(\epsilon_{cc}/2)N} \right\} \left(\prod_{c=1}^n \prod_{i=1}^N \int_{-\infty}^{\infty} dS_i^c \right) e^{(1/2) \sum_{i=1}^N \sum_{a,b} \epsilon_{ab} S_i^a S_i^b} \\
&= \prod_{c=1}^n \left\{ N \int_{-i\infty}^{i\infty} \frac{d(\epsilon_{cc}/2)}{2\pi i} e^{-(\epsilon_{cc}/2)N} \right\} e^{N \ln \sqrt{\frac{(2\pi)^n}{\det(-\hat{\epsilon})}}}
\end{aligned} \tag{VI.59}$$

where we introduced $\epsilon_{aa}/2 = \lambda_a$.

Thus we find,

$$-\beta G_{n,0}[\hat{\epsilon}]/N = -\frac{1}{2} \sum_{c=1}^n \epsilon_{cc} + \frac{n}{2} \ln(2\pi) - \frac{1}{2} \ln \det(-\hat{\epsilon}) \quad (\text{VI.60})$$

and

$$\begin{aligned} -\beta F_{n,0}[\hat{q}]/N &= -\beta G_{n,0}[\hat{\epsilon}_0^*]/N - \sum_{a < b} (\epsilon_0^*)_{ab} q_{ab} \\ &= -\frac{1}{2} \sum_{a,b=1}^n (\epsilon_0^*)_{ab} q_{ab} + \frac{n}{2} \ln(2\pi) - \frac{1}{2} \ln \det(-\hat{\epsilon}_0^*) \\ &= \frac{n}{2} + \frac{n}{2} \ln(2\pi) + \frac{1}{2} \ln \det \hat{q} \end{aligned} \quad (\text{VI.61})$$

with $q_{aa} = 1$. Here we took into account that $(\epsilon_0^*)_{ab} = (\epsilon_0^*)_{ab}[\hat{q}]$ ($a \neq b$) is determined by Eq. (VI.48) and also that the diagonal ones ϵ_{aa} s must be fixed by doing saddle point integrations in Eq. (VI.59). Indeed these can be done all together by taking derivatives of the 2nd equation of Eq. (VI.61),

$$0 = \frac{\partial}{\partial(\epsilon_0)_{ab}} \left[-\frac{1}{2} \sum_{a,b=1}^n (\epsilon_0)_{ab} q_{ab} + \frac{n}{2} \ln(2\pi) - \frac{1}{2} \ln \det(-\hat{\epsilon}_0) \right] \quad (\text{VI.62})$$

which yields (using Eq. (A.1)),

$$q_{ab} = ((-\hat{\epsilon}_0)^{-1})_{ab} \quad (\text{VI.63})$$

2. Interaction part of the free-energy

Now we examine the cumulant expansion

$$\frac{1}{N} \ln \langle e^{-\sqrt{\lambda}\beta \sum_{a=1}^n H[\{S_i^a\}]} \rangle_{\epsilon,0} = \frac{\sqrt{\lambda}}{N} \sum_{a=1}^n \langle (-\beta H[\{S_a\}]) \rangle_{\epsilon,0} + \frac{\lambda}{2N} \sum_{a,b=1}^n (\langle (\beta H_a)(\beta H_b) \rangle_{\epsilon,0} - \langle (\beta H_a) \rangle_{\epsilon,0} \langle (\beta H_b) \rangle_{\epsilon,0}) + \dots \quad (\text{VI.64})$$

with

$$\epsilon_{ab} = (\epsilon_0)_{ab} + \lambda(\epsilon_1)_{ab} + \frac{\lambda^2}{2}(\epsilon_2)_{ab} \dots \quad (\text{VI.65})$$

The 1st cumulant vanishes because of Eq. (VI.38),

$$\frac{\lambda^{1/2}}{N} \sum_{a=1}^n \langle (-\beta H[\{S_a\}]) \rangle_{\epsilon,0} = -\frac{\sqrt{\lambda}}{N} \frac{J}{\sqrt{c/\alpha}} \sum_a \sum_{\blacksquare} \langle \prod_{j \in \partial \blacksquare} S_j^a \rangle_{\epsilon,0} = 0. \quad (\text{VI.66})$$

Note that in the averages $\langle \dots \rangle_{\epsilon,0}$ (see Eq. (VI.37)) spins at different sites i are mutually indecent from each other so that $\langle \prod_{j \in \partial \blacksquare} S_j^a \rangle_{\epsilon,0} = \prod_{j \in \partial \blacksquare} \langle S_j^a \rangle_{\epsilon,0}$.

The 2nd cumulant is evaluated as,

$$\begin{aligned} &\frac{\lambda}{N} \sum_{a,b=1}^n (\langle (\beta H_a)(\beta H_b) \rangle_{\epsilon,0} - \langle (\beta H_a) \rangle_{\epsilon,0} \langle (\beta H_b) \rangle_{\epsilon,0}) \\ &= \lambda \frac{(\beta J)^2}{N(c/\alpha)} \sum_{a,b} \sum_{\blacksquare_1, \blacksquare_2} \left[\langle \prod_{j_1 \in \partial \blacksquare_1} S_{j_1}^a \prod_{j_2 \in \partial \blacksquare_2} S_{j_2}^b \rangle_{\epsilon,0} - \langle \prod_{j_1 \in \partial \blacksquare_1} S_{j_1}^a \rangle_{\epsilon,0} \langle \prod_{j_2 \in \partial \blacksquare_2} S_{j_2}^b \rangle_{\epsilon,0} \right] \\ &= \lambda \frac{(\beta J)^2}{N(c/\alpha)} \sum_{\blacksquare_1, \blacksquare_2} \sum_{a,b} q_{ab}^p \delta_{\blacksquare_1, \blacksquare_2} = \lambda \gamma (\beta J)^2 \sum_{a,b} q_{ab}^p \end{aligned} \quad (\text{VI.67})$$

Note that terms with $\blacksquare_1 \neq \blacksquare_1$ cannot survive because odd moments vanish Eq. (VI.38). Finally we used Eq. (III.2) which implies $N_{\blacksquare} = N\gamma(c/\alpha)$

There are three kinds of contributions to higher order cumulants,

- For the 4th order cumulant, the obvious one comes from the case that $\blacksquare_1 = \blacksquare_2 = \blacksquare_3 = \blacksquare_4$,

$$\frac{\lambda^2}{c/\alpha}(\beta J)^2 \sum_{a,b,c,d} \frac{1}{N(c/\alpha)} \sum_{\blacksquare} \prod_{j \in \partial \blacksquare} \langle S_j^a S_j^b S_j^c S_j^d \rangle_{\epsilon,0}^c = O((c/\alpha)^{-1}) \quad (\text{VI.68})$$

Thus this contribution vanishes in the dense limit $c \rightarrow \infty$. Obviously analogous terms which appear in higher order cumulants, vanish even more rapidly in the dense limit $c \rightarrow \infty$.

- Another contribution at the 4th order cumulant, which contributes to $G_2(\hat{\epsilon})$, is due to a connected diagram in which one spin is shared by two factor nodes, i. e. one particle reducible ones. (see Fig. 53 in appendix L). Two replicas, say replicas a and b are attributed one factor node and the other two replicas c and d are attributed to the other factor node. This is exactly the analogue of the contribution to $G_2(h)$ discussed in sec. IVC1. Thus it becomes eliminated by the Legendre transformation to $F_2(\hat{q})$. Similarly, one particles reducible diagrams do not contribute to higher orders. The remaining possible contributions are those due to loop diagrams.
- Our graphs are locally tree-like and closed loops can be neglected (see sec. IIIA) so that contribution by loop diagrams are absent in our case.

For example, consider the diagram shown in Fig. 11 for $p = 2$ model which consists of 3 interactions. For each interaction we associate 1 replica. For a given node 0 (out of N possible nodes), there are c choices for i connected to 0 and $c - 1$ choices for j , different from i , connected to 0.

- If the loop is part of a random graph, the probability that an arbitrary chosen remaining (unconnected) arm of i is connected to one of the remaining arm of j is $\sim (c - 1)/N$. Then the over-all contribution of this type of diagram **associated with 2 replicas** is $(\beta J / \sqrt{c/\alpha})^6 \times c(c - 1) \times (c - 1)/N \sim (\beta J)^6/N$ which vanishes in the limit $N \rightarrow \infty$.

To sum up we find the interaction part of the free-energy as,

$$-\beta F_1[\hat{q}]/N = \frac{\gamma(\beta J)^2}{2} \sum_{a,b} q_{ab}^p \quad (\text{VI.69})$$

Thus including both the Ising and spherical models we find the total free-energy Eq. (VI.45) as,

$$-\beta F/N = \partial_n \text{ entropic part} \Big|_{n=0} + \partial_n \frac{\gamma(\beta J)^2}{2} \sum_{a,b} q_{ab}^p \Bigg|_{n=0} \quad (\text{VI.70})$$

The internal energy is obtained as,

$$\beta e = -\beta \frac{\partial}{\partial \beta} (-\beta F/N) = \left(-\beta \frac{\partial}{\partial \beta} \right) \partial_n \frac{\gamma(\beta J)^2}{2} \sum_{a,b} q_{ab}^p \Bigg|_{n=0} \quad (\text{VI.71})$$

3. Total free-energy, variational equation and the Hessian matrix

- Ising model

$$\begin{aligned} -\beta F_n[\hat{q}]/N &= -\frac{1}{2} \sum_{a \neq b} \epsilon_{ab}^* q_{ab} + \ln e^{\frac{1}{2} \sum_{a \neq b} \epsilon_{ab}^* \frac{\partial^2}{\partial h_a \partial h_b}} \prod_{c=1}^n 2 \cosh(h_c) \Big|_{h=0} + \frac{\gamma(\beta J)^2}{2} \sum_{a,b} q_{ab}^p \\ &= -\frac{1}{2} \sum_{a,b} \epsilon_{ab}^* q_{ab} + \ln e^{\frac{1}{2} \sum_{a,b} \epsilon_{ab}^* \frac{\partial^2}{\partial h_a \partial h_b}} \prod_{c=1}^n 2 \cosh(h_c) \Big|_{h=0} + \frac{\gamma(\beta J)^2}{2} \sum_{a,b} q_{ab}^p \end{aligned} \quad (\text{VI.72})$$

where $\hat{\epsilon}^* = \epsilon_0^*[\hat{q}]$ is given by Eq. (VI.48) or Eq. (VI.57). We also assumed assumed $q_{aa} = 1$ in the last equation. Taking a derivative we find

$$\frac{\partial}{\partial q_{a < b}}(-\beta F_n[\hat{q}]/N) = -\epsilon_{ab}^* + \gamma(\beta J)^2 p q_{ab}^{p-1} \quad (\text{VI.73})$$

At the saddle point $0 = \frac{\partial}{\partial q_{a < b}}(-\beta F_n[\hat{q}]/N)$ we find

$$\epsilon_{ab}^{**} = \gamma(\beta J)^2 p q_{ab}^{p-1} \quad a \neq b, \quad (\text{VI.74})$$

Here and in the following

$$\frac{\partial}{\partial q_{a < b}} = \frac{\partial}{\partial q_{ab}} + \frac{\partial}{\partial q_{ba}} \quad (\text{VI.75})$$

since the matrix \hat{q} is symmetric.

Using Eq. (VI.74) in the last equation of Eq. (VI.72) we obtain

$$-\beta F_n[\hat{q}]/N = -\frac{\gamma(\beta J)^2}{2}(p-1) \sum_{a,b} q_{ab}^p + \ln e^{\frac{1}{2} \sum_{a,b} \epsilon_{ab}^{**} \frac{\partial^2}{\partial h_a \partial h_b}} \prod_{c=1}^n 2 \cosh(h_c) \Big|_{h=0} \quad (\text{VI.76})$$

Taking a derivative of the free-energy we find,

$$\frac{\partial}{\partial q_{a < b}}(-\beta F_n[\hat{q}]/N) = -\gamma(\beta J)^2 p(p-1) q_{ab}^{p-1} + \gamma(\beta J)^2 p(p-1) q_{ab}^{p-2} \langle S_a S_b \rangle_{\epsilon^{**}} \quad (\text{VI.77})$$

where $\langle \dots \rangle_\epsilon$ is the one defined by Eq. (VI.37) (see also Eq. (VI.54)),

$$\begin{aligned} \lim_{n \rightarrow 0} \langle S_a S_b \rangle_\epsilon &= \lim_{n \rightarrow 0} \frac{\partial}{\partial \epsilon_{ab}} \ln e^{\sum_{a < b} \epsilon_{ab} \frac{\partial^2}{\partial h_a \partial h_b}} \prod_c (2 \cosh(h_c)) \Big|_{h=0} \\ &= \lim_{n \rightarrow 0} \frac{\partial^2}{\partial h_a \partial h_b} e^{\sum_{a < b} \epsilon_{ab} \frac{\partial^2}{\partial h_a \partial h_b}} \prod_c (2 \cosh(h_c)) \Big|_{h=0} = q_{ab} \end{aligned} \quad (\text{VI.78})$$

Taking another derivative, we obtain the Hessian matrix as,

$$\begin{aligned} -M_{a \neq b, c \neq d} &= \frac{\partial^2}{\partial q_{a < b} \partial q_{c < d}}(-\beta F_n[\hat{q}]/N) \\ &= \left[-\gamma(\beta J)^2 p(p-1)^2 q_{ab}^{p-2} + \gamma(\beta J)^2 p(p-1)(p-2) q_{ab}^{p-3} \langle S_a S_b \rangle_{\epsilon^{**}} \right] (\delta_{ac} \delta_{bd} + \delta_{ad} \delta_{bc}) \\ &\quad + \left(\gamma(\beta J)^2 p(p-1) \right)^2 q_{ab}^{p-2} q_{cd}^{p-2} \langle S_a S_b S_c S_d \rangle_{\epsilon^{**}} \\ &= -2\gamma(\beta J)^2 p(p-1) q_{ab}^{p-2} \left[\frac{\delta_{ac} \delta_{bd} + \delta_{ad} \delta_{bc}}{2} - \frac{\gamma(\beta J)^2 p(p-1) q_{cd}^{p-2}}{2} \langle S_a S_b S_c S_d \rangle_{\epsilon^{**}}^c \right] \end{aligned} \quad (\text{VI.79})$$

where

$$\begin{aligned} \lim_{n \rightarrow 0} \langle S_a S_b S_c S_d \rangle_{\epsilon^*}^c &= \lim_{n \rightarrow 0} \frac{\partial^2}{\partial \epsilon_{ab} \partial \epsilon_{cd}} \ln e^{\sum_{a < b} \epsilon_{ab} \frac{\partial^2}{\partial h_a \partial h_b}} \prod_c (2 \cosh(h_c)) \Big|_{h=0} \\ &= \lim_{n \rightarrow 0} \frac{\partial^2}{\partial h_a \partial h_b} \frac{\partial^2}{\partial h_c \partial h_d} e^{\sum_{a < b} \epsilon_{ab} \frac{\partial^2}{\partial h_a \partial h_b}} \prod_c (2 \cosh(h_c)) \Big|_{h=0} - q_{ab} q_{cd} \end{aligned} \quad (\text{VI.80})$$

- Spherical model

$$\begin{aligned} -\beta F_n[\hat{q}]/N &= \frac{n}{2} + \frac{n}{2} \ln(2\pi) + \frac{1}{2} \ln \det \hat{q} \\ &\quad + \frac{\gamma(\beta J)^2}{2} \sum_{a,b} q_{ab}^p \end{aligned} \quad (\text{VI.81})$$

Taking derivatives of the free-energy we find ⁵,

$$\frac{\partial}{\partial q_{a**}} (-\beta F_n[\hat{q}]/N) = (q^{-1})_{ab} + \gamma(\beta J)^2 p q_{ab}^{p-1} \quad (\text{VI.82})**$$

and the Hessian matrix⁶

$$\begin{aligned} M_{a \neq b, c \neq d} &= \frac{\partial^2}{\partial q_{a**} \partial q_{c<d}} (\beta F_n[\hat{q}]/N) \\ &= (q^{-1})_{ac}(q^{-1})_{bd} + (q^{-1})_{ad}(q^{-1})_{bc} - \gamma(\beta J)^2 p(p-1) q_{ab}^{p-2} (\delta_{ac}\delta_{bd} + \delta_{ad}\delta_{bc}) \end{aligned} \quad (\text{VI.83})**$$

4. Models with quenched disorder

The models with quenched disorder introduced in sec. III A 5 lead to *exactly* the same free-energy expressions in terms of the glass order parameter q_{ab} , including both the strong quenched disorder limit $\lambda = 0$ and disorder-free limit $\lambda = \sqrt{c/\alpha}$ in Eq. (III.11). One can see in the cumulant expansion to obtain the interaction part of the free-energy that, in the 2nd order term Eq. (VI.67), 'self-generated disorder' and 'quenched disorder' act additively [15].

Comparing the distribution of the global coupling used in the conventional p -spin mean-field glass models Eq. (III.18) with ours Eq. (III.11) one would notice a difference. This is due to the self-generated disorder which is not took into account in previous studies.

Show here the phase diagram similar to Fig. 6 but with horizontal axis $j_0/J \rightarrow \lambda/\sqrt{c/\alpha}$.

The scaling used for the intermediately disordered systems Eq. (III.11) (or Eq. (III.18)) is useful to study competition between the ferromagnetic state and paramagnetic-glass states. One can write down free-energy in terms of the glass order parameter q_{ab} as well as the ferromagnetic order parameter m [15]. With $\lambda = O(1)$, the energy scale for the ferromagnetism is brought down to that of the glass.

In the case of $p = 2$, we have seen that the paramagnetic state $m = 0$ becomes unstable. Thus in this case one has to use strongly disordered model like the SK model [22] to study glass physics. ⁷

D. M -component vectorial p -spin models with a generic potential

Here we set up for the replica theory [15] for the M -component vectorial spin models introduced in sec. IIIC which are relevant for vectorial CSPs and inference problems as discussed in sec. IIIE. Here we consider the case of continuous spins which meet the constraint Eq. (III.22).

$$H[\{S\}] = \sum_{\blacksquare} v(r_{\blacksquare}) \quad r_{\blacksquare} = \frac{1}{\sqrt{M}} \sum_{\mu=1}^M \underbrace{\prod_{j \in \blacksquare} S_j^\mu}_{p-body} \quad (\text{VI.84})$$

⁵ This can be obtained using the formula in appendix A. Note that $\partial q_{a<b} = \partial q_{ab} + \partial q_{ba}$ since the matrix \hat{q} is symmetric as written in Eq. (VI.75).

⁶ Here we use the following. From $A(x)^{-1}A(x) = I$, one finds $(d/dx)A^{-1} = -A^{-1}(dA/dx)A^{-1}$.

⁷ In [15] stability of the system against the ferromagnetic transition was examined using the free-energy $F[\hat{q}, m]$. It was found $\partial^2 F[\hat{q}, m]/\partial q_{ab} \partial m = 0$ for $p > 2$. Thus the stability against the ferromagnetic transition is solely determined by $\partial^2 F^2[\hat{q}, m]/\partial m^2|_{m=0} = 1$ which is positive. Thus the paramagnetic (possibly glassy) state $m = 0$ is always metastable.

1. Entropic part of the free-energy

The entropic part of the free-energy is obtained as,

$$-\beta F_{n,0}[\hat{q}]/NM = \frac{n}{2} + \frac{n}{2} \ln(2\pi) + \frac{1}{2} \ln \det \hat{q} \quad (\text{VI.85})$$

2. Interaction part of the free-energy

It is convenient to introduce a Fourier transform,

$$e^{-\beta v(x)} = \int \frac{d\kappa}{2\pi} e^{i\kappa x} Z_\kappa \quad (\text{VI.86})$$

Then we can write,

$$\langle e^{-\beta \sum_{a=1}^n H[\{S^a\}]} \rangle_{\epsilon,0} = \prod_{\blacksquare} \prod_{a=1}^n \left(\int \frac{d\kappa_{\blacksquare}^a}{2\pi} Z_{\kappa_{\blacksquare}^a} \right) \left\langle \exp \left[\sum_{\blacksquare} \sum_a \frac{i\kappa_{\blacksquare}^a}{\sqrt{M}} \sum_{\mu=1}^M \prod_{j \in \blacksquare} (S_j^\mu)^a \right] \right\rangle_{\epsilon,0} \quad (\text{VI.87})$$

We need to evaluate the cumulant expansion

$$\begin{aligned} & \ln \left\langle \exp \left[\sum_{\blacksquare} \sum_a \frac{i\kappa_{\blacksquare}^a}{\sqrt{M}} \sum_{\mu=1}^M \prod_{j \in \blacksquare} (S_j^\mu)^a \right] \right\rangle_{\epsilon,0} \\ &= \sum_{\blacksquare} \sum_a \frac{i\kappa_{\blacksquare}^a}{\sqrt{M}} \sum_{\mu=1}^M \langle \prod_{j \in \blacksquare} (S_j^\mu)^a \rangle_{\epsilon,0} \\ &+ \frac{1}{2} \sum_{\blacksquare_1, \blacksquare_2} \sum_{a,b} \frac{i\kappa_{\blacksquare_1}^a}{\sqrt{M}} \sum_{\mu_1=1}^M \frac{i\kappa_{\blacksquare_2}^b}{\sqrt{M}} \sum_{\mu_2=1}^M \underbrace{\langle \prod_{j_1 \in \blacksquare_1} (S_{j_1}^{\mu_1})^a \prod_{j_2 \in \blacksquare_2} (S_{j_2}^{\mu_2})^b \rangle_{\epsilon,0}^c}_{q_{ab}^p \delta_{\blacksquare_1, \blacksquare_2} \delta_{\mu_1, \mu_2}} + \dots \end{aligned} \quad (\text{VI.88})$$

The 1st cumulant vanish. For the 2nd cumulant we find

$$\begin{aligned} & \sum_{\blacksquare_1, \blacksquare_2} \sum_{a,b} \frac{i\kappa_{\blacksquare_1}^a}{\sqrt{M}} \sum_{\mu_1=1}^M \frac{i\kappa_{\blacksquare_2}^b}{\sqrt{M}} \sum_{\mu_2=1}^M \underbrace{\langle \prod_{j_1 \in \blacksquare_1} (S_{j_1}^{\mu_1})^a \prod_{j_2 \in \blacksquare_2} (S_{j_2}^{\mu_2})^b \rangle_{\epsilon,0}^c}_{q_{ab}^p \delta_{\blacksquare_1, \blacksquare_2} \delta_{\mu_1, \mu_2}} \\ &= \sum_{\blacksquare} \sum_{a,b} (i\kappa_{\blacksquare}^a)(i\kappa_{\blacksquare}^b) q_{ab}^p \end{aligned} \quad (\text{VI.89})$$

Contributions of higher order terms can be neglected similarly to the scalar model discussed in sec. [VIC 2](#). To sum up, we find the interaction part of the free-energy as,

$$\begin{aligned} -\beta F_{n,1}[\hat{q}] &= \ln \prod_{\blacksquare, a} \int \frac{d\kappa_{\blacksquare}^a}{2\pi} e^{\sum_{\blacksquare} \frac{1}{2} \sum_{a,b} q_{ab}^p (i\kappa_{\blacksquare}^a)(i\kappa_{\blacksquare}^b)} \prod_{\blacksquare, a} \int dh_{\blacksquare}^a e^{-i\kappa_{\blacksquare}^a h_{\blacksquare}^a} e^{-\beta v(h_{\blacksquare}^a)} \\ &= \ln \prod_{\blacksquare, a} \int dh_{\blacksquare}^a \int \frac{d\kappa_{\blacksquare}^a}{2\pi} \left(e^{\frac{1}{2} \sum_{\blacksquare} \sum_{a,b} q_{ab}^p \frac{\partial^2}{\partial h_{\blacksquare}^a \partial h_{\blacksquare}^b}} e^{-i\kappa_{\blacksquare}^a h_{\blacksquare}^a} \right) e^{-\beta \sum_{\blacksquare} \sum_a v(h_{\blacksquare}^a)} \\ &= \ln \prod_{\blacksquare, a} \int dh_{\blacksquare}^a \underbrace{\int \frac{d\kappa_{\blacksquare}^a}{2\pi} e^{-i\kappa_{\blacksquare}^a h_{\blacksquare}^a}}_{\delta(h_{\blacksquare}^a)} e^{\frac{1}{2} \sum_{\blacksquare} \sum_{a,b} q_{ab}^p \frac{\partial^2}{\partial h_{\blacksquare}^a \partial h_{\blacksquare}^b}} \prod_{\blacksquare, a} e^{-\beta \sum_{\blacksquare} \sum_a v(h_{\blacksquare}^a)} \\ &= \ln \left[e^{\frac{1}{2} \sum_{a,b} q_{ab}^p \frac{\partial^2}{\partial h^a \partial h^b}} e^{-\beta \sum_a v(h^a)} \Big|_{h=0} \right]^{N_{\blacksquare}} \end{aligned} \quad (\text{VI.90})$$

where we repeated integrations by parts to derive the 3rd equation. To sum up we obtain,

$$-\beta F_{n,1}[\hat{q}]/NM = \gamma \ln e^{\frac{1}{2} \sum_{a,b} q_{ab}^p \frac{\partial^2}{\partial h^a \partial h^b}} e^{-\beta \sum_a v(h^a)} \Big|_{h=0} \quad (\text{VI.91})$$

where we used $N_{\blacksquare} = \gamma NM$.

3. Total free-energy

$$-\beta F_n[\hat{q}]/NM = \frac{n}{2} + \frac{n}{2} \ln(2\pi) + \frac{1}{2} \ln \det \hat{q} + \gamma \ln e^{\frac{1}{2} \sum_{a,b} q_{ab}^p \frac{\partial^2}{\partial h^a \partial h^b}} e^{-\beta \sum_a v(h^a)} \Big|_{h=0} \quad (\text{VI.92})$$

Taking derivatives of the free-energy we find,

$$\frac{\partial}{\partial q_{ab}} (-\beta F_n[\hat{q}]/N) = (q^{-1})_{ab} + \gamma p q_{ab}^{p-1} \langle \Pi_a \Pi_b \rangle_{\epsilon^*} \quad (\text{VI.93})$$

and the Hessian matrix,

$$\begin{aligned} M_{a \neq b, c \neq d} &= \frac{\partial^2}{\partial q_{a< b} \partial q_{c< d}} (\beta F_n[\hat{q}]/N) \\ &= (q^{-1})_{ac} (q^{-1})_{bd} + (q^{-1})_{ad} (q^{-1})_{bc} \\ &\quad - \gamma p (p-1) q_{ab}^{p-2} (\delta_{ac} \delta_{bd} + \delta_{ad} \delta_{bc}) \frac{\partial^2}{\partial h_a \partial h_b} e^{\frac{1}{2} \sum_{a,b} q_{ab}^p \frac{\partial^2}{\partial h^a \partial h^b}} e^{-\beta \sum_a v(h^a)} \Big|_{h=0} \\ &\quad - \gamma p^2 q_{ab}^{p-1} q_{cd}^{p-1} \frac{\partial^2}{\partial h_a \partial h_b} \frac{\partial^2}{\partial h_c \partial h_d} e^{\frac{1}{2} \sum_{a,b} q_{ab}^p \frac{\partial^2}{\partial h^a \partial h^b}} e^{-\beta \sum_a v(h^a)} \Big|_{h=0} \\ &= (q^{-1})_{ac} (q^{-1})_{bd} - (q^{-1})_{ad} (q^{-1})_{bc} \\ &\quad - \gamma p (p-1) q_{ab}^{p-2} \langle \Pi_a \Pi_b \rangle_{\epsilon^*} (\delta_{ac} \delta_{bd} + \delta_{ad} \delta_{bc}) \\ &\quad - \gamma p^2 q_{ab}^{p-1} q_{cd}^{p-1} \langle \Pi_a \Pi_b \Pi_c \Pi_d \rangle_{\epsilon^*} \end{aligned} \quad (\text{VI.94})$$

where we defined

$$\Pi = (e^{-\beta v(h)})' / e^{-\beta v(h)} \quad (\text{VI.95})$$

and $\langle \dots \rangle_{\epsilon^*}$ is the one defined by Eq. (VI.37).

In the case of linear potential $v(x) = -J(x)$ we find

$$-\beta F_n[\hat{q}]/NM = \frac{n}{2} + \frac{n}{2} \ln(2\pi) + \frac{1}{2} \ln \det \hat{q} + \gamma e^{\frac{(\beta J)^2}{2} \sum_{a,b} q_{ab}^p} \quad (\text{VI.96})$$

which implies

$$-\beta f[\hat{q}] = -\partial_n \beta F_n[\hat{q}] \Big|_{n=0} / NM = \frac{1}{2} + \frac{1}{2} \ln(2\pi) + \frac{1}{2} \partial_n \ln \det \hat{q} \Big|_{n=0} + \frac{\gamma(\beta J)^2}{2} \partial_n \sum_{a,b} q_{ab}^p \Big|_{n=0} \quad (\text{VI.97})$$

Note that this agrees with Eq. (VI.81).

E. Density functional approach

Another strategy to derive the replicated free-energy is to use the density functional approach [15] (see appendix A of the latter) which closely follows the strategy used to derive replicated liquid theory for hard-spheres in large dimensional limit [56–58]. In [15], the replicated free-energy for the M -component vectorial models with generic potential (linear/non-linear) was derived both by the approach explained above and the density functional approach. Such density functional approach can also be applied for the scalar p -spin models.

VII. REPLICA SYMMETRIC (RS) SOLUTION

A. Scalar Ising p -spin model

1. RS solution

Here we consider the scalar p -spin models with Ising spins Eq. (VI.72).

For the RS ansatz ($k = 0$) we assume (see Eq. (VI.23)),

$$q_{ab} = (1 - q)\delta_{ab} + q \quad \epsilon_{ab} = \epsilon \quad (\text{VII.1})$$

Remember that we have introduced $q_{aa} = 1$ and ϵ_{aa} where the latter is arbitrary in the Ising case. (see sec. VIC 1). Here we made a simple choice. Using Eq. (VII.1) we find,

$$\sum_{a,b=1}^n q_{ab}^p = n(1 + (n - 1)q^p). \quad (\text{VII.2})$$

which is needed for the interaction part of the free-energy.

For the Ising model Eq. (VI.72) we find,

$$\sum_{a,b=1}^n \epsilon_{ab} q_{ab} = n(\epsilon + (n - 1)\epsilon q), \quad (\text{VII.3})$$

and (see Appendix D)

$$\begin{aligned} e^{\frac{\epsilon}{2} \sum_{a,b} \frac{\partial^2}{\partial h_a \partial h_b}} \prod_{c=1}^n 2 \cosh(h_c) \Big|_{h=0} &= e^{\frac{\epsilon}{2} \frac{\partial^2}{\partial h^2}} (2 \cosh(h))^n \Big|_{h=0} \\ &= \gamma_\epsilon \otimes (2 \cosh(h))^n = \int Dz (2 \cosh(\sqrt{\epsilon}z))^n \end{aligned} \quad (\text{VII.4})$$

The 1st equation is due to Eq. (D.3). In the 2nd and 3rd equations we used Eq. (D.7) and introduced the following notations

$$\gamma_a \otimes f(x) = \int Dz f(x - \sqrt{a}z) \quad (\text{VII.5})$$

and

$$\int Dz \dots \equiv \int_{-\infty}^{\infty} \frac{dz}{\sqrt{2\pi}} e^{-\frac{z^2}{2}} \dots \quad (\text{VII.6})$$

Collecting the above results, we find the last two equations of Eq. (VI.72) yield,

$$\begin{aligned} -\beta F_n^{\text{RS}}(q)/N &= -\frac{1}{2}n(\epsilon + (n - 1)\epsilon q) + \ln e^{\frac{\epsilon}{2} \frac{\partial^2}{\partial h^2}} (2 \cosh(h))^n \Big|_{h=0} \\ &\quad + \frac{\gamma(\beta J)^2}{2} n(1 + (n - 1)q^p) \end{aligned} \quad (\text{VII.7})$$

thus

$$\begin{aligned} -\beta f_{\text{RS}}(q) &= -\beta \partial_n F_n^{\text{RS}}(q)|_{n=0}/N \\ &= -\frac{1}{2}(\epsilon - \epsilon q) + \int Dz \log(2 \cosh(\sqrt{\epsilon}z)) + \frac{\gamma(\beta J)^2}{2}(1 - q^p) \\ &= \frac{\gamma(\beta J)^2}{2} + \frac{1}{2}\gamma(\beta J)^2(p - 1)q^p - \frac{\gamma(\beta J)^2}{2}pq^{p-1} + \int Dz \log(2 \cosh(\sqrt{\epsilon}z)) \end{aligned} \quad (\text{VII.8})$$

The last equation follows from the 1st one using Eq. (VII.11) shown below. Here $\epsilon = \epsilon(q)$ is given by,

$$q = \int Dz \tanh^2(\sqrt{\epsilon}z) \quad (\text{VII.9})$$

which follow from Eq. (VI.57) or taking a derivative ∂_ϵ of the 2nd equation of Eq. (VII.8)⁸. The saddle point equation

$$0 = \frac{d}{dq} \partial_n (-\beta F_n^{\text{RS}}(q)|_{n=0})/N \Big|_{q=q^*} \quad (\text{VII.10})$$

leads to

$$\epsilon = \gamma(\beta J)^2 pq^{p-1} \quad (\text{VII.11})$$

Using this in Eq. (VII.9) we find the self-consistent equation for q ,

$$q = \int Dz \tanh^2(\sqrt{\gamma(\beta J)^2 pq^{p-1}} z). \quad (\text{VII.12})$$

The internal energy is obtained as,

$$\frac{e}{J} = \frac{\partial}{\partial(\beta J)} \beta f_{\text{RS}}(q) = -\gamma(\beta J)(1 - q^p) \quad (\text{VII.13})$$

The Hessian matrix Eq. (VI.79) becomes

$$M_{a \neq b, c \neq d} = \gamma(\beta J)^2 p(p-1)q^{p-2} [\delta_{ac}\delta_{bd} + \delta_{ad}\delta_{bc}] - \left(\gamma(\beta J)^2 p(p-1)q^{p-2} \right)^2 (A(q) - q^2) \quad (\text{VII.14})$$

where

$$\begin{aligned} \lim_{n \rightarrow 0} A(q) &= \lim_{n \rightarrow 0} \frac{\partial^2}{\partial h_a \partial h_b} \frac{\partial^2}{\partial h_c \partial h_d} e^{\frac{\epsilon_0}{2} \sum_{a,b=1}^n \frac{\partial^2}{\partial h_a \partial h_b}} \prod_c (2 \cosh(h_c)) \Big|_h \\ &= \gamma_\epsilon \otimes \left\{ (\delta_{ac}\delta_{bd} + \delta_{ad}\delta_{bc}) \right. \\ &\quad + [\delta_{ac} + \delta_{bc} + \delta_{ad} + \delta_{bd} - 2(\delta_{ad}\delta_{bc} + \delta_{ac}\delta_{bd})] \tanh^2(h) \\ &\quad \left. + [1 - (\delta_{ac} + \delta_{bc} + \delta_{ad} + \delta_{bd}) + (\delta_{ad}\delta_{bc} + \delta_{ac}\delta_{bd})] \tanh^4(h) \right\} \end{aligned} \quad (\text{VII.15})$$

where we used Eq. (D.9). As explained in sec K, this implies,

$$\lambda_R = M_1 = 2\gamma(\beta J)^2 p(p-1)q^{p-2} \left\{ 1 - \gamma(\beta J)^2 p(p-1)q^{p-2} \int Dz (1 - \tanh^2(\sqrt{\epsilon}z))^2 \right\} \quad (\text{VII.16})$$

For convenience let us introduce normalized replicon eigen-value

$$\tilde{\lambda}_R = 1 - \gamma(\beta J)^2 p(p-1)q^{p-2} \int Dz (1 - \tanh^2(\sqrt{\epsilon}z))^2. \quad (\text{VII.17})$$

Thus stability of the RS solution requires⁹

$$\frac{1}{\gamma(\beta J)^2 p(p-1)q^{p-2}} > \int Dz \operatorname{sech}^4(\Xi) \quad \Xi = \sqrt{\gamma(\beta J)^2 pq^{p-1}} z \quad (\text{VII.18})$$

This is the so called d'Almeida-Thouless condition [55].¹⁰ We see that $q = 0$ is always a solution of Eq. (VII.11) for $p > 1$. The free-energy is obtained as,

$$-\beta f_{\text{RS}}(q=0) = \ln 2 + \frac{\gamma}{2}(\beta J)^2 \quad (\text{VII.19})$$

which is independent of p . For $p > 2$, we find that the $q = 0$ solution always satisfies (marginally) the AT condition Eq. (VII.18) so that glass transition(s), if any, should take place in discontinuous ways.

Note that the free-energy Eq. (VII.8) expanded around $q = 0$ becomes,

$$-\beta f_{\text{RS}}(q) = \log 2 + \frac{\gamma(\beta J)^2}{2} + \frac{\gamma(\beta J)^2}{2}(p-1)q^p - \frac{(\gamma(\beta J)^2)^2}{4}p^2q^{2(p-1)} + O(q^{4(p-1)}) + \dots \quad (\text{VII.20})$$

so that $\beta f_{\text{RS}}(q)$ is locally 'maximum' at $q = 0$ for $p = 2$ at $T > T_c$ and for $p > 2$ at all temperatures! This does not mean instability of the $q = 0$ solution. The confusion is fixed by recalling that one has to study the stability through the Hessian matrix in $n \rightarrow 0$ dimensional space as done above.

⁸ Derivation becomes easier considering $0 = \partial_\epsilon(-\beta F_n^{\text{RS}}(q)/N)$, with the expression Eq. (VII.7). We find $\partial_\epsilon e^{\frac{\epsilon}{2} \partial_h^2} (2 \cosh(h))^n = \frac{n}{2} e^{\frac{\epsilon}{2} \partial_h^2} (2 \cosh(h))^n [1 + (n-1) \tanh^2(h)] \xrightarrow{n \rightarrow 0} \frac{n}{2} e^{\frac{\epsilon}{2} \partial_h^2} (1 - \tanh^2(h)) = \frac{n}{2} \int Dz (1 - \tanh^2(\sqrt{\epsilon}z))$.

⁹ $\int Dz (1 - \tanh^2(\Xi))^2 = \int Dz \cosh^{-4}(\Xi)$

¹⁰ From sec. K, we find $\lambda_L = \lambda_A = \lambda_R - M_2$. One can check that $-M_2 \propto \int Dz \tanh^2(\Xi) (1 - \tanh^2(\Xi))^2 > 0$ using the results shown above. Thus the replicon eigenvalue controls the stability of the RS ansatz.

2. SK model : $p = 2$ Ising

The RS solution $p = 2$ was analyzed by Sherrington-Kirkpatrick [22]. The equation of state Eq. (VII.12) reads in this case as

$$q = \int \frac{dz}{\sqrt{2\pi}} e^{-\frac{z^2}{2}} \tanh^2(h_{\text{ext}} + \sqrt{\epsilon}z) \quad \epsilon = 2\gamma(\beta J)^2 q \quad (\text{VII.21})$$

here we included the effect of weak external field h_{ext} . Assuming q, h_{ext} are small and using $\tanh(x) = x - x^3/3 + \dots$ and thus $\tanh^2(x) = x^2 - 2/3x^4 + \dots$ for small x and using $\langle z^2 \rangle_z = 1, \langle z^4 \rangle_z = 3$, we find,

$$q = h_{\text{ext}}^2 + \epsilon \langle z^2 \rangle_z - \frac{2}{3} \langle (h_{\text{ext}} + z\sqrt{\epsilon})^4 \rangle_z + \dots = h_{\text{ext}}^2 + (\sqrt{2\gamma}\beta J)^2 q - 2(\sqrt{2\gamma}\beta J)^4 q^2 + \dots \quad (\text{VII.22})$$

Under zero external magnetic field $h_{\text{ext}} = 0$ we find from the AT condition Eq. (VII.18) that the $q = 0$ paramagnetic solution is stable only at $T > T_c$, with

$$k_B T_c / J = \sqrt{2\gamma}. \quad (\text{VII.23})$$

Note that vanishing of the eigen values of the Hessian matrix means divergence of the glass susceptibility. Then we find a continuous emergence of a finite glass order parameter passing T_c ,

$$q = \frac{(\sqrt{2\gamma}\beta J)^2 - 1}{2(\sqrt{2\gamma}\beta J)^4} \simeq 1 - \frac{T}{T_c}. \quad (\text{VII.24})$$

Under small magnetic field we find,

$$q = \chi_{\text{SG}} h_{\text{ext}}^2 \quad \chi_{\text{SG}} = \frac{1}{1 - 2\gamma(\beta J)^2} \quad (\text{VII.25})$$

suggesting a glass transition signaled by divergence of the spinglass susceptibility χ_{SG} approaching the spinglass transition temperature $T \rightarrow T_c^+$. Similarly one can observe

$$\begin{aligned} m &= \int \frac{dz}{\sqrt{2\pi}} e^{-\frac{z^2}{2}} \tanh(h_{\text{ext}} + \sqrt{\epsilon}z) = h_{\text{ext}} - \frac{1}{3} h_{\text{ext}}^3 - h_{\text{ext}} 2\gamma(\beta J)^2 q + \dots \\ &= h_{\text{ext}} - \frac{1}{3} h_{\text{ext}}^3 - 2\gamma(\beta J)^2 \chi_{\text{SG}} h_{\text{ext}}^3 + \dots \end{aligned}$$

Thus the non-linear susceptibility is proportional to the spinglass susceptibility χ_{SG} and diverges negatively as $T \rightarrow T_c^+$. These observations suggest that the spinglass transition is a second order phase transition.

However one can show that the $q > 0$ RS solution actually violates the AT condition Eq. (VII.18) [55] so that we have to consider breaking of the replica symmetry as can be seen in Fig. 19 b) where we show the normalized replicon eigenvalue $\tilde{\lambda}_R$ Eq. (VII.17).

3. Random Energy Model (RSM) : $p = \infty$ Ising

The random energy model corresponds to $p \rightarrow \infty$ as discussed in sec. V A. Note that in the $p \rightarrow \infty$ limit, the equation of state Eq. (VII.12) only admits $q = 0$ and 1 as possible solutions.

The free-energy of the RS ansatz with $q = 0$ obtained as Eq. (VII.19) agrees with the free-energy of in the paramagnetic phase $T > T_c$ Eq. (V.19).

The free-energy of the RS ansatz with $q = 1$, in $p \rightarrow \infty$ limit, can be obtained as,

$$-\beta f_{\text{RS}}(q = 1) = \ln 2 + \frac{\gamma}{2}(\beta J)^2 \quad (\text{VII.26})$$

which is the same as Eq. (VII.19). (We do not show the details of the derivation here but it is the same for the 1RSB solution with $m \rightarrow 1$ discussed in sec. VIII A 2.) But we know that below T_c , the free-energy of the REM becomes $-\beta F/N = -\beta J e_{\min}$ with $e_{\min} = -\sqrt{2\gamma \ln 2}$ (see Eq. (V.20) and Eq. (V.13)). Thus apparently the RS solution with $q = 1$ does not give the correct answer.

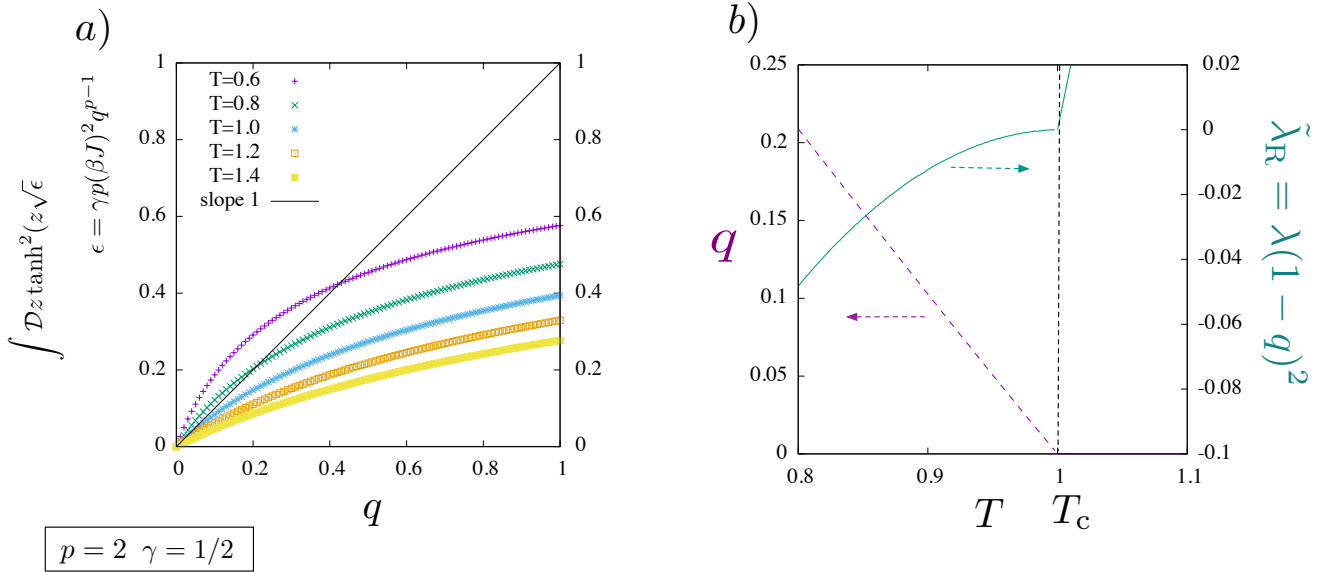


FIG. 19. RS solution of the $p = 2$ Ising model. a) Graphical representation of the saddle point equation for q . Here $\gamma = 1/2$. The curves are the r.h.s of Eq. (VII.21) and the solutions of the saddle point equation is given by the crossing points between these curves and the straight line with slope 1. At $T < T_c$ with $T_c = 1.0$, $q > 0$ solution emerge continuously. b) Temperature dependence of the stable $q > 0$ solution and the value of the normalized eigen-value λ_R Eq. (VII.17) of the solution.

B. Scalar spherical p -spin model

Here we consider the scalar p -spin models with spherical spins Eq. (VI.81). The RS ansatz is given by Eq. (VII.1),

$$q_{ab} = (1 - q)\delta_{ab} + q \quad (\text{VII.27})$$

Then using Eq. (B.2) we find Eq. (VI.81) becomes,

$$\ln \det \hat{q} = \ln[1 + (n - 1)q] + (n - 1) \ln(1 - q). \quad (\text{VII.28})$$

Thus we find, neglecting constant terms,

$$-\beta f_{\text{RS}}(q) = -\beta \partial_n F_n^{\text{RS}}(q)|_{n=0}/N = \frac{1}{2} \left(\frac{q}{1-q} + \ln(1-q) \right) + \frac{\gamma(\beta J)^2}{2} (1 - q^p) \quad (\text{VII.29})$$

The self-consistent equation for the order parameter q is found as,

$$0 = \frac{q}{(1-q)^2} - \gamma(\beta J)^2 p q^{p-1} \quad (\text{VII.30})$$

which implies $q = 0$ is always a solution for $p > 1$.

The Hessian matrix Eq. (VI.83) becomes with the RS ansatz Eq. (VII.1),

$$M_{a \neq b, c \neq d} = \left[\frac{1}{(1-q)^2} - \gamma(\beta J)^2 p(p-1)q^{p-2} \right] (\delta_{ac}\delta_{bd} + \delta_{ad}\delta_{bc}) + \dots \quad (\text{VII.31})$$

where we used the inverse of the inverse of q_{ab} is,

$$q_{ab}^{-1} = \frac{1}{1-q}\delta_{ab} - \frac{q}{1 + (n-2)q - (n-1)q^2} \xrightarrow{n \rightarrow 0} \frac{1}{1-q}\delta_{ab} - \frac{q}{(1-q)^2} \quad (\text{VII.32})$$

Thus we find the replicon eigen value as,

$$\lambda_R = \frac{1}{(1-q)^2} \left\{ 1 - \gamma(\beta J)^2 p(p-1)(1-q)^2 q^{p-2} \right\} \quad (\text{VII.33})$$

This implies $q = 0$ solution is always stable for $p > 2$. Note that from Eq. (VII.29) one finds $d^2/dq^2\beta df_{\text{RS}}(q)|_{q=0} = -1/2 < 0$ for $p > 2$ but this does not mean instability of $q = 0$ solution. The stability of the solution must be examined through the analysis of the Hessian matrix in $n \rightarrow 0$ limit. We have made the same comment for the Ising model.

C. Vectorial p -spin models

1. RS solution

We assume the RS ansatz

$$q_{ab} = (1 - q)\delta_{ab} + q \quad (\text{VII.34})$$

and evaluate the free-energy Eq. (VI.92).

To evaluate the entropic part of the free-energy, we find,

$$\ln \det \hat{q} = \ln[1 + (n - 1)q] + (n - 1) \ln(1 - q) \quad (\text{VII.35})$$

$$\begin{aligned} e^{\frac{1}{2} \sum_{a,b} q_{ab}^p \frac{\partial^2}{\partial h^a \partial h^b}} e^{-\beta \sum_c v(h^c)} \Big|_{h=0} &= e^{\frac{1}{2} q^p \sum_{a,b} \frac{\partial^2}{\partial h^a \partial h^b}} \prod_{c=1}^n g(h_c) \Big|_{h=0} \\ &= e^{\frac{1}{2} q^p \frac{\partial^2}{\partial h^2}} g^n(h) \Big|_{h=0} = \int \mathcal{D}z_0 g^n(\sqrt{q^p} z_0) \end{aligned} \quad (\text{VII.36})$$

where we introduced

$$g(h) = e^{\frac{(1-q^p)}{2} \frac{\partial^2}{\partial h^2}} e^{-\beta v(h)} = \int \mathcal{D}x e^{-\beta v(h+x)} \Big|_{x=\sqrt{1-q^p}z} \quad (\text{VII.37})$$

Let us also introduce,

$$f(h) = -\ln g(h) \quad (\text{VII.38})$$

Collecting the above results we obtain the variational free-energy within the RS ansatz as

$$\begin{aligned} -\beta f_{\text{RS}}(q) &= \partial_n (-\beta F_n^{\text{RS}}(q))|_{n=0}/N = \frac{1}{2} \left(\frac{q}{1-q} + \ln(1-q) \right) \\ &\quad + \frac{\alpha}{p} \int \mathcal{D}z_0 \ln g(\sqrt{q^p} z_0) \end{aligned} \quad (\text{VII.39})$$

where we have dropped off irrelevant constants.

The saddle point equation for the order parameter q is obtained as,^{11 12}

$$\begin{aligned} 0 &= \frac{\partial(-\beta f_{\text{RS}}(q))}{\partial q} = \frac{1}{2} \frac{q}{(1-q)^2} - \frac{\alpha}{p} \frac{pq^{p-1}}{2} \int \mathcal{D}z_0 (f'(x))^2 \Big|_{x=\sqrt{q^p}z_0} \\ &= \frac{1}{2} \frac{q}{(1-q)^2} \mathcal{G}(q) \end{aligned} \quad (\text{VII.40})$$

where we introduced

$$\mathcal{G}(q) \equiv 1 - \alpha(1-q)^2 q^{p-2} \int \mathcal{D}z_0 (f'(x))^2 \Big|_{x=\sqrt{q^p}z_0} \quad (\text{VII.41})$$

¹¹ Note that $f(h)$ also depends on q .

¹² The computation becomes easier by noting $\frac{\partial}{\partial \lambda} e^{\frac{\lambda}{2} \partial_h^2} (e^{\frac{1-\lambda}{2} \partial_h^2} e^{-\beta v(h)})^n = \frac{1}{2} n(n-1) e^{\frac{\lambda}{2} \partial_h^2} \left(e^{\frac{1-\lambda}{2} \partial_h^2} e^{-\beta v(h)} \right)^n \left(\frac{e^{\frac{1-\lambda}{2} \partial_h^2} (e^{-\beta v(h)})'}{e^{\frac{1-\lambda}{2} \partial_h^2} e^{-\beta v(h)}} \right)^2$ and take $n \rightarrow 0$ afterwards.

For $p > 1$, we find $q = 0$ is always a solution while non-zero solution $q \neq 0$ may be found solving $\mathcal{G}(q) = 0$.

The Hessian matrix Eq. (VI.94) becomes,

$$M_{a \neq b, c \neq d} = \frac{M_1}{2} (\delta_{ac}\delta_{bd} + \delta_{ad}\delta_{bc}) + \dots \quad (\text{VII.42})$$

with

$$\begin{aligned} \frac{M_1}{2} = & \left\{ \frac{1}{(1-q)^2} - \gamma p(p-1)q^{p-2} \int \mathcal{D}z_0 (f'(x))^2 \Big|_{x=\sqrt{q^p}z_0} \right. \\ & \left. - \gamma p^2 q^{2(p-1)} \int \mathcal{D}z_0 (f''(x))^2 \Big|_{x=\sqrt{q^p}z_0} \right\} + \dots \end{aligned} \quad (\text{VII.43})$$

where we used Eq. (D.8) and Eq. (D.9),

$$\begin{aligned} \frac{\partial^2}{\partial h_a \partial h_b} e^{\frac{q^p}{2} \sum_{a,b} \frac{\partial^2}{\partial h_a \partial h_b}} \prod_{c=1}^n \underbrace{e^{\frac{(1-q^p)}{2} \frac{\partial^2}{\partial h_c^2}} e^{-\beta v(h_c)}}_{g(h_c)} \Big|_{h_c=h} &= \gamma_{q^p} \otimes \begin{pmatrix} g'(h) \\ \underbrace{g(h)}_{-f'(h)} \end{pmatrix}^2 \\ \frac{\partial^2}{\partial h_a \partial h_b} \frac{\partial^2}{\partial h_c \partial h_d} e^{\frac{q^p}{2} \sum_{a,b} \frac{\partial^2}{\partial h_a \partial h_b}} \prod_{c=1}^n g(h_c) \Big|_{h_c=h} &= (\delta_{ac}\delta_{bd} + \delta_{ad}\delta_{bc}) \gamma_{q^p} \otimes (f''(h))^2 + \dots \end{aligned} \quad (\text{VII.44})$$

From the above expression we find the replicon eigen-value (see sec K) as

$$\lambda_R = M_1 \quad (\text{VII.45})$$

We see that $q = 0$ solution which always exist for $p > 1$ is stable for $p > 2$. For $p = 2$ there can be some α_c where the λ_R vanishes suggesting possibilities of continuous phase transitions.

2. hardcore potential

By using the hardcore potential for the vectorial p -spin model, we can study the family of constraint satisfaction problems of continuous variables discussed in sec. III E [15]. The special case $p = 1$ amounts to the analysis of the Gardner volume of the perceptron problem [32, 33].

For the hardcore potential

$$e^{-\beta v(x)} = \theta(\delta - x) \quad (\text{VII.46})$$

for which we find the function $g(h)$ defined by Eq. (VII.37) as,

$$g(h) = \Theta \left(\frac{\delta - h}{\sqrt{2(1-q^p)}} \right) \quad (\text{VII.47})$$

where we introduced,

$$\Theta(x) \equiv \int_{-\infty}^x \frac{dz}{\sqrt{\pi}} e^{-z^2} = \gamma_{1/2} \otimes \theta(x) = \frac{1}{2}(1 + \text{erf}(x)), \quad (\text{VII.48})$$

where $\text{erf}(x)$ is the error function,

$$\text{erf}(x) = \frac{2}{\sqrt{\pi}} \int_0^x \frac{dz}{\sqrt{\pi}} e^{-z^2}. \quad (\text{VII.49})$$

With this we find the RS free-energy given by Eq. (VII.39) as,

$$-\beta f_{\text{RS}}(q) = \frac{1}{2} \left(\frac{q}{1-q} + \ln(1-q) \right) + \frac{\alpha}{p} \int \mathcal{D}z_0 \ln \Theta \left(\frac{\delta - \sqrt{q^p}z}{\sqrt{2(1-q^p)}} \right) \quad (\text{VII.50})$$

The $q = 0$ solution always exist for $p > 1$. The saddle point equation for $q \neq 0$ becomes,

$$0 = \mathcal{G}(q) = 1 - \alpha(1-q)^2 q^{p-2} \frac{1}{2(1-q^p)} \int \mathcal{D}z_0 r^2(x) \Big|_{x=\frac{\delta-\sqrt{q^p}z_0}{\sqrt{2(1-q^p)}}} \quad (\text{VII.51})$$

or

$$\alpha = \alpha(q) \quad \alpha(q) = 2 \frac{1-q^p}{(1-q)^2 q^{p-2}} \frac{1}{\int \mathcal{D}z_0 r^2(x) \Big|_{x=\frac{\delta-\sqrt{q^p}z_0}{\sqrt{2(1-q^p)}}}} \quad (\text{VII.52})$$

where we introduced

$$r(x) \equiv \frac{\Theta'(x)}{\Theta(x)} = \frac{e^{-x^2}}{\sqrt{\pi}} / \Theta(x) \quad (\text{VII.53})$$

As shown in Fig. 20, q monotonically increases with α . The location of the jamming point where $q \rightarrow 1$ is obtained as,

$$\alpha_j(\delta) = \lim_{q \rightarrow 1} \alpha(q) = \lim_{q \rightarrow 1} \frac{2p}{1-q} \frac{1}{\int \mathcal{D}z_0 r^2(x) \Big|_{x=\frac{\delta-z_0}{\sqrt{2(1-q^p)}}}} = \frac{p^2}{\int_0^\infty \frac{dy}{\sqrt{2\pi}} e^{-(\delta+y)^2/2} y^2} \quad (\text{VII.54})$$

In the last equation we used the asymptotic behavior of the function $r(x)$ given in Eq. (G.5). For $\delta = 0$ we find in particular

$$\alpha_j(0) = 2p^2 \quad (\text{VII.55})$$

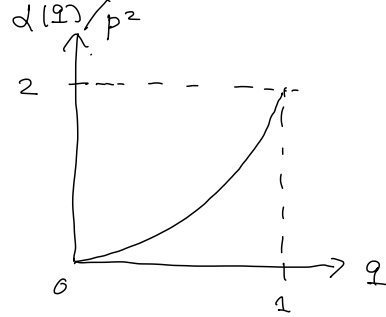


FIG. 20. Glass order parameter (RS) of the hardcore model for $\delta = 0$

3. hardcore $p = 1$ model: Perceptron

As we discussed in III F, the $p = 1$ model maps exactly to the perceptron problem studied by Gardner [32]. Here let us mention the interesting connection to the problem of dichotomy (see sec 6.2 of [59]): consider M points $\mu = 1, 2, \dots, M$ in N dimensional space which are colored black $S_0^\mu = 1$ or white $S_0^\mu = -1$. The coordinate of the μ -th point is given by $\mathbf{S}^\mu = (S_1^\mu, S_2^\mu, \dots, S_N^\mu)$. Then the coloring is called a *dichotomy* if there exists a hyperplane passing the origin which separates the points such that all black points are on one side of it and all white points are on the other side of it. Now consider the perceptron which satisfies Eq. (III.44). Clearly the hyperplane which is normal to the vector $\mathbf{J}^\mu = (J_1, J_2, \dots, J_N)$ is such a hyperplane.

In a mathematical analysis by Cover [60] the number of dichotomies $c(M, N)$ was evaluated under a weak assumption that the vectors \mathbf{S}^μ $\mu = 1, 2, \dots, M$ are linearly independent from each other. Cover found $c(M, N) = 2^{\sum_{i=0}^{N-1} M-i C_i}$ where $_n C_r = \binom{n}{r}$. It was shown that the probability that a random coloring of the M points produces a dichotomy $c(M, N)/2^M$ becomes $\theta(2 - \alpha)$ with $\alpha = M/N$ in $N \rightarrow \infty$ limit. Note that Gardner's analysis [32] which predicts $\alpha_j = 2$ discussed above agrees with this.

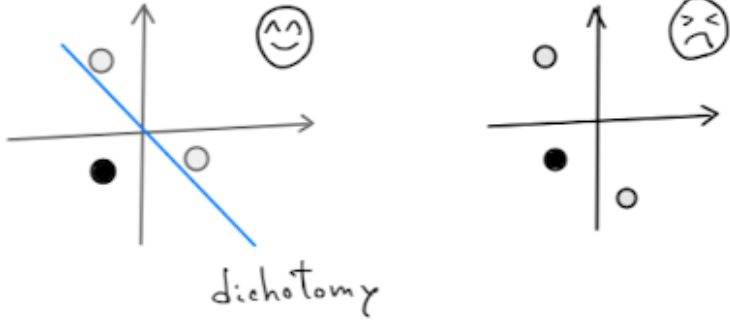


FIG. 21. $M = 3$ points in $N = 2$ dim space which are colored black and white. The case of dichotomy and the case which is not.

Interestingly the Cover's analysis shows that for *finite* N , $c(M, N)/2^M = 1$ for $\alpha < 1$ while $c(M, N)/2^M = O(e^{-N})$ in the range $1 < \alpha < 2$. This means there are instances which are *not* dichotomy below $\alpha_c = 2$ but they are *very rare*. The replica computation at $n = 0$ picks up the behaviour of the most probable instances (See VIA 5).

The RS solution for the perceptron problem (hardcore $p = 1$ model) is known to be stable for $\kappa \geq 0$ ($\delta \leq 0$) [32] (see sec III F for the correspondence). However RSB solutions emerge for $\kappa \leq 0$ ($\delta \geq 0$). The latter regime is interesting as it provides the simplest model with non-trivial jamming of the same universality classes as that of hard-spheres [34].

$p = 2$ model

In the figure shown below we show the phase diagram of the $p = 2$ hardcore model [15]. The upper solid line is $\alpha = \alpha_j(\delta)$ given by Eq. (VII.54), which is the jamming line within the RS ansatz. $q > 0$ RS solution emerges continuously at the lower curve which represents $\alpha = \alpha_c(\delta)$ which with the AT line at which the replicon eigenvalue λ_R (Eq. (VII.45)+Eq. (VII.44)). The dotted line is the jamming line obtained by the continuous continuous RSB solution which is discussed later.

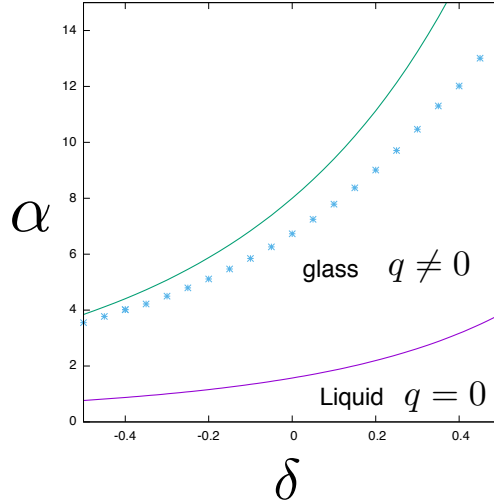


FIG. 22. The phase diagram of the $p = 2$ body hardcore model within the replica symmetric (RS) ansatz (Taken from [15])

VIII. GLASS TRANSITIONS WITH ONE STEP REPLICA SYMMETRY BREAKING (1RSB)

A. Scalar Ising p -spin models

1. 1RSB solution

For the 1RSB ansatz ($k = 1$) we assume (see Eq. (VI.23))

$$q_{ab} = (1 - q_1)\delta_{ab} + (q_1 - q_0)I_{ab}^m + q_0 \quad \epsilon_{ab} = (\epsilon_1 - \epsilon_0)I_{ab}^m + \epsilon_0 \quad (\text{VIII.1})$$

Rememeber again that ϵ_{aa} was arbitrary in the Ising case (see sec. VIC 1). Here we made a simple choise $\epsilon_{aa} = \epsilon_1$.

Using this we can evaluate the free-energy function of the Ising model Eq. (VI.72) and the spherical model Eq. (VI.81) within the 1RSB ansatz as the following. We find

$$\sum_{a,b=1}^n q_{ab}^p = n[1 + (m - 1)q_1^p + (n - m)q_0^p]. \quad (\text{VIII.2})$$

which is needed to evaluate the interaction part of the free-energy.

For the Ising model, we find,

$$\sum_{a,b=1}^n \epsilon_{ab} q_{ab} = n[\epsilon_1 + (m - 1)\epsilon_1 q_1 + (n - m)\epsilon_0 q_0], \quad (\text{VIII.3})$$

and

$$\begin{aligned} & e^{\frac{\epsilon_0}{2} \sum_{a,b} \frac{\partial^2}{\partial h_a \partial h_b}} \prod_{c=1}^{n/m} e^{\frac{(\epsilon_1 - \epsilon_0)}{2} \sum_{a,b \in C} \frac{\partial^2}{\partial h_a \partial h_b}} \prod_{c=1}^n 2 \cosh(h_c) \Big|_{h=0} = e^{\frac{\epsilon_0}{2} \frac{\partial^2}{\partial h^2}} \left(e^{\frac{(\epsilon_1 - \epsilon_0)}{2} \frac{\partial^2}{\partial h^2}} (2 \cosh(h))^m \right)^{n/m} \Big|_{h=0} \\ & = \gamma_{\epsilon_0} \otimes (\gamma_{\epsilon_1 - \epsilon_0} \otimes (2 \cosh(h))^m)^{n/m} = \int Dz_0 \left(\int Dz_1 (2 \cosh \Xi)^m \right)^{n/m} \end{aligned} \quad (\text{VIII.4})$$

where we introduced a shorthand notation

$$\Xi = h_{\text{ext}} + \sqrt{\epsilon_1 - \epsilon_0} z_1 + \sqrt{\epsilon_0} z_0 \quad (\text{VIII.5})$$

This is an generalization of Eq. (VII.4) in the replica symmetric computation. The hierarchical differentiation can be done using Eq. (D.4). Here we included external magnetic field h_{ext} .

Collecting the above results, we find the last two equations of Eq. (VI.72) yield,

$$\begin{aligned} & -\beta F_n^{\text{1RSB}}(q_1, q_0, m)/N \\ & = -\frac{1}{2} n[\epsilon_1 + (m - 1)\epsilon_1 q_1 + (n - m)\epsilon_0 q_0] + \ln e^{\frac{\epsilon_0}{2} \frac{\partial^2}{\partial h^2}} \left(e^{\frac{(\epsilon_1 - \epsilon_0)}{2} \frac{\partial^2}{\partial h^2}} (2 \cosh(h))^m \right)^{n/m} \Big|_{h=0} \\ & + \frac{\gamma(\beta J)^2}{2} n[1 + (m - 1)q_1^p + (n - m)q_0^p]. \end{aligned} \quad (\text{VIII.6})$$

so that

$$\begin{aligned} -\beta f_{\text{1RSB}}(q_1, q_0, m) & = -\beta \partial_n F_n^{\text{1RSB}}(q_1, q_0, m)|_{n=0}/N \\ & = -\frac{1}{2} [\epsilon_1 + (m - 1)\epsilon_1 q_1 - m\epsilon_0 q_0] + \frac{1}{m} \int Dz_0 \ln \left(\int Dz_1 (2 \cosh \Xi)^m \right) \\ & + \frac{\gamma(\beta J)^2}{2} [1 + (m - 1)q_1^p - mq_0^p] \\ & = \frac{\gamma(\beta J)^2}{2} - \frac{\gamma(\beta J)^2}{2} (p - 1) [(m - 1)q_1^p - mq_0^p] - \frac{\gamma(\beta J)^2}{2} pq_1^{p-1} \\ & + \frac{1}{m} \int Dz_0 \ln \left(\int Dz_1 (2 \cosh \Xi)^m \right) \end{aligned} \quad (\text{VIII.7})$$

The last equation follows from the 1st one using Eq. (VIII.10) shown below. Comparing with the RS free-energy Eq. (VII.8), one can see,

$$f_{1\text{RSB}}(q_1 = q, q_0 = q, m \rightarrow 0) = f_{\text{RS}}(q). \quad (\text{VIII.8})$$

and for any q_1 ,

$$f_{1\text{RSB}}(q_1, q_0 = q, m = 1) = f_{\text{RS}}(q). \quad (\text{VIII.9})$$

Taking derivatives we find,

$$0 = \frac{\partial f_{1\text{RSB}}}{\partial q_i} \rightarrow \epsilon_i = p\gamma(\beta J)^2 q_i^{p-1} \quad (i = 0, 1) \quad (\text{VIII.10})$$

and after some algebra ¹³ we find

$$0 = \frac{\partial f_{1\text{RSB}}}{\partial \epsilon_0} \rightarrow q_0 = \int \mathcal{D}z_0 \left(\frac{\int Dz_1 \cosh^m(\Xi) \tanh(\Xi)}{\int Dz_1 \cosh^m(\Xi)} \right)^2 \quad (\text{VIII.11})$$

and

$$0 = \frac{\partial f_{1\text{RSB}}}{\partial \epsilon_1} \rightarrow q_1 = \int \mathcal{D}z_0 \frac{\int Dz_1 \cosh^m(\Xi) \tanh^2(\Xi)}{\int Dz_1 \cosh^m(\Xi)} \quad (\text{VIII.12})$$

The latter two results can also be obtained from Eq. (VI.57).

Finally the parameter m must be extremized.¹⁴ Thus we find,

$$\begin{aligned} 0 = \frac{\partial f_{1\text{RSB}}}{\partial m} \rightarrow 0 = & -(p-1) \frac{\gamma(\beta J)^2}{2} (q_0^p - q_1^p) + \frac{1}{m^2} \int \mathcal{D}z_0 \ln \int \mathcal{D}z_1 [2 \cosh(\Xi)]^m \\ & - \frac{1}{m} \int \mathcal{D}z_0 \frac{\int \mathcal{D}z_1 [2 \cosh(\Xi)]^m \ln [2 \cosh(\Xi)]}{\int \mathcal{D}z_1 [2 \cosh(\Xi)]^m} \end{aligned} \quad (\text{VIII.13})$$

The (dimension-less) internal energy is obtained as,

$$e = \frac{\partial}{\partial(\beta J)} \beta f_{1\text{RSB}}(q_1, q_0, m) = -\gamma(\beta J)(1 + (m-1)q_1^p - mq_0^p) \quad (\text{VIII.14})$$

Assuming $h_{\text{ext}} = 0$, we easily find that $q_0 = 0$ (and thus $\epsilon_0 = 0$) is a solution. We limit ourselves to this case in the following. In this case the calculation simplifies a lot. For clarity let us display the results below. The free-energy becomes

$$\begin{aligned} -\beta f_{1\text{RSB}}(q_1 = q, q_0 = 0, m) = & -\frac{1}{2}\epsilon[1 - (1-m)q] + \frac{1}{m} \log \int \mathcal{D}z [2 \cosh(z\sqrt{\epsilon})]^m \\ & + \gamma \frac{(\beta J)^2}{2} [1 - (1-m)q^p] \end{aligned} \quad (\text{VIII.15})$$

where q and ϵ are given by

$$q = \frac{\int \mathcal{D}z \cosh^m(z\sqrt{\epsilon}) \tanh^2(z\sqrt{\epsilon})}{\int \mathcal{D}z \cosh^m(z\sqrt{\epsilon})} \quad \epsilon = \gamma p(\beta J)^2 q^{p-1} \quad (\text{VIII.16})$$

In this simplified case $q_0 = 0$, the hessian matrix Eq. (VI.79) becomes similar to that of the RS solution Eq. (VII.14). One just need to replace $A(q)$ in Eq. (VII.14) with

$$\lim_{n \rightarrow 0} A(q) = \lim_{n \rightarrow 0} \frac{\partial^2}{\partial h_a \partial h_b} \frac{\partial^2}{\partial h_c \partial h_d} \Bigg|_{a,b,c,d \in 1} \prod_{c=1}^{n/m} \left[e^{\frac{\epsilon_0}{2} \sum_{a,b \in \mathcal{C}} \frac{\partial^2}{\partial h_a \partial h_b}} \prod_{c \in \mathcal{C}} (2 \cosh(h_c)) \right]_h \quad (\text{VIII.17})$$

¹³ Derivations become easier considering $0 = \partial_{\epsilon_0}(-\beta F_n^{RSB}(q_1, q_0, m)/N)$, $0 = \partial_{\epsilon_1}(-\beta F_n^{RSB}(q_1, q_0, m)/N)$ using the expression Eq. (VIII.6) and taking $n \rightarrow 0$ afterwards.

¹⁴ This amount to impose vanishing of the complexity as first noted by Monasson [51]. We will discuss this later in sec. VIII D.

thus

$$M_{a \neq b, c \neq d} = (\delta_{ac}\delta_{bd} + \delta_{ad}\delta_{bc})\gamma(\beta J)^2 p(p-1)q^{p-2} \left\{ 1 - \frac{\gamma(\beta J)^2 p(p-1)q^{p-2}}{\int Dz \cosh^m(\sqrt{\epsilon}z) \left(\frac{\int Dz \cosh^m(\sqrt{\epsilon}z)(1 - \tanh^2(\sqrt{\epsilon}z))^2}{\int Dz \cosh^m(\sqrt{\epsilon}z)} - q^2 \right)} \right\} \quad (\text{VIII.18})$$

Thus we find the stability of the 1RSB solution ($q_1 = q, q_0 = 0$)

$$\frac{1}{\gamma(\beta J)^2 p(p-1)q^{p-2}} > \frac{\int Dz \cosh^m(\sqrt{\epsilon}z) \operatorname{sech}^4(\sqrt{\epsilon}z)}{\int Dz \cosh^m(\sqrt{\epsilon}z)} \quad (\text{VIII.19})$$

This is the analogue of the AT condition Eq. (VII.18) [55] adjusted to 1RSB by E. Gardner [61].

2. $p = \infty$ Ising model

In particular let us examine the case $p \rightarrow \infty$ to compare with the random energy model. We notice that in the limit $p \rightarrow \infty$, if we assume $0 < q < 1$ the 2nd equation of Eq. (VIII.16) implies $\epsilon = 0$ which cannot satisfy the 1st equation. The only possibilities are $(q, \epsilon) = (0, 0)$ and $(1, \infty)$.

Let us evaluate the free-energy Eq. (VIII.15) for the solution $q = 1, \epsilon = \infty$. To this end we have to examine the integral,

$$I(r) = \int Dz [2 \cosh(z\sqrt{\epsilon})]^r \quad (\text{VIII.20})$$

in $\epsilon \rightarrow \infty$ limit. By noting that $2 \cosh(z\sqrt{\epsilon}) \simeq e^{z\sqrt{\epsilon}\operatorname{sgn}(z)}$ we find

$$\lim_{\epsilon \rightarrow \infty} I(r) = \begin{cases} 2e^{\frac{r^2\epsilon}{2}} & r > 0 \\ \sqrt{\frac{2}{\pi}} \frac{1}{|r|\sqrt{\epsilon}} & r < 0 \end{cases}$$

With this we find Eq. (VIII.15) becomes

$$-\beta f_{1\text{RSB}}(q_1 = 1, q_0 = 0, m) = \frac{\gamma(\beta J)^2}{2} m + \frac{\ln 2}{m} \quad (\text{VIII.21})$$

Finally we require $0 = \partial_m \beta F_{1\text{RSB}}$ which yields

$$m = \frac{k_B T}{J} \sqrt{\frac{2 \ln 2}{\gamma}} \quad (\text{VIII.22})$$

which continuously decreases with the temperature.¹⁵

Let us check stability of the $q = 1$ 1RSB solution. We see l.h.s of Eq. (VIII.19) is $1/p(p-1)$ while r.h.s behaves as $\epsilon^{-1/2} e^{-m^2\epsilon/2}$ with $\epsilon \propto p$. Thus in $p \rightarrow \infty$ limit the stability condition Eq. (VIII.19) is satisfied.

Comparing with the RS free-energy Eq. (VII.8) we find the 1RSB free-energy becomes lower than the RS energy for $m < 1$ suggesting a critical temperature T_c such that $m(T_c) = 1$. Thus we find

$$k_B T_c = J \sqrt{\frac{\gamma}{2 \ln 2}} \quad (\text{VIII.23})$$

with which we can write

$$m = \frac{T}{T_c}. \quad (\text{VIII.24})$$

¹⁵ One can see easily that the free-energy becomes maximum by this! The meaning of this operation become clear later in sec. VIII D.

As the result the 1RSB free-energy becomes independent of the temperature below T_c ;

$$f_{\text{1RSB}}/J = -\sqrt{2\gamma \ln 2} = e_{\min} \quad (\text{VIII.25})$$

where e_{\min} is given by Eq. (V.13).

The (dimension-less) internal energy is obtained from Eq. (VIII.14) using $m = T/T_c$, $q_1 = 1$, and $q_0 = 0$ as,

$$e = -\gamma(\beta J)(1 - (1 - m)) = -\gamma(\beta J) \frac{T}{T_c} = -\sqrt{\gamma 2 \ln 2} \quad (\text{VIII.26})$$

while $e = -\gamma(\beta J)$ in the $q = 0$ RS solution Eq. (VIII.14).

From the above results we realize that the exact results of the REM is recovered by the 1RSB solution.

B. Distribution of overlap $P(q)$

Now we have to ask : *what is the physical meaning of the replica symmetry breaking?*. Let us consider two *real* replicas, say 1 and 2 and examine the probability distribution $P(q)$ of the overlap q between them. More precisely we consider the *disorder average* of this distribution function,

$$\overline{P(q)} = \lim_{N \rightarrow \infty} \overline{\delta(q - \frac{1}{N} \sum_{i=1}^N \sigma_i^1 \sigma_i^2)} \quad (\text{VIII.27})$$

Here the overline $\overline{\dots}$ represents the disorder average. It can be 1) average over quenched disorder Eq. (III A 5) or 2) the random pinning field discussed in sec VI A 3.

We wish to evaluate this using the 1RSB solution. To this end we just need to add $n - 2$ more replicas so that we have n replicas as a whole. We apply the 1RSB ansatz for this n replica system as discussed above. At this point we have to remember that there is a family of equivalent solutions which can be obtained by permuting the replica indices of the Parisi's matrix and that all of them has the same statistical weights as discussed in sec VI A 6. The overlap between the two replicas q_{12} can take either q_0 or q_1 depending on the permutations. Then assuming equal weights of all of these permuted solutions we find,

$$\overline{P(q)} = \frac{m(m-1)\frac{n}{m}}{n(n-1)} \delta(q - q_1) + \left(1 - \frac{m(m-1)\frac{n}{m}}{n(n-1)}\right) \delta(q - q_0) \xrightarrow{n \rightarrow 0} (1-m)\delta(q - q_1) + m\delta(q - q_0) \quad (\text{VIII.28})$$

To be specific let us consider the case of REM for which we know $q_1 = 1$, $q_0 = 0$ and $m = T/T_c$ at $0 < T < T_c$. In the limit $T \rightarrow 0$, $m \rightarrow 0$ so that $\overline{P(q)} = \delta(q - 1)$ which is expected since the two replicas should stay in the ground state at zero temperature.

In the other limit $T \rightarrow T_c$, $m \rightarrow 1$ so that $\overline{P(q)} = \delta(q)$. This could also be expected because down to T_c the two replicas are allowed to stay in arbitrarily different states which happen to have almost the same energy. As discussed in sec V A Eq. (V.6) the overlap between such states are typically 0.

More generally, in the spinglass phase, $0 < T < T_c$, we find an intriguing situation: the two distinct delta peaks one at $q = q_1 = 1$ and the other at $q = q_0 = 0$ coexists in $P(q)$ whose relative weights evolves with temperature. For example in the REM we found $m = T/T_c$. See Fig. 36 a) for a schematic picture.

In the case of REM, actually this result can be obtained without using the replicas but directly developing a low temperature expansion of the REM as we discuss in Appendix I. With this approach the picture becomes clearer. In the low temperature limit, the peak at $q = 1$ with amplitude accounts for the case that both of the replicas remain in the ground state and the peak at $q = 0$ accounts for the situation that one of the two replicas stay at the 1st excited state while the other one remains in the ground state. Note that typical overlap between the ground state and the excited states are 0. The amplitude $m = T/T_c$ of the peak at $q = 0$ is essentially the disorder average of the (relative) Boltzmann weight of the 1st excited state. One can see that this is not a self-averaging quantity. (Sample to sample fluctuations of $P(q)$ can be computed both by the replica method and by the low temperature expansion approach.) The energy gap between the ground state and the 1st excited state fluctuate between different realizations of quenched disorder in usual spinglass models or the random pinning field in the disorder-free Ising p -spin ferromagnetic model discussed in sec. V A.

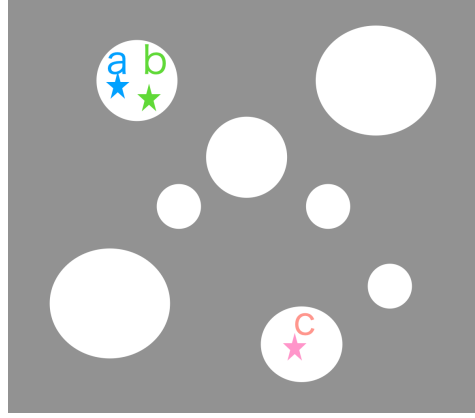


FIG. 23. Schematic picture of the phase space of a glass which is decomposed into disconnected components (basins) $\alpha = 1, 2, \dots$. Replicas a, b, c may or may not belong to the same basins.

C. Systems with many metastable states

Based on the above observation in the $p \rightarrow \infty$ limit (REM), we may interpret the 1RSB solution in more general cases in the following way. In the 1RSB phase, there are multiple metastable spinglass states $\alpha = 1, 2, \dots$ whose mutual overlap is typically q_0 . On the other hand q_1 would be interpreted as the EA order parameter q_{EA} , which can be regarded as *self-overlap* of metastable states (see below). Then in REM ($p \rightarrow \infty$) it happens that $q_{\text{EA}} = 1$ suggesting that there is no thermal fluctuation within a metastable state of REM. This means that every spin configuration becomes a metastable state in the $p \rightarrow \infty$ limit.

Then similarly to the case of REM Eq. (V.10), we naturally expect that the partition function of a generic p -spin model can be represented as a summation over the metastable states,

$$Z = \sum_{\alpha} e^{-\beta N f_{\alpha}(T)} \quad (\text{VIII.29})$$

where $f_{\alpha}(T)$ is the free-energy/spin of the metastable state α . The above representation is just the same as that of the REM Eq. (V.10) but here the energy e_{α} is replaced by the free-energy f_{α} . It may be decomposed as

$$f_{\alpha} = e_{\alpha} - T s_{\alpha} \quad (\text{VIII.30})$$

with e_{α} and s_{α} being the internal energy and the entropy of the metastable state α . This reflects the fact that $q_1 = q_{\text{EA}}$, which is 1 in the REM ($p \rightarrow \infty$), is smaller than 1 for general p suggesting thermal fluctuations within metastable states. In other words, for generic p , a free-energy minimum consists of not only an energy minimum but nearby spin configurations which defines a basin around the minimum in the phase space. Then the thermal averages would be decomposed as

$$\langle \dots \rangle = \sum_{\alpha} w_{\alpha} \langle \dots \rangle_{\alpha} \quad w_{\alpha} = \frac{e^{-N\beta f_{\alpha}}}{\sum_{\alpha} e^{-N\beta f_{\alpha}}} \quad (\text{VIII.31})$$

where $\langle \dots \rangle_{\alpha}$ is the thermal average with respect to the thermal fluctuation within α .

For example the $P(q)$ function can be rewritten as follows,

$$\begin{aligned} P(q) &= \lim_{N \rightarrow \infty} \langle \delta(q - \frac{1}{N} \sum_{i=1}^N \sigma_i^1 \sigma_i^2) \rangle = \sum_{\alpha} \sum_{\alpha'} w_{\alpha} w_{\alpha'} \langle \delta(q - \frac{1}{N} \sum_{i=1}^N \sigma_i^1 \sigma_i^2) \rangle_{\alpha, \alpha'} = \sum_{\alpha} \sum_{\alpha'} w_{\alpha} w_{\alpha'} \delta(q - q_{\alpha \alpha'}) \\ &= \sum_{\alpha} w_{\alpha}^2 \delta(q - q_{\alpha \alpha}) + \sum_{\alpha \neq \alpha'} w_{\alpha} w_{\alpha'} \delta(q - q_{\alpha \alpha'}) \end{aligned} \quad (\text{VIII.32})$$

where

$$q_{\alpha, \alpha'} \equiv \frac{1}{N} \sum_{i=1}^N m_{i, \alpha} m_{i, \alpha'} \quad m_{i, \alpha} \equiv \langle \sigma_i \rangle_{\alpha} \quad (\text{VIII.33})$$

is the mutual overlap between the metastable states α and α' . For $\alpha' = \alpha$, it is the self-overlap, which should be identified as the Edwards-Anderson order parameter q_{EA} . To derive Eq. (VIII.32) we assumed the clustering property. (See Appendix H).

In the case of 1RSB we have found Eq. (VIII.28) which implies $q_{\alpha,\alpha} = q_1$, $q_{\alpha,\alpha'} = q_0$ for $\alpha \neq \alpha'$, $\sum_{\alpha} w_{\alpha}^2 = 1 - m$ and $\sum_{\alpha \neq \alpha'} w_{\alpha} w_{\alpha'} = m$. We discuss later general connection between the Parisi's ansatz Eq. (VI.23) and the overlap distribution function $P(q)$.

D. Complexity

Similarly to the case of REM we may rewrite the partition function Eq. (VIII.29) as

$$Z = \sum_{\alpha} e^{-\beta N f_{\alpha}(T)} = \int df e^{N(\Sigma(f,T) - \beta f)} \quad (\text{VIII.34})$$

where the number the states in the sum σ_{α} is exponentially large in N so that we introduced the so called *structural entropy* or *complexity*

$$\Sigma(f, T) \equiv \frac{1}{N} \log \sum_{\alpha} \delta(f - f_{\alpha}(T)). \quad (\text{VIII.35})$$

The above representations Eq. (VIII.29), Eq. (VIII.34) and Eq. (VIII.35) are justified by studying the solutions of the equations of state of the p-spin model, which is the so called Thouless-Anderson-Palmer (TAP) equations [62, 63].

Monasson[51] proposed to introduce an extra parameter m into the game,

$$-N\beta m\phi_m \equiv \ln Z_m \quad Z_m \equiv \sum_{\alpha} e^{-Nm\beta f_{\alpha}(T)} = \int df e^{N(\Sigma(f,T) - \beta mf)}. \quad (\text{VIII.36})$$

Formally evaluating the integral by the saddle point method we find,

$$-\beta m\phi_m = \Sigma(f^*, T) - \beta mf^* \quad \left. \frac{\partial \Sigma(f, T)}{\partial f} \right|_{f=f^*(T,m)} = \frac{m}{k_B T} \quad (\text{VIII.37})$$

From this we find

$$f^* = \partial_m(m\phi_m) \quad \Sigma^* = \beta m^2 \partial_m \phi_m \quad (\text{VIII.38})$$

The complexity function $\Sigma(f, T)$ can be extracted from the above result varying m as a parameter.¹⁶ Here we see that the role of the parameter m is to select a certain group of metastable states.

Now the above construction can be implemented using the replicas as follows: consider m replicas which are *forced* to stay together such that at any instance their configuration belong to a common metastable state. In the case of n replicas this amount to consider a situation such that n replicas are divided into n/m groups and that replicas belonging to a common group move around different states together while different groups move around independently from each other;

$$Z_{\text{1RSB}}^n = Z_m^{n/m} = \left(\sum_{\alpha} e^{-Nm\beta f_{\alpha}(T)} \right)^{n/m} \quad (\text{VIII.39})$$

Actually this is readily realized precisely by the 1RSB ansatz : the n replicas are divided into n/m groups of size m and the replicas belonging to each of the groups have mutual overlap which is equal to q_{EA} while mutual overlap $q_0 = 0$ between different groups. Here let us recall that, as we noted in sec. VIA 3, the hierarchical structure of the order parameter q_{ab} assumed in the Parisi's ansatz imply we are assuming the same hierarchical structure in the symmetry breaking or pinning field ϵ_{ab} . In the case of 1RSB, we indeed apply pinning field with the 1RSB structure

¹⁶ The parameter m plays the role of conjugated field for the free-energy f and the complexity Σ can be viewed as the Legendre transform of the free-energy f . (This is analogous to the relation between the entropy and energy: the entropy is the Legendre transform of the energy with the inverse temperature playing the role of the conjugated field.)

to create the replica groups of size m , and the send $\epsilon_{ab} \rightarrow 0$ after $N \rightarrow \infty$. The partition function Eq. (VIII.39) can be regarded as the reflection of such an operation.

Now based on the above arguments we find,

$$-N\beta f_{1\text{RSB}}(q_1, q_0 = 0, m) = \partial_n(Z_m)^{n/m} \Big|_{n=0} = \ln Z_m/m. \quad (\text{VIII.40})$$

Thus we find

$$\phi_m = f_{1\text{RSB}}(q_1, q_0 = 0, m) \quad (\text{VIII.41})$$

- An important observation made by Monasson [51] is that the condition $0 = \partial_m f_{1\text{RSB}}$ Eq. (VIII.13) for $T \leq T_c$ is equivalent to require vanishing complexity $\Sigma = 0$ because of Eq. (VIII.38).
- In the limit $m \rightarrow 1$ we find Eq. (VIII.9) so that $\lim_{m \rightarrow 1} \phi_m(q) = f_{1\text{RSB}}(q, 0, m = 1) = f_{\text{RS}}(0)$ which is the correct thermodynamic free-energy of the liquid phase. The Monnason's trick Eq. (VIII.37) allow us to decompose the liquid free-energy

$$-\beta f_{\text{RS}}(0) = \Sigma(f^*(m = 1), T) - \beta f^*(m = 1) \quad (\text{VIII.42})$$

Let us check these explicitly in the case of REM. From Eq. (VIII.21) we readily find,

$$-\beta \phi_m = -\beta f_{1\text{RSB}} = \frac{(\beta J)^2}{4}m + \frac{\ln 2}{m}. \quad (\text{VIII.43})$$

Then using the prescription Eq. (VIII.38) we find

$$\Sigma(f^*) = m^2 \partial_m \left(-\frac{(\beta J)^2}{4}m - \frac{\ln 2}{m} \right) = \ln 2 - \frac{(\beta J)^2}{4}m^2 \quad \beta f^* = \partial_m \left(-m^2 \frac{(\beta J)^2}{4} - \ln 2 \right) = -\frac{(\beta J)^2}{2}m \quad (\text{VIII.44})$$

from which we find the complexity

$$\Sigma(f) = \ln 2 - (f/J)^2 \quad (\text{VIII.45})$$

which agrees with Eq. (V.12)

- 1RSB solution continues to be present above T_c up to T_d (which is ∞ in the case of REM) where it finally disappears....
- Energy landscape changes at T_d ...
- The above ideas play key roles to develop the cloned liquid theory (replicated liquid theory) for structural glasses.[64, 65]

E. $2 < p < \infty$ Ising model

1. Search for solutions

Assuming $q_1 = q, q_0 = 0$, we can obtain q by solving Eq. (VIII.16). The stability of the solution can be checked examine the condition Eq. (VIII.19). In Fig. 24 a), we show a graphical representation of the 1RSB saddle point equation of the $p = 3$ Ising model for $m = 1$ case. Similarly, we can look for 1RSB solutions of various m as shown in Fig. 24 b). As we discussed above the role of the parameter m is to select a certain group of metastable states. There we also show the value of normalized replicon eigen-value of the Hessian matrix Eq. (IX.14).

2. Dynamical transition

Dynamical transition temperature T_d is the point where the 1RSB solution with $m = 1$ emerges (See Fig. 24 and Fig. 25). Approaching this temperature from above, the dynamics slows down. Within the mean-field model the ergodicity breaks down there (See. sec. XII), as first predicted by the mode coupling theory.

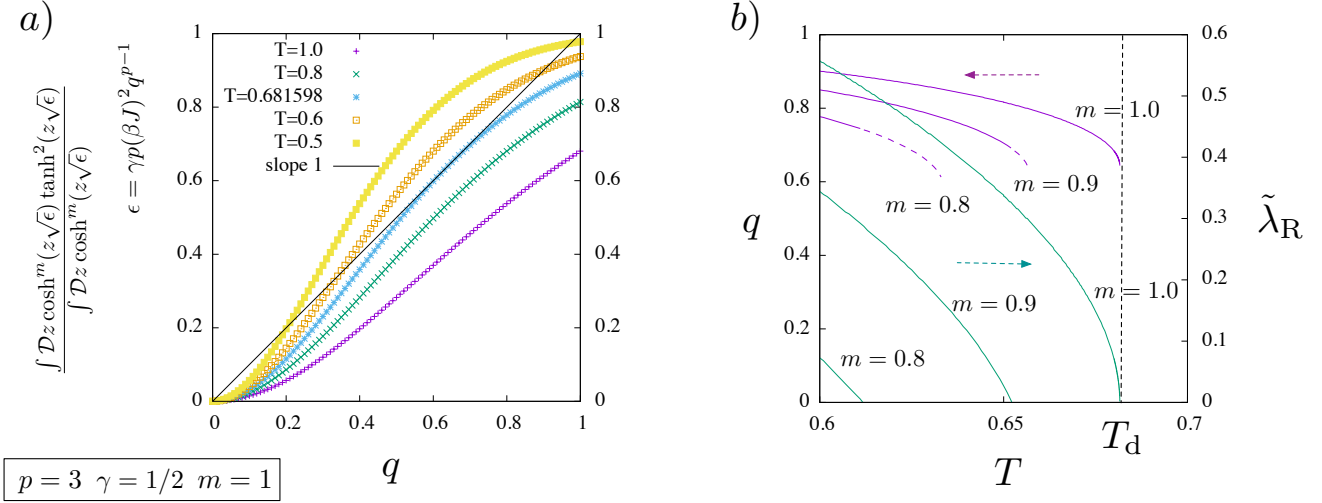


FIG. 24. 1RSB solution of the $p = 3$ Ising model. a) Graphical representation of the saddle point equation for q for the case $m = 1$. The curves are the r.h.s of Eq. (VIII.16) and the solutions of the saddle point equation is given by the crossing points between these curves and the straight line with slope 1. At $T < T_d$ with $T_d \simeq 0.681598\dots$, two $q > 0$ solutions emerge. The stable one is the larger one. b) Temperature dependence of the stable $q > 0$ solution and the value of the normalized eigen-value $\tilde{\lambda}_R$ (see text) of the solution for $m = 1.0, 0.9, 0.8$.

3. Complexity

Using the prescription Eq. (VIII.38) Eq. (VIII.41) for the p-spin model Eq. (VIII.7), we find for the case $q_1 = q, q_0 = 0$,

$$\begin{aligned} \Sigma^* &= m^2 \partial_m \beta f_{1\text{RSB}}(q, 0, m) \\ &= m^2 \frac{\gamma(\beta J)^2}{2} q^p (p-1) + \ln \int Dz (2 \cosh(\Xi))^m - m \frac{\int Dz (\cosh(\Xi))^m \ln(2 \cosh(\Xi))}{\int Dz (\cosh(\Xi))^m} \end{aligned} \quad (\text{VIII.46})$$

$$\begin{aligned} \beta f^* &= \partial_m (m \beta f_{1\text{RSB}}(q, 0, m)) \\ &= -\frac{\gamma(\beta J)^2}{2} + \frac{\gamma(\beta J)^2}{2} \left[q^p (p-1)(2m-1) + pq^{p-1} \right] - \frac{\int Dz (\cosh(\Xi))^m \ln(2 \cosh(\Xi))}{\int Dz (\cosh(\Xi))^m} \end{aligned} \quad (\text{VIII.47})$$

4. Gardner transition

At low enough temperature the 1RSB solution breaks the stability condition Eq. (VIII.19) as first noted by E. Gardner [61]. (See Fig. 25) Recently this transition has been found also in the hard-sphere glass [66, 67].

F. Disentangling hierarchy of responses

Let us discuss a generic feature of linear response in the system with many metastable state captured by the 1RSB ansatz following [42], [43] and [70].

We consider a perturbing field h which is conjugated to an extensive physical observable O . We denote the value of the observable/ N at state α as o_α and that the associated linear susceptibility as χ_α ,

$$o_\alpha = -\frac{\partial f_\alpha}{\partial h} \quad \chi_\alpha = \frac{\partial o_\alpha}{\partial h} = -\frac{\partial^2 f_\alpha}{\partial h^2} \quad (\text{VIII.48})$$

In other words o_α is the value of the observable o averaged over the intra-state fluctuation, i.e. the thermal fluctuations *within* the state α . Similarly χ_α is related to the fluctuation of o within the state α .

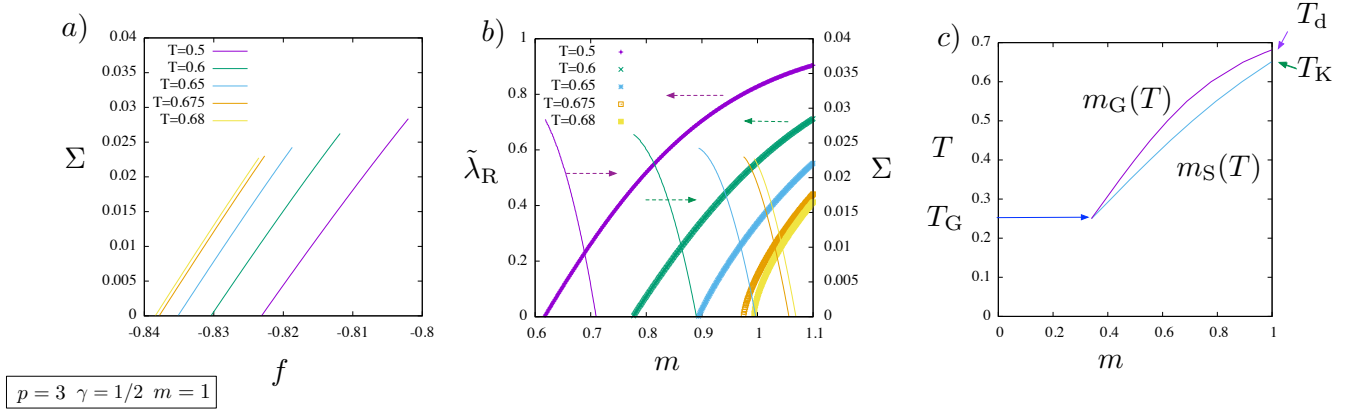


FIG. 25. Complexity and stability of the 1RSB phase ($p = 3$, $\gamma = 1/2$) : a) Complexity $\Sigma(f)$ vs f at various temperatures b) The replicon eigenvalue $\lambda_R(m, T)$ and complexity $\Sigma^*(f^*(m, T), T)$ vs m . c) the static glass transition line ('Kauzmann line') $m_s(T)$ above which the complexity is positive $\Sigma > 0$ and 'Gardner line' $m_G(T)$ below which the replicon eigen value is positive [68]. The dynamical transition takes place at $T_d = 0.681598$ The Kauzmann transition takes place at $T_K = 0.651385$. The gardner transition takes place at $T_G = 0.24026$ [68, 69].

In the 1RSB ansatz we have

$$-\beta N f_{1\text{RSB}}(T, h) = \frac{1}{m} \ln \sum_{\alpha} e^{-Nm\beta f_{\alpha}(T, h)} \quad (\text{VIII.49})$$

Then we find

$$o(T, h) = -\frac{\partial f_{1\text{RSB}}(T, h)}{\partial h} = \frac{\partial}{\partial h} \frac{\ln \sum_{\alpha} e^{-Nm\beta f_{\alpha}(T, h)}}{\beta m N} = \sum_{\alpha} w_{\alpha} o_{\alpha} = \langle o_{\alpha} \rangle_0 \quad (\text{VIII.50})$$

where

$$\langle \dots \rangle_0 \equiv \sum_{\alpha} w_{\alpha} \dots \quad (\text{VIII.51})$$

is the average over different metastable states with the statistical weight

$$w_{\alpha} \equiv \frac{e^{-Nm\beta f_{\alpha}(T, h)}}{\sum_{\alpha} e^{-Nm\beta f_{\alpha}(T, h)}} \quad (\text{VIII.52})$$

Similarly we find the susceptibility as,

$$\chi_{1\text{RSB}}(T, h) = \frac{\partial o(T, h)}{\partial h} = \sum_{\alpha} w_{\alpha} \partial_h o_{\alpha} + \sum_{\alpha} (\partial_h w_{\alpha}) o_{\alpha} = \tilde{\chi}_1 + m \tilde{\chi}_0 \quad (\text{VIII.53})$$

with

$$\tilde{\chi}_1 = \langle \chi_{\alpha} \rangle_0 \quad \tilde{\chi}_0 = N\beta(\langle o_{\alpha}^2 \rangle_0 - \langle o_{\alpha} \rangle_0^2) \quad (\text{VIII.54})$$

Physically we can interpret $\tilde{\chi}_1$ as the response within a metastable state and $\tilde{\chi}_0$ as the response due to transition between different states. The total response is the mixture. One may wish to disentangle the two qualitatively different susceptibilities.

A trick to disentangle the two susceptibilities was noticed in [42, 43] as follows. Let us apply different probing fields on each of the replicas,

$$\begin{aligned} \chi_{a,b}(T, h) &\equiv -\left. \frac{\partial^2 m f_{1\text{RSB}}(T, \{h_a\})}{\partial h_a \partial h_b} \right|_{\{h_a=h\}} = -\frac{1}{\beta N} \left. \frac{\partial^2}{\partial h_a \partial h_b} \ln \sum_{\alpha} e^{-Nm\beta \sum_{a=1}^m f_{\alpha}(h_a)} \right|_{\{h_a=h\}} \\ &= \tilde{\chi}_1 \delta_{ab} + \tilde{\chi}_0 \end{aligned}$$

We also observe that the total response is recovered as,

$$\sum_{b=1}^m \chi_{ab} = \tilde{\chi}_1 + m\tilde{\chi}_0 = \chi_{1\text{RSB}}(T, h). \quad (\text{VIII.55})$$

As an example let us consider the magnetic response of the p -spin Ising model. To this end we just need to apply different fields on $h_a = h + \delta h_a$ ($a = 1, 2, \dots, m$) on the replicas as outlined above. Then Eq. (VIII.7) becomes

$$\begin{aligned} -\beta f_{1\text{RSB}}(q_1, q_0, m) &= -\beta \partial_n F_n^{1\text{RSB}}(q_1, q_0, m)|_{n=0}/N \\ &= -\frac{1}{2}[\epsilon_1 + (m-1)\epsilon_1 q_1 - m\epsilon_0 q_0] - \frac{1}{m} \int \mathcal{D}z_0 \log \int \mathcal{D}z_1 \prod_{a=1}^m [2 \cosh(\beta h_a + \sqrt{\lambda_1 - \lambda_0} z_1 + \sqrt{\lambda_0} z_0)] \\ &\quad + \frac{\gamma(\beta J)^2}{2}[1 + (m-1)q_1^p - mq_0^p] \end{aligned} \quad (\text{VIII.56})$$

from this we find the following susceptibility matrix,

$$\chi_{ab} = -\left. \frac{\partial^2 m f_{1\text{RSB}}(\{h_1, \dots, h_m\})}{\partial h_a \partial h_b} \right|_{h_a=h} = \tilde{\chi}_1 \delta_{ab} + \tilde{\chi}_0 \quad (\text{VIII.57})$$

with

$$\tilde{\chi}_1 = \int \mathcal{D}z_0 \frac{\int \mathcal{D}z_1 [2 \cosh \Xi]^m \beta (1 - \tanh^2 \Xi)}{\int \mathcal{D}z_1 [2 \cosh \Xi]^m} = \beta(1 - q_1) \quad (\text{VIII.58})$$

where $\Xi = \beta h + \sqrt{\epsilon_1 - \epsilon_0} z_1 + \sqrt{\epsilon_0} z_0$ and

$$\tilde{\chi}_0 = \beta \left[\int \mathcal{D}z_0 \frac{\int \mathcal{D}z_1 [2 \cosh \Xi]^m \tanh^2 \Xi}{\int \mathcal{D}z_1 [2 \cosh \Xi]^m} - \left(\frac{\int \mathcal{D}z_1 [2 \cosh \Xi]^m \tanh \Xi}{\int \mathcal{D}z_1 [2 \cosh \Xi]^m} \right)^2 \right] = \beta(q_1 - q_0) \quad (\text{VIII.59})$$

The total susceptibility becomes

$$\chi_{1\text{RSB}} = \beta[1 - q_1 + m(q_1 - q_0)] \quad (\text{VIII.60})$$

which of course includes the RS result with $m = 1$, $\chi_{\text{RS}} = \beta(1 - q_0)$.

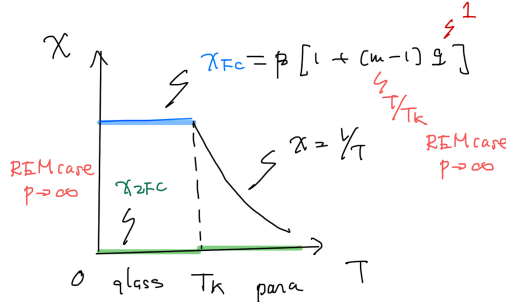


FIG. 26. FC/ZFC susceptibilities in REM ($p = \infty$)

Experimentally it is well known that the magnetic response in spin-glasses exhibit strong hysteresis[71]. In Fig. 26 we show the FC/ZFC susceptibilities of the simplest model, REM ($p = \infty$). The susceptibility in the paramagnetic phase, above the glass transition temperature T_K follows the Curie's law $\chi_{\text{RS}} = \beta$ (since $q_0 = 0$). Below T_K , total magnetic response $\chi_{1\text{RSB}} = \beta((1 + (1 - m)q_1)$ (since $q_0 = 0$) could be associated with the so called field-cooled (FC) susceptibility χ_{FC} . In REM we know $m = T/T_K$ and $q_1 = 1$ so that $\chi_{\text{FC}} = \chi_{1\text{RSB}} = 1/T_K$ which is independent of the temperature T . Interestingly χ_{FC} measured in experiments [71] is also nearly independent of temperature below the spinglass transition temperature. On the other hand, the magnetic susceptibility associated with fluctuations inside basins $\chi_1 = \beta(1 - q_1)$, which may be associated with the so called zero-field cooled (ZFC) susceptibility is 0 in the case of REM. This extreme behaviour is due to the special character of REM. Nevertheless experiments show $\chi_{\text{ZFC}} < \chi_{\text{FC}}$ below the spinglass transition temperature [71] while $\chi_{\text{FC}} = \chi_{\text{ZFC}}$ in the paramagnetic phase. **TODO: show also FC/ZFC susceptibilities of $p = 3$ system.**

G. Scalar spherical p -spin model

For simplicity let us limit ourselves with $q_0 = 0$ here. Then we find

$$\ln \det \hat{q} = \frac{n}{m} \left\{ \ln[1 + (m-1)q] + (m-1) \ln(1-q) \right\}. \quad (\text{VIII.61})$$

Collecting the above results we find,

$$\begin{aligned} -\beta f_{1\text{RSB}}(q_1 = q, q_0 = 0, m) &= -\beta \partial_n F_n^{\text{1RSB}}(q_1 = q, q_0 = 0, m)|_{n=0}/N \\ &= \frac{1}{2} + \frac{1}{2} \ln(2\pi) + \frac{1}{2m} [(m-1) \ln(1-q) + \ln[1 + (m-1)q]] \\ &\quad + \frac{\gamma(\beta J)^2}{2} [1 + (m-1)q^p] \end{aligned} \quad (\text{VIII.62})$$

We find the SP equation for q as,

$$0 = \partial_q (-\beta f_{1\text{RSB}}(q_1 = q, q_0 = 0, m)) = \frac{(1-m)}{2} q \left\{ \frac{1}{(1-q)(1+(m-1)q)} - \mu q^{p-2} \right\} \quad (\text{VIII.63})$$

where we defined

$$\mu = \gamma(\beta J)^2 p \quad (\text{VIII.64})$$

Thus we find $q_1 = q = 0$ is always a solution. In the limit $m \rightarrow 1$, the equation for $q > 0$ solution is obtained as,

$$\mu(1-q)q^{p-2} = 1 \quad (\text{VIII.65})$$

Remarkably this agrees with prediction of the dynamical mean-field theory [72].

The Hessian matrix Eq. (VI.83) becomes with the 1RSB ansatz with $q_1 = q, q_0 = 0$,

$$M_{a \neq b, c \neq d} = \frac{1}{(1-q)^2} - \gamma(\beta J)^2 p(p-1)q^{p-2}(\delta_{ac}\delta_{bd} + \delta_{ad}\delta_{bc}) + \dots \quad (\text{VIII.66})$$

Thus we find the replicon eigen value as,

$$\lambda_R = \frac{1}{(1-q)^2} - \mu(p-1)q^{p-2} \quad (\text{VIII.67})$$

This implies $q = 0$ solution is always stable for $p > 2$.

(Exercise) Show that $q > 0$ solution emerges at the dynamical transition (for $m = 1$),

$$q = \frac{p-2}{p-1} \quad (\text{VIII.68})$$

that $\lambda_R = 0$ for this.

IX. STATE FOLLOWING: FRANZ-PARISI POTENTIAL

A. The idea of glass state following

$$\begin{aligned} -\beta F_{m+s} &= \ln \sum_{\alpha} e^{-N\beta(mf_{\alpha}+sf_{\alpha}(\eta))} \\ &= -N\beta mf_m - N\beta V_F(\eta)s + O(s^2) \end{aligned} \quad (\text{IX.1})$$

where

$$-N\beta mf_m = \ln \sum_{\alpha} e^{-N\beta mf_{\alpha}} \quad (\text{IX.2})$$

is the free-energy of the reference system (Monasson's free-energy). We introduced the Franz-Parisi potential[73],

$$V_{\text{FP}}(\eta) = \frac{\sum_{\alpha} e^{-N\beta mf_{\alpha}} f_{\alpha}(\eta)}{\sum_{\alpha} e^{-N\beta mf_{\alpha}}} \quad (\text{IX.3})$$

B. p -spin Ising case

Let us study the p -spin Ising model. We consider that the reference system (r) and the student system (s) are at different temperatures

$$\beta J_a = \beta J \eta_a \quad \eta_a = \begin{cases} 1 & a \in r \\ \eta & a \in s \end{cases}$$

1. Simplest ansatz

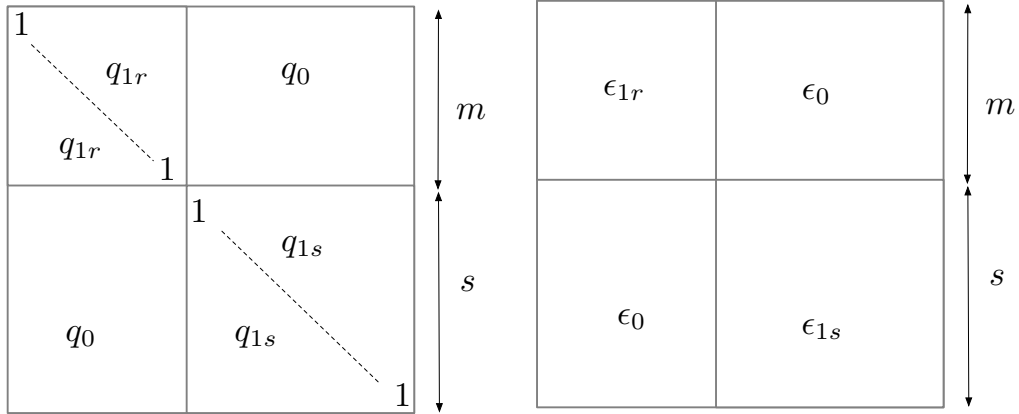


FIG. 27. Parisi matrix for state following

The program sketched above can be implemented by considering the ansatz shown in Fig. 27. Using this in

Eq. (VI.72) we find,

$$\begin{aligned}
-\beta F_{m+s}[\hat{q}] / N &= \frac{\gamma(\beta J)^2}{2}(m + \eta^2 s) - \frac{\gamma(\beta J)^2}{2}(p-1) \sum_{a \neq b} \eta_a \eta_b q_{ab}^p \\
&\quad + \ln \left[e^{\gamma(\beta J)^2 p \sum_{a < b} \eta_a \eta_b q_{ab}^{p-1} \frac{\partial^2}{\partial h_a \partial h_b}} \prod_{a=1}^m (2 \cosh(h_a)) \prod_{a=1+m}^{m+s} (2 \cosh(h_a)) \right]_{h_a=0} \\
&= \frac{\gamma(\beta J)^2}{2}(m + \eta^2 s) - \frac{\gamma(\beta J)^2}{2} [m(m-1)q_{1r}^p + \eta^2 s(s-1)q_{1s}^p + 2\eta s m q_o^p] \\
&\quad - \frac{m}{2}\gamma(\beta J)^2 p q_{1r}^{p-1} - \frac{s}{2}\eta^2 \gamma(\beta J)^2 p q_{1s}^{p-1} \\
&\quad + \ln e^{\gamma p(\beta J)^2 q_0^{p-1} \partial_h^2} \left[\left(e^{\gamma p(\beta J)^2 (q_{1r}^{p-1} - q_0^{p-1}) \partial_h^2} (2 \cosh(h))^m \right) \left(e^{\gamma p(\beta J)^2 (q_{1s}^{p-1} - q_0^{p-1}) \partial_h^2} (2 \cosh(\eta h))^s \right) \right]_{h=0} \tag{IX.4}
\end{aligned}$$

This representation fails for $q_1 < q_0$, which happens for heating case (see the case of the spherical model. We should switch to a different representation.

Using the above result in Eq. (IX.1) we find the free-energy of the reference system,

$$\begin{aligned}
-\beta f_m &= \frac{\gamma(\beta J)^2}{2} - \frac{\gamma(\beta J)^2}{2}(m-1)q_{1r}^p - \frac{m}{2}\gamma(\beta J)^2 p q_{1r}^{p-1} \\
&\quad + \frac{1}{m} \ln \int \mathcal{D}z (2 \cosh(\Xi))^m \tag{IX.5}
\end{aligned}$$

with

$$\Xi = \sqrt{\gamma(\beta J)^2} \sqrt{pq_{1r}^{p-1}} z \tag{IX.6}$$

The above result agrees with Eq. (VIII.7) (with $q_0 = 0$), as it should. We readily know Eq. (VIII.16),

$$q_{1r} = \frac{\int \mathcal{D}z (2 \cosh(\Xi))^m \tanh^2(\Xi)}{\int \mathcal{D}z (2 \cosh(\Xi))^m} \tag{IX.7}$$

For the “student” system we find,

$$\begin{aligned}
-\beta V_{\text{FP}} &= \frac{\gamma(\beta J)^2}{2} \eta^2 + \frac{\gamma(\beta J)^2}{2} \eta^2 q_{1s}^p - \gamma(\beta J)^2 \eta m q_0^p - \frac{\gamma(\beta J)^2}{2} \eta^2 p q_{1s}^{p-1} \\
&\quad + \frac{\int \mathcal{D}z_0 \int \mathcal{D}z_r (2 \cosh(\Xi_r))^m \int \mathcal{D}z_s \ln(2 \cosh(\Xi_s))}{\int \mathcal{D}z (2 \cosh(\Xi))^m} \tag{IX.8}
\end{aligned}$$

with

$$\begin{aligned}
\Xi_r &= \sqrt{\gamma(\beta J)^2} [\sqrt{pq_0^{p-1}} z_0 + \sqrt{pq_{1r}^{p-1} - pq_0^{p-1}} z_r] \\
\Xi_s &= \eta \sqrt{\gamma(\beta J)^2} [\sqrt{pq_0^{p-1}} z_0 + \sqrt{pq_{1s}^{p-1} - pq_0^{p-1}} z_s] \tag{IX.9}
\end{aligned}$$

Taking derivatives we find,

$$\begin{aligned}
q_0 &= \frac{\int \mathcal{D}z_0 \int \mathcal{D}z_r (2 \cosh(\Xi_r))^m \tanh(\Xi_r) \int \mathcal{D}z_s \tanh(\Xi_s)}{\int \mathcal{D}z (2 \cosh(\Xi))^m} \\
q_{1s} &= \frac{\int \mathcal{D}z_0 \int \mathcal{D}z_r (2 \cosh(\Xi_r))^m \int \mathcal{D}z_s \tanh^2(\Xi_s)}{\int \mathcal{D}z (2 \cosh(\Xi))^m} \tag{IX.10}
\end{aligned}$$

We can check that in the case the SP equations admit a solution with $\eta = 1$, $q_{1s} = q_0 = q$ and $V_{\text{FP}}(q_{1s} = q_0 = q)$ given by Eq. (IX.8) becomes identical to $f^*(q)$ given by Eq. (VIII.47) as it should be. We also find $-\beta V_{\text{FP}}(q_{1s} = q_0 = 0) = \frac{\gamma(\beta J)^2}{2} + \ln 2$ which is identical to the thermodynamic free-energy $f_{\text{RS}}(q = 0)$ Eq. (VII.19). Then the relation Eq. (VIII.42) implies $-\beta V_{\text{FP}}(q_{1s} = q_0 = 0) - (-\beta V_{\text{FP}}(q_{1s} = q_0 = q))$ is nothing but the complexity $\Sigma(T)$. At the Kauzmann transition $\Sigma(T_K) = 0$ which can be seen in Fig. 28.

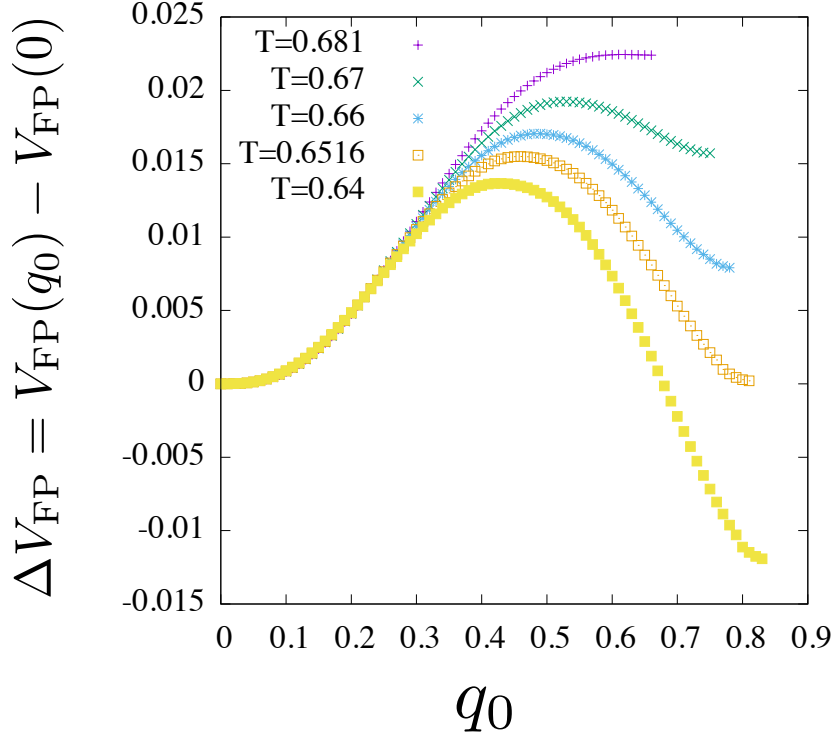


FIG. 28. FP potential of the $p = 3$ Ising model in the case $\eta = 1$. Here we consider the reference system in the temperature range $T_K < T < T_d$ so that $m = 1$. Here we set $q_{1s} = q_0$. Note that $T_K = 0.651385$ [68].

The internal energy

$$\begin{aligned}\beta_s e &= -\beta_s \frac{\partial}{\partial \beta_s} (-\beta V_{\text{FP}}) = -\eta \frac{\partial}{\partial \eta} (-\beta V_{\text{FP}}) \\ &= -\gamma(\beta_s J)^2 + \gamma(\beta_s J)^2 q_{1s}^p - \gamma(\beta J)(\beta_s J)m q_0^p\end{aligned}\quad (\text{IX.11})$$

where we introduced

$$\beta_s = \eta \beta \quad (\text{IX.12})$$

The Hessian matrix Eq. (VI.79) for the student sector is found as,

$$\begin{aligned}M_{a \neq b, c \neq d} &= (\delta_{a,d}\delta_{b,c} + \delta_{a,c}\delta_{b,d})\gamma(\beta_s J)^2 p(p-1)q_{1s}^{p-2} \{ \\ &1 - \gamma(\beta_s J)^2 p(p-1)q_{1s}^{p-2} \frac{\int \mathcal{D}z_0 \int \mathcal{D}z_r \cosh^m(\Xi_r) \int \mathcal{D}z_s \operatorname{sech}^4(\Xi_s)}{\int \mathcal{D}z \cosh^m(\Xi)} \} + \dots\end{aligned}\quad (\text{IX.13})$$

Thus the normalized replicon eigen-value is obtained as,

$$\tilde{\lambda}_R = 1 - \gamma(\beta_s J)^2 p(p-1)q_{1s}^{p-2} \frac{\int \mathcal{D}z_0 \int \mathcal{D}z_r \cosh^m(\Xi_r) \int \mathcal{D}z_s \operatorname{sech}^4(\Xi_s)}{\int \mathcal{D}z \cosh^m(\Xi)} \quad (\text{IX.14})$$

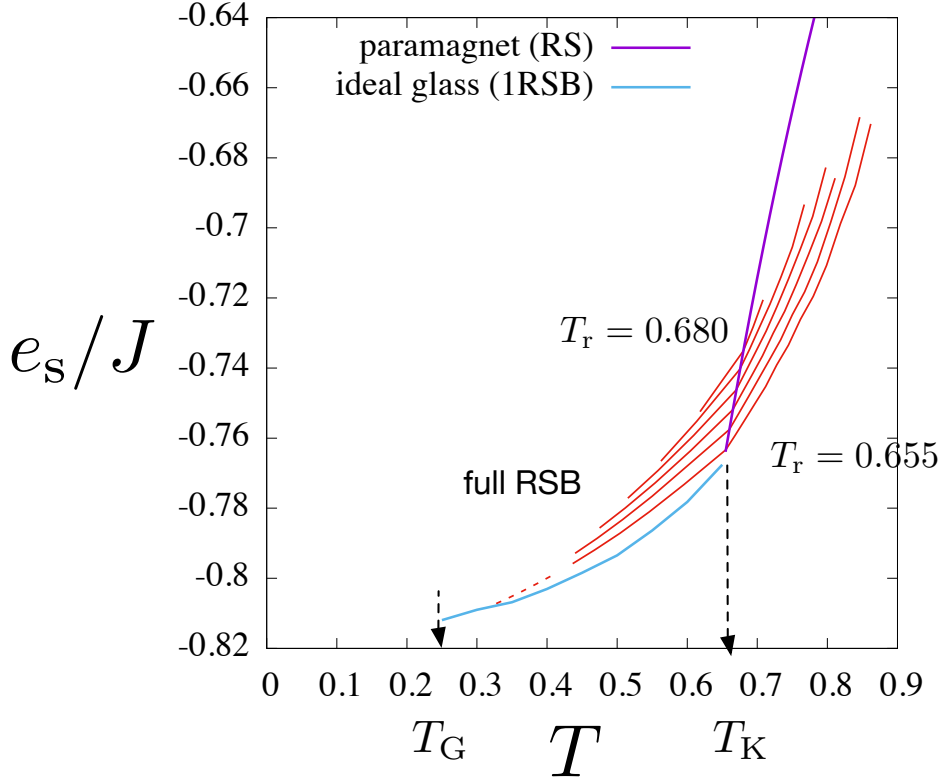


FIG. 29. Internal energy: the red lines are the state following curves. Broken lines represent region where the solution is unstable (Gardner phase). see [74] for a computation by the cavity approach.

C. p -spin spherical case

1. Basics

Let us consider the spherical p -spin model. From Eq. (VI.81) we find for $n = 1 + s$ replica system with RS ansatz Eq. (VII.1) (see sec VII B), we find the free energy as

$$-\beta F_{n=1+s}^{\text{RS}}(q)/N = \frac{1+s}{2} + \frac{1+s}{2} \ln(2\pi) + \frac{1}{2} [\ln(1+sq) + s \ln(1-q)] + \frac{\gamma(\beta J)^2}{2}(1+s)(1+sq^p) \quad (\text{IX.15})$$

In $s \rightarrow 0$ limit we find

$$-\beta f_1 = -\beta F_1[\hat{q}_{\text{statefollowing}}]/N = \frac{1}{2} + \frac{1}{2} \ln(2\pi) + \frac{\gamma(\beta J)^2}{2} \quad (\text{IX.16})$$

which agrees with the RS free-energy with $q = 0$ (see Eq. (VII.29)). We also obtain the FP potential as,

$$-\beta V_{\text{FP}}(q) = \partial_s (-\beta F_{n=1+s}^{\text{RS}}(q)/N) \Big|_{s=0} = \frac{1}{2} + \frac{1}{2} \ln(2\pi) + \frac{1}{2} (q + \ln(1-q)) + \frac{\gamma(\beta J)^2}{2}(1+q^p) \quad (\text{IX.17})$$

In Fig. 30 we display the profile of the FP potential.

The saddle point equation reads,

$$0 = \frac{\partial}{\partial q} (-\beta V_{\text{FP}}) = -\frac{q}{2(1-q)} \underbrace{\left(1 - \gamma(\beta J)^2 p q^{p-2} (1-q)\right)}_{g(q)} \quad (\text{IX.18})$$

Remarkably this agrees with the equation Eq. (XII.52)) which determines the plateau height C of the time-auto correlation function. Below the dynamical transition temperature T_d , the non-zero solution emerges signaling on set of glassiness.

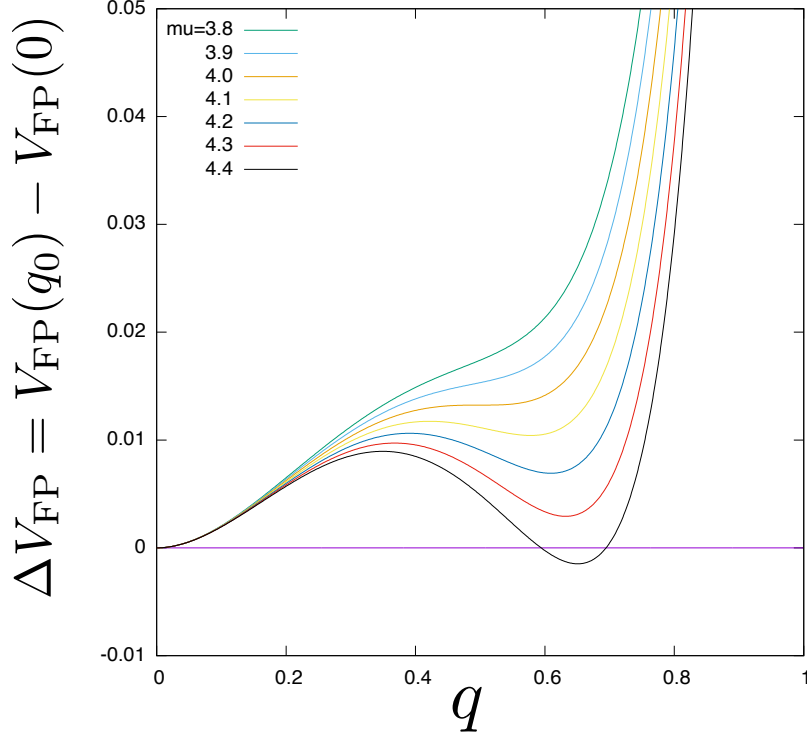


FIG. 30. FP potential of the $p = 3$ spherical model.

As in the case of the Ising model, the profile of the FP potential shown in Fig. 30 suggests the Kauzmann transition T_K at which the FP potential at the non-zero solution becomes the same as that of the $q = 0$ solution which always exist.

From the 1RSB solution of the spherical model (see sec. VIII G) we readily find,

$$\Sigma^* = -m^2 \partial_m (-\beta f_{1\text{RSB}}(q_1 = q, q_0 = 0, m)) = \frac{1}{2} \ln \left[\frac{1 + (m-1)q}{1-q} \right] - \frac{m}{2} \frac{q}{1 + (m-1)q} - m^2 \frac{\gamma(\beta J)^2}{2} q^p \quad (\text{IX.19})$$

and

$$\beta f^* = \partial_m (\beta f_{1\text{RSB}}(q_1 = q, q_0 = 0, m)) = -\frac{1}{2} \frac{q}{1 + (m-1)q} - \frac{1}{2} \ln(1-q) - \frac{\gamma(\beta J)^2}{2} (1 + (2m-1)q^p) \quad (\text{IX.20})$$

[Q] It can be seen that $-\beta V_{\text{FP}}(q) - \beta V_{\text{FP}}(0) = -\Sigma^*(m = 1)$. It can also be seen that $-\beta F(q) = -\beta f^*(m = 1)$ (apart from some constants neglected). What is the physical meaning?

2. Temperature perturbation

Now let us consider state following under temperature perturbation. To this end we study the replicated spherical p -spin model Eq. (VI.81) with the temperature perturbation Eq. (IX.4),

$$-\beta F_{1+s}[\hat{q}] / N = \frac{1+s}{2} + \frac{1+s}{2} \ln(2\pi) + \ln \det \hat{q}_{1+s} + \frac{\gamma(\beta J)^2}{2} \sum_{a,b} \eta_a \eta_b q_{ab}^{p-1} \quad (\text{IX.21})$$

Using the ansatz shown in Fig. 27, we find the free-energy become,

$$\begin{aligned} -\beta F_{1+s}[\hat{q}_{\text{state following}}] / N = & \frac{1+s}{2} + \frac{1+s}{2} \ln(2\pi) + \frac{1}{2} \left[\ln \{(1-q) + s(q-r^2)\} + (s-1) \ln(1-q) \right] + \\ & \frac{\gamma(\beta J)^2}{2} \left[(1+\eta^2 s) + \eta^2 s(s-1) q^p + 2\eta s r^p \right] \end{aligned} \quad (\text{IX.22})$$

In $s \rightarrow 0$ limit we find

$$-\beta f_1 = -\beta F_1[\hat{q}_{\text{statefollowing}}]/N = \frac{1}{2} + \frac{1}{2} \ln(2\pi) + \frac{\gamma(\beta J)^2}{2} \quad (\text{IX.23})$$

which agrees with the RS free-energy with $q = 0$ (see Eq. (VII.29)). The Franz-Parisi potential is obtained as

$$-\beta V_{\text{FP}}(q, r) = \partial_s \left(-\beta F_{1+s}[\hat{q}]/N \Big|_{s=0} \right) = \frac{1}{2} + \frac{1}{2} \ln(2\pi) + \frac{1}{2} \left(\frac{q-r^2}{1-q} + \ln(1-q) \right) + \frac{\gamma(\beta J)^2}{2} (\eta^2 - \eta^2 q^p + 2\eta r^p) \quad (\text{IX.24})$$

for $\eta = 1$ and $r = q$ this agree with Eq. (IX.17).

Taking derivatives of $-\beta V_{\text{FP}}(q, r)$ with respect to q and r we find the saddle point equations,

$$\begin{aligned} 0 &= -\frac{q-r^2}{(1-q)^2} \left[1 - \eta^2 \mu q^{p-1} \frac{(1-q)^2}{q-r^2} \right] \\ 0 &= -\frac{r}{1-q} \left[1 - \eta \mu r^{p-1} \frac{1-q}{r} \right] \end{aligned} \quad (\text{IX.25})$$

The internal energy of the reference state is

$$\beta e = -\beta \frac{\partial}{\partial \beta} (-\beta f_1) = -\gamma(\beta J)^2 \quad (\text{IX.26})$$

The internal energy is obtained as

$$\beta_s e = -\eta \frac{\partial}{\partial \eta} (-\beta V_{\text{FP}}) = -\gamma(\beta J)^2 \left[\eta^2 (1 - q^p) + \eta r^p \right] \quad (\text{IX.27})$$

where we used β_s defined in Eq. (IX.12).

(To Do) Compute also the complexity, show the Kauzmann temperature, replicon eigenvalue.

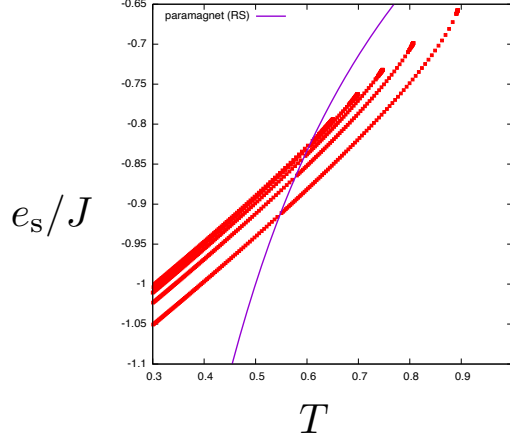


FIG. 31. Internal energy: the red lines are the state following curves of the spherical model. $\mu = 5.0, 4.5, 4.25, 4.125, 4.0625$. ($p = 3, \gamma = 1/2$) **Indicate also the Kauzmann temperature.**

D. Teacher-student setting: statistical inference of planted configuration

The state following is intimately related to the problem of statistical inference discussed in sec. II B. In the teacher-student scenario (sec. II B 2), the teacher can be regarded as the reference system.

Student infers A through the Baeyens formula,

$$P(A|B) = \frac{1}{Z_{\text{student}}(B)} P(B|A) P(A) \quad (\text{IX.28})$$

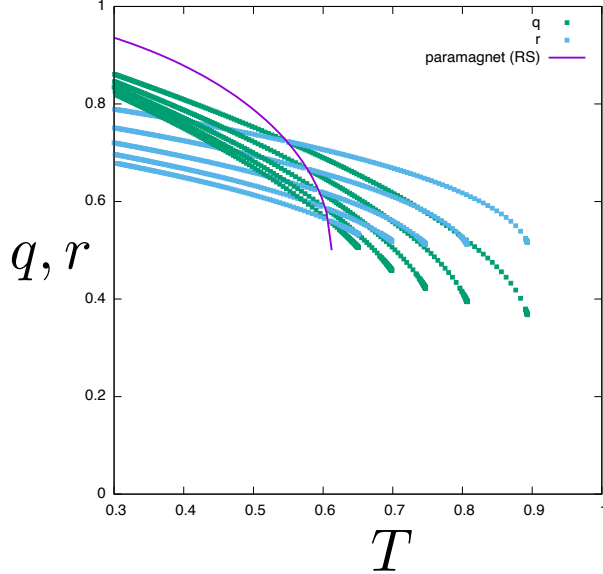


FIG. 32. Overlaps of the spherical model. $\mu = 5.0, 4.5, 4.25, 4.125, 4.0625$. ($p = 3, \gamma = 1/2$) **Indicate also the Kauzmann temperature.**

with the partition function of a student

$$Z_{\text{student}}(B) = \int dA P(B|A) P(A) = \int dA e^{-\beta_s H(A|B)} \quad (\text{IX.29})$$

which depends on B provided by the teacher. It fluctuates as B fluctuates. Replicating this we find,

$$Z_{\text{student}}^n(B) = \int \prod_{a=1}^n dA_a e^{-\beta_s \sum_{a=1}^n H(A_a|B)} \quad (\text{IX.30})$$

We are interested with 'typical inferences' which can be studied through the free-energy averaged over different realizations of B (see the discussion in sec. [VIA 5](#)),

$$-\beta F = \mathbb{E}_B[\ln Z_{\text{student}}(B)] = \partial_n \mathbb{E}_B[Z_{\text{student}}^n(B)]|_{n=0} \quad (\text{IX.31})$$

where the average over different realizations of B can be expressed as

$$\mathbb{E}_B \dots = \int dB P(B) \dots = \int dB dA^* P(B|A^*) P(A^*) \dots = \int dB dA^* e^{-\beta^* H(A^*|B)} \dots \quad (\text{IX.32})$$

Note that this reflects how the teacher generates B given ground truth A^* . Then including 0-th replica to represent the teacher we can write

$$\mathbb{E}_B[Z_{\text{student}}^n(B)] = \int dB \int \prod_{a=0}^n dA_a e^{-\sum_{a=0}^n \beta_a H(A_a|B)} \quad (\text{IX.33})$$

where $\beta_0 = \beta_*$ and $\beta_a = \beta_s$ for $a = 1, 2, \dots, n$. We can see that if $\beta_* = \beta$, the $1+n$ replica system is replica symmetric at the Hamiltonian level.

1. Planted p -spin

- The 'simple setting 1' discussed in sec [III D](#) is realized exactly in the previous section sec. [IX B](#).

The order parameter q_0 measures the overlap between the teacher and student. Thus $q_0 = 0$ means failure of the inference and larger q_0 mean successful inference. Bayes optimal inference corresponds to $\eta = 1$ where we naturally have $q_{1s} = q_0$. The latter is essentially the same as the identity $q = m$ (see Eq. [\(III.21\)](#)) which happens along the Nishimori line (see below). This holds generically in Bayes optimal inferences [\[10, 18\]](#).

- (Todo) Expand this ... discuss replica formalism for the error correcting code.

In sec III D 3 we also explained that 'simple setting 2' is equivalent to a spin-glass problem with a ferromagnetic bias Eq. (III.11) or Eq. (III.18). The phase diagrams of such models are well known (See Fig. 6). Thus one just needs to re-interpret the known spinglass phase diagrams in the context of inference. As we explained in sec III D, the magnetization m can be understood as the overlap of the inferred spin configuration S with respect to the ground truth S^* . Thus the inference is successful in the ferromagnetic phase where $m > 0$.

Along the Nishimori-line one can prove [19] the Edwards-Anderson glass order parameter q is equal to m ,

$$q = m \quad (\text{IX.34})$$

As noted above this is a generic property which happens when the inference is Bayes optimal [10, 18].

This inference scheme is exactly the Sourlas code [24] for the error correcting codes: one sends the global coupling J_{i_1, i_2, \dots, i_p} as the data to the receiver along a noisy channel. Then the receiver tries to infer the original N bits from the noisy data. In the $p \rightarrow \infty$ (corresponding to REM with a ferromagnetic bias) the Sourlas code achieves the upper limit due to the Shannon bound [75] $R < C$ ($R = N/N_\blacksquare$: transmission rate, C : capacity of the transmission line). However $R, C \rightarrow 0$ in $N \rightarrow \infty$ so that transmission actually becomes infinitely slow. This problem arise because one sends too large number of data $N_\blacksquare \propto N^p$ (see Eq. (III.13)). This problem was overcome using the sparse coding proposed by Kabashima-Saad [25]. One can also consider the planted version of the M -component vector spin problem (see sec. III A 4) studied in [15].¹⁷

Now let us examine the Sourlas code in the teacher-student setting explained in sec. III D 3. Students infer S using the Bayes formula

$$P(S|Y) = \frac{1}{Z(Y)} P(Y|S) P(S) \quad Z(Y) = \int dS P(Y|S) P(S) \quad (\text{IX.35})$$

with the prior distribution of the form

$$P(S) = \prod_{i=1}^N \phi(S_i) \quad \phi(S) = \frac{1}{2} [\delta(S+1) + \delta(S-1)] \quad (\text{IX.36})$$

and the likelihood of the form

$$P(Y|S) = \prod_{\blacksquare=1}^{N_\blacksquare} \psi(Y_\blacksquare | \{S_i\}_{i \in \partial \blacksquare}) \quad (\text{IX.37})$$

Then we find the object we have to analyze is,

$$\mathbb{E}_Y[Z_{\text{student}}^n(Y)] = \int \left(\prod_{\blacksquare=1}^{N_\blacksquare} dY_\blacksquare \right) \prod_{a=0}^n \left(\prod_{i=1}^N \underbrace{\int dS_i^a \phi(S_i^a)}_{(1/2) \sum s_i^a = \pm 1} \right) \prod_{\blacksquare=1}^{N_\blacksquare} \psi_a(Y_\blacksquare | \{S_i^a\}_{i \in \partial \blacksquare}) \quad (\text{IX.38})$$

Considering Gaussian noise we find,

$$\psi_a(Y_\blacksquare | \{S_i\}_{i \in \partial \blacksquare}) = \frac{1}{\sqrt{2\pi\Delta^2}} \exp \left[-\frac{(Y_\blacksquare - \frac{\Lambda_a}{\sqrt{c/\alpha}} \prod_{i \in \partial \blacksquare} S_i)^2}{2\Delta^2} \right] \quad (\text{IX.39})$$

where

$$\begin{aligned} \Lambda_0 &= \Lambda_* \\ \Lambda_a &= \Lambda \quad (a = 1, 2, \dots, n) \end{aligned} \quad (\text{IX.40})$$

¹⁷ Using the large- M component vector spin system on the dense graph with large connectivity $c = \alpha M \rightarrow \infty$ (with fixed α), one can attain a finite transmission rate $R = N_\blacksquare/(NM) = \gamma$ (See Eq. (III.23)) and also attain the Shannon bound in $p \rightarrow \infty$ limit with fixed $\gamma = \alpha/p$. (S. Yokoi, master thesis, Osaka Univ, 2018)(Nagasaki-Yokoi-Obuchi-Yoshino, work in progress)

The inference becomes Bayes optimal if $\Lambda = \Lambda_*$. Now performing the integration over Y_{\blacksquare} we find,

$$\int dY_{\blacksquare} \prod_{a=0}^n \psi(Y_{\blacksquare} | \{S_i^a\}_{i \in \partial \blacksquare}) = \exp \left[\frac{1}{2} \frac{1}{1+n} \sum_{a=0}^n \sum_{b=0}^n \frac{\Lambda_a/\Delta}{\sqrt{c/\alpha}} \frac{\Lambda_b/\Delta}{\sqrt{c/\alpha}} \prod_{i \in \partial \blacksquare} S_i^a S_i^b \right] \quad (\text{IX.41})$$

Here we dropped unimportant constant terms. Hence we find,

$$\mathbb{E}_Y[Z_{\text{student}}^n(Y)] = Z_{1+n} = \frac{1}{2^{N(n+1)}} \prod_{a=0}^n \left(\prod_{i=1}^N \sum_{S_i^a} \right) \prod_{\blacksquare=1}^{N_{\blacksquare}} \exp \left[\frac{1}{2} \frac{1}{1+n} \sum_{a=0}^n \sum_{b=0}^n \frac{\Lambda_a/\Delta}{\sqrt{c/\alpha}} \frac{\Lambda_b/\Delta}{\sqrt{c/\alpha}} \prod_{i \in \partial \blacksquare} S_i^a S_i^b \right] \quad (\text{IX.42})$$

We proceed as done in sec. VI.C.

$$Z_{1+n} = \int \prod_{a < b} dq^{ab} e^{-\beta F_{1+n}[q]} \quad e^{-\beta F[q]} = \int_{-i\infty}^{i\infty} \prod_{a < b} \frac{d\epsilon^{ab}}{2\pi i} e^{-\sum_{i=1}^N \sum_{a < b} \epsilon^{ab} q^{ab}} e^{-\beta G_{1+n}[\epsilon]} \quad (\text{IX.43})$$

where

$$-\beta G_{1+n}[\epsilon] = -\beta G_{1+n,0}[\epsilon] + \ln \left\langle \prod_{\blacksquare=1}^{N_{\blacksquare}} \exp \left[\frac{1}{2} \frac{1}{1+n} \sum_{a=0}^n \sum_{b=0}^n \frac{\Lambda_a/\Delta}{\sqrt{c/\alpha}} \frac{\Lambda_b/\Delta}{\sqrt{c/\alpha}} \prod_{i \in \partial \blacksquare} S_i^a S_i^b \right] \right\rangle_{\epsilon,0} \quad (\text{IX.44})$$

with the entropic part of the free-energy given by (see Eq. (VI.55)),

$$\begin{aligned} \frac{-\beta G_{n,0}[\epsilon]}{N} &= \ln \prod_{a=0}^n \sum_{S^a=\pm 1} e^{\frac{1}{2} \sum_{a,b=0}^n \epsilon_{ab} S_a S_b} = \ln \prod_{a=0}^n \sum_{S^a=\pm 1} e^{\frac{1}{2} \sum_{a,b=1}^n \epsilon_{ab} \frac{\partial^2}{\partial h_a \partial h_b} + \epsilon_{00} + S_0 \sum_{a=1}^n \epsilon_{0a} \frac{\partial}{\partial h_a} + \frac{\epsilon_{00}}{2}} e^{\sum_{c=1}^n h_c S_c} \Big|_{h=0} \\ &= \frac{\epsilon_{00}}{2} + \ln e^{\frac{1}{2} \sum_{a,b=1}^n \epsilon_{ab} \frac{\partial^2}{\partial h_a \partial h_b}} \prod_{c=1}^n (2 \cosh(h_c + \epsilon_{0c})) \Big|_{h=0} \end{aligned} \quad (\text{IX.45})$$

To derive the last equation we used the identity $e^{a(d/dh)} f(h) = f(h+a)$ for a generic a and a function $f(h)$, and $\cosh(h) = \cosh(-h)$. The cumulare expansion $\ln \langle \dots \rangle_{\epsilon,0}$ can be done as before and we find,

$$\frac{1}{N} \ln \langle \dots \rangle_{\epsilon,0} = \frac{\gamma}{2} \frac{1}{1+n} \sum_{a=0}^n \sum_{b=0}^n \frac{\Lambda_a}{\Delta} \frac{\Lambda_b}{\Delta} q_{ab}^p \quad (\text{IX.46})$$

dropping terms which vanish in $c \rightarrow \infty$. To sum up we find

$$\frac{-\beta F_{1+n}[q]}{N} = -\frac{1}{2} \sum_{a,b=0}^n \epsilon_{ab}^* q_{ab} + \ln e^{\frac{1}{2} \sum_{a,b=1}^n \epsilon_{ab}^* \frac{\partial^2}{\partial h_a \partial h_b}} \prod_{c=0}^n 2 \cosh(h_c + \epsilon_{0c}) \Big|_{h=0} + \frac{\gamma}{2} \sum_{a,b=0}^n \frac{\Lambda_a}{\Delta} \frac{\Lambda_b}{\Delta} q_{ab}^p \quad (\text{IX.47})$$

where we have replaced $1+n$ by 1 anticipating to take $n \rightarrow 0$ limit.

We consider the ansatz like Fig. 27 but considering $m = 1$ case. We also rewrite $s \rightarrow n$ (just for the notational consistency) $q_0 \rightarrow m$ ('magnetization'). Then

$$\sum_{a,b=0}^n \frac{\Lambda_a}{\Delta} \frac{\Lambda_b}{\Delta} q_{ab}^p = \left(\frac{\Lambda_*}{\Delta} \right)^2 + 2n \frac{\Lambda_*}{\Delta} \frac{\Lambda}{\Delta} m^p + \left(\frac{\Lambda}{\Delta} \right)^2 \sum_{a,b=1}^n q_{ab}^p \quad (\text{IX.48})$$

and

$$\sum_{a,b=0}^n \epsilon_{ab}^* q_{ab} = \epsilon_{00}^* + 2n \epsilon_0^* m + \sum_{a,b=1}^n \epsilon_{ab}^* q_{ab} \quad (\text{IX.49})$$

To sum up we find

$$\begin{aligned} \frac{-\beta F_{1+n}[q]}{N} &= -\frac{1}{2} \left[2n \epsilon_0^* m + \sum_{a,b=1}^n \epsilon_{ab}^* q_{ab} \right] + \ln e^{\frac{1}{2} \sum_{a,b=1}^n \epsilon_{ab}^* \frac{\partial^2}{\partial h_a \partial h_b}} \prod_{c=0}^n 2 \cosh(h_c + \epsilon_0^*) \Big|_{h=0} \\ &\quad + \frac{\gamma}{2} \left[2n \frac{\Lambda_*}{\Delta} \frac{\Lambda}{\Delta} m^p + \left(\frac{\Lambda}{\Delta} \right)^2 \sum_{a,b=1}^n q_{ab}^p \right] \end{aligned} \quad (\text{IX.50})$$

where we dropped some constant terms.

Now let us consider replica symmetric ansatz for the n student replicas (see sec VII A 1) : we assume Eq. (VII.1). Then we find (see Eq. (VII.7)),

$$\begin{aligned} \frac{-\beta F_{1+n}^{\text{RS}}[q, m]}{N} &= -n\epsilon_0 m + n\gamma \frac{\Lambda_*}{\Delta} \frac{\Lambda}{\Delta} m^p \\ &\quad - \frac{1}{2} n(\epsilon + (n-1)\epsilon q) + \ln e^{\frac{\epsilon}{2} \frac{\partial^2}{\partial h^2}} (2 \cosh(h + \epsilon_0))^n \Big|_{h=0} + \frac{\gamma}{2} \left(\frac{\Lambda}{\Delta} \right)^2 n(1 + (n-1)q^p) \end{aligned} \quad (\text{IX.51})$$

from which we find (see Eq. (VII.8)),

$$\begin{aligned} -\beta f_{\text{student}}^{\text{RS}}[q, m] &= \partial_n \left(\frac{-\beta F_{1+n}^{\text{RS}}[q, m]}{N} \right)_{n=0} \\ &= -\epsilon_0 m + \gamma \frac{\Lambda_*}{\Delta} \frac{\Lambda}{\Delta} m^p - \frac{1}{2}(\epsilon - \epsilon q) + \frac{\gamma}{2} \left(\frac{\Lambda}{\Delta} \right)^2 (1 - q^p) + \int Dz \log(2 \cosh(\sqrt{\epsilon}z + \epsilon_0)) \end{aligned} \quad (\text{IX.52})$$

Taking derivatives with respect to m and q we find,

$$\epsilon_0 = \gamma p \frac{\Lambda_*}{\Delta} \frac{\Lambda}{\Delta} m^{p-1} \quad (\text{IX.53})$$

$$\epsilon = \gamma p \left(\frac{\Lambda}{\Delta} \right)^2 q^{p-1} \quad (\text{IX.54})$$

And taking derivatives with respect to ϵ_0 and ϵ we find,

$$m = \int Dz \tanh(\sqrt{\epsilon}z + \epsilon_0) \quad (\text{IX.55})$$

$$q = \int Dz \tanh^2(\sqrt{\epsilon}z + \epsilon_0) \quad (\text{IX.56})$$

Let us recall the correspondence Eq. (III.40) between the spin-glass problem with ferromagnetic bias and the Sourlas code,

$$\begin{aligned} \beta J &\rightarrow \frac{\Lambda}{\Delta} \\ \lambda &\rightarrow \frac{\Lambda^*}{\Delta} \end{aligned} \quad (\text{IX.57})$$

which also implied the equivalence of Bayes optimal inference and the SG problem along the Nishimori line Eq. (III.42),

$$\frac{\Lambda^*}{\Delta} = \frac{\Lambda}{\Delta} \Leftrightarrow \beta J = \lambda \quad (\text{IX.58})$$

In this case $m = q$. Then we just had single equation of states,

$$m = \int Dz \tanh(\sqrt{\gamma p(\Lambda/\Delta)^2 m^{p-1}} z + \gamma p(\Lambda/\Delta)^2 m^{p-1}) \quad (\text{IX.59})$$

2. Shannon's bound

The transmission rate is given by

$$R = \frac{N}{N_{\blacksquare}} = \frac{p}{c} = \frac{1}{\gamma} \frac{1}{c/\alpha} \quad (\text{IX.60})$$

using $N_{\blacksquare} = N(c/p)$ (see Eq. (III.1)) and $\gamma = \alpha/p$ (see Eq. (III.2)). It quantifies the degree of redundancy of the coding. The Shannon's channel capacity theorem [75] says that for perfect recovery of the data $m = 1$ out of the noisy data is possible only for sufficiently redundant coding such that

$$R \leq C \quad (\text{IX.61})$$

where C is the so called channel capacity. In our case, we are considering a transmission channel with Gaussian noise. The capacity of Gaussian channel [9] is given by,

$$C = \frac{1}{2} \log_2 \left[1 + \left(\frac{\Lambda}{\sqrt{c/\alpha}\Delta} \right)^2 \right] \xrightarrow{c \rightarrow \infty} \frac{1}{2 \ln 2} \left(\frac{\Lambda}{\Delta} \right)^2 \frac{1}{c/\alpha} \quad (\text{IX.62})$$

where the second term in the bracket [...] is the square of the S/N (signal to noise ratio). Here we used the fact that the bias of the noise is $\Lambda/(\sqrt{c/\alpha})$ and the standard deviation of the noise is Δ (see Eq. (IX.39)). Thus the Shannon's theorem Eq. (IX.61) requires

$$\frac{\Lambda}{\Delta} \geq \sqrt{\frac{2 \ln 2}{\gamma}} \quad (\text{IX.63})$$

for perfect denoising.

Interestingly one can show that in $p \rightarrow \infty$ limit, the Sourlas code [24] exhibit a 1st order transition from the paramagnetic phase $m = 0$ (complete failure of inference) to the fully magnetized ferromagnetic phase $m = 1$ (perfect inference) at, in the case of Bayes optimal inference,

$$\left(\frac{\Lambda}{\Delta} \right)_c = \sqrt{\frac{2 \ln 2}{\gamma}}. \quad (\text{IX.64})$$

Indeed one can recognize easily that the equation of states Eq. (IX.59) admits only two solutions $m = 0$ and $m = 1$ in $p \rightarrow \infty$ limit. Thus the Soulas code can achieve perfect inference in $p \rightarrow \infty$ limit with the lowest possible redundancy of the code.

[Exercise] Compute the transition point Eq. (IX.64) comparing the difference of the free-energy Eq. (IX.52) between the two solutions: $m = 0$ and $m = 1$.

3. Perceptron learning

Here we consider the teacher-student setting in the context of learning by the perceptron mentioned in sec IX D 3. We consider the following scenario (Model B proposed in the unfinished work of E. Gardner [27]).

We consider two machines which are the simple perceptrons introduced in sec. III F (see Fig. 8). We call one the teacher machine and the other the student machine. They have exactly the same architecture including the number of neurons N .

- Teacher: Teacher's J_i $i = 1, 2, \dots, N$ are created randomly. Each J_i is an iid Gaussian random number of average 0 and variance 1. And this set of weights is the ground truth. Then teacher creates M different sets of inputs $S_i^\mu = \pm 1$ ($i = 1, 2, \dots, N$) ($\mu = 1, 2, \dots, M$) randomly. Then teacher computes the corresponding outputs S_0^μ ($\mu = 1, 2, \dots, M$) using the teacher's machine. The M set of inputs/outputs is the data which is sent to the student.
- Student: Student receives the M sets of data from the teacher. The task of the student is to infer teachers weights J_i 's using the data. The student knows exactly how the data was created (except the actual values of J_i 's). So the student does a Bayes optimal inference.

This problem can be studied in the same way as we did the state following in sec. IX B of the p -spin Ising model. Instead of the p -spin Ising model we use the large- M component vectorial spin model with $p = 1$. In sec III F we found the partition function of the system is just the same as the Gardner's volume of the perceptron.

In sec we have studied such a model in the context of constraint satisfaction problem using n replicas. Here we use the model with $1 + s$ replicas, 1 for the teacher and s for the student and take $s \rightarrow 0$ limit. The structure of the order parameter is the same as the one shown in Fig ?? with $m = 1$. We set $m = 1$ because the teacher's machine is just a random machine. For convenience we label the teacher's replica as the 0 th replica and label the students replicas as $a = 1, 2, \dots, s$.

Within the simplest ansatz we have,

$$\hat{Q}_{ab} = R + (1 - R)\delta_{a,0}\delta_{b,0} + (\hat{Q}_{\text{student}} - R)(1 - \delta_{a,0})(1 - \delta_{b,0}) \quad (\text{IX.65})$$

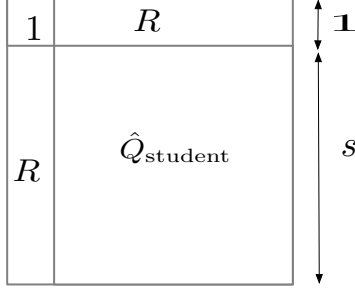


FIG. 33. Parisi matrix for perceptron learning (random teacher)

Here R represents the overlap between the teacher and student machines while \hat{Q}_{student} represent the overlaps among the students.

To compute the entropic part of the free-energy of the M -component spin system Eq. (VI.92) we need the determinant of the Parisi matrix. We find,

$$\det(Q) = \det(\hat{Q}_{\text{student}} - R^2). \quad (\text{IX.66})$$

Assuming RS ansatz for the student part,

$$\hat{Q}_{\text{student}} = Q + (1 - Q)\delta_{a,b} \quad a, b \in \text{students} \quad (\text{IX.67})$$

we find

$$\begin{aligned} \det(Q) &= \ln \left[1 - R^2 + (s - 1)(Q - R^2) \right] \\ &\quad + (s - 1) \ln(1 - Q) \end{aligned} \quad (\text{IX.68})$$

Using this we find the free-energy Eq. (VI.92) as

$$\begin{aligned} -\beta F_{1+s}[\hat{q}] / NM &= \frac{s}{2} + \frac{s}{2} \ln(2\pi) + \frac{1}{2} \ln \left[1 - R^2 + (s - 1)(Q - R^2) \right] + \frac{1}{2}(s - 1) \ln(1 - Q) \\ &\quad + \alpha \ln e^{\frac{R}{2} \partial_h^2} \left\{ \left(e^{\frac{1-R}{2} \partial_h^2} \theta(h) \right) \left[e^{\frac{Q-R}{2} \partial_h^2} \left(e^{\frac{1-Q}{2} \partial_h^2} \theta(h) \right)^s \right] \right\} \Big|_{h=0} \end{aligned} \quad (\text{IX.69})$$

Note that $p = 1$ in the perceptron problem so that $\gamma = \alpha$. From this, we extract the Franz-Parisi potential, or the logarithm of the Gardner's volume of the students as,

$$\begin{aligned} -\beta V_{\text{FP}}(Q, R) &= \partial_s (-\beta F_{1+s}[\hat{q}] / NM) \Big|_{s=0} = \frac{1}{2} + \frac{\ln(2\pi)}{2} + \frac{1}{2} \frac{Q - R^2}{1 - Q} + \frac{1}{2} \ln(1 - Q) \\ &\quad + \alpha \partial_s \ln e^{\frac{R}{2} \partial_h^2} \left\{ \left(e^{\frac{1-R}{2} \partial_h^2} \theta(h) \right) \left[e^{\frac{Q-R}{2} \partial_h^2} \left(e^{\frac{1-Q}{2} \partial_h^2} \theta(h) \right)^s \right] \right\} \Big|_{h=0} \Bigg|_{s=0} \end{aligned} \quad (\text{IX.70})$$

Saddle point equations are

$$\begin{aligned} 0 &= \frac{\partial}{\partial Q} (-\beta V_{\text{FP}}(Q, R)) \\ &= \frac{1}{2} \frac{Q - R^2}{(1 - Q)^2} - \frac{\alpha}{2} \frac{\int \mathcal{D}z_{\text{com}} \int \mathcal{D}z_{\text{teacher}} \theta(\Xi_{\text{teacher}}) \int \mathcal{D}z_0 \left(\frac{\int \mathcal{D}z \theta'(\Xi_{\text{student}})}{\int \mathcal{D}z \theta(\Xi_{\text{student}})} \right)^2}{\int \mathcal{D}z_{\text{com}} \int \mathcal{D}z_{\text{teacher}} \theta(\Xi_{\text{teacher}})} \end{aligned} \quad (\text{IX.71})$$

and

$$\begin{aligned} 0 &= \frac{\partial}{\partial R} (-\beta V_{\text{FP}}(Q, R)) \\ &= \frac{1}{2} \frac{-2R}{1 - Q} + \alpha \frac{\int \mathcal{D}z_{\text{com}} \int \mathcal{D}z_{\text{teacher}} \theta'(\Xi_{\text{teacher}}) \int \mathcal{D}z_0 \frac{\int \mathcal{D}z \theta'(\Xi_{\text{student}})}{\int \mathcal{D}z \theta(\Xi_{\text{student}})}}{\int \mathcal{D}z_{\text{com}} \int \mathcal{D}z_{\text{teacher}} \theta(\Xi_{\text{teacher}})} \end{aligned} \quad (\text{IX.72})$$

where

$$\Xi_{\text{teacher}} = \sqrt{1-R}z_{\text{teacher}} + \sqrt{R}z_{\text{com}} \quad (\text{IX.73})$$

$$\Xi_{\text{student}} = \sqrt{1-Q}z + \sqrt{Q-R}z_0 + \sqrt{R}z_{\text{com}} \quad (\text{IX.74})$$

To derive the 2nd equation see¹⁸.

We see that $Q = R$ is a solution (Nishimori condition). Using this we find,

$$0 = \frac{1}{2} \frac{Q}{1-Q} \left[1 - \frac{\alpha}{2} \frac{1}{Q} \frac{\int \mathcal{D}z_{\text{com}} \Theta(x) r^2(x)}{\int \mathcal{D}z_{\text{com}} \Theta(x)} \Big|_{x=\frac{\sqrt{Q}z_{\text{com}}}{\sqrt{2(1-Q)}}} \right] \quad (\text{IX.75})$$

where we used Eq. (VII.48) and Eq. (VII.53).

Let us focus on the regime $Q = 1 - \epsilon$ with $\epsilon \ll 1$. We find,

$$[\dots] \simeq 1 - \alpha \sqrt{2\epsilon} \int_{-\infty}^{\infty} \frac{dy}{\sqrt{2\pi}} \Theta(y) r^2(y) \quad (\text{IX.76})$$

this yields

$$\epsilon = \frac{1}{2\alpha^2} \frac{1}{\left[\int_{-\infty}^{\infty} \frac{dy}{\sqrt{2\pi}} \Theta(y) r^2(y) \right]^2} \quad (\text{IX.77})$$

Generalization error - what is the probability that the student gives wrong answer? Consider the internal field within the teacher and student machines subjected to some random test data $S_i^{\text{test}} = \pm 1$,

$$\begin{aligned} u &= \sum_{i=1}^N \frac{J_i^{\text{teacher}}}{\sqrt{N}} S_i^{\text{test}} \\ v &= \sum_{i=1}^N \frac{J_i^{\text{student}}}{\sqrt{N}} S_i^{\text{test}} \end{aligned} \quad (\text{IX.78})$$

Let us denote $\overline{\dots}^{\text{test}}$ the average over different realizations of the random test data,

$$\overline{S_i^{\text{test}}}^{\text{test}} = 0 \quad \overline{S_i^{\text{test}} S_j^{\text{test}}}^{\text{test}} = \delta_{ij} \quad (\text{IX.79})$$

Then we find,

$$\overline{u}^{\text{test}} = \overline{v}^{\text{test}} = 0 \quad \overline{u^2}^{\text{test}} = \overline{v^2}^{\text{test}} = 1 \quad (\text{IX.80})$$

while

$$\overline{uv}^{\text{test}} = \frac{1}{N} \sum_{i=1}^N J_i^{\text{teacher}} J_i^{\text{student}} = R \quad (\text{IX.81})$$

then

$$P(u, v) = \frac{1}{2\pi\sqrt{1-R^2}} \exp\left(-\frac{u^2 + v^2 - 2Ruv}{2(1-R^2)}\right) \quad (\text{IX.82})$$

which implies the generalization error

$$E(R) = \int du dv P(u, v) \theta(-uv) = \frac{1}{\pi} \cos^{-1}(R) \quad (\text{IX.83})$$

¹⁸ $(1/2)(f(h)g(h))'' = (1/2)f''(h)g(h) + (1/2)f(h)g''(h) + f'(h)g'(h)$.

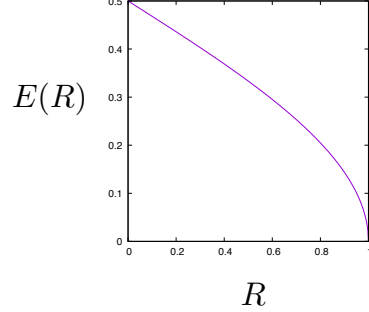


FIG. 34. Generalization error of a single perceptron

From Eq. (IX.69) we find,

$$\begin{aligned}
 -\beta V_{\text{FP}}(Q, R) = & \frac{1}{2} + \frac{\ln(2\pi)}{2} + \frac{1}{2} \frac{Q - R^2}{1 - Q} + \frac{1}{2} \ln(1 - Q) \\
 & + \alpha \frac{\int \mathcal{D}z_{\text{com}} \int \mathcal{D}z_{\text{teacher}} \theta(\Xi_{\text{teacher}}) \int \mathcal{D}z_0 \ln \int \mathcal{D}z \theta(\Xi_{\text{student}})}{\int \mathcal{D}z_{\text{com}} \int \mathcal{D}z_{\text{teacher}} \theta(\Xi_{\text{teacher}})} \\
 & \frac{1}{2} + \frac{\ln(2\pi)}{2} + \frac{1}{2} \frac{Q - R^2}{1 - Q} + \frac{1}{2} \ln(1 - Q) \\
 & + \alpha \frac{\int \mathcal{D}z_{\text{com}} \int \mathcal{D}z_{\text{teacher}} \theta(\Xi_{\text{teacher}}) \int \mathcal{D}z_0 \ln \int \mathcal{D}z \theta(\Xi_{\text{student}})}{\int \mathcal{D}z_{\text{com}} \int \mathcal{D}z_{\text{teacher}} \theta(\Xi_{\text{teacher}})} \quad (\text{IX.84})
 \end{aligned}$$

X. FURTHER REPLICA SYMMETRY BREAKINGS

A. Hierarchical energy landscape and responses with $2, 3, \dots, k$ RSB

In sec. VIIID we have argued that the 1RSB ansatz is equivalent to assume factorization of the replicated partition function as,

$$-\beta N f_{1\text{RSB}} = \partial_n Z_{1\text{RSB}}^n|_{n=0} \quad Z_{1\text{RSB}}^n = \left(\sum_{\alpha_1} \exp[-N\beta m_1 f_{\alpha_1}] \right)^{n/m_1}. \quad (\text{X.1})$$

Here n replicas are group into n/m_1 clusters of size m_1 and all the replicas belonging to a given cluster are forced to stay in the same state.

Then it is natural to expect that the 2RSB ansatz is equivalent to make a further decomposition,

$$\exp[-N\beta f_{\alpha_1}] = \sum_{\alpha_2 \in \alpha_1} \exp[-N\beta m_2 f_{\alpha_2}]^{1/m_2} \quad (\text{X.2})$$

using this in Eq. (X.1) we find

$$-\beta N f_{2\text{RSB}} = \partial_n Z_{2\text{RSB}}^n|_{n=0} \quad Z_{2\text{RSB}}^n \equiv \left(\sum_{\alpha_1} \left(\sum_{\alpha_2 \in \alpha_1} \exp[-N\beta m_2 f_{\alpha_2}] \right)^{m_1/m_2} \right)^{n/m_1} \quad (\text{X.3})$$

Here we recognize that each clusters is decomposed into m_1/m_2 sub-clusters of size m_2 such that the replicas belonging to a given sub-cluster are forced to stay in the same state. Moreover we see that in the 2RSB ansatz the states labeled by α_2 are grouped into meta-states or *meta-basins* labeled by α_1 such that the sub-clusters belonging to a given cluster are forced to stay in the same *meta-basin*, which is a union of states.

Now we wish to extend VIIIF [42], [43] to 2-RSB (and ultimately to k -RSB) so that we can disentangle the linear responses in the hierarchical energy landscape [70]. One has

$$o(T, h) = -\frac{\partial f_{2\text{RSB}}(T, h)}{\partial h} = \langle \langle o_{\alpha_2} \rangle \rangle_0 = \sum_{\alpha_1} w_{\alpha_1} \sum_{\alpha_2 \in \alpha_1} w_{\alpha_1|\alpha_2} o_{\alpha_2} \quad (\text{X.4})$$

where $o_\alpha = -\partial_h f_\alpha$ is the value of the physical observable o averaged over the thermal fluctuation within the state α . We also introduced

$$\langle \dots \rangle_0 \equiv \sum_{\alpha_1} w_{\alpha_1} \dots \quad \langle \dots \rangle_1 \equiv \sum_{\alpha_2} w_{\alpha_2} \dots \quad (\text{X.5})$$

with w_{α_1} and $w_{\alpha_2|\alpha_1}$, which can be interpreted as the statistical weights of the meta-basins and states,

$$w_{\alpha_1} = \frac{Z_{\alpha_1}^{m_1/m_2}}{\sum_{\alpha_1} Z_{\alpha_1}^{m_1/m_2}} \quad w_{\alpha_2|\alpha_1} = \frac{e^{-Nm_2\beta f_{\alpha_2}}}{Z_{\alpha_1}} \quad Z_{\alpha_1} = \sum_{\alpha_2 \in \alpha_1} e^{-Nm_2\beta f_{\alpha_2}}. \quad (\text{X.6})$$

Now one can find,

$$\begin{aligned} \chi_{2\text{RSB}} &= \sum_{\alpha_1} w_{\alpha_1} \sum_{\alpha_2 \in \alpha_1} w_{\alpha_2|\alpha_1} \partial_h o_{\alpha_2} + \sum_{\alpha_1} w_{\alpha_1} \sum_{\alpha_2 \in \alpha_1} \partial_h w_{\alpha_2|\alpha_1} o_{\alpha_2} + \sum_{\alpha_1} \partial_h w_{\alpha_1} \sum_{\alpha_2 \in \alpha_1} w_{\alpha_2|\alpha_1} o_{\alpha_2} \\ &= \tilde{\chi}_2 + m_2 \tilde{\chi}_1 + m_1 \tilde{\chi}_0 \end{aligned} \quad (\text{X.7})$$

with

$$\tilde{\chi}_2 = \langle \langle \chi_{\alpha_2} \rangle \rangle_0 \quad \tilde{\chi}_1 = N\beta[\langle \langle o_{\alpha_2}^2 \rangle \rangle_1 - \langle \langle o_{\alpha_2} \rangle \rangle_0^2] \quad \tilde{\chi}_0 = N\beta[\langle \langle o_{\alpha_2} \rangle \rangle_1^2 - \langle \langle o_{\alpha_2} \rangle \rangle_0^2] \quad (\text{X.8})$$

Physically we can interpret $\tilde{\chi}_2$ as the response within a state, $\tilde{\chi}_1$ as the response due to transition between different states within a common meta-basin and finally $\tilde{\chi}_0$ as the response due to transition between different meta-basins. The total response is the mixture. Just as we did for the 1RSB case we wish to disentangle the three qualitatively different susceptibilities.



FIG. 35. An example of ultrametric tree

Again let us suppose that each of the replica is subjected to difference probing fields. Then one easily finds,

$$\chi_{a,b}(T, h) \equiv -m_1 \frac{\partial^2 f_{\text{RSB}}(T, \{h_a\})}{\partial h_a \partial h_b} \Bigg|_{\{h_a=h\}} = \tilde{\chi}_2 \delta_{ab} + \tilde{\chi}_1 I_{ab}^{m_2} + \tilde{\chi}_0$$

and

$$\sum_{b=1}^{m_1} \chi_{ab} = \tilde{\chi}_2 + m_2 \tilde{\chi}_1 + m_1 \tilde{\chi}_0 = \chi_{\text{RSB}}(T, h). \quad (\text{X.9})$$

Generalization to k -RSB is now straightforward but we do not attempt it here because it would require heavier notation to describe the hierarchy of the clusters.

TODO: discuss FC/ZFC susceptibilities $\chi_{\text{total}} = \beta(1 - \bar{q})$ and $\chi_{\text{EA}} = \beta(1 - q_{\text{EA}})$

B. Overlap distribution function $P(q)$ and the order parameter function $q(x)$

We have already discussed the overlap distribution $P(q)$ for the case of 1RSB. Here we discuss the connection between $P(q)$ and the Parisi's ansatz Eq. (VI.23) for the more general cases. The structure of the matrix is shown in Fig. 18.

We can repeat the argument in sec VIII B for the general case:

$$\overline{P(q)} = \frac{\sum_{a \neq b} \delta(Q_{ab} - q)}{n(n-1)} \quad (\text{X.10})$$

The probability to observe the overlap q within the section $\delta q_i = q_{i+1} - q_i$, averaged over the disorder, can be evaluated within the Parisi's ansatz as,

$$\overline{P(q)} dq_i = \frac{m_i(m_i-1)\frac{n}{m_i} - m_{i+1}(m_{i+1}-1)\frac{n}{m_{i+1}}}{n(n-1)} = \frac{m_i - m_{i+1}}{n-1} \xrightarrow{n \rightarrow 0} \delta m_i \quad (\text{X.11})$$

where $\delta m_i = m_{i+1} - m_i$. In the continuous limit $k \rightarrow \infty$ ($\delta m_i \rightarrow 0$) we find,

$$\overline{P(q)} = \frac{dx(q)}{dq} \quad (\text{X.12})$$

where we recalled m as x . This establishes the connection between the order parameter function $q(x)$ which parameterized the Parisi's ansatz and the overlap distribution function $P(q)$. In Fig. 36 we display the two important examples: 1RSB and continuous RSB cases.

Now considering three replicas, one can ask distribution of mutual overlaps, q_{12} , q_{23} and q_{31} . By doing the same argument as above one finds,

$$\overline{P(q_{12}, q_{23}, q_{31})} = \lim_{n \rightarrow 0} \frac{1}{n(n-1)(n-2)} \sum_{a \neq b \neq c} \delta(Q_{ab} - q_{12}) \delta(Q_{ac} - q_{23}) \delta(Q_{bc} - q_{31}) \quad (\text{X.13})$$

Then, just from the structure of the matrix, we find, the smallest two among q_{12}, q_{23}, q_{31} are equal, which means *ultrametricity* [1].

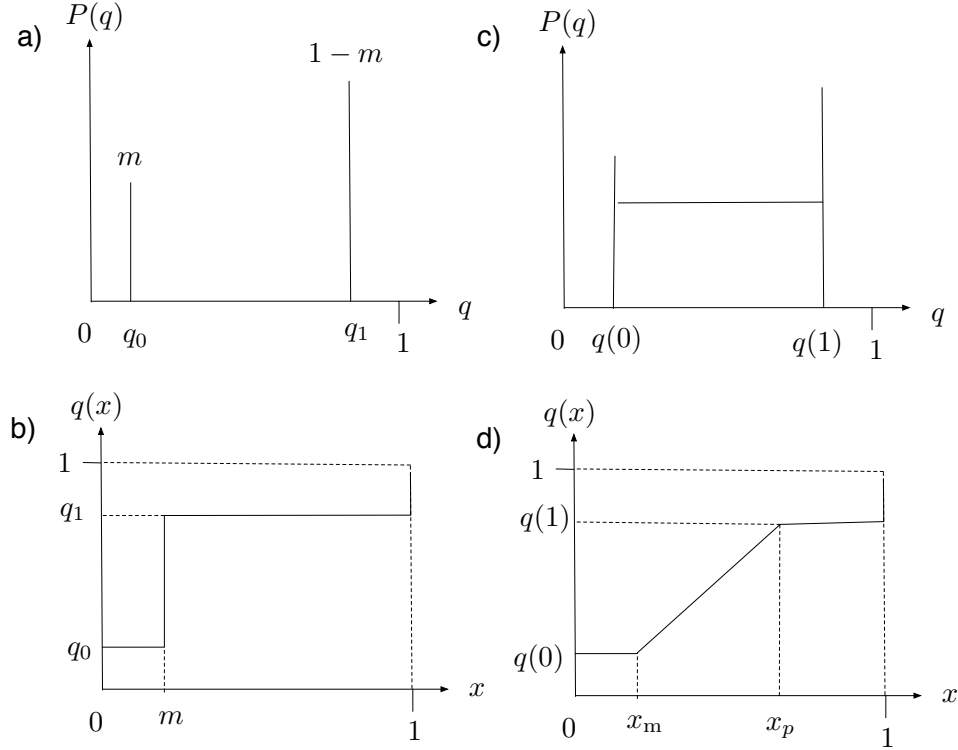


FIG. 36. Schematic pictures of the overlap distribution function $P(q)$ and the order parameter function $q(x)$. a) and b) are for the 1RSB case. c) and d) are for the full RSB case. (For simplicity we assumed flat distribution of $P(q)$ in the continuous part.)

C. p -spin Ising model

1. Free-energy of k -RSB ansatz

Here we evaluate the free-energy Eq. (VI.72) using the generic Parisi's ansatz Eq. (VI.23) (See Fig. 18), which reads,

$$q_{ab} = q_0 + \sum_{i=1}^{k+1} (q_i - q_{i-1}) I_{ab}^{m_i} = \sum_{i=0}^{k+1} q_i (I_{ab}^{m_i} - I_{ab}^{m_{i+1}}) \quad (\text{X.14})$$

First, we easily obtain,

$$\begin{aligned} \frac{1}{n} \sum_{a,b} q_{ab}^p &= \frac{1}{n} \sum_{a,b} \sum_{i=0}^{k+1} q_i^p (I_{ab}^{m_i} - I_{ab}^{m_{i+1}}) = 1 + \sum_{i=0}^k q_i^p ((m_i - 1) - (m_{i+1} - 1)) \\ &= 1 + \sum_{i=0}^k q_i^p (m_i - m_{i+1}) \end{aligned} \quad (\text{X.15})$$

In the last equation $dm_i = m_i - m_{i+1} \rightarrow -dx$ (note m_i decreases with increasing i when n becomes smaller than 1 (See Fig. 18 d)). Similarly we find,

$$\frac{1}{n} \sum_{a,b} \epsilon_{ab} q_{ab} = \epsilon_k + \sum_{i=0}^k q_i \epsilon_i (m_i - m_{i+1}) \quad (\text{X.16})$$

Rememeber again that ϵ_{aa} was arbitrary in the Ising case (see sec. VI C 1). Here we made a simple choise $\epsilon_{aa} = \epsilon_k$.

Next step is to evaluate

$$A_k = \exp \left[\frac{1}{2} \sum_{a,b} \epsilon_{ab} \frac{\partial^2}{\partial h_a \partial h_b} \right] \prod_a 2 \cosh(h_a) \Big|_{h_a=0} \quad (\text{X.17})$$

$$= \exp \left[\frac{1}{2} \epsilon_0 \sum_{a,b} \frac{\partial^2}{\partial h_a \partial h_b} \right] \prod_{i=1}^k \exp \left[\frac{1}{2} (\epsilon_i - \epsilon_{i-1}) \sum_{a,b} I_{ab}^{m_i} \frac{\partial^2}{\partial h_a \partial h_b} \right] \prod_a 2 \cosh(h_a) \Big|_{h_a=0} \quad (\text{X.18})$$

$$= e^{\frac{\epsilon_0}{2} \frac{\partial^2}{\partial h^2}} \left(e^{\frac{\epsilon_1 - \epsilon_0}{2} \frac{\partial^2}{\partial h^2}} \left(\cdots e^{\frac{\epsilon_k - \epsilon_{k-1}}{2} \frac{\partial^2}{\partial h^2}} (2 \cosh(x))^{m_k/m_{k+1}} \cdots \right)^{m_1/m_2} \right)^{m_0/m_1} \Big|_{h=0} \quad (\text{X.19})$$

Note that $m_0 = n$ and $m_{k+1} = 1$.

Now we are naturally lead to define a family of functions $g(m_i, y)$ and $f(m_i, y)$

$$f(m_i, y) = -\frac{1}{m_i} \ln g(m_i, y) \quad (\text{X.20})$$

for $i = 1, 2, \dots, k$ which satisfy recursion relations Eq. (E.1) and Eq. (E.3) respectively with

$$\Lambda_0 = \epsilon_0 \quad \Lambda_i = \epsilon_i - \epsilon_{i-1} \quad (i = 1, 2, \dots, k) \quad (\text{X.21})$$

and 'the boundary condition',

$$g(m_{k+1} = 1, y) = 2 \cosh(y). \quad (\text{X.22})$$

and

$$-f(m_{k+1} = 1, y) = \ln 2 \cosh(y). \quad (\text{X.23})$$

as shown in appendix E.

With these we find, remembering $m_0 = n$,

$$A_k = g(m_0, 0) = e^{-nf(m_0, 0)} = e^{\frac{\epsilon_0}{2} \frac{\partial^2}{\partial h^2}} e^{-nf(m_1, h)} \Big|_{h=0} \quad (\text{X.24})$$

which is valid for $k = 0, 1, 2, \dots, \infty$. The contribution of the interaction to the free-energy becomes

$$\partial_n \ln A_k \Big|_{n=0} = -f(m_0, 0) = e^{\frac{\epsilon_0}{2} \frac{\partial^2}{\partial h^2}} (-f(m_1, h)) \Big|_{h=0} = - \int \mathcal{D}z_0 f(m_1, \sqrt{\epsilon_0} z_0) \quad (\text{X.25})$$

Collecting the above results we find the free-energy Eq. (VI.72) as,

$$\begin{aligned} -\beta f_{k-RSB} &= (-\beta \partial_n F_n^{k-RSB}[\hat{q}]) / N \Big|_{n=0} \\ &= -\frac{1}{2} \epsilon_k - \frac{1}{2} \sum_{i=0}^k q_i \epsilon_i (m_i - m_{i+1}) \\ &\quad - \int \mathcal{D}z_0 f(m_1, \sqrt{\epsilon_0} z_0) + \frac{\gamma(\beta J)^2}{2} + \frac{\gamma(\beta J)^2}{2} \sum_{i=0}^k q_i^p (m_i - m_{i+1}) \end{aligned} \quad (\text{X.26})$$

2. Variational equations

We find for $i \neq k$,

$$\begin{aligned}
\frac{\partial}{\partial \epsilon_i} g(m_i, h) &= \frac{\partial}{\partial \epsilon_i} \left[e^{\frac{\epsilon_i - \epsilon_{i-1}}{2} \frac{\partial}{\partial h^2}} \left(\underbrace{e^{\frac{\epsilon_{i+1} - \epsilon_i}{2} \frac{\partial}{\partial h^2}} g(m_{i+2}, h)^{m_{i+1}/m_{i+2}}}_{g(m_{i+1}, h)} \right)^{m_i/m_{i+1}} \right] \\
&= \frac{1}{2} m_i (m_i - m_{i+1}) e^{\frac{\epsilon_i - \epsilon_{i-1}}{2} \frac{\partial}{\partial h^2}} \left\{ e^{-m_i f(m_{i+1}, h)} (f'(m_{i+1}, h))^2 \right\} \\
&= \frac{1}{2} m_i (m_i - m_{i+1}) \int dh' e^{\frac{\epsilon_i - \epsilon_{i-1}}{2} \frac{\partial}{\partial h^2}} e^{-m_i f(m_{i+1}, h)} \delta(h - h') (f'(m_{i+1}, h'))^2 \\
&= \frac{1}{2} m_i (m_i - m_{i+1}) \int dh' e^{\frac{\epsilon_i - \epsilon_{i-1}}{2} \frac{\partial}{\partial h^2}} e^{-m_i f(m_{i+1}, h)} \frac{\delta f(m_{i+1}, h)}{\delta f(m_{i+1}, h')} (f'(m_{i+1}, h'))^2 \\
&= -\frac{1}{2} (m_i - m_{i+1}) \int dh' \frac{\delta}{\delta f(m_{i+1}, h')} e^{\frac{\epsilon_i - \epsilon_{i-1}}{2} \frac{\partial}{\partial h^2}} e^{-m_i f(m_{i+1}, h)} (f'(m_{i+1}, h'))^2 \\
&= -\frac{1}{2} (m_i - m_{i+1}) \int dh' \frac{\delta g(m_i, h)}{\delta f(m_{i+1}, h')} (f'(m_{i+1}, h'))^2
\end{aligned} \tag{X.27}$$

Thus

$$\frac{\partial}{\partial \epsilon_i} f(m_i, h) = -\frac{1}{2} (m_i - m_{i+1}) \int dh' \frac{\delta f(m_i, h)}{\delta f(m_{i+1}, h')} (f'(m_{i+1}, h'))^2 \tag{X.28}$$

Similarly, for $i = k$, we find,

$$\begin{aligned}
\frac{\partial}{\partial \epsilon_k} g(m_k, h) &= \frac{\partial}{\partial \epsilon_k} \left[e^{\frac{\epsilon_k - \epsilon_{k-1}}{2} \frac{\partial}{\partial h^2}} (2 \cosh(h))^{m_k} \right] = \frac{1}{2} e^{\frac{\epsilon_k - \epsilon_{k-1}}{2} \frac{\partial}{\partial h^2}} \frac{\partial^2}{\partial h^2} (2 \cosh(h))^{m_k} \\
&= \frac{1}{2} e^{\frac{\epsilon_k - \epsilon_{k-1}}{2} \frac{\partial}{\partial h^2}} \left\{ m_k (m_k - 1) (2 \cosh(h))^{m_k} \tanh^2(h) + m_k (2 \cosh(h))^{m_k} \right\} \\
&= -\frac{1}{2} \int dh' \frac{\delta g(m_k, h)}{\delta f(m_{k+1}, h')} \left((m_k - 1) (f'(m_{k+1}, h'))^2 + 1 \right)
\end{aligned} \tag{X.29}$$

More generally we can show for $0 \leq j \leq i$,

$$\begin{aligned}
-\frac{\partial}{\partial \epsilon_i} f(m_j, h) &= \int d\eta \frac{\delta f(m_j, h)}{\delta f(m_i, \eta)} \left(-\frac{\partial}{\partial \epsilon_i} f(m_i, \eta) \right) \\
&= \frac{1}{2} \int dh' P_{j,i+1}(h, h') \left[(m_i - m_{i+1}) (f'(m_{i+1}, h'))^2 + \delta_{i,k} \right]
\end{aligned} \tag{X.30}$$

where we introduced

$$P_{i,j}(h, h') = \frac{\delta f(m_i, h)}{\delta f(m_j, h')} \tag{X.31}$$

and used the chain rule

$$\int d\eta P_{j,i}(h, \eta) P_{i,i+1}(\eta, h') = P_{j,i+1}(h, h'). \tag{X.32}$$

The functions $P_{i,j}(h, h')$ follows a recursion formula Eq. (F.4) with the boundary condition Eq. (F.5).

Now from Eq. (X.26) we find saddle point equations

$$\begin{aligned}
0 &= \frac{\partial}{\partial \epsilon_i} (-\beta f_{k-RSB}[\hat{\epsilon}, \hat{q}]) \\
&= -\frac{1}{2} \delta_{i,k} - \frac{1}{2} q_i (m_i - m_{i+1}) - \int \mathcal{D}z_0 \frac{\partial}{\partial \epsilon_i} f(m_1, \sqrt{\epsilon_0} z_0) \\
&= -\frac{1}{2} \delta_{i,k} - \frac{1}{2} q_i (m_i - m_{i+1}) \\
&\quad + \int \mathcal{D}z_0 \frac{1}{2} \int dh' P_{1,i+1}(\sqrt{\epsilon_0} z_0, h') [(m_i - m_{i+1}) (f'(m_{i+1}, h'))^2 + \delta_{i,k}]
\end{aligned} \tag{X.33}$$

Thus we find, for $i = 1, 2, \dots, k$,

$$q_i = \int dh P_i(h) m^2(m_{i+1}, h) \quad (\text{X.34})$$

where we introduced

$$m(m_i, h) = -f'(m_i, h) \quad (\text{X.35})$$

which can be interpreted as 'magnetizations' which follow a recursion relation Eq. (E.5) with the boundary condition

$$m(m_{k+1}, h) = -f'(m_{k+1}, h) = \tanh(h) \quad (\text{X.36})$$

We also introduced

$$P_i(h) = \int \mathcal{D}z_0 P_{1,i+1}(\sqrt{\epsilon_0}z_0, h) \quad (\text{X.37})$$

which follows follows the same recursion formula as Eq. (F.4),

$$P_j(h) = e^{-m_j f(m_{j+1}, h)} \gamma_{\Lambda_j} \otimes_h \frac{P_{j-1}(h)}{e^{-m_j f(m_j, h)}} \quad j = 1, 2, \dots, k+1 \quad (\text{X.38})$$

with the 'boundary condition',

$$P_0(h) = \frac{1}{\sqrt{2\pi\epsilon_0}} e^{-\frac{h^2}{2\epsilon_0}}. \quad (\text{X.39})$$

which follows from Eq. (X.37) and Eq. (F.5). The functions $P_i(h)$ is also normalized such that

$$\int dh P_i(h) = 1 \quad (\text{X.40})$$

reflecting Eq. (F.6). Physically $P_i(h)$ can be interpreted as internal field distributions.

We also find from Eq. (X.26),

$$0 = \frac{\partial}{\partial q_i} (-\beta f_{k-RSB})[\hat{\epsilon}, \hat{q}] \rightarrow \epsilon_i = \gamma(\beta J)^2 p q_i^{p-1} \quad (\text{X.41})$$

To solve the saddle point equations, we can follow the following steps. The values of $q_i = 0, 1, 2, \dots, k$ in the $k (\geq 1)$ RSB ansatz with m_i 's fixed as $0 = m_0 < m_1 < \dots < m_k < m_{k+1} = 1$ can be solved numerically by iterating the following steps:

1. Make an initial guess on q_i for $i = 0, 1, 2, \dots, k$ by which we also obtain ϵ_i for $i = 0, 1, 2, \dots, k$ via Eq. (X.41): $\epsilon_i = \gamma(\beta J)^2 p q_i^{p-1}$.
2. Evaluate the functions $f(m_i, h)$ for an appropriate range of h doing 'Gaussian' convolutions recursively in the order ($i = k \rightarrow k-1 \rightarrow \dots \rightarrow 2 \rightarrow 1$) using the recursion formula Eq. (E.3) with the boundary condition Eq. (X.23) $-f(m_{k+1}, h) = \ln(2 \cosh(h))$. Simultaneously compute also $m(m_i, h) = -f'(m_i, h)$ using the recursion formula Eq. (E.5) with the boundary condition $m(m_{k+1}, h) = -f'(m_{k+1}, h) = \tanh(h)$.
3. Evaluate the functions $P_i(h)$ by doing another series of 'Gaussian' convolutions recursively in the opposite direction ($i = 1 \rightarrow 2 \rightarrow \dots \rightarrow k-1 \rightarrow k$) using the recursion formula Eq. (F.4) with the boundary condition Eq. (X.39) $P_0(z) = e^{-z^2/2\epsilon_0}/\sqrt{2\pi\epsilon_0}$. Then q_i for $i = 0, 1, 2, \dots, k$ can be determined using Eq. (X.34). Go back to the initial step.

3. Stability

Now let us examine the stability of the full RSB phase. Within the k -RSB ansatz Eq. (VI.23), n replicas are divided into n/m_1 groups of size m_1 and each of the latter is divided into m_1/m_2 groups of size m_2 , and so on as shown in Fig. 18. Finally we find n/m_k groups of size m_k . Within each of the groups of size m_k , the replica symmetry remains. As we did in the RS and 1-RSB case, here we only analyze stability of the replica symmetry within such

a most inner-core group. Thus we just consider the Hessian matrix $M_{a \neq b, c \neq d}^{\mathcal{C}}$ given by Eq. (VI.79) with Eq. (VI.80) assuming that all indexes a, b, c, d are in the same most-inner core replica group of size m_k , which we denote as \mathcal{C} in the following. Then we find, for simplicity,

$$M_{(a \neq b, c \neq d)}^{\mathcal{C}} = 2\gamma(\beta J)^2 p(p-1) q_k^{p-2} \left[\frac{\delta_{ac}\delta_{bd} + \delta_{ad}\delta_{bc}}{2} - \frac{\gamma(\beta J)^2 p(p-1) q_k^{p-2}}{2} \langle S_a S_b S_c S_d \rangle_{\epsilon^*} \right] \quad (\text{X.42})$$

where

$$\begin{aligned} \langle S_a S_b S_c S_d \rangle_{\epsilon^*} &= \exp \left(\sum_{l=0}^k \frac{\Lambda_l}{2} \sum_{e,f=1}^n I_{ef}^{m_l} \frac{\partial^2}{\partial h_e \partial h_f} \right) \left(\prod_{a \notin \mathcal{C}} g(m_{k+1}, h_a) \right) \frac{\partial^4}{\partial h_a \partial h_b \partial h_c \partial h_d} \prod_{a \in \mathcal{C}} g(m_{k+1}, h_a) \Big|_{\{h_a=0\}} \\ &= \int dy \gamma_{\Lambda_0} \otimes \left\{ g^{m_0/m_1-1}(m_1, h) \gamma_{\Lambda_1} \otimes \left\{ g^{m_1/m_2-1}(m_2, h) \gamma_{\Lambda_2} \otimes \{ \dots \right. \right. \\ &\quad \dots g^{m_{k-1}/m_k-1}(m_k, h) \gamma_{\Lambda_k} \otimes \left. \left. \left\{ g^{m_k}(m_{k+1}, h) \delta(h-y) \left[S_1(y) \frac{\delta_{ac}\delta_{bd} + \delta_{ad}\delta_{bc}}{2} \right. \right. \right. \right. \\ &\quad \left. \left. \left. \left. + S_2(y) \frac{\delta_{ac} + \delta_{ad} + \delta_{bc} + \delta_{bd}}{4} + S_3(y) \right] \right\} \right|_{h=0} \\ &= - \int dy \frac{m_{k+1}}{m_0} \frac{\delta g(m_0, 0)}{\delta f(m_{k+1}, y)} \left[S_1(y) \frac{\delta_{ac}\delta_{bd} + \delta_{ad}\delta_{bc}}{2} + S_2(y) \frac{\delta_{ac} + \delta_{ad} + \delta_{bc} + \delta_{bd}}{4} + S_3(y) \right] \\ &\xrightarrow[m_0=n \rightarrow 0]{} \int dh P_k(h) \left[S_1(h) \frac{\delta_{ac}\delta_{bd} + \delta_{ad}\delta_{bc}}{2} + S_2(h) \frac{\delta_{ac} + \delta_{ad} + \delta_{bc} + \delta_{bd}}{4} + S_3(h) \right] \end{aligned} \quad (\text{X.43})$$

In the last equation we used the following, remembering $m_{k+1} = 1$, using Eq. (X.20) and Eq. (E.3),

$$\begin{aligned} -\frac{m_{k+1}}{m_0} \frac{\delta g(m_0, 0)}{\delta f(m_{k+1}, h)} &= -\frac{1}{m_0} \frac{\delta}{\delta f(m_{k+1}, h)} e^{\frac{\epsilon_0}{2} \frac{\partial^2}{\partial y^2}} e^{-m_0 f(m_1, y)} \Big|_{y=0} \\ &= e^{\frac{\epsilon_0}{2} \frac{\partial^2}{\partial y^2}} e^{-m_0 f(m_1, y)} \frac{\delta f(m_1, y)}{\delta f(m_{k+1}, h)} \Big|_{y=0} = e^{\frac{\epsilon_0}{2} \frac{\partial^2}{\partial y^2}} e^{-m_0 f(m_1, y)} P_{1,k+1}(y, h) \Big|_{y=0} \xrightarrow[m_0 \rightarrow 0]{} P_k(h) \end{aligned} \quad (\text{X.44})$$

In the last equation we used Eq. (X.37). We also used $S_1(h), S_2(h), S_3(h)$ defined in Eq. (D.10).

Collecting the above results we find the Hessian matrix at the most-inner core part $M_{a \neq b, c \neq d}^{\mathcal{C}}$ takes the RS form Eq. (K.1) with,

$$M_1 = 2\gamma(\beta J)^2 p(p-1) q_k^{p-2} \left(1 - \gamma(\beta J)^2 p(p-1) q_k^{p-2} \int dh P_k(h) (f''(m_{k+1}, h))^2 \right) \quad (\text{X.45})$$

$$M_2 = -4 \left(\gamma(\beta J)^2 p(p-1) q_k^{p-2} \right)^2 \int dh P_k(h) (-f''(h)) (f'(m_{k+1}, h))^2 \quad (\text{X.46})$$

$$M_3 = - \left(\gamma(\beta J)^2 p(p-1) q_k^{p-2} \right)^2 \int dh P_k(h) (f'(m_{k+1}, h))^4 \quad (\text{X.47})$$

where $f''(m_{k+1}, h) = (\tanh(h))' = 1 - \tanh^2(h)$.

Using the results in sec. K we find the normalized replicon eigen value

$$\tilde{\lambda}_R = 1 - \gamma(\beta J)^2 p(p-1) q_k^{p-2} \int dh P_k(h) (f''(m_{k+1}, h))^2 \quad (\text{X.48})$$

This result reproduces the RS case ($k = 0$) Eq. (VII.17) (see Eq. (X.39)) and 1RSB case ($k = 1$) Eq. (VIII.19) (Exercise: check this) as it should.

4. Continuous RSB: $k \rightarrow \infty$ limit

Finally let us consider $k \rightarrow \infty$ limit [54, 61]. Here and in the following we use the following shorthand notation

$$\dot{A}(x, y) \equiv \frac{\partial A(x, y)}{\partial x} \quad A'(x, y) \equiv \frac{\partial A(x, y)}{\partial y} \quad (\text{X.49})$$

In $k \rightarrow \infty$ limit, writing $m_i = x - \delta x, m_{i+1} = x$ and $\Lambda_i = \dot{\epsilon}(x)\delta x$, the recursion relations Eq. (E.1), Eq. (E.1) and Eq. (E.5) become partial differential equations, called as Parisi's equations,

$$-\dot{g}(x, y) = \frac{\dot{\epsilon}(x)}{2} g''(x, y) - \frac{1}{x} g(x, y) \ln g(x, y) \quad (\text{X.50})$$

Equivalently for,

$$-f(x, y) \equiv \frac{1}{x} \ln g(x, y) \quad (\text{X.51})$$

we find,

$$\dot{f}(x, y) = -\frac{\dot{\epsilon}(x)}{2} \left[f''(x, y) - x(f'(x, y))^2 \right] \quad (\text{X.52})$$

And for

$$m(x, y) = -f'(x, y) \quad (\text{X.53})$$

we find, Eq. (E.5) becomes

$$\dot{m}(x, h) = -\frac{\dot{\epsilon}(x)}{2} (m''(x, h) + 2xm(x, h)m'(x, h)) \quad (\text{X.54})$$

The boundary conditions are given by

$$g(1, y) = 2 \cosh(y). \quad (\text{X.55})$$

$$-f(1, y) = \ln(2 \cosh(y)). \quad (\text{X.56})$$

and

$$m(1, y) = \tanh(y) \quad (\text{X.57})$$

Finally the recursion relation for the distribution of the internal field $P_i(h)$ Eq. (XIII.104) becomes, in the $k \rightarrow \infty$ limit a partial differential equation

$$\dot{P}(x, h) = \frac{1}{2} \dot{\epsilon}(x) [P''(x, h) + 2x(P(x, h)f'(x, h))'] \quad (\text{X.58})$$

with a boundary condition

$$P(0, h) = \frac{1}{\sqrt{2\pi\epsilon(0)}} e^{-\frac{h^2}{2\epsilon(0)}}. \quad (\text{X.59})$$

With these the free-energy becomes

$$\beta f_{\infty \text{RSB}} = -\frac{(\beta J)^2}{4} + \frac{(\beta J)^2}{4} \int_0^1 dx q^p(x) - \frac{1}{2} \int_0^1 dx \epsilon(x) q(x) + \frac{1}{2} \epsilon(1) - \int Dz_0 f(m_1, \beta h + \sqrt{\epsilon(0)} z_0) \quad (\text{X.60})$$

where

$$\epsilon(x) = \gamma(\beta J)^2 p q(x)^{p-1} \quad q(x) = \int dh P(x, h) m^2(x, h). \quad (\text{X.61})$$

Marginal stability

It can be shown that the (reduced) replicon eigen value Eq. (X.48) in the most-inner core sector vanishes in the continuous limit

$$\tilde{\lambda}_R = 1 - \gamma(\beta J)^2 p(p-1)q(1)^{p-2} \int dh P(1, h) (f''(1, h))^2 = 0 \quad (\text{X.62})$$

meaning marginal stability of the full RSB solution.

This can be shown as follows. Taking both sides of Eq. (X.61) we find

$$\begin{aligned}\dot{q} &= \int dh [\dot{P}m^2 + 2Pm\dot{m}] \\ &= \frac{\dot{\epsilon}}{2} \int dh [(p'' - 2x(pm)'')m^2 - 2p(m'' + 2xmm')m] \\ &= \gamma(\beta J)^2 p(p-1)q^{p-2}\dot{q} \int dh P(m')^2\end{aligned}\quad (\text{X.63})$$

In the 2nd equation we used Eq. (X.58) and Eq. (X.54). To derive the last equation we used some integrations by parts and used Eq. (VI.74). Thus we find an identity

$$1 = \gamma(\beta J)^2 p(p-1)q^{p-2}\dot{q} \int dh P(f'')^2 \quad (\text{X.64})$$

using $m = -f'$. This proves Eq. (X.62): vanishing of the replicon eigen value $\tilde{\lambda}_R = 0$.

5. Analysis of k -RSB solution: $p = 2$ case (SK model)

In Fig. 37 we show an example of the numerical analysis done for the SK model ($p = 2$). An interesting feature emerges at low temperature on the distribution of the internal field $P(1, h)$: opening of a pseudo-gap.

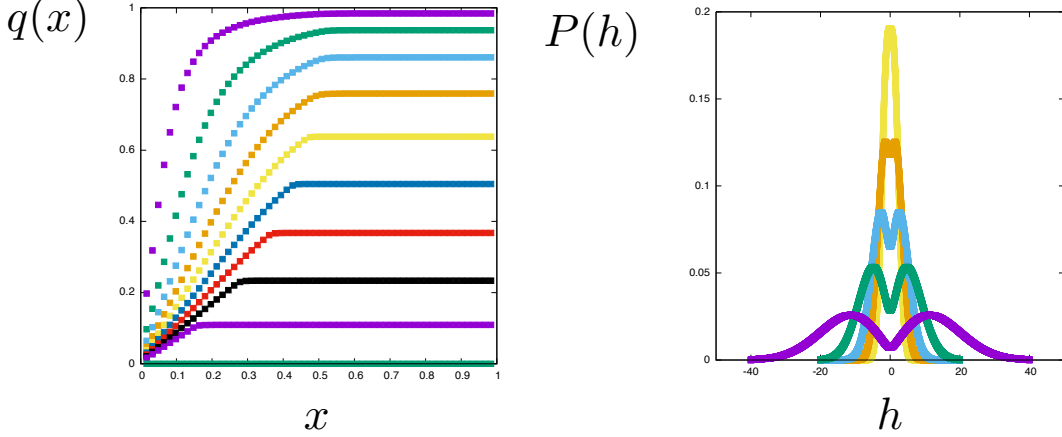


FIG. 37. Numerical solution of the k -RSB ansatz in the case of the SK model ($p = 2$) whose critical temperature is $T_c/J = 1$. Here $k = 60$. (Left panel) The order parameter function $q(x)$ and (Right panel) for $T = 0.1, 0.2, 0.3, 0.4, 0.5, 0.6, 0.7, 0.8, 0.9, 1.0$ form top to bottom and the internal field distribution $P_k(h)$ for $T = 0.1, 0.2, 0.3, 0.4, 0.5$ form bottom to top. A comparison between the replica and TAP (cavity) approaches was done in [76].

TODO: discuss FC/ZFC susceptibilities showing results of $\chi_{\text{total}} = \beta(1 - \bar{q})$ and $\chi_{\text{EA}} = \beta(1 - q_{\text{EA}})$ computed using the RSB solution.

D. Vectorial p -spin models with soft/hardcore potential

Here we study the RSB of the M -vector p -spin model with the hardcore Eq. (III.26) and soft-core Eq. (III.27) interactions.

In this model we can define 'pressure' as

$$\Pi = -\frac{1}{N_\blacksquare} \frac{\partial \beta F}{\partial \delta} \quad (\text{X.65})$$

and distribution function of gap,

$$g(r) = \langle \delta(r - r_\blacksquare) \rangle = \frac{1}{N_\blacksquare} \frac{\delta \beta F}{\delta \ln e^{-\beta v(r)}} \quad (\text{X.66})$$

We can evaluate the fraction of interactions whose gaps are *closed* as,

$$f_{\text{closed}} = \lim_{\epsilon \rightarrow 0} \int_{-\infty}^{\epsilon} dr g(r) \quad (\text{X.67})$$

which means there are $N_{\blacksquare} f_{\text{closed}}$ constraints. Then isostaticity implies

$$N(M - 1) = N_{\blacksquare} f_{\text{closed}} \quad (\text{X.68})$$

or

$$1 = \frac{\alpha}{p} f_{\text{closed}} \quad (\text{X.69})$$

where we used Eq. (III.23).

1. *k-RSB ansatz and $k \rightarrow \infty$ limit*

2. *Analysis of k -RSB solution*

- In Fig. 38 we show the phase diagram of the vectorial $p = 2$ soft/hardcore model. The planes (AT/G1/G2) are obtained by investigating the replicon eigen-value of the RS and 1RSB phases.

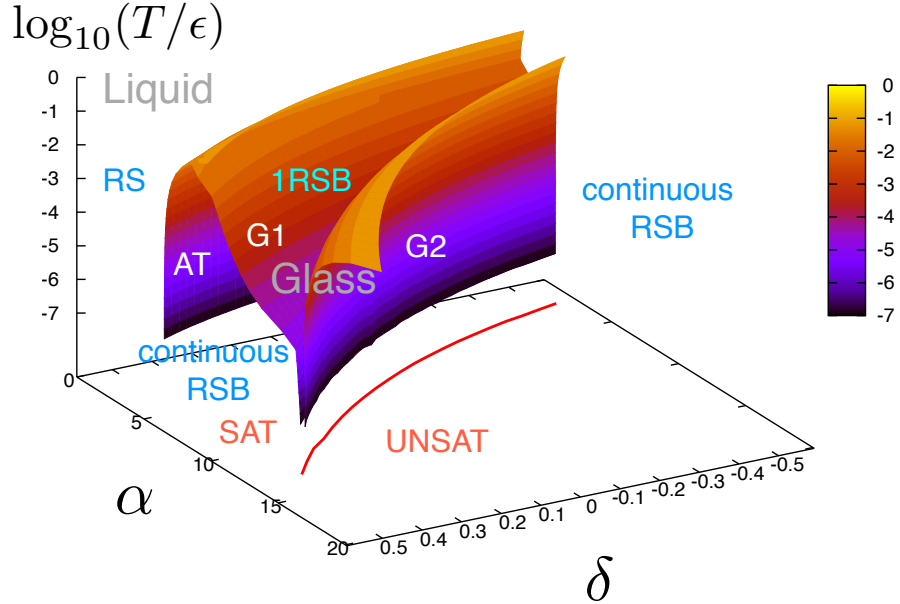


FIG. 38. Phase diagram of the soft/hardcore model ($p = 2$). On the plane AT separating the liquid (RS) and glass (RSB) the d'Almeida-Thouless (AT) instability occurs. The 1RSB solution becomes unstable below the two planes G1 and G2 on which the Gardner transition occurs. The G1 plane separates from the AT plane at finite temperatures. The red line on the bottom represents the jamming line $\alpha = \alpha_j(\delta)$ at $T = 0$. (Taken from [15])

- In Fig. 39 we show the $q(x)$ function obtained numerically solving the $k = 100$ RSB ansatz. The power law behaviour $1 - q(x) \propto x^{-\kappa}$ with $\kappa \sim 1.4$ agree with the semi-analytical prediction based on a scaling ansatz (see below).

3. *Marginal stability*

The replicon eigen value $\lambda_R = 0$ in the full RSB solution.

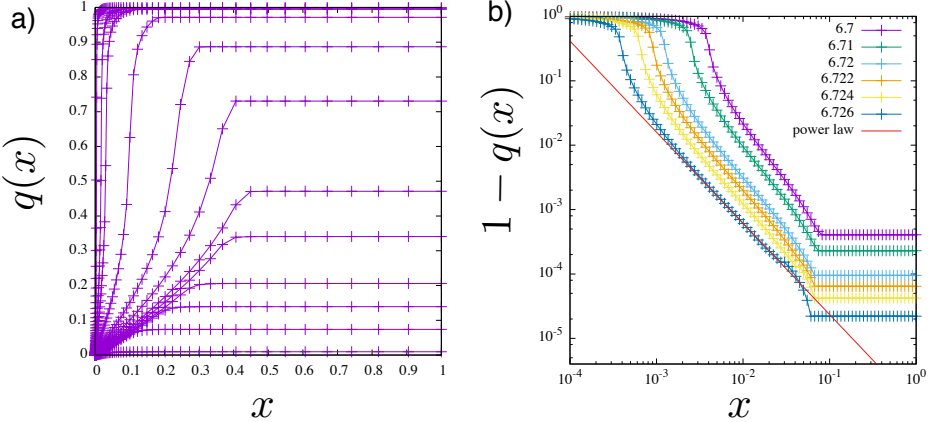


FIG. 39. The $q(x)$ function of the hardcore model with $p = 2$, $\delta = 0$ for which $\alpha_c = 1.5708..$ and $\alpha_j = 6.732...$ a) $\alpha = 1.6, 1.8, 2.0, 2.2, 2.4, 2.6, 2.8, 3.0, 4.0, 5.0, 6.0, 6.5, 6.6, 6.7$ from the bottom to the top. b) The straight line represents the power law fit $ax^{-\kappa}$ with $\kappa = 1.4157$, the same exponent as that for the hardspheres[58]. (Taken from [15]).

4. Jamming

One can show that for *general* p that following happens at jamming (SAT/UNSTAT transition)

1. Isostaticity Eq. (X.69) holds at jamming, similarly to the hard-spheres
2. Critical properties at jamming is the same as that of the hard-spheres

These were shown for the perceptron [34] ($p = 1$) and extended to general $p \geq 1$ in [15].

First of all the $g(x)$ function exhibits a power law behaviour $1 - g(x) \propto x^{-\kappa}$ approaching jamming $\alpha \rightarrow \alpha_j(\delta)$. The exponent κ can be obtained semi-analytically through a scaling argument, which can be checked numerically (see Eq. (39)). Then critical properties of physical observables can be deduced. The 'cage size' vanishes as

$$1 - q(1) \propto \Pi^{-\kappa} \quad \kappa = 1.41575 \quad (\text{X.70})$$

with the pressure Π Eq. (X.65) which diverges at jamming. The distribution of the gap Eq. (X.66) exhibits a contact δ peak at $r = 0$ + power law tail $r^{-\alpha}$ approaching jamming. These are perfectly analogous to the finding in the hard-sphere system in the $d \rightarrow \infty$ limit, which we discuss later.

XI. CAVITY APPROACH

Let us consider a system of spins S_i ($i = 1, 2, \dots, N$) whose equilibrium probability distribution is given by,

$$P(S_1, S_2, \dots, S_N) = \frac{1}{Z} \prod_{\blacksquare=1}^{N_\blacksquare} \psi_\blacksquare(\{S_i\}_{i \in \partial \blacksquare}) \prod_{i=1}^N \psi_i(S_i) \quad (\text{XI.1})$$

where

$$Z = \left(\prod_{i=1}^N \text{Tr}_{S_i} \right) \prod_{\blacksquare=1}^{N_\blacksquare} \psi_\blacksquare(\{S_i\}_{i \in \partial \blacksquare}) \prod_{i=1}^N \phi(S_i) \quad (\text{XI.2})$$

is the partition function.

As we see below, the cavity approach allows us to compute the marginal probabilities

$$P(S_i) = \prod_{j \neq i} \text{Tr}_{S_j} P(S_1, S_2, \dots, S_N) \quad i = 1, 2, \dots, N \quad (\text{XI.3})$$

with some low computational costs.

A. Belief Propagation(BP) equations

Because our graphs are locally tree-like, we can write down the belief propagation (BP) equations as,

$$\tilde{\phi}_{\blacksquare \rightarrow i}^t(S_i) = \left(\prod_{j \in \partial \blacksquare \setminus i} \text{Tr}_{S_j} \right) \psi_\blacksquare(\{S_i\}_{i \in \partial \blacksquare}) \prod_{j \in \partial \blacksquare \setminus i} \phi_{j \rightarrow \blacksquare}^t(S_j) \quad (\text{XI.4})$$

$$\phi_{i \rightarrow \blacksquare}^{t+1}(S_i) = \frac{1}{Z_{i \rightarrow \blacksquare}^{t+1}} \psi_i(S_i) \prod_{\square \in \partial i \setminus \blacksquare} \tilde{\phi}_{\square \rightarrow i}^t(S_i) \quad (\text{XI.5})$$

where $\tilde{\phi}_{\blacksquare \rightarrow i}(S_i)$ and $\phi_{i \rightarrow \blacksquare}$ are *messages* from interaction node \blacksquare to variable node i and vice versa. $Z_{i \rightarrow \blacksquare}$ is a normalization constant such that $\text{Tr}_{S_i} \phi_{i \rightarrow \blacksquare}(S_i) = 1$. The message $\tilde{\phi}_{\blacksquare \rightarrow i}(S_i)$ is proportional to the probability distribution of spin S_i when it is only connected to \blacksquare . On the other hand $\phi_{i \rightarrow \blacksquare}(S_i)$ is proportional to the probability distribution of spin S_i when only the connection to \blacksquare is missing.

Our goal is to obtain the marginal distribution function for each S_i which is obtained as,

$$\phi_i^{t+1}(S_i) = \frac{1}{Z_i^t} \prod_{\blacksquare \in \partial i} \tilde{\phi}_{\blacksquare \rightarrow i}^t(S_i) \quad (\text{XI.6})$$

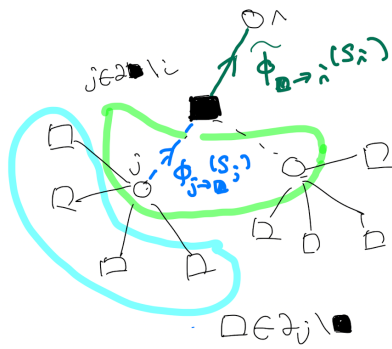
which is similar to Eq. (XI.5) but this is really the probability distribution (marginal distribution) of S_i within the *complete* network (no missing elements). Here Z_i is a normalization constant defined such that $\text{Tr}_{S_i} \phi_i(S_i) = 1$.

The BP equations presented above can be non-practical if the computation of Tr_{S_j} 's take too much time. So we wish to avoid it if it is possible. Fortunately, in the case of the Ising model, we can parametrize the probability distribution functions simply as,

$$\phi_{i \rightarrow \blacksquare}(S_i) = \frac{e^{h_{i \rightarrow \blacksquare} S_i}}{2 \cosh(h_{i \rightarrow \blacksquare})} \quad \tilde{\phi}_{\blacksquare \rightarrow i}(S_i) = \frac{e^{\tilde{h}_{\blacksquare \rightarrow i} S_i}}{2 \cosh(\tilde{h}_{\blacksquare \rightarrow i})} \quad (\text{XI.7})$$

Then one can find practical BP equations for $h_{i \rightarrow \blacksquare}(S_i)$ and $\tilde{h}_{\blacksquare \rightarrow i}(S_i)$ [10]. Here we skip discussions about it.

Now let us pay attention to the fact that our graphs are *dense* $c \gg 1$. Then we can derive the so called Approximate Message Passing (AMP) algorithm which is equivalent to the TAP equation [62] from the BP equation following the standard steps [10, 28]. The 1st step is to derive a set of equations called relaxed BP (r-BP) equations.

FIG. 40. Messages in a p -spin model. Here $p = 3$, $c = 4$.

B. relaxed-BP equations

As an example we consider in the following the p -spin Ising model,

$$H = -\frac{J}{\sqrt{c/\alpha}} \sum_{\blacksquare} \prod_{\substack{j \in \partial \blacksquare \\ p-\text{body}}} S_j \quad (\text{XI.8})$$

with Ising spins $S_i = \pm 1$ ($i = 1, 2, \dots, N$). Then we have,

$$\psi_{\blacksquare} = e^{\frac{\beta J}{\sqrt{c/\alpha}} \prod_{j \in \partial \blacksquare} S_j} \quad \psi_i(S_i) = 1 \quad (\text{XI.9})$$

and we can use the parameterization Eq. (XI.7).

Let us introduce

$$m_{i \rightarrow \blacksquare} = \sum_{S_i = \pm 1} \phi_{i \rightarrow \blacksquare}(S_i) S_i = \tanh(h_{i \rightarrow \blacksquare}) \quad (\text{XI.10})$$

Then Eq. (XI.4) becomes,

$$\tilde{\phi}_{\blacksquare \rightarrow i}(S_i) = \prod_{j \in \partial \blacksquare \setminus i} (2 \cosh(h_{j \rightarrow \blacksquare})) \left\langle e^{\frac{\beta J}{\sqrt{c/\alpha}} \prod_{j \in \partial \blacksquare} S_j} \right\rangle_h \quad (\text{XI.11})$$

where we introduced

$$\langle \cdots \rangle_h = \prod_{j \in \partial \blacksquare \setminus i} \phi_{j \rightarrow \blacksquare}(S_j) \cdots = \prod_{j \in \partial \blacksquare \setminus i} \frac{\text{Tr}_{S_j} e^{h_{j \rightarrow \blacksquare} S_j}}{2 \cosh(h_{j \rightarrow \blacksquare})} \cdots \quad (\text{XI.12})$$

By doing a cumulant expansion we find,

$$\begin{aligned} \ln \left\langle e^{\frac{\beta J}{\sqrt{c/\alpha}} \prod_{j \in \partial \blacksquare} S_j} \right\rangle_h &= \frac{\beta J}{\sqrt{c/\alpha}} S_i \prod_{j \in \partial \blacksquare \setminus i} m_{j \rightarrow \blacksquare} \\ &+ \frac{1}{2} \frac{(\beta J)^2}{c/\alpha} \left(1 - \prod_{j \in \partial \blacksquare \setminus i} m_{j \rightarrow \blacksquare}^2 \right) + \dots \end{aligned} \quad (\text{XI.13})$$

Thus we find

$$\tilde{\phi}_{\blacksquare \rightarrow i}^t(S_i) \propto e^{\frac{\beta J}{\sqrt{c/\alpha}} S_i \prod_{j \in \partial \blacksquare \setminus i} m_{j \rightarrow \blacksquare}^t} \quad (\text{XI.14})$$

Using this in Eq. (XI.5) and using Eq. (XI.7) we find,

$$h_{i \rightarrow \blacksquare}^{t+1} = \frac{\beta J}{\sqrt{c/\alpha}} \sum_{\square \in \partial i \setminus \blacksquare} \prod_{j \in \partial \square \setminus i} m_{j \rightarrow \square}^t \quad (\text{XI.15})$$

then using Eq. (XI.10) we find

$$m_{i \rightarrow \blacksquare}^{t+1} = \tanh \left(\frac{\beta J}{\sqrt{c/\alpha}} \sum_{\square \in \partial i \setminus \blacksquare} \prod_{j \in \partial \square \setminus i} m_{j \rightarrow \square}^t \right) \quad (\text{XI.16})$$

This is the so called relaxed BP (r-BP) [10]. Here we have $N \times N_\blacksquare = N^2(c/p)$ (since $N_\blacksquare = N(c/p)$ see Eq. (III.1)) equations and each of the equation contains a summation over c terms so that the computational cost scales as $N^2 c(c/p)$. For the global coupling $c \propto N^{p-1}$ (see Eq. (III.14)) so that the computational cost becomes very high.

We find the marginal distribution of S_i defined by Eq. (XI.6) as,

$$\phi_i^{t+1}(S_i) = \frac{1}{Z_i} e^{S_i(h_i^{\text{eff}})^{t+1}} \quad (\text{XI.17})$$

where

$$(h_i^{\text{eff}})^{t+1} = \frac{\beta J}{\sqrt{c/\alpha}} \sum_{\blacksquare \in \partial i} \prod_{j \in \partial \blacksquare \setminus i} m_{j \rightarrow \blacksquare}^t \quad (\text{XI.18})$$

This allows us to evaluate the 'local magnetization' as

$$m_i = \sum_{S_i=\pm 1} \phi_i(S_i) S_i = \tanh(h_i^{\text{eff}}) \quad (\text{XI.19})$$

C. Approximate Message Passing (AMP) or TAP equations

Let us look more closely into the effective field we found above. We find with a recursive use of Eq. (XI.16),

$$\begin{aligned} (h_i^{\text{eff}})^{t+1} &= \frac{\beta J}{\sqrt{c/\alpha}} \sum_{\blacksquare \in \partial i} \prod_{j \in \partial \blacksquare \setminus i} m_{j \rightarrow \blacksquare}^t \\ &= \frac{\beta J}{\sqrt{c/\alpha}} \sum_{\blacksquare \in \partial i} \prod_{j \in \partial \blacksquare \setminus i} \tanh \underbrace{\left(\frac{\beta J}{\sqrt{c/\alpha}} \sum_{\square \in \partial j \setminus \blacksquare} \prod_{k \in \partial \square \setminus j} m_{k \rightarrow \square}^{t-1} \right)}_{(h_j^{\text{eff}})^t} \\ &\quad \underbrace{\frac{\beta J}{\sqrt{c/\alpha}} \sum_{\square \in \partial j} \prod_{k \in \partial \square \setminus j} m_{k \rightarrow \square}^{t-1} - \frac{\beta J}{\sqrt{c/\alpha}} \prod_{k \in \partial \blacksquare \setminus j} m_{k \rightarrow \blacksquare}^{t-1}}_{(h_j^{\text{eff}})^t} \\ &\simeq \frac{\beta J}{\sqrt{c/\alpha}} \sum_{\blacksquare \in \partial i} \prod_{j \in \partial \blacksquare \setminus i} m_j^t \\ &\quad - \frac{(\beta J)^2}{c/\alpha} \sum_{\blacksquare \in \partial i} \sum_{l \in \partial \blacksquare \setminus i} (1 - \tanh^2((h_l^{\text{eff}})^t)) \left(\prod_{k \in (\partial \blacksquare \setminus l)} m_{k \rightarrow \blacksquare}^{t-1} \right) \prod_{j \in (\partial \blacksquare \setminus i) \setminus l} m_{j \rightarrow \blacksquare}^t \\ &\simeq \frac{\beta J}{\sqrt{c/\alpha}} \sum_{\blacksquare \in \partial i} \prod_{j \in \partial \blacksquare \setminus i} m_j^t - \gamma(\beta J)^2 p(p-1)(1-q_t) q_{t-1}^{p-2} m_i^{t-1} \end{aligned} \quad (\text{XI.20})$$

From the 3rd to 4th equation we expanded $\tanh(..)$ function assuming the term $\frac{\beta J}{\sqrt{c/\alpha}} \prod_{k \in \partial \blacksquare \setminus j} m_{k \rightarrow \blacksquare}$ is small. In the last equation we assumed $m_{i \rightarrow \blacksquare} \simeq m_i$ with m_i being the local magnetization Eq. (XI.19) neglecting higher order corrections. We also introduced

$$q = \frac{1}{N} \sum_{i=1}^N m_i^2 \quad (\text{XI.21})$$

and assumed $\sum_{\blacksquare \in \partial_i} \dots \simeq c \times \text{average of } \dots$ since our graphs are dense $c \gg 1$. Note that $\gamma = \alpha/p$ as defined in Eq. (III.2).

To sum up, putting correct 'time indices' we find the TAP or AMP equation for the p-spin Ising model [62, 77],

$$m_{i,t} = \tanh h_{i,t}^{\text{eff}} \quad h_{i,t}^{\text{eff}} = h_{\text{ext}} + \frac{\beta J}{\sqrt{c/\alpha}} \sum_{\blacksquare \in \partial_i} \prod_{j \in \partial \blacksquare \setminus i} m_{j,t-1} - \gamma(\beta J)^2 p(p-1)(1-q_{t-1})q_{t-2}^{p-2} m_{i,t-2} \quad (\text{XI.22})$$

The last term in the h_i^{eff} is the Onsager's reaction term. Here we have N equations and each of the equation contains a summation over c terms so that the computational cost scales as Nc . Note that the computational cost is dramatically reduced compared with the relaxed BP.

D. State Evolution

For the overlap q we can write,

$$q = \frac{1}{N} \sum_{i=1}^N m_i^2 = \frac{1}{N} \sum_{i=1}^N \tanh^2(h_i^{\text{eff}}) = \int dh P(h) \tanh^2(h) \quad P(h) = \frac{1}{N} \sum_{i=1}^N \delta(h - h_i^{\text{eff}}) \quad (\text{XI.23})$$

Assuming the magnetization m_i Eq. (XI.19) are uncorrelated at different sites i , we find the variance of the 'random field' h_i^{eff} Eq. (XI.18) created by neighbors of i as,

$$\lim_{N \rightarrow \infty} \frac{1}{N} \sum_{i=1}^N (h_i^{\text{eff}})^2 = \lim_{N \rightarrow \infty} \frac{1}{N} \sum_{i=1}^N \left[\frac{\beta J}{\sqrt{c/\alpha}} \sum_{\blacksquare \in \partial_i} \prod_{j \in \partial \blacksquare \setminus i} m_{j \rightarrow \blacksquare} \right]^2 = \gamma(\beta J)^2 p q^{p-1} \quad (\text{XI.24})$$

while the average is zero,

$$\lim_{N \rightarrow \infty} \frac{1}{N} \sum_{i=1}^N (h_i^{\text{eff}}) = 0 \quad (\text{XI.25})$$

Higher order cumulants vanish in dense limit $c \rightarrow \infty$. Thus we find (the so called state evolution equation),

$$q_t = \int \mathcal{D} \tanh^2(\sqrt{\epsilon} z) \quad \epsilon = \gamma(\beta J)^2 p q_{t-1}^{p-1} \quad (\text{XI.26})$$

This agrees with Eq. (VII.12).

XII. DYNAMICAL MEAN-FIELD THEORY

We can study slow dynamics of our ferromagnetic p -spin model of the dense graph introduced in sec. III A in the supercooled paramagnetic regime by developing a dynamical mean-field theory. In the following we work on the spherical model, for which we will find the same equations as found in the spinglass model [47]. We work on the Martin-Siggia-Rose (MSR) generating functional [78] of the Langevin dynamics following similar steps as we did for the statics. In appendix M we summarized some basics of the Langevin equation and the MSR generating functional.

A. Model

Here let us consider specifically the ferromagnetic p -spin model on the dense graph,

$$H = -\frac{J}{\sqrt{c/\alpha}} \sum_{\blacksquare} \underbrace{\prod_{j \in \partial \blacksquare} S_j}_{p\text{-body}} \quad (\text{XII.1})$$

with scalar spins S_i ($i = 1, 2, \dots, N$) with the spherical constraint Eq. (III.7)

$$\sum_{i=1}^N S_i^2 = N. \quad (\text{XII.2})$$

The spherical p -spin model is very useful in the sense that it allows one to analyze theoretically the dynamics [49, 72] as well as statics [79] in great detail (see [6]).

We consider the relaxationla dynamics of the system which obeys the following Langevin equation for (dimensionless) time $0 < t < \infty$,

$$\frac{d}{dt} S_i = -\frac{1}{J} \frac{\delta H}{\delta S_i} - z(t) S_i + h_i(t) + \xi_i(t) \quad (\text{XII.3})$$

with the white noise,

$$\langle \xi_i(t) \xi_j(t') \rangle_\xi = \delta_{ij} 2\tilde{T} \delta(t - t') \quad \tilde{T} = \frac{1}{\beta J} \quad (\text{XII.4})$$

We have also introduced external field $h_i(t)$.

B. MSR generating functional

We start from an identity

$$1 = \left\langle \int \mathcal{D}[S] \prod_t \delta \left(-\frac{d}{dt} S_i - \frac{1}{J} \frac{\delta H}{\delta S_i} - z(t) S_i + h_i(t) + \xi_i(t) \right) \right\rangle_\xi = \int \mathcal{D}[S] \mathcal{D}[\hat{S}] e^{\mathcal{S}[S, \hat{S}] + \int_0^\infty dt \sum_{i=1}^N h_i(t) i \hat{S}_i(t)} \quad (\text{XII.5})$$

where $\int \mathcal{D}[S]$ and $\int \mathcal{D}[\hat{S}]$ represent path-integrals. In the last equation we used a (path) integral representation of the delta functions introducing,

$$\mathcal{S}[S, \hat{S}] = \int_0^\infty dt \sum_{i=1}^N i \hat{S}_i(t) \left[-\frac{d}{dt} S_i(t) - z(t) S_i(t) + T i \hat{S}_i(t) \right] + \mathcal{S}_{\text{int}}[S, \hat{S}] \quad (\text{XII.6})$$

with

$$\mathcal{S}_{\text{int}}[S, \hat{S}] = -\frac{1}{\sqrt{c/\alpha}} \int_0^\infty dt \sum_i \sum_{\blacksquare \in \partial_i} i \hat{S}_i(t) \prod_{j \in \partial \blacksquare \setminus i} S_j(t) \quad (\text{XII.7})$$

The MSR generating function is defined, slightly extending the above functional as,

$$Z_{\text{MSR}}[h, \hat{h}] = \int \mathcal{D}[s] \mathcal{D}[\hat{s}] \exp \left[\mathcal{S}[S, \hat{S}] + \sum_i \int_0^\infty dt [h_i(t) i \hat{S}_i(t)] + \hat{h}_i(t) S_i(t) \right] \quad (\text{XII.8})$$

where we introduced a field $\hat{h}_i(t)$ conjugated to $S_i(t)$.

For example, the time auto-correlation function and linear-response functions can be obtained as

$$C_{ij}(t_1, t_2) = \langle S_i(t_1) S_j(t_2) \rangle_\xi = \frac{\delta^2 Z_{\text{MSR}}[h, \hat{h}]}{\delta \hat{h}_i(t_1) \delta \hat{h}_j(t_2)} \Big|_{h, \hat{h}=0} \quad (\text{XII.9})$$

and

$$R_{ij}(t_1, t_2) = \left\langle \frac{\delta S_i(t_1)}{\delta h_j(t_2)} \right\rangle_\xi = \langle S_i(t_1) i \hat{S}_j(t_2) \rangle_\xi = \frac{\delta^2 Z_{\text{MSR}}[h, \hat{h}]}{\delta \hat{h}_i(t_1) \delta h_j(t_2)} \Big|_{h, \hat{h}=0} \quad (\text{XII.10})$$

Some remarks:

- $Z_{\text{MSR}}[h, \hat{h} = 0] = 1$ by construction.
- The causality implies $R_{ij}(t_1, t_2) = 0$ for $t_1 < t_2$.
- We follow the Ito'sprescription (see appendix M 3 b) which implies $\lim_{t_2 \rightarrow t_1^-} R_{ij}(t_1, t_2) = \delta_{ij}$ (see Eq. (M.32)).
- In the ensemble of paths included in the MSR generating functional introduced above we have assumed a flat measure for the initial configuration $S_i(t=0)$ for $i = 1, 2, \dots, N$: a completely random configuration.
- An important property which holds in equilibrium (or in stationary states) is that the time-translational invariance (TTI) which implies

$$C_{ij}(t_1, t_2) = C_{ij}(t_1 - t_2) \quad R_{ij}(t_1, t_2) = R_{ij}(t_1 - t_2) \quad (\text{XII.11})$$

- Another very important property which holds in equilibrium is the fluctuation-dissipation theorem (FDT),

$$R_{ij}(t_1, t_2) = \frac{1}{\bar{T}} \frac{\partial C_{ij}(t_1, t_2)}{\partial t_2}. \quad (\text{XII.12})$$

C. Dynamical order parameters and the effective Langevin equation

Let us introduce dynamical order parameters,

$$Q_1(t, t') = \frac{1}{N} \sum_{i=1}^N \left\langle i \hat{S}_i(t) i \hat{S}_i(t') \right\rangle \quad (\text{XII.13})$$

$$Q_2(t, t') = \frac{1}{N} \sum_{i=1}^N \left\langle S_i(t) S_i(t') \right\rangle = C(t, t') \quad (\text{XII.14})$$

$$Q_3(t, t') = \frac{1}{N} \sum_{i=1}^N \left\langle i \hat{S}_i(t) S_i(t') \right\rangle = R(t', t) \quad (\text{XII.15})$$

$$Q_4(t, t') = \frac{1}{N} \sum_{i=1}^N \left\langle S_i(t) i \hat{S}_i(t') \right\rangle = R(t, t') \quad (\text{XII.16})$$

Note that $C(t, t') = (1/N) \sum_{i=1}^N C_{ii}(t, t')$ is nothing but the spin autocorrelation function Eq. (VI.7). Apparently we have,

$$C(t_1, t_2) = C(t_2, t_1) \quad (\text{XII.17})$$

On the other hand $R(t, t') = (1/N) \sum_{i=1}^N R_{ii}(t, t')$ is the conjugated response function which is related to $C(t, t)$ via FDT (see Eq. (XII.12)) as

$$R(t_1, t_2) = \frac{1}{\tilde{T}} \frac{\partial C(t_1, t_2)}{\partial t_2}. \quad (\text{XII.18})$$

in equilibrium.

We can write

$$\begin{aligned} \int \mathcal{D}[S] \mathcal{D}[\hat{S}] \dots &= \int \mathcal{D}[Q_1] \mathcal{D}[Q_2] \mathcal{D}[Q_3] \mathcal{D}[Q_4] \int \mathcal{D}[S] \mathcal{D}[\hat{S}] \\ &\prod_{t,t'} \left\{ \delta \left(NQ_1(t, t') - \sum_i i\hat{S}_i(t)i\hat{S}_i(t') \right) \delta \left(NQ_2(t, t') - \sum_i S_i(t)S_i(t') \right) \right. \\ &\quad \left. \delta \left(NQ_3(t, t') - \sum_i i\hat{S}_i(t)S_i(t') \right) \delta \left(NQ_4(t, t') - \sum_i S_i(t)i\hat{S}_i(t') \right) \right\} \end{aligned} \quad (\text{XII.19})$$

We can introduce integral representations of the delta functions as,

$$\prod_{t,t'} \delta \left(NQ_1(t, t') - \sum_i i\hat{S}_i(t)i\hat{S}_i(t') \right) = \int \mathcal{D}[\lambda] \exp \left[N \int_0^\infty dt \int_0^\infty dt' \left[\lambda_1(t, t')Q_1(t, t') - \lambda_1(t, t') \frac{1}{N} \sum_i i\hat{S}_i(t)i\hat{S}_i(t') \right] \right] \quad (\text{XII.20})$$

We express other delta functions similarly by introducing $\lambda_2(t, t')$, $\lambda_3(t, t')$ and $\lambda_4(t, t')$. As the result we have,

$$\begin{aligned} Z_{\text{MSR}} &= \int \mathcal{D}[\lambda_1] \mathcal{D}[\lambda_2] \mathcal{D}[\lambda_3] \mathcal{D}[\lambda_4] \mathcal{D}[Q_1] \mathcal{D}[Q_2] \mathcal{D}[Q_3] \mathcal{D}[Q_4] \\ &\exp \left[N \int_0^\infty dt \int_0^\infty dt' [\lambda_1(t, t')Q_1(t, t') + \lambda_2(t, t')Q_2(t, t') + \lambda_3(t, t')Q_3(t, t') + \lambda_4(t, t')Q_4(t, t')] \right] \\ &\int \mathcal{D}[S] \mathcal{D}[\hat{S}] \prod_{i=1}^N e^{\mathcal{S}_{\text{local}}[S_i, \hat{S}_i, \lambda]} \langle e^{\mathcal{S}_{\text{int}}} \rangle_\lambda \end{aligned} \quad (\text{XII.21})$$

where we introduced

$$\begin{aligned} \mathcal{S}_{\text{local}}[S_i, \hat{S}_i, \lambda] &= \int_0^\infty dt i\hat{S}_i(t) \left[-\frac{d}{dt} S_i(t) - z(t)S_i(t) + Ti\hat{S}_i(t) \right] \\ &- \int_0^\infty dt \int_0^\infty dt' [\lambda_1(t, t')i\hat{S}_i(t)i\hat{S}_i(t') + \lambda_2(t, t')S_i(t)S_i(t') + \lambda_3(t, t')i\hat{S}_i(t)S_i(t')w + \lambda_4(t, t')S_i(t)i\hat{S}_i(t')] \end{aligned} \quad (\text{XII.22})$$

and

$$\langle \dots \rangle_\lambda = \frac{\int \mathcal{D}[S] \mathcal{D}[\hat{S}] \prod_i \exp[\mathcal{S}_{\text{local}}[S_i, \hat{S}_i, \lambda]] \dots}{\int \mathcal{D}[S] \mathcal{D}[\hat{S}] \prod_i \exp[\mathcal{S}_{\text{local}}[S_i, \hat{S}_i, \lambda]]} \quad (\text{XII.23})$$

Note that different sites i s are uncorrelated in this averaging.

Now we can proceed much as we did for the statics. We evaluate the cumulant expansion of the interaction part,

$$\begin{aligned}
\ln \langle e^{S_{\text{int}}} \rangle_\lambda &= \ln \left\langle \exp \left[-\frac{1}{\sqrt{c/\alpha}} \int_0^\infty dt \sum_i \sum_{\blacksquare \in \partial_i} i \hat{S}_i(t) \prod_{j \in \partial \blacksquare \setminus i} S_j(t) \right] \right\rangle_\lambda \\
&= -\frac{1}{\sqrt{c/\alpha}} \int_0^\infty dt \sum_i \sum_{\blacksquare \in \partial_i} \langle i \hat{S}_i(t) \rangle_\lambda \prod_{j \in \partial \blacksquare \setminus i} \langle S_j(t) \rangle_\lambda \\
&\quad + \frac{1}{2} \frac{1}{c/\alpha} \int_0^\infty dt_1 \int_0^\infty dt_2 \left\langle \sum_i \sum_{\blacksquare_1 \in \partial_i} i \hat{S}_i(t_1) \prod_{j \in \partial \blacksquare_1 \setminus i} S_j(t_1) \sum_k \sum_{\blacksquare_2 \in \partial_k} i \hat{S}_k(t_2) \prod_{l \in \partial \blacksquare_2 \setminus k} S_l(t_2) \right\rangle_\lambda + \dots \\
&= \frac{1}{2} \frac{1}{c/\alpha} \sum_{\blacksquare} \int_0^\infty dt_1 \int_0^\infty dt_2 \left[\sum_{i \in \partial \blacksquare} \langle i \hat{S}_i(t_1) i \hat{S}_i(t_2) \rangle_\lambda \prod_{j \in \partial \blacksquare \setminus i} \langle S_j(t_1) S_j(t_2) \rangle_\lambda \right. \\
&\quad \left. + \sum_{i \in \partial \blacksquare} \langle i \hat{S}_i(t_1) S_i(t_2) \rangle_\lambda \sum_{j \in \partial \blacksquare \setminus i} \langle S_j(t_1) i \hat{S}_j(t_2) \rangle_\lambda \prod_{k \in \partial \blacksquare \setminus i, j} \langle S_k(t_1) S_k(t_2) \rangle_\lambda \right] + \dots \\
&= \frac{\gamma N}{2} \int_0^\infty dt_1 \int_0^\infty dt_2 \left[p \langle i \hat{S}(t_1) i \hat{S}(t_2) \rangle_\lambda \langle S(t_1) S(t_2) \rangle_\lambda^{p-1} \right. \\
&\quad \left. + p(p-1) \langle i \hat{S}(t_1) S(t_2) \rangle_\lambda \langle S(t_1) i \hat{S}(t_2) \rangle_\lambda \langle S(t_1) S(t_2) \rangle_\lambda^{p-2} \right] \tag{XII.24}
\end{aligned}$$

where we used Eq. (III.2) $N_{\blacksquare} = N \frac{c}{\alpha} \gamma$. The cumulants can be represented by diagrams much as in the replica theory. The replica indices a, b should be replaced by times t_1, t_2 . Concerning higher order terms we point out again that only 1PI diagrams (loop diagrams) remain after the Legendre transform $\lambda_1(t_1, t_2) \rightarrow Q_1(t_1, t_2), \dots$. Higher order terms due to the loops vanish in $N \rightarrow \infty$ limit.

Collecting the above results we find,

$$\begin{aligned}
Z_{\text{MSR}} &= \int \mathcal{D}[Q_1] \mathcal{D}[Q_2] \mathcal{D}[Q_3] \mathcal{D}[Q_4] \mathcal{D}[\lambda_1] \mathcal{D}[\lambda_2] \mathcal{D}[\lambda_3] \mathcal{D}[\lambda_4] \int \mathcal{D}[S] \mathcal{D}[\hat{S}] \exp \left[\sum_i \int_0^\infty dt i \hat{S}_i(t) \left[-\frac{d}{dt} S_i(t) - z(t) S_i(t) + T i \hat{S}_i(t) \right] \right] \\
&\quad \exp \left[- \sum_i \int_0^\infty dt \int_0^\infty dt' \left[\lambda_1(t, t') i \hat{S}_i(t) i \hat{S}_i(t') + \lambda_2(t, t') S_i(t) S_i(t') + \lambda_3(t, t') i \hat{S}_i(t) S_i(t') + \lambda_4(t, t') S_i(t) i \hat{S}_i(t') \right] \right] \\
&\quad \exp \left[N \int_0^\infty dt_1 \int_0^\infty dt_2 \left[\frac{\gamma}{2!} p Q_1(t_1, t_2) Q_2^{p-1}(t_1, t_2) + \frac{\gamma}{2!} p(p-1) Q_3(t_1, t_2) Q_4(t_1, t_2) Q_2^{p-2}(t_1, t_2) \right. \right. \\
&\quad \left. \left. + \lambda_1(t_1, t_2) Q_1(t_1, t_2) + \lambda_2(t_1, t_2) Q_2(t_1, t_2) + \lambda_3(t_1, t_2) Q_3(t_1, t_2) + \lambda_4(t_1, t_2) Q_4(t_1, t_2) \right] \right] \tag{XII.25}
\end{aligned}$$

The integrations over λ 's and Q 's can be done by saddle point integrations for $N \gg 1$. Saddle point equations for integrations over Q 's are obtained as,

$$-\lambda_1(t_1, t_2) = \frac{\gamma p}{2} Q_2^{p-1}(t_1, t_2) \tag{XII.26}$$

$$-\lambda_2(t_1, t_2) = \frac{\gamma p(p-1)}{2} Q_1(t_1, t_2) Q_2^{p-2}(t_1, t_2) + \frac{\gamma p(p-1)(p-2)}{2} Q_3(t_1, t_2) Q_4(t_1, t_2) Q_2^{p-3}(t_1, t_2) \tag{XII.27}$$

$$-\lambda_3(t_1, t_2) = \frac{\gamma p(p-1)}{2} Q_4(t_1, t_2) Q_2^{p-2}(t_1, t_2) \tag{XII.28}$$

$$-\lambda_4(t_1, t_2) = \frac{\gamma p(p-1)}{2} Q_3(t_1, t_2) Q_2^{p-2}(t_1, t_2) \tag{XII.29}$$

Here let us note that

$$Q_3(t_1, t_2) Q_4(t_1, t_2) = R(t_1, t_2) R(t_2, t_1) = 0 \tag{XII.30}$$

because of the causality. We also have,

$$Q_1(t_1, t_2) = N^{-1} \sum_{i=1}^N \partial_{h_i}^2 Z_{\text{MSR}}(h_i, \hat{h}) \Big|_{\hat{h}=0} = 0 \tag{XII.31}$$

because $Z_{\text{MSR}}(h, \hat{h} = 0) = 1$ holds.

Combining the above results, we find an effective Langevin equation,

$$\frac{d}{dt} S_i(t) = -z(t)S_i(t) + \gamma p(p-1) \int_0^t dt' R(t, t') C^{p-2}(t, t') S_i(t') + \xi(t) \quad (\text{XII.32})$$

with an effective random force,

$$\langle \xi(t)\xi(t') \rangle = D(t, t') \quad D(t, t') \equiv 2T\delta(t-t') + \gamma p C^{p-1}(t, t'). \quad (\text{XII.33})$$

D. Self-consistent equations of the correlation and response functions

Using the effective Langevin equation Eq. (XII.32)- Eq. (XII.33), we obtain self-consistent equations for the correlation and response functions as follows.

Using Eq. (M.30) we can write,

$$R(t_1, t_2) = \left\langle \frac{\partial S(t_1)}{\partial \xi(t_2)} \right\rangle \quad (\text{XII.34})$$

Then we find,

$$\begin{aligned} \frac{\partial}{\partial t_1} R(t_1, t_2) &= \frac{\partial}{\partial t_1} \left\langle \frac{\delta S(t_1)}{\delta \xi(t_2)} \right\rangle = \left\langle \frac{\partial}{\partial t_1} \frac{\delta S(t_1)}{\delta \xi(t_2)} \right\rangle \\ &= -z(t_1)R(t_1, t_2) + \gamma p(p-1) \int_{t_2}^{t_1} dt' R(t_1, t') C^{p-2}(t_1, t') R(t', t_2) + \delta(t_1 - t_2) \end{aligned} \quad (\text{XII.35})$$

We also find

$$\begin{aligned} \frac{\partial}{\partial t_1} C(t_1, t_2) &= \frac{\partial}{\partial t_1} \langle S(t_1)S(t_2) \rangle = \langle \frac{dS(t_1)}{dt_1} S(t_2) \rangle \\ &= -z(t_1)C(t_1, t_2) + \gamma p(p-1) \int_0^{t_1} dt' R(t_1, t') C^{p-2}(t_1, t') C(t', t_2) + \langle \xi(t_1)S(t_2) \rangle \\ &= -z(t_1)C(t_1, t_2) + \gamma p(p-1) \int_0^{t_1} dt' R(t_1, t') C^{p-2}(t_1, t') C(t', t_2) \\ &\quad + 2\tilde{T}R(t_2, t_1) + \gamma p \int_0^{t_2} dt'' C^{p-1}(t_1, t'') R(t_2, t'') \end{aligned} \quad (\text{XII.36})$$

In the last equation we used

$$\langle \xi(t_1)S(t_2) \rangle = \int dt'' D(t_1, t'') R(t_2, t'') = 2\tilde{T}R(t_2, t_1) + \gamma p \int_0^{t_2} dt'' C^{p-1}(t_1, t'') R(t_2, t'') \quad (\text{XII.37})$$

which follows from Eq. (M.34) and Eq. (XII.33).

Let us recall the spherical constraint Eq. (XII.2) which implies

$$C(t, t) = 1 \quad (\text{XII.38})$$

so that

$$\begin{aligned} 0 &= \frac{dC(s, s)}{ds} = \left[\frac{\partial}{\partial t_1} C(t_1, t_2) + \frac{\partial}{\partial t_2} C(t_1, t_2) \right] \Big|_{t_1=t_2=s} \\ &= -2z(s) \underbrace{C(s, s)}_1 + 2\gamma p^2 \int_0^s dt' R(s, t') C^{p-1}(s, t') + 2\tilde{T} \underbrace{[R(t_2, t_1) + R(t_1, t_2)]}_1 \Bigg|_{t_1=t_2=s} \end{aligned} \quad (\text{XII.39})$$

here we used Eq. (M.32). Then we find,

$$z(t) = \gamma p^2 \int_0^t dt' R(t, t') C^{p-1}(t, t') + \tilde{T} \quad (\text{XII.40})$$

E. Equilibrium dynamics

We can consider large time limits with *fixed* time-difference,

$$t_1, t_2 \rightarrow \infty \quad \text{with fixed} \quad \tau \equiv t_1 - t_2 \quad (\text{XII.41})$$

In this limit, we have TTI (time-translational invariance) Eq. (XII.11),

$$C(t_1, t_2) \rightarrow C(\tau) \quad R(t_1, t_2) \rightarrow R(\tau) \quad (\text{XII.42})$$

and FDT Eq. (XII.12),

$$R(t_1, t_2) = \frac{1}{\tilde{T}} \frac{\partial C(t_1, t_2)}{\partial t_2} \quad \text{or} \quad R(\tau) = -\frac{1}{\tilde{T}} \frac{dC(\tau)}{d\tau} \quad (\text{XII.43})$$

We also assume

$$\lim_{t_1 \rightarrow \infty} C(t_1, t_2) = 0 \quad (\text{XII.44})$$

Using these we find Eq. (XII.40) becomes in the large time limit,

$$z(t) = \tilde{T} + \gamma p^2 \int_0^t d\tau R(t, t - \tau) C^{p-1}(t, t - \tau) \xrightarrow{t \rightarrow \infty} \tilde{T} + \gamma p^2 \int_0^\infty d\tau \underbrace{R(\tau) C^{p-1}(\tau)}_{\frac{1}{\tilde{T}} \frac{1}{p} \left(-\frac{d}{d\tau} \right) C^p(\tau)} = \tilde{T} + \frac{\gamma p}{\tilde{T}}$$

here we assume $\lim_{\tau \rightarrow \infty} C(\tau) = 0$ Eq. (XII.44).

Let us consider Eq. (XII.36) in the equilibrium limit defined in Eq. (XII.41). Using FDT Eq. (XII.43) we find,

$$\gamma p \int_0^{t_2} dt'' C^{p-1}(t_1, t'') R(t_2, t'') = \frac{\gamma p}{\tilde{T}} \int_0^{t_2} dt'' C^{p-1}(t_1 - t'') \frac{\partial C(t_2 - t'')}{\partial t''} = \frac{\gamma p}{\tilde{T}} \int_0^{t_2} dt'' C^{p-1}(t_1 - t'') \frac{\partial C(t'' - t_2)}{\partial t''} \quad (\text{XII.45})$$

in the last step we used Eq. (XII.17). Similarly we also find,

$$\begin{aligned} \gamma p(p-1) \int_0^{t_1} dt' R(t_1, t') C^{p-2}(t_1, t') C(t', t_2) &= \frac{\gamma p}{\tilde{T}} \int_0^{t_1} dt' \frac{\partial C^{p-1}(t_1 - t')}{\partial t'} C(t' - t_2) \\ &= \frac{\gamma p}{\tilde{T}} \underbrace{C^{p-1}(t_1 - t') C(t' - t_2)}_{C(t_1 - t_2) - C^{p-1}(t_1) C(-t_2)} \Big|_{t'=0}^{t'=t_1} - \frac{\gamma p}{\tilde{T}} \int_0^{t_1} dt' C^{p-1}(t_1 - t') \frac{\partial C(t' - t_2)}{\partial t'} \\ &\xrightarrow{\text{large time limit Eq. (XII.41)}} \frac{\gamma p}{\tilde{T}} C(t_1 - t_2) - \frac{\gamma p}{\tilde{T}} \int_0^{t_1} dt' C^{p-1}(t_1 - t') \frac{\partial C(t' - t_2)}{\partial t'} \end{aligned} \quad (\text{XII.46})$$

here we assumed $\lim_{\tau \rightarrow \infty} C(\tau) = 0$ Eq. (XII.44).

Combining the above results we find Eq. (XII.36) becomes in the equilibrium limit Eq. (XII.41),

$$\frac{\partial}{\partial t_1} C(t_1, t_2) = -\tilde{T} C(t_1, t_2) - \frac{\gamma p}{\tilde{T}} \int_{t_2}^{t_1} dt' C^{p-1}(t_1 - t') \frac{\partial C(t' - t_2)}{\partial t'} + 2\tilde{T} R(t_2 - t_1) \quad (\text{XII.47})$$

Finally we obtain,

$$\frac{dC(\tau)}{d\tau} = -\tilde{T} C(\tau) - \frac{\gamma p}{\tilde{T}} \int_0^\tau d\tau' C^{p-1}(\tau - \tau') \frac{\partial C(\tau')}{\partial \tau'} \quad (\tau > 0) \quad (\text{XII.48})$$

here we used the causality Eq. (M.7): $R(\tau) = 0$ for $\tau < 0$. In Fig. 41 we show a plot of the autocorrelation function obtained numerically solving Eq. (XII.48).

[Q] Show that the same equation can be derived starting from Eq. (XII.35).

The solution of the equation exhibit two step relaxations with a plateau as shown in Fig. 41. The plateau is nothing but the Edwards-Anderson order parameter q_{EA} Eq. (VI.6).

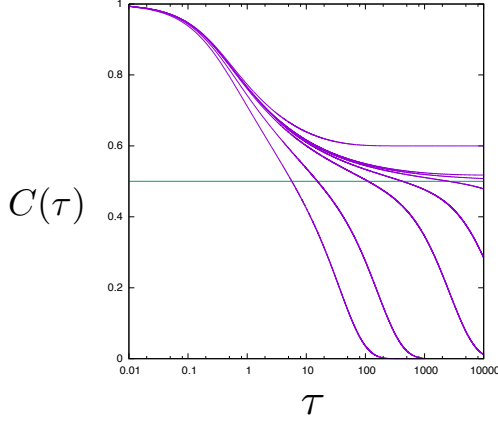


FIG. 41. Autocorrelation function $C(\tau)$: $p = 3$ $\gamma = 1/2$ for which $\tilde{T}_d = 0.612372..$ (see Eq. (XII.54)) and $q_{EA}(T_d) = C_d(T_d) = 0.5$ (see Eq. (XII.53)). This is obtained solving Eq. (XII.48) numerically. The lines are for $\tilde{T} = 0.6, 0.612, 0.612372, 0.613, 0.615, 0.62, 0.65, 0.7$ from the top to the bottom. The horizontal line indicates C_d .

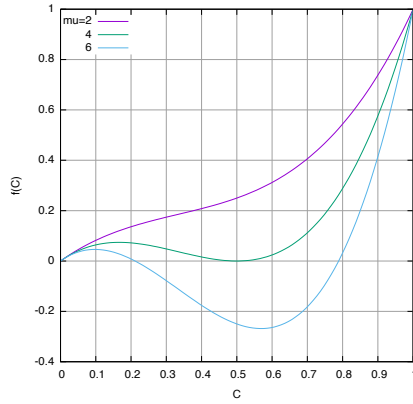


FIG. 42. function $f(C)$ for $p = 3$ $\gamma = 1/2$

As long as $C(\tau)$ decays with time τ so that $dC(\tau)/d\tau < 0$, Eq. (XII.48) implies the following inequality must hold,

$$C(\tau) + \frac{\gamma p}{\tilde{T}^2} \int_0^\tau d\tau' C^{p-1}(\tau - \tau') \frac{\partial C(\tau')}{\partial \tau'} > 0 \quad (\text{XII.49})$$

By observing that $dC(\tau')/d\tau' < 0$ and $C(\tau - \tau') > C(\tau)$ for $0 < \tau' < \tau$ in the integral, the above inequality requires the following

$$C(\tau) + \mu C^{p-1}(\tau) \int_0^\tau d\tau' \frac{\partial C(\tau')}{\partial \tau'} = C(\tau) + \mu C^{p-1}(\tau)(C(\tau) - 1) > 0 \quad (\text{XII.50})$$

with

$$\mu = \frac{\gamma p}{\tilde{T}^2} \quad (\text{XII.51})$$

To sum up we find the following condition

$$f(C) > 0 \quad f(C) = Cg(C) \quad g(C) = 1 + \mu C^{p-2}(C - 1) \quad (\text{XII.52})$$

In Fig. 42 we display the function $f(C)$ for the case of $p = 3$ and $\gamma = 1/2$. It can be seen that for sufficiently small μ , $f(C) > 0$ for the entire range $0 < C < 1$ while the condition breaks down for sufficiently large μ where $f(C) > 0$ holds

only for some limited range $C_p(\mu) < C < 1$. The value of $C_p(\mu)$ is precisely the plateau height of the auto-correlation function which can be seen in Fig. 41. The critical point can be found solving $g(C) = g'(C) = 0$. The plateau height at the critical point is obtained as

$$C_d = C_p(\mu_d) = \frac{p-2}{p-1}. \quad (\text{XII.53})$$

and the location of the critical point is

$$\mu_d = \frac{(p-1)^{p-1}}{(p-2)^{p-2}} \quad \text{or} \quad \tilde{T}_d = \sqrt{\frac{\gamma p(p-2)^{p-2}}{(p-1)^{p-1}}}. \quad (\text{XII.54})$$

Let us discuss connection to the statics.

- The saddle point equation of 1RSB solution of the model in the limit $m \rightarrow 1$ (assuming $q_0 = 0$), shown in Eq. (VIII.65) turns out to be,

$$f(q_1) = 0 \quad (\text{XII.55})$$

with $f(q_1)$ being exactly the same function $f(c)$ defined in Eq. (XII.52). See also Eq. (VIII.68).

- Similar obserbation can be seen also in the state following set up discussed in sec IX C.

[Q] What is the physical meaning of this? Pure coincidence?

F. Out-of-equilibrium dynamics

Dynamics at longer time scales, outside the equilibrium regime Eq. (XII.41).

- Breakdown of TTI

$$C(t_1, t_2) \neq C(t_1 - t_2) \quad R(t_1, t_2) \neq R(t_1 - t_2) \quad (\text{XII.56})$$

- Violation of FDT

$$R(t_1, t_2) = \frac{X(t_1, t_2)}{\tilde{T}} \frac{\partial C(t_1, t_2)}{\partial t_2} \quad X \neq 1 \quad (\text{XII.57})$$

DMFT for the p -spin spherical model[49] revealed the following features in the long time limit $t_1, t_2 \rightarrow \infty$ with *fixed* $C(t_1, t_2) = C$

- Equilibrium regime $C_d (= q_{\text{EA}}) < C < 1$
 - TTI holds
 - FDT holds $X(C) = 1$
- Aging regime $0 < C < C_d$
 - TTI breaks down - waiting time effect
 - Generalized FDT $X(C) < 1$

Correspondence with statics? [50, 80].

$$X(C) \stackrel{?}{=} x(c) \quad (\text{XII.58})$$

where $x(c)$ is related to $P(q)$ as Eq. (X.12),

$$x(q) = \int_0^q dq' P(q'). \quad (\text{XII.59})$$

The generalized FDT implies 'effective temperature'[80, 81],

$$T_{\text{eff}}(C) = \frac{T}{X(C)} \quad (\text{XII.60})$$

Part III

Spheres in large dimensional limit

We consider an assembly of spherical particles of 'size' D , whose number density is ρ . We assume that the particles are spherical and that interaction between them is given by a two body potential $v(r) = v(r/D)$ which only depends on the mutual distance r between the particles. The important length scale is the 'size' D of the particles, which controls the interaction between particles. For hard-spheres, it is the diameter. For convenience let us introduce the 'volume fraction' (fraction of the volume occupied by the particles),

$$\varphi = \rho \Omega_d (D/2)^d \quad \rho = \frac{N}{V} \quad (\text{XII.61})$$

where Ω_d is the volume of a unit sphere.

XIII. REPLICATED LIQUID

The following is a review note on the recent progress of the replica approach to the glass transitions and jamming of spheres in large- d limit [12]. To derive the replica theory, we follow the same steps we used for the spin systems discussed in previous chapters without going through the density functional theory [35].

A. Replicated system of spheres

We consider replicated system with n replicas. Here we consider a situation in which the replicas are divided into n/m subgroups $\mathcal{C} = 1, 2, \dots, n/m$ each of which consists of m replicas. Group $\mathcal{C} = 1$ consists of replicas $a = 1, 2, \dots, m$, $\mathcal{C} = 2$ consists of replicas $a = m + 1, m + 2, \dots, 2m$ and so on. The total Hamiltonian is given by

$$H_n = \sum_{\mathcal{C}=1}^{n/m} H_{m,\mathcal{C}} \quad (\text{XIII.1})$$

where $H_{m,\mathcal{C}}$ is for the group \mathcal{C} . For instance the group $\mathcal{C} = 1$ has,

$$-\beta H_{m,1} = -\beta \sum_{a=1}^m H[\{\mathbf{p}_i^a, \mathbf{r}_i^a\}] + \frac{D^2}{2} \sum_{i=1}^N \sum_{a,b=1}^{m-1} (\epsilon_i)_{ab} \eta_i^a \cdot \eta_i^b. \quad (\text{XIII.2})$$

Note that the additional term breaks replica symmetry (invariance under permutations of replicas $a = 1, 2, \dots, n$) and also the permutation symmetry of particles (permutations of the labels $i = 1, 2, \dots, N$ put on them). This amounts to create a sort of 'molecules made of replicas' $i = 1, 2, \dots, N$ as shown in Fig. 43.

The Hamiltonian for each replica is

$$H[\{\mathbf{p}_i, \mathbf{r}_i\}] = \sum_{i=1}^N \frac{|\mathbf{p}_i|^2}{2m} + \sum_{i < j} v(r_{ij}) \quad r_{ij} = |\mathbf{x}_i - \mathbf{x}_j|$$

where we decomposed the coordinates as

$$\mathbf{x}_i^a = \mathbf{R}_i + \mathbf{u}_i^a \quad \mathbf{u}_i^a = \frac{D}{\sqrt{d}} \eta_i^a \quad (\text{XIII.3})$$

with \mathbf{R}_i being the center of mass of the 'molecule'

$$\mathbf{R}_i = \frac{1}{m} \sum_{a=1}^m \mathbf{x}_i^a. \quad (\text{XIII.4})$$

Thus we have a sum rule,

$$\sum_{a=1}^m \mathbf{u}_i^a = 0 \quad (\text{XIII.5})$$

Note that in Eq. (XIII.2) the external field ϵ is applied only to $m - 1$ replicas. The reason is that position of the remaining replica is fixed by the sum rule.

Let us introduce the glass order parameter,

$$q_{ab} = \frac{1}{N} \sum_{i=1}^N \langle \mathbf{u}_i^a \cdot \mathbf{u}_i^b \rangle_\epsilon = \frac{1}{N} \sum_{i=1}^N \frac{D^2}{d} \sum_{\mu=1}^d \langle (\eta_i^\mu)^a (\eta_i^\mu)^b \rangle_\epsilon \quad (\text{XIII.6})$$

Note the sum rule Eq. (XIII.5) implies,

$$q_{mb} = - \sum_{a=1}^{m-1} q_{ab} \quad q_{mm} = \sum_{a,b=1}^{m-1} q_{ab} \quad (\text{XIII.7})$$

where $1 \leq b \leq m - 1$ in the 1st equation.

B. Derivation of the free-energy in $d \rightarrow \infty$ limit

In the $d \rightarrow \infty$ limit, we may also define *local* glass order parameter,

$$(q_i)_{ab} = \langle \mathbf{u}_i^a \cdot \mathbf{u}_i^b \rangle_{\epsilon_i} = \frac{D^2}{d} \sum_{\mu=1}^d \langle (\eta_i^\mu)^a (\eta_i^\mu)^b \rangle_\epsilon \quad (\text{XIII.8})$$

Now similarly to Eq. (VI.34) we start from an identity,

$$1 = \int_{-\infty}^{\infty} \int_{-i\infty}^{i\infty} \prod_{a < b} \left(\frac{d}{2\pi i} \right) d(q_i)_{ab} d(\epsilon_i)_{ab} e^{\frac{d}{2} \sum_{a,b=1}^{m-1} (\epsilon_i)_{ab} ((D^2/d) \sum_{\mu=1}^d (\eta_i^\mu)^a (\eta_i^\mu)^b - (q_i)_{ab})} \quad (\text{XIII.9})$$

$$\begin{aligned} \overline{Z_n}[\hat{\epsilon}_{\text{ext}}^{m,m}] &= \frac{1}{N!} \int \prod_{i=1}^N \prod_{a=1}^m \frac{d^d x_i^a}{\lambda_{\text{th}}^d} e^{-\beta \sum_a \sum_{i < j} v(r_{ij}^a) + \frac{D^2}{2} \sum_{i=1}^N \sum_{a,b=1}^{m-1} (\epsilon_i^{\text{ext}})_{ab} (\eta_i^a \cdot \eta_i^b)} \\ &= \frac{1}{N!} \prod_i \left\{ \prod_{a < b} d \int d(q_i)_{ab} \int_{-i\infty}^{i\infty} \prod_{a < b} \frac{d(\epsilon_i)_{ab}}{2\pi i} e^{-\frac{d}{2} \sum_{a,b=1}^{m-1} (\epsilon_i)_{ab} (q_i)_{ab}} \right\} \\ &\quad \int \prod_{i=1}^N \prod_{a=1}^m \frac{d^d x_i^a}{\lambda_{\text{th}}^d} e^{\frac{D^2}{2} \sum_{i=1}^N \sum_{a,b=1}^{m-1} ((\epsilon_i^{\text{ext}})_{ab} + (\epsilon_i)_{ab}) \eta_i^a \cdot \eta_i^b} e^{-\beta \sum_a \sum_{i < j} v(r_{ij}^a)} \\ &= \prod_{i=1}^N \left\{ \prod_{a < b} d \int d(q_i)_{ab} e^{\frac{d}{2} \sum_{a,b=1}^{m-1} (\epsilon_i^{\text{ext}})_{ab} (q_i)_{ab}} \int_{(\epsilon_i)_{ab}^{\text{ext}} - i\infty}^{(\epsilon_i)_{ab}^{\text{ext}} + i\infty} \frac{d(\epsilon_i)_{ab}}{2\pi i} e^{-\frac{d}{2} \sum_{a,b=1}^{m-1} (\epsilon_i)_{ab} (q_i)_{ab}} \right\} \\ &\quad e^{-\beta G_{m,0}(\hat{\epsilon}^{m,m})} \langle e^{-\beta \sum_a \sum_{i < j} v(r_{ij}^a)} \rangle_{\epsilon,0} \\ &= \prod_{i=1}^N \left\{ \prod_{a < b} d \int d(q_i)_{ab} e^{\frac{d}{2} \sum_{a,b=1}^{m-1} \epsilon_{ab}^{\text{ext}} q_{ab}} \int_{\epsilon_{ab}^{\text{ext}} - i\infty}^{\epsilon_{ab}^{\text{ext}} + i\infty} \frac{d(\epsilon_i)_{ab}}{2\pi i} e^{-\frac{d}{2} \sum_{a,b=1}^{m-1} (\epsilon_i)_{ab} (q_i)_{ab}} \right\} e^{-\beta G(\hat{\epsilon}^{m,m})} \\ &= \prod_{i=1}^N \prod_{a < b} d \int d(q_i)_{ab} e^{\frac{d}{2} \sum_{i=1}^N \sum_{a,b=1}^{m-1} (\epsilon_i^{\text{ext}})_{ab} (q_i)_{ab} - \beta F(\hat{q}^{m,m})} = e^{\frac{d}{2} \sum_{i=1}^N \sum_{a,b=1}^{m-1} (\epsilon_i)_{ab}^{\text{ext}} (q_i)_{ab}^* - \beta F((\hat{q}^*)^{m,m})} \end{aligned} \quad (\text{XIII.10})$$

where $\hat{\epsilon}^{m,m}$ and $\hat{q}^{m,m}$ are matrices of size $(m - 1) \times (m - 1)$ obtained by subtracting the m -th low and column of the original $m \times m$ matrix $\hat{\epsilon}$ and \hat{q} respectively.

In the 3rd equation we introduced,

$$-\beta G_{m,0}[\hat{\epsilon}^{m,m}] = -\ln N! + Nd \ln I \quad I = \int \prod_{a=1}^m \frac{dx^a}{\lambda_{\text{th}}} e^{\frac{d}{2} \sum_{a,b=1}^{m-1} \epsilon_{ab} u^a u^b} \quad (\text{XIII.11})$$

and

$$\langle \dots \rangle_{\epsilon,0} = \frac{\prod_{i=1}^N \prod_{a=1}^m \int \frac{d^d x_i^a}{\lambda_{\text{th}}^d} e^{\frac{D^2}{2} \sum_{a,b=1}^{m-1} \epsilon_{ab} \eta_i^a \cdot \eta_i^b} \dots}{\prod_{i=1}^N \prod_{a=1}^m \int \frac{d^d x_i^a}{\lambda_{\text{th}}^d} e^{\frac{D^2}{2} \sum_{a,b=1}^{m-1} \epsilon_{ab} \eta_i^a \cdot \eta_i^b}} \quad (\text{XIII.12})$$

The subscript $\langle \dots \rangle_{h,0}$ is meant to emphasize that the interaction is absent in this averaging. Note that different replica-molecule $i = 1, 2, \dots$ are mutually independent from each other in this averaging.

We can evaluate the integral I as follows. By noting that $\int \prod_{a=1}^m dx^a = \int dR \prod_{a=1}^m du^a \delta(R - (1/m) \sum_{a=1}^m x^a) = m \int dR \prod_{a=1}^m du^a \delta(\sum_{a=1}^m u^a)$

$$I = \frac{m}{\lambda_{\text{th}}^m} \int dR \int \prod_{a=1}^{m-1} du^a e^{\frac{1}{2} \sum_{a,b=1}^{m-1} d\epsilon_{ab} u^a u^b} = \frac{m}{\lambda_{\text{th}}^m} V^{1/d} \sqrt{\frac{(2\pi)^{m-1}}{\det(-d\hat{\epsilon})^{m,m}}} \quad (\text{XIII.13})$$

Here V is the volume of the system ($\int dR)^d = V$. Thus we find

$$-\beta G_{m,0} = -N \ln(\rho \lambda_{\text{th}}^d) + N + \sum_{i=1}^N d \ln \left(\frac{m}{\lambda_{\text{th}}^{m-1}} \sqrt{\frac{(2\pi)^{m-1}}{\det(-d\hat{\epsilon}_i)^{m,m}}} \right) \quad (\text{XIII.14})$$

where $\rho = N/V$. We used the Stirling's formula $\ln N! \sim N \ln N - N$.

In the 4th equation we introduced

$$-\beta G_m[\hat{\epsilon}^{m,m}] = -\beta G_{m,0}[\hat{\epsilon}^{m,m}] + \ln \langle e^{-\beta \sum_a \sum_{i < j} v(r_{ij}^a)} \rangle_{\epsilon,0} \quad (\text{XIII.15})$$

The integration over $\hat{\epsilon}_i$ can be done by the saddle point method assuming $d \gg 1$.

In the 5th equation we performed the integration over \hat{q} again by the saddle point method and defined the Legendre transform (similarly to Eq. (VI.29)),

$$-\beta F_m[\hat{q}^{m,m}] = -\beta G_m[\hat{\epsilon}^{m,m}] - \frac{d}{2} \sum_{i=1}^N \sum_{a,b=1}^{m-1} (\epsilon_i^*)_{ab} (q_i)_{ab} \quad (\text{XIII.16})$$

where $\hat{\epsilon}_i^{*,m,m}$ is determined by, for $a, b = 1, 2, \dots, m-1$,

$$(q_i)_{ab} = \frac{1}{d} \frac{\partial(-\beta G_m)}{\partial(\epsilon_i)_{ab}} \Big|_{\hat{\epsilon}_i^{m,m} = \hat{\epsilon}_i^{*,m,m}[\hat{q}_i^{m,m}]} = \langle \mathbf{u}_i^a \cdot \mathbf{u}_i^b \rangle_{\epsilon} = \frac{D^2}{d} \sum_{\mu=1}^d \langle (\eta_i^{\mu})^a (\eta_i^{\mu})^b \rangle_{\epsilon} \quad (\text{XIII.17})$$

Let us emphasize that here $\langle \dots \rangle_{\epsilon}$ is the averaging *in the presence of the interactions* so that it is different from $\langle \dots \rangle_{\epsilon,0}$ defined in Eq. (XIII.12).

Now we derive the free-energy functional for the $d\infty$ replicated liquid system using again the Plefka expansion Eq. (VI.46) we used in sec. VIB2 to derive the free-energy functional for the replicated spin system. Fortunately, much as the spin system with dense coupling, the Plefka expansion stops at 1st order.

At the 0 th order of the Plefka expansion we find,

$$(q_i)_{ab} = \frac{1}{d} \frac{\partial(-\beta G_{m,0})}{\partial(\epsilon_i)_{ab}} \Big|_{\hat{\epsilon}_i^{m,m} = \hat{\epsilon}_i^{*,m,m}[\hat{q}_i^{m,m}]} = \frac{1}{d} \frac{\partial}{\partial(\epsilon_i)_{ab}} \left(-\frac{d}{2} \right) \ln \det(-d(\hat{\epsilon}_i^*)^{m,m}) = -((\hat{\epsilon}_i^*)^{m,m})_{ab}^{-1} \quad (\text{XIII.18})$$

where we used Eq. (A.1). Here ϵ is at the 0-th order, i.e. $\epsilon = \epsilon_0$ (see Eq. (VI.46)). Thus the entropic part of the free-energy is obtained as

$$\begin{aligned} -\beta F_{m,0}[\hat{q}^{m,m}] &= N \left(1 - \ln(\rho \lambda_{\text{th}}^d) \right) + d \sum_{i=1}^N \ln \left(\frac{m}{\lambda_{\text{th}}^{m-1}} \sqrt{\frac{(2\pi)^{m-1}}{\det(-d\hat{\epsilon}_i^*)^{m,m}}} \right) - \frac{d}{2} \sum_{i=1}^N \sum_{a,b=1}^{m-1} (\epsilon_i^*)_{ab} (q_i)_{ab} \\ &= N \left(1 - \ln(\rho \lambda_{\text{th}}^d) + d \ln m + \frac{(m-1)d}{2} \ln \left(\frac{2\pi e}{d} \right) \right) + \sum_{i=1}^N \frac{d}{2} \ln \left[\frac{\det \hat{q}_i^{m,m}}{\lambda_{\text{th}}^{2(m-1)}} \right] \end{aligned} \quad (\text{XIII.19})$$

This is the free-energy of an ideal gas of molecules made of replicas.

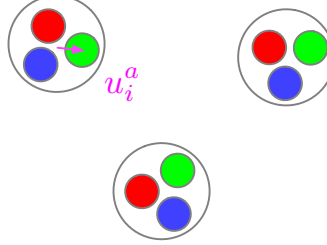


FIG. 43. Gas of molecules made of replicas

Now we extract the interaction part of the free-energy limiting ourselves to $d \rightarrow \infty$ limit. First let us introduce the Mayer function of the replicated system as,

$$e^{-\beta \sum_a \sum_{i < j} v(r_{ij}^a)} = \prod_{i < j} (1 + f_{ij}) \quad f_{ij} = \prod_a e^{-\beta v(r_{ij}^a)} - 1 \quad (\text{XIII.20})$$

Using this we find,

$$\begin{aligned} \ln \langle e^{-\beta \sum_a \sum_{i < j} v(r_{ij}^a)} \rangle_{\epsilon,0} &= \ln \langle (1 + f_{ij}) \rangle_{\epsilon,0} = \sum_{i < j} \langle f_{ij} \rangle_{\epsilon,0} + \dots \\ &= \frac{N(N-1)}{2} \langle f_{12} \rangle_{\epsilon,0} + \dots \end{aligned} \quad (\text{XIII.21})$$

[After legendre transform] As noted in sec. III G the Mayer expansion stops at the 1st correction (see Eq. (III.62)) in $d \rightarrow \infty$ limit.

Let us note that the Mayer function depends on the displacement vector between the centers of the mass of the two 'molecules' $\mathbf{R}_{ij} = \mathbf{R}_i - \mathbf{R}_j$ and the fluctuations $\mathbf{u}_i^a, \mathbf{u}_j^a$ of the replicas within the molecules as,

$$f_{ij} = f(\{|r_i^a - r_j^a|^2\}) = f(\{R_{ij}^2 + 2R_{ij}\hat{R}_{ij} \cdot (\mathbf{u}_i^a - \mathbf{u}_j^a) + (\mathbf{u}_i^a - \mathbf{u}_j^a)^2\}) \quad (\text{XIII.22})$$

where $R_{ij} = |\mathbf{R}_{ij}|$ and $\hat{R}_{ij} = \mathbf{R}_{ij}/R_{ij}$. Then

$$\langle f_{ij} \rangle_{\epsilon,0} = \frac{\Omega_d d}{V} \int_0^\infty dR_{ij} R_{ij}^{d-1} \langle \langle f(\{R_{ij}^2 + 2R_{ij}\hat{R}_{ij} \cdot (\mathbf{u}_i^a - \mathbf{u}_j^a) + (\mathbf{u}_i^a - \mathbf{u}_j^a)^2\}) \rangle_{\Omega_{ij}} \rangle_{\epsilon_i, \epsilon_j, 0} \quad (\text{XIII.23})$$

Here we introduced

$$\langle \dots \rangle_{\Omega_{ij}} = \frac{\int d\Omega_{ij} \dots}{d\Omega_d} \quad (\text{XIII.24})$$

where Ω_d is the volume of d-dimensional unit sphere. Here $\int d\Omega_{ij} \dots$ is the integration over the solid angle of \hat{R}_{ij} (total solid angle is $d\Omega_d$). By introducing $\hat{R} = \mathbf{y}/\sqrt{d}$ we find a cumulant expansion,

$$\begin{aligned} \ln \langle e^{\sum_{\mu=1}^d h_\mu \hat{R}_\mu} \rangle_\Omega &= \ln \langle e^{\frac{1}{\sqrt{d}} \sum_{\mu=1}^d h_\mu y_\mu} \rangle_\Omega \\ &= \frac{1}{\sqrt{d}} \sum_{\mu=1}^d h_\mu \langle y_\mu \rangle_\Omega + \frac{1}{2d} \sum_{\mu, \nu} h_\mu h_\nu \langle y_\mu y_\nu \rangle_\Omega^c + \dots \xrightarrow{d \rightarrow \infty} \frac{1}{2d} \sum_{\mu=1}^d h_\mu^2 \end{aligned} \quad (\text{XIII.25})$$

which implies the probability distribution of the components of the vector \hat{R} is a Gaussian in $d \rightarrow \infty$ limit ¹⁹,

$$P(\hat{R}) = \prod_{\mu=1}^d \frac{e^{-\frac{d\hat{R}_\mu^2}{2}}}{\sqrt{2\pi/d}} \quad (\text{XIII.26})$$

¹⁹ Here we used that $\langle y_\mu \rangle_\Omega = 0$, $\langle y_\mu y_\nu \rangle_\Omega = \delta_{\mu\nu}$, which are obvious by the rotational symmetry and the normalization condition. We also used that different components are independent from each other. This can be seen by writing

$$\langle \dots \rangle_\Omega = \Omega^{-1} \int \prod_{\mu=1}^d dx_\mu \delta(\sum_{\mu=1}^d x_\mu^2 - 1) \propto \int \prod_{\mu=1}^d dy_\mu \delta(\sum_{\mu=1}^d y_\mu^2 - d) = \int \frac{d\kappa}{2\pi} e^{-i\kappa d} \prod_{\mu=1}^d \int dy_\mu e^{i\kappa y_\mu^2} \dots$$

In $d \rightarrow \infty$ limit the integration over κ can be done (formally) by the saddle point method so that different y_μ 's can actually be regarded as independent random variables.

Collecting the above results we find,

$$\begin{aligned}
& \langle\langle f(\{R_{ij}^2 + 2R_{ij}\hat{R}_{ij} \cdot (\mathbf{u}_i^a - \mathbf{u}_j^a) + (\mathbf{u}_i^a - \mathbf{u}_j^a)^2\}) \rangle\rangle_{\Omega_{ij}} \rangle_{\epsilon_i, \epsilon_j, 0} \\
&= \int \prod_{a=1}^m \frac{d\lambda^a}{2\pi} \langle e^{i \sum_{a=1}^m \lambda_a ((\mathbf{u}_i^a - \mathbf{u}_j^a)^2)} \langle e^{i \sum_{a=1}^m \lambda_a (2R_{ij}\hat{R}_{ij} \cdot (\mathbf{u}_i^a - \mathbf{u}_j^a))} \rangle_{\Omega_{ij}} \rangle_{\epsilon_i, \epsilon_j, 0} \tilde{f}(\{\lambda_a\}) \\
&= \int \prod_{a=1}^m \frac{d\lambda^a}{2\pi} \langle e^{i \sum_{a=1}^m \lambda_a ((\mathbf{u}_i^a - \mathbf{u}_j^a)^2)} e^{-\frac{1}{2d} \sum_{a,b=1}^m (2R_{ij})^2 \lambda_a \lambda_b (\mathbf{u}_i^a - \mathbf{u}_j^a) \cdot (\mathbf{u}_i^b - \mathbf{u}_j^b)} \rangle_{\epsilon_i, \epsilon_j, 0} \tilde{f}(\{\lambda_a\}) \\
&= \int \prod_{a=1}^m \frac{d\lambda^a}{2\pi} e^{i \sum_{a=1}^m \lambda_a ((q_i)_{aa} + (q_j)_{aa})} e^{-\frac{1}{2d} \sum_{a,b=1}^m (2R_{ij})^2 \lambda_a \lambda_b ((q_i)_{ab} + (q_j)_{ab})} \tilde{f}(\{\lambda_a\}) \\
&= e^{\sum_{a=1}^m ((q_i)_{aa} + (q_j)_{aa}) \frac{\partial}{\partial y_a}} e^{\frac{1}{2d} \sum_{a,b=1}^m (2R_{ij})^2 ((q_i)_{ab} + (q_j)_{ab}) \frac{\partial^2}{\partial y_a \partial y_b}} f(\{R_{ij}^2 + y_a\}) \Big|_{y_a=0} \tag{XIII.27}
\end{aligned}$$

In the 2nd equation we introduced a Fourier transform,

$$f(\{R^2 + \mathbf{y}^a\}) = \int \prod_{a=1}^m \frac{d\lambda^a}{2\pi} e^{i \sum_{a=1}^m \lambda_a y^a} \tilde{f}(\{\lambda_a\}) \tag{XIII.28}$$

To derive the 3rd equation we noted that we have defined the *local glass order parameter* as Eq. (XIII.8) which is enforced via Eq. (XIII.9).

In the following we assume homogeneous solution : $(q_i)_{ab} = q_{ab}$ for $i = 1, 2, \dots, N$.

To evaluate the integral Eq. (XIII.23) in $d \rightarrow \infty$ limit, we introduce a scaled variable ξ ,

$$R = D \left(1 + \frac{\xi}{d} \right) \tag{XIII.29}$$

and α_{ab} via

$$q_{ab} = \frac{D^2}{d} \alpha_{ab} \tag{XIII.30}$$

Then we find in $d \rightarrow \infty$ limit²⁰

$$\begin{aligned}
& \ln \langle e^{-\beta \sum_a \sum_{i < j} v(r_{ij}^a)} \rangle_{\epsilon, 0} \\
&= \frac{N}{2} \rho \Omega_d d \int_0^\infty dR R^{d-1} e^{\sum_{a=1}^m 2q_{aa} \frac{\partial}{\partial y_a}} e^{\frac{1}{2d} \sum_{a,b=1}^m (2R)^2 2q_{ab} \frac{\partial^2}{\partial y_a \partial y_b}} f(\{R^2 + y_a\}) \Big|_{y_a=0} \\
&= \frac{N}{2} \rho \Omega_d D^d \int_{-\infty}^\infty d\xi e^\xi e^{\alpha_d (\sum_a \frac{\partial}{\partial \xi_a} + 1) \sum_b \frac{\partial}{\partial \xi_b}} e^{-\frac{1}{2} \sum_{a,b} \Delta_{ab} \frac{\partial^2}{\partial \xi_a \partial \xi_b}} f \left(\left\{ D^2 \left(1 + \frac{\xi_a}{d} \right)^2 \right\} \right) \Big|_{\{\xi_a=\xi\}} \\
&= \frac{N}{2} \rho \Omega_d D^d \int_{-\infty}^\infty d\xi e^\xi e^{-\frac{1}{2} \sum_{ab} \Delta_{ab} \frac{\partial^2}{\partial \xi_a \partial \xi_b}} f \left(\left\{ D^2 \left(1 + \frac{\xi_a}{d} \right)^2 \right\} \right) \Big|_{\{\xi_a=\xi\}} \tag{XIII.31}
\end{aligned}$$

where we assumed the diagonal elements are uniform $\alpha_{aa} = \alpha_d$ and introduced

$$\Delta_{ab} = \alpha_{aa} + \alpha_{bb} - 2\alpha_{ab}. \tag{XIII.32}$$

To derive the last equation we used integrations by parts.

²⁰ Note that $\lim_{d \rightarrow \infty} (R/D)^d = e^\xi$ and that $d(R^2) = 2RdR = 2(D^2/d)(1 + \xi/d)d\xi \xrightarrow{d \rightarrow \infty} 2(D^2/d)d\xi$

After the Legendre-transform $G_m[\hat{\epsilon}] \rightarrow F_m[\hat{q}]$ (see Eq. (XIII.16)), only 1PI diagrams (closed loops) in the Mayer expansion contribute. Thus the next order is due to a triangle diagram. But it's contribution becomes exponentially small in d (see sec 2.3 of [12]) like in sparse graphs. Thus contributions due to higher order terms in the Mayer expansion become negligible in $d \rightarrow \infty$ limit.

To summarize we obtained the free-energy of the assembly of spheres in $d \rightarrow \infty$ limit as,

$$\begin{aligned} -\frac{\beta F_m[\hat{\alpha}^{mm}]}{N} = & 1 - \ln(\rho \lambda_{\text{th}}^d) + d \ln m + \frac{(m-1)d}{2} \ln \left(\frac{2\pi e(D/\lambda_{\text{th}})^2}{d^2} \right) + \frac{d}{2} \ln \det \hat{\alpha}^{m,m} \\ & + \underbrace{\frac{d}{2} \hat{\varphi} \int_{-\infty}^{\infty} d\xi e^{\xi} \left(e^{-\frac{1}{2} \sum_{ab} \Delta_{ab} \frac{\partial^2}{\partial \xi_a \partial \xi_b}} \prod_{a=1}^m e^{-\beta v(D^2(1+\frac{\xi_a}{d})^2)} - 1 \right)}_{-\mathcal{F}_{\text{int}}} \Big|_{\{\xi_a=\xi\}} \end{aligned} \quad (\text{XIII.33})$$

where we introduced the volume fraction φ and a scaled volume fraction $\hat{\varphi}$,

$$\hat{\varphi} = 2^d \varphi / d \quad \varphi = \rho \Omega_d (D/2)^d \quad (\text{XIII.34})$$

Note that the total free-energy of the n -replicas is given simply by

$$F_n = (n/m) F_m \quad (\text{XIII.35})$$

so that the thermodynamic free-energy is obtained as,

$$\frac{-\beta F}{N} = \frac{\partial_n (-\beta F_n)|_{n=0}}{N} = \frac{(-\beta F_m)}{mN} \quad (\text{XIII.36})$$

Note that in the case $m = 1$ we find the free-energy of the liquid,

$$-\frac{\beta F_{\text{liq}}}{N} = 1 - \ln(\rho \lambda_{\text{th}}^d) + \frac{d}{2} \hat{\varphi} \int_{-\infty}^{\infty} d\xi e^{\xi} \left[\left(e^{-\beta v(D(1+\frac{\xi}{d}))^2} \right) - 1 \right] \quad (\text{XIII.37})$$

C. Variational equation and Hessian matrix

Let us rewrite the free-energy expression as

$$-\frac{\beta F_m[\hat{\Delta}]}{N} = c_{\text{nt}} + \frac{d}{2} \mathcal{S}[\hat{\Delta}] \quad (\text{XIII.38})$$

where

$$\mathcal{S}[\hat{\Delta}] = \ln \det \hat{\alpha}^{mm} + \hat{\varphi}(-\mathcal{F}_{\text{int}}) \quad (\text{XIII.39})$$

with

$$-\mathcal{F}_{\text{int}} = \int_{-\infty}^{\infty} d\xi e^{\xi} \left(e^{-\frac{1}{2} \sum_{ab} \Delta_{ab} \frac{\partial^2}{\partial \xi_a \partial \xi_b}} \prod_{a=1}^m e^{-\beta v(D^2(1+\frac{\xi_a}{d})^2)} - 1 \right) \Big|_{\{\xi_a=\xi\}} \quad (\text{XIII.40})$$

We have to solve the variational equations,

$$0 = \frac{\partial}{\partial \Delta_{ab}} \mathcal{S}[\hat{\Delta}]. \quad (\text{XIII.41})$$

The stability of the solution can be examined by studying the Hessian matrix,

$$M_{a \neq b, c \neq d} = -\frac{\partial^2 \mathcal{S}[\hat{\Delta}]}{\partial \Delta_{a<b} \partial \Delta_{c<d}} \quad (\text{XIII.42})$$

D. Radial distribution function $g(r)$ or the effective potential

In $d \rightarrow \infty$ limit Eq. (III.61) becomes

$$-\beta F_1^{\text{ex}}/N = \frac{d}{2} \hat{\varphi} \underbrace{\int_{-\infty}^{\infty} d\xi e^{\xi} (e^{-\beta v(\xi)} - 1)}_{-\mathcal{F}_{\text{int}}^{\text{liq}}} \quad (\text{XIII.43})$$

so that we simply have, from Eq. (III.61) ,

$$g_{\text{liq}}(\xi) = e^{-\xi} \frac{\delta}{\delta(-\beta v(\xi))} (-\mathcal{F}_{\text{int}}^{\text{liq}}) = e^{-\beta v(\xi)} \quad (\text{XIII.44})$$

On the other hand we may obtain radial distribution function $g_{\text{glass}}(r)$ or effective potential $v_{\text{eff}}(\xi)$ within a glass as

$$g_{\text{glass}}(\xi) = e^{-\beta v_{\text{eff}}(\xi)} = e^{-\xi} \frac{\delta}{\delta(-\beta v(\xi))} \frac{(-\mathcal{F}_{\text{int}})}{m} \quad (\text{XIII.45})$$

E. Compression and Decompression

Let us discuss compression (or decompression) of our system. Let us parameterize the changes of the volume as

$$V(\eta) = V_0 e^{-\eta} \quad (\text{XIII.46})$$

Thus we are compressing for $\eta > 0$ and decompressing for $\eta < 0$. A change of the volume amounts to a change of the boundary condition. By writing the original coordinate system as x'_1, x'_2, \dots, x'_d , we can introduce a new coordinate system x_1, x_2, \dots, x_d with $x_\mu = x'_\mu(1 + \eta/d)$ for $\mu = 1, 2, 3, \dots, d$. With the new coordinate system, the boundary condition is brought back to the original one.

In the replicated system we may consider to compress each replica differently using η_a ($a = 1, 2, \dots, m$). The expression for the free-energy of the replicated system Eq. (XIII.2) become,

$$\begin{aligned} & -\beta G_m[\hat{\epsilon}^{mm}, \{\eta_a\}] \\ &= \ln \frac{1}{N!} \int_{\{V(\eta_a)\}} \prod_{i=1}^N \prod_{a=1}^m \frac{d^d(x_i^a)'}{\lambda_{\text{th}}^d} e^{-\beta \sum_a \sum_{i < j} v((r_{ij}^a)') + \frac{1}{2} \sum_{a,b=1}^{m-1} \epsilon_{ab} \sum_{i=1}^N (\mathbf{u}^a)_i' \cdot (\mathbf{u}^a)_i'} \\ &= \ln \frac{1}{N!} \underbrace{\prod_a \left(1 - \frac{\eta_a}{d}\right)^d}_{e^{-\sum_a \eta_a} \text{ in } d \rightarrow \infty} \int_{V(0)} \prod_{i=1}^N \prod_{a=1}^m \frac{d^d(x_i^a)}{\lambda_{\text{th}}^d} e^{-\beta \sum_a \sum_{i < j} v((1 - \eta_a/d)r_{ij}^a) + \frac{1}{2} \sum_{a,b=1}^{m-1} \sum_{i=1}^N \epsilon'_{ab} (\mathbf{u}^a)_i \cdot (\mathbf{u}^a)_i} \end{aligned} \quad (\text{XIII.47})$$

where $\epsilon'_{ab} = (1 - \eta_a/d)(1 - \eta_b/d)\epsilon_{ab}$. This ϵ' play the same role as ϵ in Eq. (VI.48), i.e. by taking a derivative of the free-energy obtained above by ϵ' yields $q_{ab} = \langle u^a u^b \rangle_{\epsilon'}$. Now it is easy to see that the free-energy of the replicated system under compression is

$$\begin{aligned} & -\frac{\beta F_m[\hat{\alpha}^{mm}, \{\eta_a\}]}{N} = 1 - \sum_{a=1}^m \eta_a - \ln(\rho \lambda_{\text{th}}^d) - d \ln m + \frac{(m-1)d}{2} \ln \left(\frac{2\pi e(D/\lambda_{\text{th}})^2}{d^2} \right) + \frac{d}{2} \ln \det \hat{\alpha}^{mm} \\ &+ \underbrace{\frac{d}{2} \hat{\varphi} \int_{-\infty}^{\infty} d\xi e^{\xi} \left(e^{-\frac{1}{2} \sum_{ab} \Delta_{ab} \frac{\partial^2}{\partial \xi_a \partial \xi_b}} \prod_{a=1}^m e^{-\beta v(D^2(1 + \frac{\xi_a}{d} - \frac{\eta_a}{d})^2) - 1} \right)}_{-\mathcal{F}_{\text{int}}(\{\eta_a\})} \Big|_{\{\xi_a = \xi\}} \end{aligned} \quad (\text{XIII.48})$$

We can compute the pressure,

$$P = -\frac{\partial F}{\partial V} \quad (\text{XIII.49})$$

considering uniform compression $\eta_a = \eta$ for $\forall a$. Then using Eq. (XIII.36) and

$$V \frac{\partial}{\partial V} = -\frac{\partial}{\partial \eta} \quad (\text{XIII.50})$$

we find the 'reduced pressure' as,

$$\begin{aligned} p &= \frac{\beta P}{\rho} = V \frac{\partial}{\partial V} \frac{-\beta F}{N} = \left(-\frac{\partial}{\partial \eta} \right) \frac{-\beta F_m(\eta)}{m N} \Big|_{\eta=0} \\ &= 1 + \frac{1}{m} \frac{d}{2} \hat{\varphi} \left(-\frac{\partial}{\partial \eta} \right) (-\mathcal{F}_{\text{int}}(\eta)) \Big|_{\eta=0} \\ &= 1 + \frac{1}{m} \frac{d}{2} \hat{\varphi} \mathcal{F}'_{\text{int}}(0) \end{aligned} \quad (\text{XIII.51})$$

The term 1 is just that of the ideal gas. In the last equation we did an integration by parts. Note that p diverges in $m \rightarrow 0$ limit suggesting jamming.

F. Shear

1. Simple shear

Here let us consider how to put shear on a generic system of spheres (at any dimension). We put simple shear strain γ on the bounding box of the system as shown in Fig. 44. This amount to change the boundary condition of the system. By writing the original coordinate system as x'_1, x'_2, \dots, x'_d , we can introduce a new coordinate system x_1, x_2, \dots, x_d with $x_1 = x'_1 - \gamma x'_2$ and $x_\mu = x'_\mu$ for $\mu = 2, 3, \dots, d$. With the new coordinate system, the boundary condition is brought back to the original rectangular one.

The displacement vector between the particles i and j , which is \mathbf{r}'_{ij} in the original coordinate, can be written as,

$$\mathbf{r}'_{ij} = S(\gamma) \mathbf{r}_{ij} \quad (\text{XIII.52})$$

with

$$S(\gamma)_{\mu\nu} = \delta_{\mu\nu} + \gamma \delta_{\mu,1} \delta_{\nu,2} \quad (\text{XIII.53})$$

Note that $\det S = 1$ which means the shear does not change the volume (and thus the density) of the system.

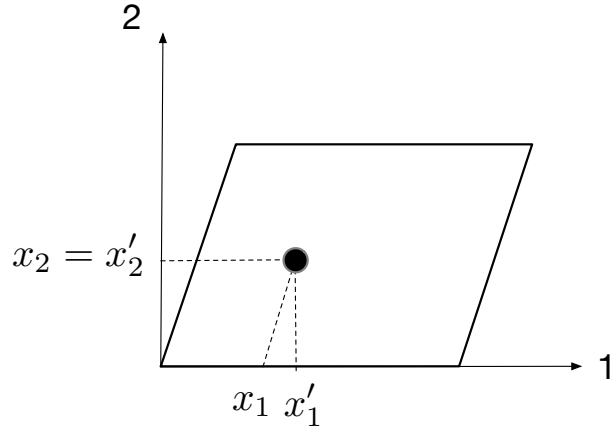


FIG. 44. Shear on the container

2. Metastable states under shear

Let us consider a glassy system with many metastable states $\alpha = 1, 2, \dots$, under shear. The free-energy of a state α under shear $\gamma + \delta\gamma$ may be expanded in power series of $\delta\gamma$ as

$$f_\alpha(\gamma + \delta\gamma) = f_\alpha(\gamma) + \sigma_\alpha(\gamma)\delta\gamma + \frac{1}{2}\mu_\alpha(\gamma)\delta\gamma^2 + \dots \quad (\text{XIII.54})$$

Here σ_α is the shear-stress of the state α and μ_α is the shear-modulus of the state α . (See Fig. 45) We can rephrase the discussion in sec. VIII F by the following replacements,

$$\begin{aligned} o_\alpha &= -\frac{\partial f_\alpha}{\partial h} \rightarrow \sigma_\alpha = \frac{\partial f_\alpha}{\partial \gamma} \\ \chi_\alpha &= \frac{\partial o_\alpha}{\partial h} = -\frac{\partial^2 f_\alpha}{\partial h^2} \rightarrow \mu_\alpha = \frac{\partial \sigma_\alpha}{\partial \gamma} = \frac{\partial^2 f_\alpha}{\partial \gamma^2} \end{aligned} \quad (\text{XIII.55})$$

Essentially the shear strain γ plays the role of the field h . Then the discussion sec. VIII F motivates us to consider replicated liquid under shear [42, 43].

This motivates us to consider replicas subjected to different shear strains γ_a . For instance we can rewrite Eq. (VIII.55) as,

$$\begin{aligned} \mu_{ab} &= \frac{\partial^2 f_{1RSB}(T, \{\gamma_a\})}{\partial \gamma_a \partial \gamma_b} = \frac{1}{\beta m N} \frac{\partial^2}{\partial \gamma_a \partial \gamma_b} \ln \sum_\alpha e^{-N\beta \sum_{a=1}^m f_\alpha(\gamma_a)} \Big|_{\{\gamma_a = \gamma\}} \\ &= \tilde{\mu}_1 \delta_{ab} + \tilde{\mu}_0 \end{aligned} \quad (\text{XIII.56})$$

where $\tilde{\mu}_1$ can be interpreted as the shear-modulus of metastable states,

$$\tilde{\mu}_1 = \sum_\alpha w_\alpha \mu_\alpha \quad \mu_\alpha = \frac{\partial^2 f_\alpha}{\partial \gamma^2} \quad w_\alpha = \frac{e^{-N\beta f_\alpha}}{\sum_\alpha e^{-N\beta f_\alpha}} \quad (\text{XIII.57})$$

while $\tilde{\mu}_0$ can be interpreted as due to inter-state fluctuation,

$$\tilde{\mu}_0 = -N\beta \left(\langle \sigma^2 \rangle_0 - \langle \sigma \rangle_0^2 \right) = -N\beta \left(\sum_\alpha w_\alpha \sigma_\alpha^2 - (\sum_\alpha w_\alpha \sigma_\alpha)^2 \right). \quad (\text{XIII.58})$$

The latter is a non-affine correction of the shear-modulus which corresponds to stress-relaxation due to α relaxation [42, 43].

Actually thermodynamics requires that the total shear-modulus vanishes,

$$\mu_{\text{total}} = \sum_b \mu_{ab} = \sum_a \mu_{ab} = m \tilde{\mu}_0 + \tilde{\mu}_1 = 0 \quad (\text{XIII.59})$$

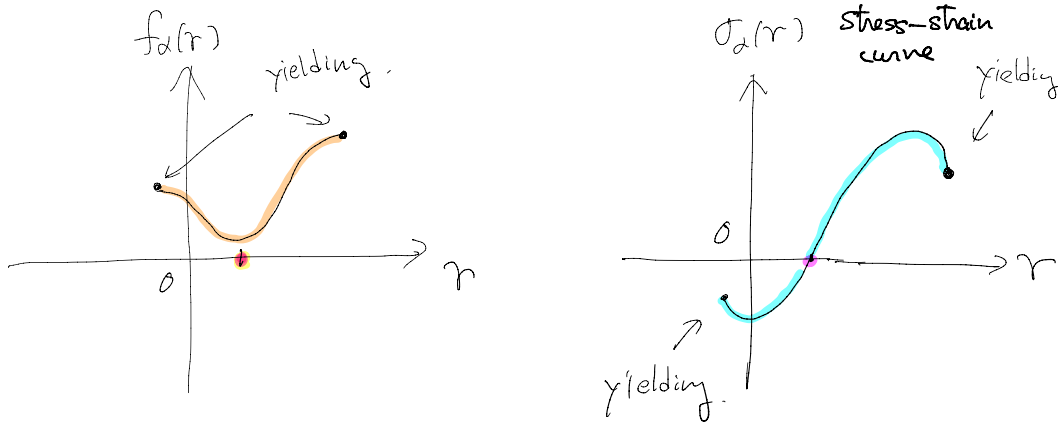


FIG. 45. Shear on a metastable state

This is because the free-energy (per unit volume) should not depend on the shape of the container, which is just a specific choice of the boundary condition, in the thermodynamic limit. Then we must have

$$\tilde{\mu}_0 = -m\tilde{\mu}_1 \quad (\text{XIII.60})$$

so that we anticipate the shear-modulus matrix in the following form within 1RSB,

$$\tilde{\mu}_{ab} = \hat{\mu} \left(\delta_{ab} - \frac{1}{m} \right) \quad \hat{\mu} = \tilde{\mu}_1 \quad (\text{XIII.61})$$

This encodes the positive shear-modulus of metastable states which is exactly canceled out by the non-affine correction due to the α relaxation.²¹

3. Replicas under shear

Following sec. VIII F and sec. X A let us consider replicas subjected to different shear strains γ_a . The displacement between the centers of mass of the molecules i and j made of replicas $a = 1, 2, \dots, n$ can be written in the new coordinate system as $\mathbf{R} = \mathbf{R}_\perp + (R_1 + \gamma_a R_2)\hat{e}_1 + R_2 \hat{e}_2$ where we dropped the subscript ij for simplicity and introduced \hat{e}_1 and \hat{e}_2 which are unit vectors into the directions 1 and 2, and the vector \vec{R}_\perp which represents the components perpendicular to 1 and 2. The displacement vector between particles i and j of the replica, say a , can be written as, with $\mathbf{v}^a = \mathbf{u}_i^a - \mathbf{u}_j^a$,

$$\begin{aligned} |r_{ij}^a|^2 &= |\mathbf{v}^a + \mathbf{R}_\perp + (R_1 + \gamma_a R_2)\hat{e}_1 + R_2 \hat{e}_2|^2 \\ &= R^2 \left[1 + 2\hat{R}_1 \hat{R}_2 \gamma_a + (\hat{R}_2)^2 \gamma_a^2 \right] + 2R\hat{R} \cdot \mathbf{v}^a + (\mathbf{v}^a)^2 + 2R(\hat{R}_2 \gamma_a)v_1^a \end{aligned} \quad (\text{XIII.64})$$

Using the above results we find,

$$\begin{aligned} &\langle\langle f(\{R^2 [1 + 2\hat{R}_1 \hat{R}_2 \gamma_a + (\hat{R}_2)^2 \gamma_a^2] + 2R\hat{R} \cdot \mathbf{v}^a + (\mathbf{v}^a)^2 + 2R(\hat{R}_2 \gamma_a)v_1^a\})\rangle_\Omega\rangle_{\epsilon_i, \epsilon_j} \\ &= \int \prod_{a=1}^m \frac{d\lambda^a}{2\pi} \langle e^{i \sum_{a=1}^m \lambda_a ((\mathbf{v}^a)^2)} \langle e^{i \sum_{a=1}^m \lambda_a (R^2 [2\hat{R}_1 \hat{R}_2 \gamma_a + (\hat{R}_2)^2 \gamma_a^2] + 2R\hat{R} \cdot \mathbf{v}^a) + 2R(\hat{R}_2 \gamma_a)v_1^a)} \rangle_\Omega \rangle_{\epsilon_i, \epsilon_j} \tilde{f}(\{\lambda_a\}) \\ &= \int \prod_{a=1}^m \frac{d\lambda^a}{2\pi} \int \frac{d\hat{R}_1}{\sqrt{2\pi/d}} e^{-\frac{d\hat{R}_1^2}{2}} \int \frac{d\hat{R}_2}{\sqrt{2\pi/d}} e^{-\frac{d\hat{R}_2^2}{2}} e^{i \sum_{a=1}^m \lambda_a R^2 [2\hat{R}_1 \hat{R}_2 \gamma_a + (\hat{R}_2)^2 \gamma_a^2]} \\ &\quad e^{i \sum_{a=1}^m \lambda_a 2q_{aa} e^{-\frac{1}{2d} \sum_{a,b=1}^m (2R)^2 \lambda_a \lambda_b 2q_{ab}}} \tilde{f}(\{\lambda_a\}) \\ &= \int \frac{dz_1}{\sqrt{2\pi}} e^{-\frac{z_1^2}{2}} \int \frac{dz_2}{\sqrt{2\pi}} e^{-\frac{z_2^2}{2}} e^{\sum_{a=1}^m \frac{R^2}{d} (2z_1 z_2 \gamma_a + z_2^2 \gamma_a^2) \frac{\partial}{\partial y_a}} \\ &\quad e^{\sum_{a=1}^m 2q_{aa} \frac{\partial}{\partial y_a} e^{\frac{1}{2d} \sum_{a,b=1}^m (2R)^2 2q_{ab} \frac{\partial^2}{\partial y_a \partial y_b}}} f(\{R^2 + y_a\}) \Big|_{y_a=0} \end{aligned} \quad (\text{XIII.65})$$

²¹ The shear-modulus of metastable states $\tilde{\mu}_1$ include non-affine correction do to stress fluctuation by the β -relaxation: $\mu_\alpha = \mu_\alpha^{\text{BORN}} - \beta N[\langle\sigma^2\rangle_\alpha - \langle\sigma\rangle_\alpha^2]$. Here $\langle\dots\rangle_\alpha$ in the 2nd term represents thermal average within the metastable state α . On the other hand μ_α^{BORN} is the so called Born term which represents the affine response.

Microscopic expression of the shear-stress is

$$\sigma = \frac{1}{N} \frac{\partial}{\partial \gamma} \sum_{i < j} v(S(\gamma) \mathbf{r}_{ij}) \quad (\text{XIII.62})$$

while that of the Born term is

$$\mu^{\text{BORN}} = \frac{1}{N} \frac{\partial^2}{\partial \gamma^2} \sum_{i < j} v(S(\gamma) \mathbf{r}_{ij}) \quad (\text{XIII.63})$$

which then implies that the interaction part of the free-energy becomes,

$$\begin{aligned}
-\frac{d}{2}\hat{\varphi}\mathcal{F}_{\text{int}} &= \ln\langle e^{-\beta\sum_a\sum_{i<j}v(r_{ij}^a)}\rangle_\epsilon \\
&= \frac{N}{2}\rho\Omega_d\int_0^\infty dRR^{d-1}\int\frac{dz_1}{\sqrt{2\pi}}e^{-\frac{z_1^2}{2}}\int\frac{dz_2}{\sqrt{2\pi}}e^{-\frac{z_2^2}{2}} \\
&\quad e^{\sum_{a=1}^m\frac{R^2}{d}(2z_1z_2\gamma_a+z_2^2\gamma_a^2)\frac{\partial}{\partial y_a}} \\
&\quad e^{\sum_{a=1}^m2q_{aa}\frac{\partial}{\partial y_a}}e^{\frac{1}{2d}\sum_{a,b=1}^m(2R_{ij})^22q_{ab}\frac{\partial^2}{\partial y_a\partial y_b}}f(\{R_{ij}^2+y_a\})\Big|_{y_a=0} \\
&= \frac{d}{2}\hat{\varphi}\int_{-\infty}^\infty d\xi\int\frac{dz_1}{\sqrt{2\pi}}e^{-\frac{z_1^2}{2}}\int\frac{dz_2}{\sqrt{2\pi}}e^{-\frac{z_2^2}{2}}e^{\sum_a(2z_1z_2\gamma_a+z_2^2\gamma_a^2)\frac{\partial}{\partial\xi_a}} \\
&\quad e^{\alpha_d(\sum_a\frac{\partial}{\partial\xi_a}+1)\sum_b\frac{\partial}{\partial\xi_b}}e^{-\frac{1}{2}\sum_{ab}\Delta_{ab}\frac{\partial^2}{\partial\xi_a\partial\xi_b}}f\left(\left\{D^2\left(1+\frac{\xi_a}{d}\right)\right\}\right)\Big|_{\{\xi_a=\xi\}} \\
&= \frac{d}{2}\hat{\varphi}\int_{-\infty}^\infty d\xi\int\frac{dz_1}{\sqrt{2\pi}}\int\frac{dz_2}{\sqrt{2\pi}} \\
&\quad e^{-\frac{1}{2}(z_1-z_2\sum_a\gamma_a\frac{\partial}{\partial\xi_a})^2-\frac{1}{2}z_2^2+z_2^2\left[-\frac{1}{4}\sum_{a,b}\frac{\partial^2}{\partial\xi_a\partial\xi_b}(\gamma_a-\gamma_b)^2+\frac{1}{2}\sum_a\partial\xi_a\gamma_a^2(\sum_b\frac{\partial}{\partial\xi_b}+1)\right]} \\
&\quad e^{\alpha_d(\sum_a\frac{\partial}{\partial\xi_a}+1)\sum_b\frac{\partial}{\partial\xi_b}}e^{-\frac{1}{2}\sum_{ab}\Delta_{ab}\frac{\partial^2}{\partial\xi_a\partial\xi_b}}f\left(\left\{D^2\left(1+\frac{\xi_a}{d}\right)\right\}\right)\Big|_{\{\xi_a=\xi\}} \\
&= \frac{d}{2}\hat{\varphi}\int_{-\infty}^\infty d\xi\int\mathcal{D}\lambda e^{-\frac{1}{2}\sum_{ab}(\Delta_{ab}+\frac{\lambda^2}{2}(\gamma_a-\gamma_b)^2)\frac{\partial^2}{\partial\xi_a\partial\xi_b}}f\left(\left\{D^2\left(1+\frac{\xi_a}{d}\right)\right\}\right)\Big|_{\{\xi_a=\xi\}} \tag{XIII.66}
\end{aligned}$$

To derive the last equation we used integrations by parts.

Obviously the entropic part of the free-energy does not change under shear. It is also instructive to observe in Eq. (XIII.66) that putting uniform shear $\gamma_a = \gamma$ for $\forall a$ do not change the free-energy of the system. This is consistent with the thermodynamics which says, as we noted before, that the free-energy (per unit volume) should *not* depend on the shape of the container, which is just a specific choice of the boundary condition, in the thermodynamic limit. Expanding the replicated free-energy in power series of the shear strains γ_a we would obtain,

$$F_m[\{\gamma + \gamma_a\}]/N = F_m[\{\gamma\}]/N + \sigma(\gamma)\sum_{a=1}^n\gamma_a + \frac{1}{2}\sum_{a,b=1}^n\mu_{ab}(\gamma)\gamma_a\gamma_b + \tag{XIII.67}$$

We know that $F_m[\{\gamma\}]/N$ actually do not depend on the uniform strain γ as discussed above, which also implies $\sigma(\gamma) = 0$ and $\sum_a\mu_{ab} = \sum_b\mu_{ab} = 0$. However we may find something interesting in the shear-modulus matrix μ_{ab} as discussed before [42, 43]. Indeed we find, expanding around $\gamma = 0$,

$$\begin{aligned}
-\frac{\beta F_m[\hat{\alpha}^{mm}][\{\gamma_a\}]}{N} &= -\frac{\beta F_m[\hat{\alpha}^{mm}][\{0\}]}{N} \\
&+ \frac{d}{2}\hat{\varphi}\underbrace{\sum_{ab}\frac{1}{2}(\gamma_a-\gamma_b)^2\frac{\partial}{\partial\Delta_{ab}}\int_{-\infty}^\infty d\xi e^\xi}_{\sum_{ab}(\delta_{ab}-1)\gamma_a\gamma_b}\underbrace{\left(e^{-\frac{1}{2}\sum_{ab}\Delta_{ab}\frac{\partial^2}{\partial\xi_a\partial\xi_b}}\prod_{a=1}^m e^{-\beta v(D^2(1+\frac{\xi_a}{d}))}-1\right)}_{-\mathcal{F}_{\text{int}}}\Big|_{\{\xi_a=\xi\}} \\
&+ \dots \tag{XIII.68}
\end{aligned}$$

Thus we find

$$\beta\mu_{ab} = d\hat{\varphi}\left[\delta_{ab}\sum_{c(\neq a)}\frac{\partial\mathcal{F}_{\text{int}}}{\partial\Delta_{ac}}-(1-\delta_{ab})\frac{\partial\mathcal{F}_{\text{int}}}{\partial\Delta_{ab}}\right] \tag{XIII.69}$$

We can check that $\sum_a\mu_{ab} = \sum_b\mu_{ab} = 0$ as it should be.

G. Parisi's ansatz

In the following section we adopt a slightly different notation: $m_0 = m < m_1 < m_2 \cdots m_k = 1$ for k -RSB. (So far we assumed $m_0 = n < m_1 < m_2 \cdots m_{k+1} = 1$.) The Δ_{ab} matrix is parameterized as,

$$\begin{aligned}\Delta_{ab} &= \sum_{i=1}^k (I_{ab}^{m_{i-1}} - I_{ab}^{m_i}) \Delta_i = \Delta_1 - \sum_{l=1}^{k-1} (\Delta_l - \Delta_{l+1}) I_{ab}^{m_i} - \Delta_k \delta_{ab} \\ &= \sum_{l=0}^{k-1} (\Delta_{l+1} - \Delta_l) I_{ab}^{m_l} - \Delta_k \delta_{ab}\end{aligned}\quad (\text{XIII.70})$$

with $\Delta_0 = 0$.

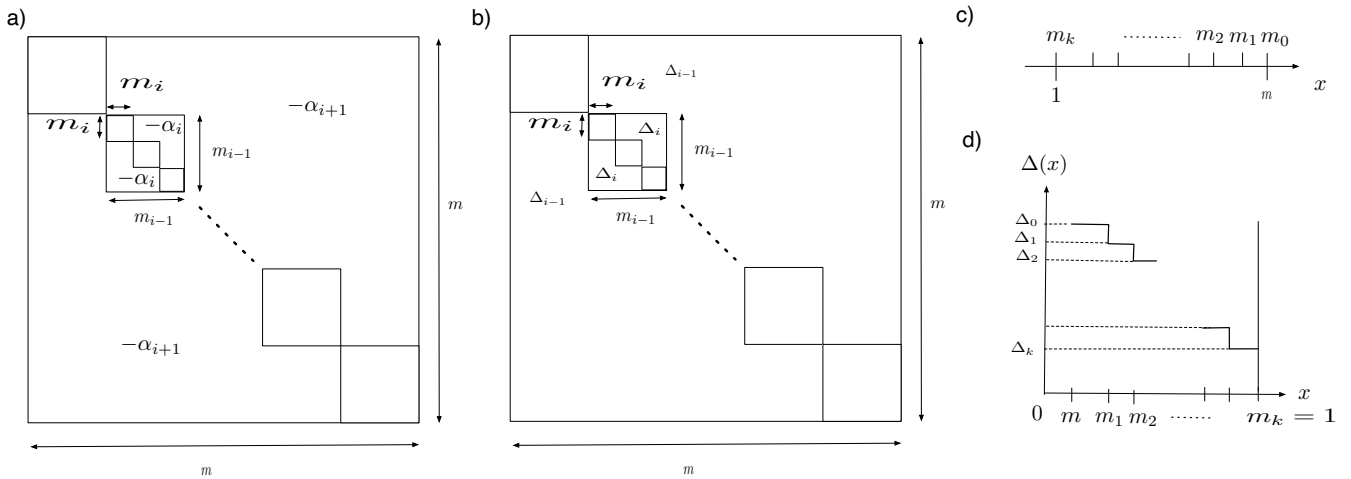


FIG. 46. Parisi's matrix for $\hat{\alpha}$ and $\hat{\Delta}$. The diagonal elements are α_d and 0 respectively. The parameter α_d is determined such that the sum rule $\sum_a \alpha_{ab} = \sum_b \alpha_{ab} = 0$ is satisfied.

H. 1RSB ansatz

1. Free-energy

Let us consider $k = 1$ RSB ansatz with $m_0 = m$, $m_1 = 1$. The simplest ansatz is $\alpha_{ab} = (\alpha_d + \alpha)I - \alpha$. Note that the sum rule Eq. (XIII.5) implies $\alpha_d = (m - 1)\alpha$. Thus we assume

$$\hat{\alpha} = (mI - 1)\alpha \quad \Delta_{ab} = \Delta_1(1 - I) \quad (\text{XIII.71})$$

where

$$\Delta_1 = 2(\alpha_d + \alpha_1) = 2m\alpha_1 \quad (\text{XIII.72})$$

where I is the identity matrix of size $m \times m$. Note that the sum rules in Eq. (XIII.7) are satisfied. Now we evaluate the free-energy Eq. (XIII.33) within this ansatz.

First, for the entropic part of the free-energy, we find using Eq. (B.5),

$$\ln \det \hat{\alpha}^{m,m} = (m - 1) \ln(m\alpha) - \ln m = (m - 1) \ln \left(\frac{\Delta}{2} \right) - \ln m \quad (\text{XIII.73})$$

Then for the interaction part of the free-energy we find,

$$\begin{aligned} -\mathcal{F}_{\text{int}}(\Delta_g) &= \int_{-\infty}^{\infty} d\xi e^{\xi} \left[e^{-\frac{1}{2}\Delta_1 \frac{\partial^2}{\partial \xi^2}} \left(\underbrace{e^{\frac{1}{2}\Delta_1 \frac{\partial^2}{\partial \xi^2}} e^{-\beta v(D(1+\frac{\xi}{d}))}}_{g(m_1, \xi)} \right)^m - 1 \right] \\ &= \int_{-\infty}^{\infty} d\xi e^{\xi} \left[e^{-\frac{1}{2}\Delta_1 \frac{\partial^2}{\partial \xi^2}} g^m(m_1, \xi) - 1 \right] = \int_{-\infty}^{\infty} d\xi e^{\xi - \Delta_1/2} [g^m(m_1, \xi) - 1] \end{aligned} \quad (\text{XIII.74})$$

In the last step we have performed integrations by parts. We have introduced

$$g(m_1, \xi) = e^{\frac{1}{2}\Delta_1 \frac{\partial^2}{\partial \xi^2}} e^{-\beta v(D(1+\frac{\xi}{d}))} = \int \mathcal{D}z e^{-\beta v(D(1+\frac{\xi+\sqrt{\Delta_1}z}{d}))} \quad (\text{XIII.75})$$

Collecting the above results we find

$$-\frac{\beta F_m^{\text{1RSB}}(\Delta_1)}{N} = c_{nt} + \frac{d}{2} \left\{ \left[(m-1) \ln \left(\frac{\Delta}{2} \right) - \ln m \right] - \hat{\varphi} \mathcal{F}_{\text{int}} \right\} \quad (\text{XIII.76})$$

where

$$c_{nt} = 1 - \ln(\rho \lambda_{\text{th}}^d) + d \ln m + \frac{(m-1)d}{2} \ln \left(\frac{2\pi e(D/\lambda)^2}{d^2} \right) \quad (\text{XIII.77})$$

2. Effective potential

The radial distribution function or the effective interaction Eq. (XIII.45) is obtained as

$$\begin{aligned} e^{-\beta v_{\text{eff}}(\xi)} &= \frac{e^{-\xi}}{m} \frac{\delta}{\delta(-\beta v(\xi))} \int_{-\infty}^{\infty} d\eta e^{\eta - \Delta_1/2} \left[(e^{(\Delta_1/2)\partial\eta^2} e^{-\beta v(\eta)})^m - 1 \right] \\ &= \frac{e^{-\xi}}{m} \int_{-\infty}^{\infty} d\eta e^{\eta - \Delta_1/2} m (e^{(\Delta_1/2)\partial\eta^2} e^{-\beta v(\eta)})^{m-1} e^{(\Delta_1/2)\partial\eta^2} \left(e^{-\beta v(\eta)} \delta(\eta - \xi) \right) \\ &= e^{-\beta v(\xi)} \int d\eta \frac{e^{-\frac{(\eta-\xi)^2}{2\Delta_1}}}{\sqrt{2\pi\Delta_1}} e^{\eta - \xi - \Delta_1/2} g^{m-1}(m_1, \xi) \end{aligned} \quad (\text{XIII.78})$$

3. Complexity

In large- d limit the term c_{nt} defined in Eq. (XIII.77) behaves as,

$$c_{nt} = \left(\frac{1}{2} - m \right) d \ln d + \frac{d}{2} m \left(\ln(2\pi D^2) + 1 \right) + O(d^0) \quad (\text{XIII.79})$$

This is due to (see Eq. (XIII.34))

$$\rho = \hat{\varphi} \frac{d}{D^d \Omega_d} \quad \Omega_d = \frac{\pi^{d/2}}{\Gamma(1+d/2)} \quad (\text{XIII.80})$$

with the Gamma function which behaves as,

$$\Gamma(1+z) \sim \sqrt{2\pi z} (z/e)^z \quad z \gg 1. \quad (\text{XIII.81})$$

Thus the free-energy behaves in large- d limit as,

$$-\frac{\beta F_m^{\text{1RSB}}(\Delta_1)}{N} = \left(\frac{1}{2} - m \right) d \ln d + \frac{d}{2} \left\{ \left[(m-1) \ln \left(\frac{\Delta}{2} \right) - \ln m \right] - \hat{\varphi} \mathcal{F}_{\text{int}} \right\} \quad (\text{XIII.82})$$

As discussed in sec. VIII D, this give the function ϕ_m ,

$$\phi_m = -\beta f_{1\text{RSB}} = -\beta F_m^{\text{1RSB}}/(mN) \quad (\text{XIII.83})$$

from which we can obtain the complexity. Using Eq. (VIII.38) we find,

$$\begin{aligned} -\beta f^* &= -d \ln d + \frac{d}{2} \left[\ln(2\pi D^2) + 1 + \frac{1}{m} + \hat{\varphi} \partial_m(-\mathcal{F}_{\text{int}}) \right] + O(d^0) \\ \Sigma^* &= \frac{d}{2} \ln d - \frac{d}{2} \left[1 + \ln \frac{\Delta}{2m} + \hat{\varphi} m^2 \partial_m m^{-1}(-\mathcal{F}_{\text{int}}) \right] + O(d^0) \end{aligned} \quad (\text{XIII.84})$$

4. Variational equation

Now let us examine the saddle point equation for Δ_1 . From the 1st equation of Eq. (XIII.74) we find, after doing some integrations by parts,

$$\frac{\partial}{\partial \Delta_1}(-\mathcal{F}_{\text{int}}) = -\frac{m(m-1)}{2} \int d\xi e^\xi e^{-\frac{\Delta_1}{2} \frac{\partial^2}{\partial \xi^2}} g^m(m_1, \xi) (f'(m_1, \xi))^2 \quad (\text{XIII.85})$$

where we introduced

$$f(m_1, \xi) = -m_1 \ln g(m_1, \xi) \quad (\text{XIII.86})$$

Note that $m_1 = 1$ in the $k = 1$ RSB. Thus saddle point equation for Δ_1 is obtained as,

$$\begin{aligned} 0 &= \frac{2}{d} \frac{\partial}{\partial \Delta_1}(-\beta F_m^{\text{1RSB}}(\Delta_1)/N) = (m-1) \frac{1}{\Delta_1} + \hat{\varphi} \frac{\partial}{\partial \Delta_1}(-\mathcal{F}_{\text{int}}) \\ &= (m-1) \left[\frac{1}{\Delta_1} - m \frac{\hat{\varphi}}{2} \int d\xi e^\xi e^{-\frac{\Delta_1}{2} \frac{\partial^2}{\partial \xi^2}} g^m(m_1, \xi) (f'(m_1, \xi))^2 \right] \end{aligned} \quad (\text{XIII.87})$$

We see that in the limit $m \rightarrow 1$ the free-energy becomes independent of Δ_1 .²² The equation for the non-trivial solution is obtained as,

$$\frac{1}{\Delta_1} = m \frac{\hat{\varphi}}{2} \int d\xi e^{\xi-\Delta_1/2} g^m(m_1, \xi) (f'(m_1, \xi))^2 \quad (\text{XIII.88})$$

5. Pressure

As discussed in sec. XIII E, (reduced) pressure can be computed using the 3rd equation of Eq. (XIII.51). In $d \gg 1$,

$$\begin{aligned} p(2/d) &= \frac{1}{m} \hat{\varphi} \left(-\frac{\partial}{\partial \eta} \right) (-\mathcal{F}_{\text{int}}(\eta)) \Big|_{\eta=0} = \hat{\varphi} \int_{-\infty}^{\infty} d\xi e^{\xi-\Delta/2} g^{m-1}(m_1, \xi) g'(m_1, \xi) \\ &= \hat{\varphi} \int_{-\infty}^{\infty} d\xi e^{\xi-\Delta/2} g^m(m_1, \xi) f'(m_1, \xi) \end{aligned} \quad (\text{XIII.89})$$

Note that $m_1 = 1$ in the $k = 1$ RSB.

6. Shear-modulus

Let us evaluate the shear-modulus matrix Eq. (XIII.69) with the $k = 1$ -RSB. From Eq. (XIII.70) we find,

$$\frac{\partial \mathcal{F}_{\text{int}}}{\partial \Delta_{ab}} = \frac{1}{m(m-1)} \frac{\partial \mathcal{F}_{\text{int}}}{\partial \Delta_1} \quad (\text{XIII.90})$$

²² Thus for $m = 1$ we can choose any Δ_1 to evaluate the free-energy. Using the simplest one $\Delta_1 = 0$ one can immediately see that the free-energy becomes the same as that of the liquid Eq. (XIII.37). We found the same in the p -spin model.

while we know from Eq. (XIII.102) together with Eq. (XIII.87)

$$-\frac{\partial \mathcal{F}_{\text{int}}}{\partial \Delta_{ab}} = -\frac{1}{m} \frac{1}{\hat{\varphi}} \frac{1}{\Delta_1} \quad (\text{XIII.91})$$

Combining the above results we find

$$\beta \frac{\mu_{ab}}{d} = \beta \hat{\mu} \left(\delta_{ab} - \frac{1}{m} \right) \quad (\text{XIII.92})$$

with

$$\hat{\mu} = \frac{1}{\Delta} \quad (\text{XIII.93})$$

Physically we can interpret $\hat{\mu}$ as the shear-modulus of glass[42, 43]. On the other hand the negative correction term can be interpreted as due to inter-state fluctuation, i. e. α -relaxation which leads to 0 total shear-modulus.

I. k -RSB ansatz and $k \rightarrow \infty$ limit

1. Free-energy

Within the k -RSB ansatz, we have [82],

$$\ln \det \hat{\alpha}^{m,m} = -\ln m + \sum_{i=1}^k \left(\frac{m}{m_i} - \frac{m}{m_{i-1}} \right) \ln \frac{G_i}{2} \quad (\text{XIII.94})$$

with

$$G_i = m_i \Delta_i + \sum_{j=i+1}^k (m_j - m_{j-1}) \Delta_j \quad i = 1, 2, \dots, k \quad (\text{XIII.95})$$

which can be converted to find

$$\Delta_i = \frac{G_i}{m_i} + \sum_{j=i+1}^k \left(\frac{1}{m_j} - \frac{1}{m_{j-1}} \right) G_j \quad i = 1, 2, \dots, k \quad (\text{XIII.96})$$

It can be easily checked that the $k = 1$ RSB case Eq. (XIII.73) can be recovered as it should.

Within the k -RSB ansatz, the interaction part of the free-energy can be written as (compare with Eq. (XIII.74)),

$$-\mathcal{F}_{\text{int}} = \int_{-\infty}^{\infty} d\xi e^{\xi} \left[e^{-\frac{1}{2} \Delta_1 \frac{\partial^2}{\partial \xi^2}} g^{m/m_1}(m_1, \xi) - 1 \right] = \int_{-\infty}^{\infty} d\xi e^{\xi} \left[e^{-m_0 f(m_0, \xi)} - 1 \right] \quad (\text{XIII.97})$$

where $g(m_i, \xi) = e^{-m_i f(m_i, \xi)}$ follows the recursion relations in sec. E with

$$\Lambda_0 = \Delta_0 \quad \Lambda_i = \Delta_i - \Delta_{i+1} \quad (i = 1, 2, \dots, k-1) \quad \Lambda_k = \Delta_k \quad (\text{XIII.98})$$

such that

$$e^{-m_i f(m_i, y)} = e^{\frac{\Delta_i - \Delta_{i+1}}{2} \frac{\partial^2}{\partial y^2}} e^{-m_i f(m_{i+1}, y)} \quad (\text{XIII.99})$$

assuming $\Delta_0 = 0$, with initial condition (see Eq. (XIII.75) for 1RSB case),

$$g(m_k, \xi) = e^{\frac{\Delta_k}{2} \frac{\partial^2}{\partial \xi^2}} e^{-\beta v(D(1 + \frac{\xi}{d}))} = \int \mathcal{D}z e^{-\beta v(D(1 + \frac{\xi + \sqrt{\Delta_k} z}{d}))} \quad (\text{XIII.100})$$

2. Variational equations

Doing similar computations as done in sec. [XC2](#) (Replace, we find,

$$-\frac{\partial}{\partial \Delta_{i+1}} f(m_j, h) = -\frac{1}{2}(m_i - m_{i+1}) \int dh' P_{j,i+1}(h, h') (f'(m_{i+1}, h'))^2 \quad (\text{XIII.101})$$

where $P_{ij}(h, h')$ is defined in Eq. [\(F.1\)](#). Using this result we find

$$\begin{aligned} \frac{\partial}{\partial \Delta_i} (-\mathcal{F}_{\text{int}}) &= m_0 \int_{-\infty}^{\infty} d\xi e^{\xi} g(m_0, \xi) \frac{\partial(-f(m_0, \xi))}{\partial \Delta_i} \\ &= -\frac{m_0(m_{i-1} - m_i)}{2} \int dh P_i(h) (f'(m_i, h))^2 \end{aligned} \quad (\text{XIII.102})$$

where we introduced²³

$$\begin{aligned} P_i(h) &= \int_{-\infty}^{\infty} d\xi e^{\xi} g(m_0, \xi) P_{0,i}(\xi, h) \\ &= \int_{-\infty}^{\infty} d\xi e^{\xi - \Delta_1/2} g^{m_0/m_1}(m_1, \xi) P_{1,i}(\xi, h) \end{aligned} \quad (\text{XIII.103})$$

Apparently $P_i(h)$ follows the same recursion formula as Eq. [\(F.4\)](#)

$$P_i(z) = e^{-m_{j-1}f(m_j, z)} \gamma_{\Lambda_{j-1}} \otimes \frac{P_{j-1}(z)}{e^{-m_{j-1}f(m_{j-1}, z)}} \quad i = 2, 3, \dots, k \quad (\text{XIII.104})$$

with the 'boundary condition'

$$P_1(h) = \int_{-\infty}^{\infty} d\xi e^{\xi - \Delta_1/2} g(m_1, \xi)^{m_0/m_1} \delta(\xi - h) = e^{h - \Delta_1/2} g^{m_0/m_1}(m_1, h) \quad (\text{XIII.105})$$

Collecting the above results we find variational equation for G_i ,

$$\begin{aligned} 0 &= \frac{2}{d} \frac{\partial}{\partial G_i} (-\beta F_m^{k-RSB}) \\ &= \left(\frac{m}{m_i} - \frac{m}{m_{i-1}} \right) \frac{1}{G_i} + \hat{\varphi} \sum_{j=1}^k \frac{\partial \Delta_j}{\partial G_i} \frac{\partial}{\partial \Delta_i} (-\mathcal{F}_{\text{int}}) \\ &= \left(\frac{m}{m_i} - \frac{m}{m_{i-1}} \right) \left[\frac{1}{G_i} - m_{i-1} \kappa_i - \sum_{j=1}^{i-1} (m_{j-1} - m_j) \kappa_j \right] \end{aligned} \quad (\text{XIII.106})$$

where we used

$$\frac{\partial \Delta_j}{\partial G_i} = \frac{1}{m_i} \delta_{ij} + \left(\frac{1}{m_i} - \frac{1}{m_{i-1}} \right) \theta(j - (i+1)) \quad (\text{XIII.107})$$

where $\theta(x) = 1$ for $x \geq 0$ and 0 for $x < 0$. We introduced

$$\kappa_i = \frac{\hat{\varphi}}{2} \int dh P_i(h) (f'(m_i, h))^2 \quad (\text{XIII.108})$$

To sum up we find the saddle point equation

$$\frac{1}{G_i} = m_{i-1} \kappa_i + \sum_{j=1}^{i-1} (m_{j-1} - m_j) \kappa_j \quad i = 1, 2, \dots, k \quad (\text{XIII.109})$$

It is easy to check that $k = 1$ case reduces to Eq. [\(XIII.88\)](#).

²³ In [58] $P_i(h)e^{\Delta_1/2}$ is denoted as $P_i(h)$.

3. Effective potential

For the effective potential Eq. (XIII.45) we find,

$$\begin{aligned} e^{-\beta v_{\text{eff}}(\xi)} &= \frac{e^{-\xi}}{m} \int_{-\infty}^{\infty} d\eta e^{\eta} e^{-mf(m_0, \eta)} \left(m \frac{\delta f(m_0, h)}{\delta f(m_{k+1}, \xi)} \right) = P_{k+1}(\xi) \\ &= e^{-\beta v(\xi)} e^{-\xi} \int_{-\infty}^{\infty} dy \frac{e^{-\frac{(y-\xi)^2}{2\Delta_k}}}{\sqrt{2\pi\Delta_k}} \frac{P_k(y)}{g(m_k, y)} \end{aligned} \quad (\text{XIII.110})$$

where we defined

$$-\beta f(m_{k+1}, h) = -\beta v(h) \quad (\text{XIII.111})$$

assuming $m_{k+1} = 1$. We recover the 1RSB result Eq. (XIII.78) for $k = 1$ case using Eq. (X.39) with $m_1 = 1$.

4. Pressure

Let us examine the pressure using the 3rd equation of Eq. (XIII.51). In $d \gg 1$ we find,

$$\begin{aligned} p(2/d) &= \frac{1}{m} \hat{\varphi} \left(-\frac{\partial}{\partial \eta} \right) (-\mathcal{F}_{\text{int}}(\eta)) \Big|_{\eta=0} = \frac{1}{m} \hat{\varphi} \int dh \int d\xi e^{\xi} \frac{\delta g(m_0, \xi)}{\delta f(m_k, h)} f'(m_k, h) \\ &= \frac{1}{m} \int dh \int d\xi e^{\xi} g(m_0, \xi) (-m_0) \frac{\delta f(m_0, \xi)}{\delta f(m_k, h)} f'(m_k, h) \\ &= \int dh \int d\xi e^{\xi} g(m_0, \xi) P_{0,i}(\xi, h) (-f'(m_k, h)) \\ &= \int dh P_i(h) \pi(m_k, h) \quad \pi(m_k, h) = -f'(m_k, h) \end{aligned} \quad (\text{XIII.112})$$

5. Shear-modulus

Let us evaluate the shear-modulus matrix Eq. (XIII.69) with the k -RSB. From Eq. (XIII.70) we find,

$$\frac{\partial \mathcal{F}_{\text{int}}}{\partial \Delta_{ab}} = \sum_{l=1}^k \frac{1}{m(m_{l-1} - m_l)} (I_{ab}^{m_{l-1}} - I_{ab}^{m_l}) \frac{\partial \mathcal{F}_{\text{int}}}{\partial \Delta_l} \quad (\text{XIII.113})$$

Using this in Eq. (XIII.69), and using Eq. (XIII.102) together with Eq. (XIII.108) we find,

$$\begin{aligned} \beta \frac{\mu_{ab}}{d} &= \hat{\varphi} \sum_{l=1}^k ((I_{ab}^{m_l} - m_l \delta_{ab}) - (I_{ab}^{m_{l-1}} - m_{l-1} \delta_{ab})) \kappa_l \\ &= \left[\kappa_k + \sum_{l=1}^k (m_{l-1} - m_l) \kappa_l \right] \delta_{ab} + \sum_{l=1}^{k-1} (\kappa_l - \kappa_{l+1}) I_{ab}^{m_k} - \kappa_1 I_{ab}^{m_0} \\ &= \frac{1}{G_k} I_{ab}^{m_k} + \sum_{l=1}^{k-1} \frac{1}{m_l} \left(\frac{1}{G_l} - \frac{1}{G_{l+1}} \right) - \frac{1}{m_0} \frac{1}{G_1} I_{ab}^m \end{aligned} \quad (\text{XIII.114})$$

In the last equation we used Eq. (XIII.109). To sum up we find

$$\mu_{ab} = \sum_{l=0}^k \tilde{\mu}_1 I_{ab}^{m_l} \quad (\text{XIII.115})$$

Then we find,

$$\hat{\mu}_i = \sum_{j=i}^k m_j \tilde{\mu}_j = \frac{1}{G_i} \quad i = 1, 2, \dots, k \quad (\text{XIII.116})$$

and

$$\hat{\mu}_0 = \frac{1}{G_1} - \frac{1}{G_1} = 0 \quad (\text{XIII.117})$$

In particular, we find using Eq. (XIII.95) for $i = k$ that $G_k = \Delta_k$ since $m_k = 1$ so that

$$\hat{\mu}_k = \tilde{\mu}_k = \frac{1}{\Delta_k}. \quad (\text{XIII.118})$$

TODO: discuss FC/ZFC shear-modulus

6. Stability of k -RSB

Now let us discuss stability of the k -RSB solution following sec.X C 3. As we did for the p -spin model, we only analyze stability of the remaining replica symmetry within the most-inner core part of the k -RSB solution. Thus we just consider the Hessian matrix a sub-block of the Hessian matrix Eq. (XIII.42) Eq. (VI.80) assuming that all indexes a, b, c, d are in the same most-inner core replica group of size m_k , which we denote as \mathcal{C} . Then we find, $M_{(a \neq b, c \neq d)}^{\mathcal{C}}$ given by with

$$M_{(a \neq b, c \neq d)}^{\mathcal{C}} = M_{(a \neq b, c \neq d)}^{\mathcal{C}, \text{ent.}} + M_{(a \neq b, c \neq d)}^{\mathcal{C}, \text{int.}} \quad (\text{XIII.119})$$

where

$$-M_{(a \neq b, c \neq d)}^{\mathcal{C}, \text{ent.}} = \frac{\partial^2}{\partial \Delta_{a < b} \partial \Delta_{c < d}} \ln \det \hat{\alpha}^{m, m} \quad (\text{XIII.120})$$

$$-M_{(a \neq b, c \neq d)}^{\mathcal{C}, \text{int.}} = \frac{\partial^2}{\partial \Delta_{a < b} \partial \Delta_{c < d}} (-\mathcal{F}_{\text{int}}) \quad (\text{XIII.121})$$

Interaction part

Let us first discuss the contribution from the interactions $M_{(a \neq b, c \neq d)}^{\mathcal{C}, \text{int.}}$. Using Eq. (XIII.97),

$$\begin{aligned} M_{(a \neq b, c \neq d)}^{\mathcal{C}, \text{int.}} &= \frac{\partial^2}{\partial \Delta_{a < b} \partial \Delta_{c < d}} \int_{-\infty}^{\infty} d\xi e^{\xi} \left[e^{-m_0 f(m_0, \xi)} - 1 \right] \\ &= \int_{-\infty}^{\infty} d\xi e^{\xi} \exp \left(\sum_{l=0}^{k-1} \frac{\Lambda_l}{2} \sum_{e, f=1}^m I_{ef}^{m_l} \frac{\partial^2}{\partial h_e \partial h_f} \right) \left(\prod_{a \notin \mathcal{C}} g(m_k, h_a) \right) \Big|_{\{h_a = \xi\}} \\ &\quad \frac{\partial^2}{\partial \Delta_{a < b} \partial \Delta_{c < d}} \prod_{a \in \mathcal{C}} g(m_k, h_a) \Big|_{\{h_a = \xi\}} \\ &= \int d\xi e^{\xi} \int dy \frac{m_k}{m_0} \frac{\delta g(m_0, \xi)}{\delta f(m_k, y)} \left[S_1(y) \frac{\delta_{ab} \delta_{bd} + \delta_{ad} \delta_b}{2} + S_2(y) \frac{\delta_{ac} + \delta_{ad} + \delta_{bc} + \delta_{bd}}{4} + S_3(y) \right] \\ &= \int dy P_k(y) \left[S_1(y) \frac{\delta_{ab} \delta_{bd} + \delta_{ad} \delta_b}{2} + S_2(y) \frac{\delta_{ac} + \delta_{ad} + \delta_{bc} + \delta_{bd}}{4} + S_3(y) \right] \end{aligned} \quad (\text{XIII.122})$$

where we used Eq. (XIII.103) and introduced

$$S_1(x) = 2(f''(m_k, x))^2 \quad S_2(x) = 4(-f''(m_k, x))(f'(m_k, x))^2 \quad S_3(x) = (f'(m_k, x))^4 \quad (\text{XIII.123})$$

The result takes the matrix structure shown in sec.K with,

$$M_1^{\text{int.}} = 2\hat{\varphi} \int dh P_k(h) (f''(m_k, h))^2 \quad (\text{XIII.124})$$

$$M_2^{\text{int.}} = 4\hat{\varphi} \int dh P_k(h) (-f''(m_k, h))(f'(m_k, h))^2 \quad (\text{XIII.125})$$

$$M_3^{\text{int.}} = \hat{\varphi} \int dh P_k(h) (-f''(m_k, h))(f'(m_k, h))^4 \quad (\text{XIII.126})$$

Entropic part

Next let us discuss the entropic contribution. For simplicity we limit ourselves with the computation of $M_1^{\text{ent.}}$ which determines the replicon eigenvalue following the trick of [58] (see sec. XII). The result is

$$M_1^{\text{ent.}} = \frac{4}{\Delta_k^2} \quad (\text{XIII.127})$$

Replicon eigen-value

To sum up we find the replicon eigenvalue as

$$\lambda_R = \frac{4}{\Delta_k^2} - 2\hat{\varphi} \int dh P_k(h) (f''(m_k, h))^2 \quad (\text{XIII.128})$$

7. Continuous RSB: $k \rightarrow \infty$ limit

Similarly to the p -spin case, let us consider the continuous RSB ($k \rightarrow \infty$). In $k \rightarrow \infty$ limit, writing $m_i = x - \delta x, m_{i+1} = x$ and $\Lambda_i = -\dot{\Delta}(x)\delta x$, the recursion relations Eq. (E.1), Eq. (E.1) and Eq. (E.5) become partial differential equations,

$$-\dot{g}(x, y) = -\frac{\dot{\Delta}(x)}{2} g''(x, y) - \frac{1}{x} g(x, y) \ln g(x, y) \quad (\text{XIII.129})$$

Equivalently for,

$$-f(x, y) \equiv \frac{1}{x} \ln g(x, y) \quad (\text{XIII.130})$$

we find,

$$\dot{f}(x, y) = \frac{\dot{\Delta}(x)}{2} \left[f''(x, y) - x(f'(x, y))^2 \right] \quad (\text{XIII.131})$$

And for

$$\pi(x, y) = -f'(x, y) \quad (\text{XIII.132})$$

we find, Eq. (E.5) becomes

$$\dot{\pi}(x, h) = \frac{\dot{\Delta}(x)}{2} (\pi''(x, h) + 2x\pi(x, h)\pi'(x, h)) \quad (\text{XIII.133})$$

The boundary conditions are

$$g(1, h) = e^{\frac{\Delta(1)}{2}\partial_h^2} e^{-\beta v(h)} = \int \mathcal{D}z e^{-\beta v(h - \sqrt{\Delta(1)}z)} \quad (\text{XIII.134})$$

$$-f(1, y) = \ln g(1, h). \quad (\text{XIII.135})$$

and

$$\pi(1, y) = -f'(1, y) \quad (\text{XIII.136})$$

Finally the recursion relation for $P_i(h)$ Eq. (XIII.104) becomes, in the $k \rightarrow \infty$ limit a partial differential equation

$$\dot{P}(x, h) = -\frac{1}{2}\dot{\Delta}(x) [P''(x, h) + 2x(P(x, h)f'(x, h))'] \quad (\text{XIII.137})$$

which is the same as Eq. (X.58) but with a different boundary condition,

$$P(m, h) = e^{h - \Delta_1/2} e^{-mf(m, h)} \quad (\text{XIII.138})$$

With these the free-energy becomes

$$\begin{aligned} -\beta F_m[\hat{\Delta}] &= c_{nt} + \frac{d}{2}\mathcal{S}[\hat{\Delta}] \\ \mathcal{S}[\hat{\Delta}] &= -m \int_m^1 \frac{dx}{x^2} [\ln G(x)/m] + \hat{\varphi} \int_{-\infty}^{\infty} d\xi e^{\xi} (e^{-mf(m,\xi)} - 1) \end{aligned} \quad (\text{XIII.139})$$

where $G(x)$ is related to $\Delta(x)$ via

$$G(x) = x\Delta(x) + \int_x^1 dy \Delta(y) \quad (\text{XIII.140})$$

which is the continuous limit of Eq. (XIII.95).

The saddle point equation Eq. (XIII.109) becomes

$$\frac{1}{G(x)} = x\kappa(x) - \int_0^x dy \kappa(y) \quad (\text{XIII.141})$$

while Eq. (XIII.108) becomes

$$\kappa(x) = \frac{\hat{\varphi}}{2} \int dh P(x,h) (f'(x,h))^2 \quad (\text{XIII.142})$$

Marginal stability

In the continuous limit $k \rightarrow \infty$ the replicon eigen value Eq. (XIII.128) becomes

$$\lambda_R = \frac{4}{\Delta^2(1)} - 2\hat{\varphi} \int dh P(1,h) (f''(1,h))^2 = 0 \quad (\text{XIII.143})$$

The vanishing of the replicon eigenvalue can be proved much as done in sec. XC4. Similarly to the computation in sec. XC4, taking a derivative d/dx of Eq. (XIII.141) and using the above expressions, taking $x \rightarrow 1$, we find,

$$-\frac{1}{\Delta^2(1)} = -\frac{\hat{\varphi}}{2} \int dh P(1,h) (\pi'(1,h))^2 \quad \pi(x,h) = -f'(x,h) \quad (\text{XIII.144})$$

which proves vanishing of the replicon eigen-value, the continuous RSB solution is marginally stable.

J. Glass state following

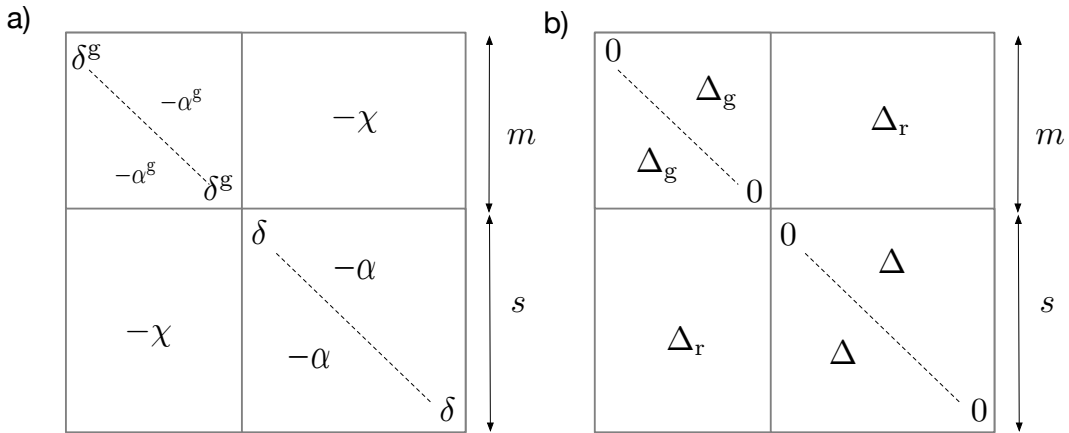


FIG. 47. Parisi matrix for state following - spheres -

1. General setting

Now we turn to the glass state following. We discussed using the p -spin model in sec. IX. We prepare the reference system in equilibrium at $\hat{\varphi}_g$ and perturb the student system . For the spheres we perturb the system by compression and shear

$$\eta_a = \begin{cases} 0 & a \in r \\ \eta & a \in s \end{cases} \quad \gamma_a = \begin{cases} 0 & a \in r \\ \gamma & a \in s \end{cases}$$

We use a $m+s$ replica system with free-energy subjected to compression $\{\eta_a\}$ and shear $\{\gamma_a\}$,

$$-\frac{\beta F_{m+s}[\hat{\alpha}, \{\gamma_a\}, \{\eta_a\}]}{N} = c_{nt} + \frac{d}{2} \ln \det \hat{\alpha}^{m+s, m+s} - \frac{d}{2} \hat{\varphi}_g \mathcal{F}_{int} \quad (\text{XIII.145})$$

where c_{nt} is (see Eq. (XIII.48)),

$$c_{nt} = 1 - \sum_a \eta_a + \ln(\rho \lambda_{th}^d) + d \ln(m+s) + \frac{(m+s-1)d}{2} \ln \left(\frac{2\pi e(D/\lambda_{th})^2}{d^2} \right) \quad (\text{XIII.146})$$

and (see Eq. (XIII.48) and Eq. (XIII.66))

$$-\mathcal{F}_{int} = \int \mathcal{D}\lambda \int_{-\infty}^{\infty} d\xi e^{\xi} \left(e^{-\frac{1}{2} \sum_{ab} (\Delta_{ab} + \frac{\lambda^2}{2} (\gamma_a - \gamma_b)^2) \frac{\partial^2}{\partial \xi_a \partial \xi_b}} \prod_{a=1}^{m+s} e^{-\beta v(D^2(1 + \frac{\xi_a}{d} - \frac{\eta_a}{d}))} - 1 \right) \Big|_{\{\xi_a = \xi\}} \quad (\text{XIII.147})$$

2. Simplest ansatz

Let us take the simplest ansatz shown in Fig. 47. By sum rules $\sum_a \alpha_{ab} = \sum_b \alpha_{ab} = 0$ we have

$$\delta^g = (m-1)\alpha^g + s\chi \quad \delta = (s-1)\alpha + m\chi \quad (\text{XIII.148})$$

and for the MSD $\Delta_{ab} = \alpha_{aa} + \alpha_{bb} - 2\alpha_{ab}$ we have

$$\begin{aligned} \Delta_g &= 2(\delta^g + \alpha^g) = 2(m\alpha^g + s\chi) \\ \Delta &= 2(\delta + \alpha) = 2(s\alpha + m\chi) \\ \Delta_r &= \delta^g + \delta + 2\chi = (m-1)\alpha^g + (s-1)\alpha + (m+s+2)\chi \end{aligned} \quad (\text{XIII.149})$$

Let us also introduce

$$\Delta_f = 2\Delta_r - \Delta_g - \Delta_r = 2(2\chi - \alpha^g - \alpha) \quad (\text{XIII.150})$$

For this ansatz we find the free-energy becomes (see SI of [83]),

$$\begin{aligned} -\frac{\beta F_{m+s}[\hat{\alpha}, \{\gamma_a\}, \{\eta_a\}]}{N} &= c_{nt} + \frac{d}{2} \left[\ln \chi + (m-1) \underbrace{\ln(m\alpha^g + s\chi)}_{\Delta_g/2} + (s-1) \underbrace{\ln \ln m}_{\Delta/2} \underbrace{(s\alpha + m\chi)}_{\Delta/2} \right] \\ &\quad - \frac{d}{2} \hat{\varphi}_g \mathcal{F}_{int} \end{aligned} \quad (\text{XIII.151})$$

with c_{nt} defined in Eq. (XIII.146) and

$$-\mathcal{F}_{int} = \int \mathcal{D}\lambda \int_{-\infty}^{\infty} d\xi e^{\xi} \left[g_{\Delta_g}^m \left(\xi + \frac{\Delta_g}{2} \right) \int \mathcal{D}z g_{\Delta}^s \left(\xi - \eta + \frac{\Delta_f(\lambda) + \Delta}{2} + \sqrt{\Delta_f(\lambda)} z \right) - 1 \right] \quad (\text{XIII.152})$$

with

$$\Delta_f(\lambda) = \Delta_f + \lambda^2 \gamma^2 \quad (\text{XIII.153})$$

and g defined as (see Eq. (XIII.75)),

$$g_{\Delta}(\xi) = e^{\frac{1}{2} \Delta \frac{\partial^2}{\partial \xi^2}} e^{-\beta v(D(1 + \frac{\xi}{d}))} = \int \mathcal{D}z e^{-\beta v(D(1 + \frac{\xi + \sqrt{\Delta} z}{d}))} \quad (\text{XIII.154})$$

3. Reference system

Using the above result we find for the reference system,

$$-\beta f_m = \lim_{s \rightarrow 0} -\frac{\beta F_{m+s}[\hat{\alpha}, \{\gamma_a\}, \{\eta_a\}]}{N} = c_{\text{nt}} + \frac{d}{2} \left\{ \left[(m-1) \ln \left(\frac{\Delta_g}{2} \right) - \ln m \right] - \hat{\varphi}_g \mathcal{F}_{\text{int}} \right\} \quad (\text{XIII.155})$$

with c_{nt}

$$c_{\mu \text{nt}} = 1 - \ln(\rho \lambda_{\text{th}}^d) + d \ln m + \frac{(m-1)d}{2} \ln \left(\frac{2\pi e(D/\lambda_{\text{th}})^2}{d^2} \right) \quad (\text{XIII.156})$$

and

$$-\mathcal{F}_{\text{int}} = \int_{-\infty}^{\infty} d\xi e^{\xi} \left[e^{-\frac{1}{2}\Delta_g \frac{\partial^2}{\partial \xi^2}} g^m(m_1, \xi) - 1 \right] = \int_{-\infty}^{\infty} d\xi e^{\xi - \Delta_g/2} [g^m(m_1, \xi) - 1] \quad (\text{XIII.157})$$

with

$$g(m_1, \xi) = e^{\frac{1}{2}\Delta_g \frac{\partial^2}{\partial \xi^2}} e^{-\beta v(D(1+\frac{\xi}{d}))} = \int \mathcal{D}z e^{-\beta v(D(1+\frac{\xi+\sqrt{\Delta_g}z}{d}))} \quad (\text{XIII.158})$$

These agree with Eq. (XIII.76) as it should. We readily know the variational equation for Δ_g (see Eq. (XIII.88)),

$$\frac{1}{\Delta_g} = m \frac{\hat{\varphi}}{2} \int d\xi e^{\xi - \Delta_g/2} g^m(m_1, \xi) (f'(m_1, \xi))^2 \quad (\text{XIII.159})$$

4. Student system

For the student system (see SI of [83]),

$$\begin{aligned} -\beta V_{\text{FP}} &= \partial_s \left(-\frac{\beta F_{m+s}[\hat{\alpha}, \{\gamma_a\}, \{\eta_a\}]}{N} \right) \Big|_{s=0} \\ &= \frac{d}{2} \ln \left(\frac{2\pi e(D/\lambda_{\text{th}})^2}{d^2} \right) + \frac{d}{2} \left[\ln \left(\frac{\Delta}{2} \right) + \frac{\Delta_g + m\Delta_f}{m\Delta} \right. \\ &\quad \left. + \hat{\varphi}_g \int \mathcal{D}\lambda \int_{-\infty}^{\infty} d\xi e^{\xi} g_{\Delta_g}^m \left(\xi + \frac{\Delta_g}{2} \right) \int \mathcal{D}z \ln g \left(\xi - \eta + \frac{\Delta_f(\lambda) + \Delta}{2} + \sqrt{\Delta_f(\lambda)}z \right) \right] \end{aligned} \quad (\text{XIII.160})$$

where

$$\Delta_f(\lambda) = \Delta_f + \lambda^2 \gamma^2 \quad \Delta_f = 2\Delta_r - \Delta_g - \Delta \quad (\text{XIII.161})$$

Now taking derivatives we can find variational equations for Δ , Δ_f (see SI of [83]).

5. Pressure and shear-stress

From the Franz-Parisi potential obtained above, we can obtain the pressure and shear-stress of the glass. The reduced pressure Eq. (XIII.51) of the glass is obtained as,

$$p = -\frac{\partial}{\partial \eta} (-\beta V_{\text{FP}}) = \frac{d}{2} \hat{\varphi}_g \int \mathcal{D}\lambda \int d\xi e^{\xi} g_{\Delta_g}^m \left(\xi + \frac{\Delta}{2} \right) \int \mathcal{D}z \frac{g'_{\Delta}(y)}{g_{\Delta}(y)} \Big|_{y=\xi-\eta+\frac{\Delta_f(\lambda)+\Delta}{2}+\sqrt{\Delta_f(\lambda)}z} \quad (\text{XIII.162})$$

The (reduced) shear-stress of the glass is obtained as,

$$\begin{aligned} \beta\sigma &= \frac{\partial}{\partial \gamma} (\beta V_{\text{FP}}) \\ &= -\frac{d}{2} \hat{\varphi}_g \int \mathcal{D}\lambda \int d\xi e^{\xi} g_{\Delta_g}^m \left(\xi + \frac{\Delta}{2} \right) \int \mathcal{D}z \frac{g'_{\Delta}(y)}{g_{\Delta}(y)} \Big|_{y=\xi-\eta+\frac{\Delta_f(\lambda)+\Delta}{2}+\sqrt{\Delta_f(\lambda)}z} \left(1 + \frac{z}{\Delta_f(\lambda)} \right) \lambda^2 \gamma \end{aligned} \quad (\text{XIII.163})$$

6. Gardner transition

XIV. HARD SPHERE GLASS

As the simplest system, let us discuss the hard-spheres in large- d limit [56–58, 66, 84]. It is the simplest glass forming system but it is also a bit special in the sense that entropy controls everything. Quantities like $-\beta f$ (free-entropy), βp (reduced pressure), $\beta\mu$ (reduced shear-modulus) do not depend on the temperature. Temperature just fixes the Maxwell-Boltzmann distribution of the momentum of the hard particles, or the time scale of free flights of the hard particles between collisions. Pressure and shear-stress can be regarded as entropic forces (or equivalently as due to the exchange of momentum between hard particles, between hard particles and bounding boxes through collisions).

A. 1RSB ansatz ($k = 1$)

For the hardcore potential

$$e^{-\beta v(D^2(1+\frac{\xi}{d}))} = \theta(\xi) \quad (\text{XIV.1})$$

we find

$$g(m_k, \xi) = \int \mathcal{D}z \theta(\xi - \sqrt{\Delta_k} z) = \Theta\left(\frac{\xi}{\sqrt{2\Delta_k}}\right) \quad (\text{XIV.2})$$

where $\Theta(x)$ is defined in Eq. (VII.48). Then remembering that $m_k = 1$ we find,

$$-f'(m_k, \xi) = \frac{\frac{e^{-\frac{\xi^2}{2\Delta_k}}}{\sqrt{2\pi\Delta_k}}}{\Theta\left(\frac{\xi}{\sqrt{2\Delta_k}}\right)} \quad (\text{XIV.3})$$

The saddle point equation Eq. (XIII.88) becomes,

$$\frac{1}{\hat{\varphi}} = \zeta_m(\Delta) \quad \zeta_m(\Delta) = \frac{m\Delta}{2} \int d\xi e^{\xi - \Delta/2} \Theta^{m-2}\left(\frac{\xi}{\sqrt{2\Delta}}\right) \left(\frac{e^{-\frac{\xi^2}{2\Delta}}}{\sqrt{2\pi\Delta}}\right)^2 \quad (\text{XIV.4})$$

1. Dynamical transition

Let us consider the dynamical transition of the hard-spheres. We display in Fig. 48 a graphical representation of the saddle point equation. By increasing the scaled volume fraction, we meet the dynamical transition point with $\hat{\varphi}_d \sim 4.8$ and $\alpha_d \sim 0.576$ [85]. (see Fig. 48 a)) At higher density we find a solution with the cage size α decreases, which is the physical solution,

$$\Delta = \Delta_d - \text{const} \sqrt{\frac{\hat{\varphi} - \hat{\varphi}_d}{\hat{\varphi}_d}} \quad (\text{XIV.5})$$

which means the shear-modulus Eq. (XIII.93),

$$\hat{\mu} = \frac{1}{\Delta_d} + \text{const} \sqrt{\frac{\hat{\varphi} - \hat{\varphi}_d}{\hat{\varphi}_d}} \quad (\text{XIV.6})$$

also exhibits the discontinuous behaviour at the dynamical transition.

2. Jamming

Saddle point equation

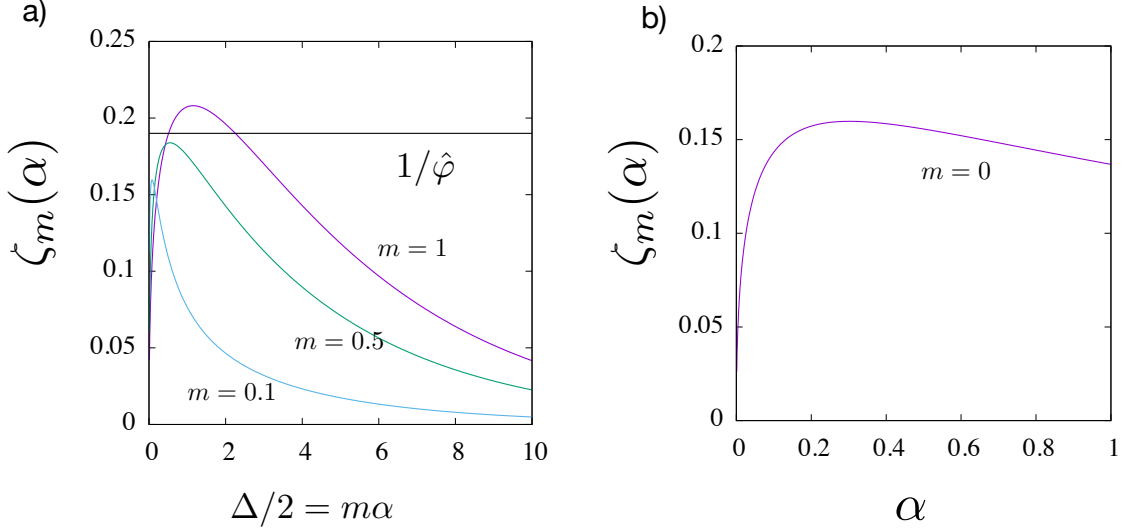


FIG. 48. Graphical representation of the saddle point equation for the hardspheres in $d \rightarrow \infty$ limit (1RSB) a) for finite m b) jamming limit $m \rightarrow 0$

In the $m \rightarrow 0$ limit, the pressure Eq. (XIII.51) diverges suggesting jamming. Let us recall that the MSD $\Delta = 2m\alpha$ so that it also vanishes in the jamming limit $m \rightarrow 0$. Now let us discuss the saddle point equation in this limit. Using $\Delta = 2m\alpha$ we find,

$$\begin{aligned} \zeta_m(\Delta) &= m^2 \alpha \int d\xi e^{\xi - m\alpha} \Theta^{m-2} \left(\frac{\xi}{\sqrt{4m\alpha}} \right) \left(\frac{e^{-\frac{\xi^2}{4m\alpha}}}{\sqrt{4\pi m\alpha}} \right)^2 \\ &\xrightarrow{m \rightarrow 0} \frac{1}{4\alpha} \int_0^\infty dy y^2 e^{-y-y^2/4\alpha} \end{aligned} \quad (\text{XIV.7})$$

The last equation can be obtained using formulae shown in G. Thus we find in the $m \rightarrow 0$ limit

$$\frac{1}{\hat{\varphi}} = \frac{1}{4\alpha} \int_0^\infty dy y^2 e^{-y-y^2/4\alpha} \quad (\text{XIV.8})$$

From this we find the lowest density where jammed configuration appears as $\hat{\varphi}_{\text{th}} = 6.26$ with $\alpha_{\text{th}} = 0.302$ [85].(see Fig. 48 b))

Pressure, Cage size and shear-modulus

Note that $m \propto 1/p$ as in Eq. (XIII.51). From the above result we also find that, within the 1RSB ansatz the MSD vanishes as

$$\Delta = m\alpha \propto 1/p \quad (\text{XIV.9})$$

which then means the shear-modulus scales as

$$\hat{\mu} \propto p \quad (\text{XIV.10})$$

Effective potential

Now let us examine the behaviour of $g(r)$ or the effective potential Eq. (XIII.78). We have

$$g(\xi) = \theta(\xi) \int d\eta \frac{e^{-\frac{(\eta-\xi)^2}{2\Delta}}}{\sqrt{2\pi\Delta}} e^{\eta-\xi-\Delta/2} \Theta^{m-1} \left(\frac{\eta}{\sqrt{2\Delta}} \right) \quad (\text{XIV.11})$$

We can make the following observations in the jamming limit $m \rightarrow 1$ which induces $\Delta = m\alpha \rightarrow 0$,

- fix ξ and take $m \rightarrow 0$

$$g(\xi) \xrightarrow{m \rightarrow 0} \theta(\xi) \quad (\text{XIV.12})$$

- fix $\lambda = \xi/\Delta$ and take $m \rightarrow 0$. From Eq. (G.3) we find dominant contribution comes from $\eta < 0$ side of the integral. We find,

$$\begin{aligned} g(\xi) &\simeq \theta(\xi) \int_{-\infty}^0 d\eta \frac{e^{-\frac{(\eta-\lambda\Delta)^2}{2\Delta}}}{\sqrt{2\pi\Delta}} e^{\eta-\lambda\Delta-\Delta/2} (2\sqrt{\pi} X e^{X^2}) \Big|_{X=-\eta/\sqrt{2\Delta}} \\ &\xrightarrow[m \rightarrow 0]{(\Delta=m\alpha \rightarrow 0)} \frac{\theta(\xi)}{\Delta} \int_0^\infty dy y e^{-(1+\lambda)y} \end{aligned} \quad (\text{XIV.13})$$

This means divergence of the contact peak $g(0^+) \propto 1/\Delta$ of width Δ approaching jamming.

Pressure again, (Contact Number)

As discussed in sec. XIII E, (reduced) pressure can also be computed using the 3rd equation of Eq. (XIII.51). In $d \gg 1$,

$$\begin{aligned} p/d &= \frac{1}{m} \hat{\varphi} \left(-\frac{\partial}{\partial \eta} \right) (-\mathcal{F}_{\text{int}}(\eta)) \Big|_{\eta=0} = \hat{\varphi} \int_{-\infty}^\infty d\xi e^{\xi-\Delta/2} \Theta^{m-1} \left(\frac{\xi}{\sqrt{2\Delta}} \right) \frac{e^{-\frac{\xi^2}{2\Delta}}}{\sqrt{2\pi\Delta}} \\ &\xrightarrow[m \rightarrow 0]{} \hat{\varphi} \int_{-\infty}^\infty d\xi e^{\xi-\Delta/2} \frac{e^{-\frac{\xi^2}{2\Delta}}}{\sqrt{2\pi\Delta}} 2\sqrt{\pi} X e^{X^2} \Big|_{X=\xi/\sqrt{2\Delta}} = \hat{\varphi} \frac{1}{\Delta} \int_0^\infty dy y e^y \end{aligned} \quad (\text{XIV.14})$$

In the 2nd equation we used again Eq. (G.3). Again we find $\Delta \propto 1/p$.

3. Kauzmann transition

Let us also examine the saddle point equation at very large densities $\hat{\varphi} \gg 1$ where Δ becomes small. We find,

$$\Delta \sim \frac{1}{I^2(m)} (\hat{\varphi})^{-2} \quad (\text{XIV.15})$$

where we introduced $I(m)$ as follows

$$\zeta_m(\Delta) \xrightarrow{\Delta \rightarrow 0} I(m) \sqrt{\Delta} \quad I(m) = \frac{m}{2\sqrt{2}} \int_{-\infty}^\infty dy \Theta^{m-2}(y) e^{-2y^2} \quad (\text{XIV.16})$$

Thus at larger densities the cage size Δ becomes smaller as one expects.

Now let us consider the complexity (see Eq. (XIII.84)),

$$\begin{aligned} \Sigma^* &= \frac{d}{2} \ln d - \frac{d}{2} \left[1 + \ln \frac{\Delta}{2m} + \hat{\varphi} m^2 \partial_m m^{-1} (-\mathcal{F}_{\text{int}}) \right] + O(d^0) \\ &= \frac{d}{2} (\ln d - \hat{\varphi}) - \frac{d}{2} \left[1 + \ln \frac{\Delta}{2m} + \hat{\varphi} m^2 \partial_m m^{-1} (-\mathcal{F}_{\text{int}} + 1) \right] + O(d^0) \end{aligned} \quad (\text{XIV.17})$$

where

$$-\mathcal{F}_{\text{int}} + 1 = \int_{-\infty}^\infty d\xi e^\xi \left[\Theta^m \left(\frac{\xi + \Delta/2}{\sqrt{2\Delta}} \right) - \theta(\xi) \right] \xrightarrow{\Delta \rightarrow 0} \sqrt{2\Delta} \underbrace{\int_{-\infty}^\infty dy [\Theta^m(y) - \theta(y)]}_{J(m)} \quad (\text{XIV.18})$$

Thus at large densities with $\Delta \propto \hat{\varphi}^{-2}$ we find,

$$\Sigma^* \sim \frac{d}{2} (\ln d - \hat{\varphi} + O(\hat{\varphi}^0)) \quad (\text{XIV.19})$$

which implies the Kauzmann transition happens at

$$\hat{\varphi}_K \propto \ln d \quad (\text{XIV.20})$$

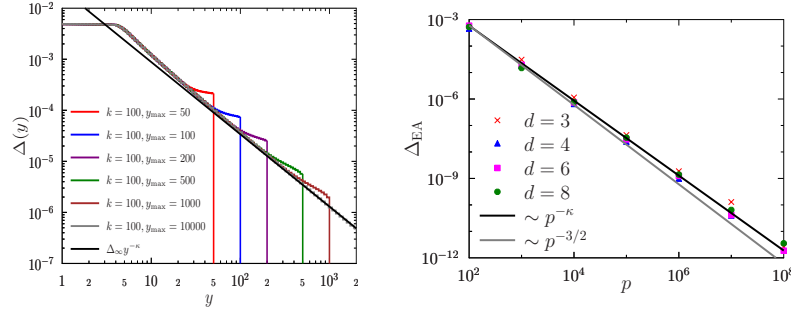


FIG. 49. The behavior of order parameters. (Left panel) $\Delta(y)$ plotted against $y = x/m$. This figure is taken from Fig.9 of [58] obtained by numerically solving the k -RSB problem. The straight line represents the power law $\Delta(y) = \Delta_\infty y^{-\kappa}$ with the κ extracted from theoretical analysis. (Right panel) The scaling property of Δ_{EA} extracted from the simulation data of the hardspheres in finite dimensional systems. The cage size Δ_{EA} is associated with the plateau value of the MSD. This figure is taken from Fig. 13 of [58].

4. Gardner transition

B. k -RSB ansatz and $k \rightarrow \infty$

C. Jamming

1. Scaling analysis of the full RSB solution approaching jamming

Here we sketch the very interesting observations on the critical properties of hardspheres approaching the jamming $m \rightarrow 0$ revealed by the full RSB ansatz.[58].

Here we are interested with the most-inner core $x \rightarrow x_1$ in the jamming limit $\Delta_{EA} = \Delta(x_1) \rightarrow 0$.

By numerically solving the k -RSB problem with large k [58], it was realized that the order parameter $\Delta(x)$ exhibit a non-trivial scaling feature as shown in the left panel of Fig. 49),

$$\Delta(x)/\Delta_{EA} \simeq (x/x_1)^{-\kappa} \quad x \gg 1 \quad (\text{XIV.21})$$

with $\kappa \simeq 1.4$. Since pressure scales as $P \propto 1/m$, this implies that the cage size vanishing approaching the jamming as,

$$\Delta_{EA} = \Delta(x_1) \propto p^{-\kappa}. \quad (\text{XIV.22})$$

Numerical data shown in the right panel of Fig. 49 suggests that this holds actually in finite dimensional systems. Such a behaviour has been predicted independently by a phenomenological argument [86].

The full RSB solution is encoded in the partial differential equations for $P(x, h)$ (see Eq. (XIII.137)) and $\pi(x, h) = -f'(x, h)$ (see Eq. (XIII.133)) which are coupled. These are supplemented by the initial conditions and Eq. (XIII.138) Eq. (XIII.136).

We proceed by assuming the following scaling features motivated by some analysis in the regimes $h \rightarrow \pm\infty$ [15, 34, 58] for $x \rightarrow x_1$. Let us introduce

$$\hat{P}(x, h) = e^{-h} P(x, h) \quad (\text{XIV.23})$$

then

$$(0) \quad h \rightarrow -\infty$$

$$\hat{P}(x, h) \sim \Delta^{-c/\kappa} P_0(h \Delta^{-c/\kappa}) \quad \pi(x, h) \sim -\frac{h}{\Lambda(x)} \quad (\text{XIV.24})$$

with

$$c = \kappa - 1 \quad (\text{XIV.25})$$

(1) $h \sim 0$ (intermediate regime)

$$\hat{P}(x, h) \sim \Delta^{-a/\kappa} P_1(h\Delta^{-b/\kappa}) \quad \pi(x, h) \sim \frac{\Delta^{b/\kappa}}{\tilde{\Lambda}(x)} \pi_1(h\Delta^{-b/\kappa}) \quad (\text{XIV.26})$$

(2) $h \rightarrow \infty$

$$\hat{P}(x, h) \sim P_2(h) \quad \pi(x, h) \sim 0 \quad (\text{XIV.27})$$

In the above equations $P_0(x), P_1(x), \pi_1(x)$ and $P_2(x)$ are some smooth functions and a, b, c, κ are some exponents.

Now we can make the following observations:

1. Matching between (0) and (1): assuming

$$P_0(u) \propto u^\theta \quad u \rightarrow 0 \quad (\text{XIV.28})$$

$$P_1(u) \propto (-u)^\theta \quad u \rightarrow -\infty \quad (\text{XIV.29})$$

the following relation is needed,

$$\Delta^{-c/\kappa} (h\Delta^{-c/\kappa})^\theta \sim \Delta^{-a/\kappa} (h\Delta^{-b/\kappa})^\theta \quad (\text{XIV.30})$$

which implies

$$\theta = \frac{c-a}{b-c}. \quad (\text{XIV.31})$$

We also find

$$\pi_1(u) \sim -u \quad u \rightarrow -\infty \quad (\text{XIV.32})$$

must hold.

2. Matching between (1) and (2): assuming

$$P_1(z) \propto z^{-\alpha} \quad z \rightarrow \infty \quad (\text{XIV.33})$$

$$P_2(z) \propto z^{-\alpha} \quad z \rightarrow 0 \quad (\text{XIV.34})$$

we find the following relation is needed to eliminate the dependence on Δ ,

$$\alpha = \frac{a}{b} \quad (\text{XIV.35})$$

3. Analysis on the intermediate regime $h \sim 0$: Plugging Eq. (XIV.26) in Eq. (XIII.137) and using Eq. (XIII.133) we find, the contribution from the 1st term on the r.h.s. scales are $(\Delta^{-b/\kappa})^2$ while those from the 2nd term on the r.h.s and the term on the l.h.s scales like Δ^{-1} . Thus in order to have a non-trivial solution we need,

$$\frac{b}{\kappa} = \frac{1}{2}. \quad (\text{XIV.36})$$

by which we can eliminate b . Now we are left with two exponents a and $c = \kappa - 1$. At this stage we are still left with the exponent c undetermined. This is fixed by imposing an exact relation which is obtained by taking a derivative d/dx of the exact identity Eq. (XIII.144).

The exponents were found to be

$$a = 0.29213\dots \quad b = 0.70787\dots \quad c = 0.41574\dots \quad (\text{XIV.37})$$

which implies

$$\alpha = 0.41269\dots \quad \theta = 0.42311\dots \quad \kappa = 1.41574\dots \quad (\text{XIV.38})$$

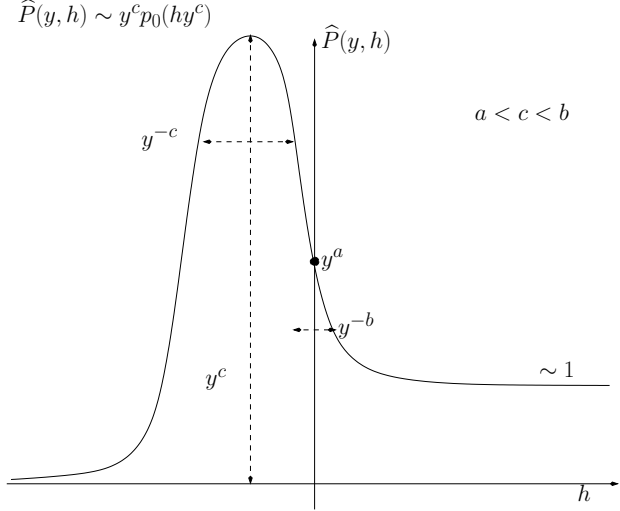


FIG. 50. Scaling of $\hat{P}(y, h) = e^{-y} P(y, h)$. Here $y = \Delta^{-1/\kappa}$. Took from Fig. 7 of [58].

2. Physical consequences

Gap distribution

Let us discuss the behaviour of the radial distribution function $g(r)$ approaching jamming using the above results in Eq. (XIII.110).

$$e^{-\beta v_{\text{eff}}(\xi)} = \theta(\xi) \int_{-\infty}^{\infty} dy \frac{e^{-\frac{(y-\xi)^2}{2\Delta_{\text{EA}}}}}{\sqrt{2\pi\Delta_{\text{EA}}}} \frac{\hat{P}_k(y)}{g(m_k, y)} \quad g(m_k, y) = \Theta\left(\frac{y}{\sqrt{2\Delta_{\text{EA}}}}\right) \quad (\text{XIV.39})$$

where $\Delta_{\text{EA}} = \Delta_k$ and $\hat{P}_k(h) = e^{-h} P_k(h)$.

1. For *fixed* finite r , sending $\Delta_{\text{EA}} = \Delta_k \rightarrow 0$ ($m \rightarrow 0$), we find,

$$g(r) = \theta(r) \hat{P}_k(r) \quad (\text{XIV.40})$$

where we used $\lim_{X \rightarrow \infty} \Theta(X) = 1$. This is a generalization of the 1RSB ($k = 1$) result Eq. (XIV.12).

In the $k \rightarrow \infty$ limit, the scaling behavior of $\hat{P}(x, h)$ close to the core $x \rightarrow x_1$ as described by Eq. (XIV.24) and Eq. (XIV.26) in the region vanishing in the jamming limit $\Delta_{\text{EA}} \rightarrow 0$ implies development of a delta peak $\delta(r)$. On the other hand, we have the scaling behavior $P(x, h) \sim h^{-\alpha}$ for fixed $h \sim 0^+$ as given by Eq. (XIV.34) with $\alpha = a/b$ given by Eq. (XIV.35). These observations implies,

$$g(r) \sim \delta(r) + c_{\text{nt}} \theta(r) r^{-\alpha}, \quad (\text{XIV.41})$$

where c_{nt} is some numerical factor.

2. In the vanishing region around $r = 0$ parametrized as $r = \Delta_{\text{EA}} \lambda$ we find, Assuming $\Delta_{\text{EA}} = \Delta_k \sim 0$ we find for $r > 0$,

$$g(r) \sim \frac{1}{\Delta_k} \int_0^{\infty} dy \hat{P}_k(-y) y e^{-\lambda y} \quad \lambda = \frac{r}{\Delta_k} \quad (\text{XIV.42})$$

This is a generalization of the 1RSB ($k = 1$) result given by Eq. (XIV.13) to *finite* $k \geq 1$.

Now in the $k \rightarrow \infty$ limit we have the non-trivial scaling behavior $P(x, h) \sim \Delta^{-c/\kappa} P_0(h\Delta^{-c/\kappa})$ for $h < 0$ in Eq. (XIV.24). Using this for $x \rightarrow x_1$ we find,

$$g(r) \sim \frac{1}{\Delta_{\text{EA}}^{1/\kappa}} \int_0^{\infty} dt P_0(-t) t e^{-t \frac{r}{\Delta_{\text{EA}}^{1/\kappa}}} \quad (\text{XIV.43})$$

where we used $c = \kappa - 1$.

Vanishing MSD, diverging shear-modulus..again

Using the above result, we repeat the analysis in the 1RSB case Eq. (XIV.14). We can find,

$$\Delta(1) \propto p^{-\kappa} \quad \mu(1) \propto p^\kappa \quad (\text{XIV.44})$$

Isostaticity

Using the above result we can evaluate the fraction of interactions or contacts which is closed. For any small but finite ϵ we have,

$$\int_0^\epsilon dr g(r) = \int_0^\infty dt P_0(-t) \int_0^{et/(p\Delta_1^{1/\kappa})} ds e^{-s} \xrightarrow{\Delta_{\text{EA}} \rightarrow 0} \int_0^\infty dt P_0(-t) \quad (\text{XIV.45})$$

On the other hand, one can find that the exact identity Eq. (XIII.144) implies,

$$1 = \frac{\hat{\varphi}}{2} \int_0^\infty dz P_0(-z) \quad (\text{XIV.46})$$

in the jamming limit. This means the average contact number at jamming

$$z = d\hat{\varphi} \int_0^\epsilon dr g(r) = 2d \quad (\text{XIV.47})$$

is just isostatic.

Mechanical marginal stability

Mechanical marginal stability [87],

$$\alpha = 1/(2 + \theta) \quad (\text{XIV.48})$$

is satisfied by the solution.

D. Glass State following

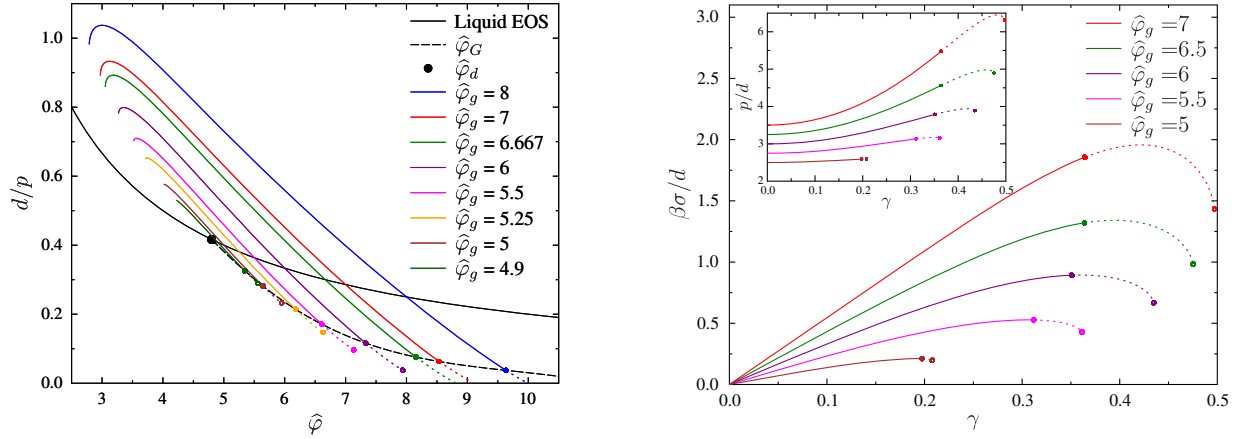


FIG. 51. Glass equation of states a) pressure b) shear-stress (stress-strain curve) obtained by state following computation. Here $m = 1$. The dotted lines represent unstable solutions (Gardner phase). Taken from [83].

1. Glass equation of states, stress-strain curves

2. Jamming and shear-jamming

ACKNOWLEDGMENTS

We thank ... This work is supported by JSPS KAKENHI (No. 19H01812).

Part IV

Appendix

Appendix A: Some useful formula

Given a matrix \hat{A} of size $n \times n$, we have,

$$\frac{\partial}{\partial A_{ab}} \ln \det A = (A^{-1})_{ab}^t \quad (\text{A.1})$$

This can be proved using the two well known relations,

$$A^{-1} = \frac{C^t}{\det A} \quad (\text{A.2})$$

and

$$\det A = \sum_{j=1}^n C_{ij} A_{ik} \quad (\text{A.3})$$

where \hat{C} is the cofactor matrix of \hat{A}

$$C_{ij} = (-1)^{i+j} |\hat{A}^{i,j}| \quad (\text{A.4})$$

with the matrix $\hat{A}^{i,j}$ obtained by subtracting i -th row and j -th column of the matrix \hat{A} .

Appendix B: Some useful formula for RS

Given a matrix of size $n \times n$ in the form

$$M_{ab} = M_1 \delta_{ab} + M_2 \quad (\text{B.1})$$

we find

- Determinant

$$\det(M_1 \delta_{ab} + M_2) = M_1^n \det(\delta_{ab} + M_2/M_1) = M_1^n (1 + nM_2/M_1) \quad (\text{B.2})$$

This can be checked easily by diagonalizing the matix.²⁴

- Inverse

$$(M^{-1})_{ab} = \frac{1}{M_1} \delta_{ab} - \frac{M_2}{M_1} \frac{1}{M_1 + nM_2} \quad (\text{B.3})$$

This can be also obtained easily assuming that the inverse matrix also has the same replica symmetric form.

Due to the cofactor expansion of the inverse matrix we have,

$$(M^{-1})_{n,n} = \frac{\det M^{n,n}}{\det M} \quad (\text{B.4})$$

where $M^{n,n}$ is obtained from M by subtracting the n th row and column. Then using Eq. (B.2) and Eq. (B.3) we find,

$$\det M^{n,n} = \det M (M^{-1})_{n,n} = M_1^{n-1} \left(1 + (n-1) \frac{M_2}{M_1} \right) \quad (\text{B.5})$$

²⁴ A matrix of the form $\delta_{ab} + A$ have only two kinds of eigenvalues: one eigenvalue is $1 + nA$ associated with an eigenvector of the form $(1, 1, \dots, 1)$ and the other eigenvalue is 1 with eigenvectors of the form $(1, -1/(n-1), -1/(n-1), \dots, -1/(n-1))$.

Appendix C: Some useful formula for state following

$$\det \begin{pmatrix} A & B \\ B^t & C \end{pmatrix} = \det A \det(C - BA^{-1}B^t) \quad (\text{C.1})$$

In particular for the matrix form shown in Fig. 27, we find,

$$\det \hat{q}_{1+s} = \det((1-q)\delta_{ab} + (q-r^2)) = (1-q)^s + s(q-r^2)(1-q)^{s-1} \quad (\text{C.2})$$

Note that the size of the matrix involved in the 2nd equation is $s \times s$. In the last equation we used Eq. (B.2).

Appendix D: Some useful formulae

- This formula can be proved directly taking derivatives,

$$\left(\frac{\partial}{\partial x_1} + \frac{\partial}{\partial x_2} \right) F(x_1, x_2) \Big|_{x_1=x_2=x} = \frac{d}{dx} F(x, x) \quad (\text{D.1})$$

which can be immediately generalized as,

$$\left(\sum_{a=1}^n \frac{\partial}{\partial x_a} \right)^p F(x_1, x_2, \dots, x_n) \Big|_{x_1=x_2=\dots=x} = \frac{d^p}{dx^p} F(x, x, \dots, x) \quad (\text{D.2})$$

Then we find, for example,

$$e^{\frac{A}{2} \sum_{a,b=1}^n \frac{\partial^2}{\partial x_a \partial x_b}} F(x_1, x_2, \dots, x_n) \Big|_{x_a=x} = e^{\frac{A}{2} \frac{d^2}{dx^2}} F(x, x, \dots, x) \quad (\text{D.3})$$

which we use in the replica symmetric computation.

- The following can be proved using Eq. (D.2) twice,

$$\begin{aligned} & \left(\frac{\partial}{\partial x_1} + \frac{\partial}{\partial x_2} + \frac{\partial}{\partial x_3} + \frac{\partial}{\partial x_4} \right) \left(\frac{\partial}{\partial x_1} + \frac{\partial}{\partial x_2} \right) \left(\frac{\partial}{\partial x_3} + \frac{\partial}{\partial x_4} \right) F_I((x_1, x_2) F_{II}(x_3, x_4)) \Big|_{x_1=x_2=x_3=x_4=x} \\ &= \frac{d}{dx} \left[\left(\frac{d}{dx} F_I(x, x) \right) \left(\frac{d}{dx} F_{II}(x, x) \right) \right] \end{aligned} \quad (\text{D.4})$$

Using Eq. (D.2) we find,

$$\begin{aligned} & \left(\frac{\partial}{\partial x_1} + \frac{\partial}{\partial x_2} + \frac{\partial}{\partial x_3} + \frac{\partial}{\partial x_4} \right) \left(\frac{\partial}{\partial x_1} + \frac{\partial}{\partial x_2} \right) \left(\frac{\partial}{\partial x_3} + \frac{\partial}{\partial x_4} \right) F_I((x_1, x_2) F_{II}(x_3, x_4)) \Big|_{x_1=x_2=x_2=x_4=x} \\ &= \frac{d}{dx} \left(\frac{\partial}{\partial x_1} + \frac{\partial}{\partial x_2} \right) \left(\frac{\partial}{\partial x_3} + \frac{\partial}{\partial x_4} \right) F_I((x_1, x_2) F_{II}(x_3, x_4)) \Big|_{x_1=x_2=x_2=x_4=x} \\ &= \frac{d}{dx} \left(\frac{\partial}{\partial x_1} + \frac{\partial}{\partial x_2} \right) F_I((x_1, x_2)) \Big|_{x_1=x_2=x} \left(\frac{\partial}{\partial x_3} + \frac{\partial}{\partial x_4} \right) F_{II}(x_3, x_4) \Big|_{x_3=x_4=x} \\ &= \frac{d}{dx} \left[\left(\frac{d}{dx} F_I(x, x) \right) \left(\frac{d}{dx} F_{II}(x, x) \right) \right] \end{aligned} \quad (\text{D.5})$$

In the last equation we used Eq. (D.2) again. This is useful in RSB computations.

- The following is just the Taylor expansion $f(h + \delta) = \sum_{n=0}^{\infty} \frac{1}{n!} \frac{d^n f(h)}{dh^n} \delta^n$,

$$e^{\delta \frac{\partial}{\partial h}} f(h) = f(h + \delta) \quad (\text{D.6})$$

- The following formula can be proved using Taylor expansion $f(h + \delta) = \sum_{n=0}^{\infty} \frac{1}{n!} \frac{d^n f(h)}{dh^n} \delta^n$,

$$e^{\frac{a}{2} \frac{\partial^2}{\partial h^2}} f(h) = \int_{-\infty}^{\infty} \frac{dz}{\sqrt{2\pi}} e^{-\frac{z^2}{2}} f(h - \sqrt{a}z) \quad (\text{D.7})$$

- The following is useful for the analysis of the Hessian matrix. By taking derivatives we find, for $a \neq b$,

$$\begin{aligned} & \frac{\partial^2}{\partial h_a \partial h_b} \exp \left(\frac{\lambda}{2} \sum_{e,f=1}^n \frac{\partial^2}{\partial h_e \partial h_f} \right) \prod_{a=1}^n g(h_a) \Big|_{h_a=h} \\ &= \exp \left(\frac{\lambda}{2} \frac{\partial^2}{\partial h^2} \right) g^n(h) \left(\frac{g'(h)}{g(h)} \right)^2 \Big|_{h_a=h} = \gamma_\lambda \otimes g^n(h) \left(\frac{g'(h)}{g(h)} \right)^2 \end{aligned} \quad (\text{D.8})$$

Similarly we obtain, for $a \neq b$ and $c \neq d$,

$$\begin{aligned} & \exp \left(\frac{\lambda}{2} \sum_{e,f=1}^n \frac{\partial^2}{\partial h_e \partial h_f} \right) \frac{\partial^4}{\partial h_a \partial h_b \partial h_c \partial h_d} \prod_{a=1}^n g(h) \Big|_{\{h_a=0\}} \\ &= \gamma_\lambda \otimes g^n(h) \left\{ (\delta_{ac}\delta_{bd} + \delta_{ad}\delta_{bc}) \left(\frac{g''(h)}{g(h)} \right)^2 \right. \\ & \quad \left. + [\delta_{ac} + \delta_{bc} + \delta_{ad} + \delta_{bd} - 2(\delta_{ad}\delta_{bc} + \delta_{ac}\delta_{bd})] \left[\frac{g''(h)}{g(h)} \left(\frac{g'(h)}{g(h)} \right)^2 \right] \right. \\ & \quad \left. + [1 - (\delta_{ac} + \delta_{bc} + \delta_{ad} + \delta_{bd}) + (\delta_{ad}\delta_{bc} + \delta_{ac}\delta_{bd})] \left(\frac{g'(h)}{g(h)} \right)^4 \right\} \\ &= \gamma_\lambda \otimes g^n(h) \left\{ S_1(h) \frac{\delta_{ac}\delta_{bd} + \delta_{ad}\delta_{bc}}{2} + S_2(h) \frac{\delta_{ac} + \delta_{ad} + \delta_{bc} + \delta_{bd}}{4} + S_3(h) \right\} \end{aligned} \quad (\text{D.9})$$

where we introduced

$$\begin{aligned} S_1(x) &= 2 \left[\left(\frac{g''(x)}{g(x)} \right)^2 - 2 \left(\frac{g''(x)}{g(x)} \right) \left(\frac{g'(x)}{g(x)} \right)^2 + \left(\frac{g'(x)}{g(x)} \right)^4 \right] = 2(f''(x))^2 \\ S_2(x) &= 4 \left[\left(\frac{g''(x)}{g(x)} \right) \left(\frac{g'(x)}{g(x)} \right)^2 - \left(\frac{g'(x)}{g(x)} \right)^4 \right] = 4(-f''(x))(f'(x))^2 \\ S_3(x) &= \left(\frac{g'(x)}{g(x)} \right)^4 = (f'(x))^4 \end{aligned}$$

where we introduced

$$f(x) = -\ln g(x) \quad (\text{D.10})$$

Appendix E: Recursion formula for $g(m_i, h)$ and $f(m_i, h)$

1. k -RSB

$$\begin{aligned} g(m_i, y) &= e^{\frac{\Lambda_i}{2} \frac{\partial^2}{\partial y^2}} g(m_{i+1}, y)^{m_i/m_{i+1}} \\ &= \gamma_{\Lambda_i} \otimes g(m_{i+1}, y)^{m_i/m_{i+1}} \\ &= \int \mathcal{D}z_i g(m_{i+1}, y + \sqrt{\Lambda_i} z_i)^{m_i/m_{i+1}} \end{aligned} \quad (\text{E.1})$$

Let us also introduce,

$$f(m_i, y) = -\frac{1}{m_i} \ln g(m_i, y) \quad (\text{E.2})$$

whose recursion relation can be obtained as,

$$-f(m_i, y) = \frac{1}{m_i} \ln \left[\gamma_{\Lambda_i} \otimes e^{-m_i f(m_{i+1}, y)} \right] = \frac{1}{m_i} \ln \int \mathcal{D}z_i e^{-m_i f(m_{i+1}, y + \sqrt{\Lambda_i} z_i)} \quad (\text{E.3})$$

One can also find from Eq. (E.3) that

$$m(m_i, h) = -f'(m_i, h) \quad (\text{E.4})$$

defined in Eq. (X.35) obeys a recursion formula,

$$m(m_i, h) = \frac{\int \mathcal{D}z_i e^{-m_i f(m_{i+1}, y + \sqrt{\Lambda_i} z_i)} (m(m_{i+1}, h))}{\int \mathcal{D}z_i e^{-m_i f(m_{i+1}, y + \sqrt{\Lambda_i} z_i)}} \quad (\text{E.5})$$

Appendix F: Recursion formula for $P_{i,j}(h, h')$

1. k -RSB

Let us define for $0 \leq i \leq j \leq k+1$,

$$P_{i,j}(y, h) \equiv \frac{\delta f(m_i, y)}{\delta f(m_j, h)}. \quad (\text{F.1})$$

Using the chain rule we can write,

$$P_{i,j}(y, z) = \int dx P_{i,j-1}(y, x) P_{j-1,j}(x, z). \quad (\text{F.2})$$

where

$$P_{j-1,j}(x, z) = \frac{\delta f(m_{j-1}, x)}{\delta f(m_j, z)} = e^{m_{j-1}(f(m_{j-1}, x) - f(m_j, z))} \frac{e^{-\frac{(x-z)^2}{2\Lambda_{j-1}}}}{\sqrt{2\pi\Lambda_{j-1}}} \quad (\text{F.3})$$

as one can easily find from the recursion relation given by Eq. (E.3). Then we find a recursion relation,

$$P_{i,j}(y, z) = e^{-m_{j-1} f(m_j, z)} \gamma_{\Lambda_{j-1}} \otimes_z \frac{P_{i,j-1}(y, z)}{e^{-m_{j-1} f(m_{j-1}, z)}} \quad (\text{F.4})$$

with the 'boundary condition'

$$P_{i,i}(y, h) = \delta(y - h). \quad (\text{F.5})$$

Here \otimes_h stands for a convolution with respect to the variable h .

A useful property to note is that the recursion relation given by Eq. (F.4) preserves the 'normalization' under the convolutions,

$$\int dh P_{i,j}(y, h) = 1 \quad (\text{F.6})$$

which can be easily checked using Eq. (E.3).

Appendix G: Asymptotic behaviour of the error function

The error function $\text{erf}(x)$,

$$\text{erf}(x) = \frac{2}{\sqrt{\pi}} \int_0^x dy e^{-y^2} = -\text{erf}(-x), \quad (\text{G.1})$$

behaves for $x \rightarrow \infty$ as,

$$\text{erf}(x) = 1 - \frac{1}{\sqrt{\pi}} \frac{e^{-x^2}}{x} \left(1 - \frac{1}{2x^2} + \frac{3}{(2x^2)^2} + \dots \right). \quad (\text{G.2})$$

This implies $\Theta(x)$ defined in Eq. (VII.48),

$$\Theta(x) = \int_{-\infty}^x \frac{dz}{\sqrt{\pi}} e^{-z^2} = \frac{1}{2}(1 + \text{erf}(x)) \simeq \begin{cases} \frac{1}{2} \frac{e^{-x^2}}{(-x)\sqrt{\pi}} \left[1 - \frac{1}{2x^2} + \frac{3}{(2x^2)^2} + \dots \right] & x \rightarrow -\infty \\ 1 & x \rightarrow \infty \end{cases} \quad (\text{G.3})$$

$$r(x) \equiv \frac{\Theta'(x)}{\Theta(x)} = \frac{e^{-x^2}}{\sqrt{\pi}} / \Theta(x) \quad (\text{G.4})$$

behaves asymptotically as,

$$r(x) \simeq \begin{cases} -2x \left(1 - \frac{1}{2x^2} + \frac{3}{(2x^2)^2} + \dots \right)^{-1} & x \rightarrow -\infty \\ 0 & x \rightarrow \infty \end{cases} \quad (\text{G.5})$$

Appendix H: Clustering property

Let us note the instantaneous value of the overlap between the replica 1 and 2 as,

$$q(\sigma^1, \sigma^2) = \frac{1}{N} \sum_{i=1}^N \sigma_i^1 \sigma_i^2 \quad (\text{H.1})$$

Let us consider the following object.

$$\langle \delta(q - q(\sigma^1, \sigma^2)) \rangle_{\alpha, \alpha'} = \int \frac{d\lambda}{2\pi} e^{i\lambda(q - q_{\alpha, \alpha'})} \langle e^{-i\lambda\delta q} \rangle_{\alpha, \alpha'} \quad \delta q \equiv q(\sigma^1, \sigma^2) - q_{\alpha, \alpha'} \quad (\text{H.2})$$

where

$$\delta q = \sum_{i=1}^N \delta q_i \quad \delta q_i = \sigma_i^1 \sigma_i^2 - q_{\alpha, \alpha'} \quad (\text{H.3})$$

$$\langle e^{-i\lambda\delta q} \rangle = 1 - i\lambda \langle \delta q \rangle_{\alpha, \alpha'} + \frac{\lambda^2}{2} \langle (\delta q)^2 \rangle_{\alpha, \alpha'} + \dots \quad (\text{H.4})$$

where $\langle \delta q \rangle_{\alpha, \alpha'} = 0$ and

$$\langle (\delta q)^2 \rangle_{\alpha, \alpha'} = \frac{1}{N^2} \sum_{i=1}^N \sum_{j=1}^N \langle \delta q_i \delta q_j \rangle \quad (\text{H.5})$$

In equilibrium states the clustering property holds, which reads as,

$$\langle \delta q_i \delta q_j \rangle \xrightarrow[|i-j|\rightarrow\infty]{} \langle \delta q_i \rangle \langle \delta q_j \rangle \quad (\text{H.6})$$

which implies

$$\begin{aligned} \langle (\delta q)^2 \rangle_{\alpha, \alpha'} &= \frac{1}{N} \sum_{i=1}^N \langle \delta q_i \rangle \frac{1}{N} \sum_{j=1}^N \langle \delta q_j \rangle + \frac{1}{N} \sum_{i=1}^N \underbrace{\frac{1}{N} \sum_{j=1}^N [\langle \delta q_i \delta q_j \rangle - \langle \delta q_i \rangle \langle \delta q_j \rangle]}_{O(N^0)} \\ &\xrightarrow[N\rightarrow\infty]{} 0 \end{aligned} \quad (\text{H.7})$$

Thus

$$\lim_{N \rightarrow \infty} \langle e^{-i\lambda\delta q} \rangle_{\alpha, \alpha'} = 1 \quad (\text{H.8})$$

To sum up

$$\langle \delta(q - q(\sigma^1, \sigma^2)) \rangle_{\alpha, \alpha'} = \int \frac{d\lambda}{2\pi} e^{i\lambda(q - q_{\alpha, \alpha'})} = \delta(q - q_{\alpha, \alpha'}) \quad (\text{H.9})$$

Appendix I: Properties of low lying states in the glass phase of the random energy model

1. Distribution of energy gaps

Suppose that M samples of random energies E (we omit $\hat{\cdot}$ in the following) are drawn from the distribution Eq. (V.24) in the range, say $0 < E < E_{\max}$ so that $A(\kappa) = \kappa/(e^{\kappa E_{\max}} - 1)$ and put then in order such that $E_1 < E_2 \dots E_M$. Let us introduce the spacing between the adjacent energy levels $y_n = E_{n+1} - E_n$ ($1 \leq n \leq M - 1$) and $y_M = E_M$. It is straightforward to show that the distribution of the energy spacing becomes[88],

$$\begin{aligned} p_M(\{y_n\}) &\equiv M! A^M(\kappa) \int_0^{E_{\max}} dE_M e^{\kappa E_M} \int_0^{E_M} dE_{M-1} e^{\kappa E_{M-1}} \dots \int_0^{E_2} dE_1 e^{\kappa E_1} \\ &\quad \delta(y_M - E_M) \prod_{n=1}^{M-1} \delta[y_n - (E_{n+1} - E_n)] \\ &= M(A(\kappa)/\kappa)^M e^{M\kappa y_M} \prod_{m=1}^{M-1} p_m(y_m) \quad p_m(y_m) = m\kappa e^{-m\kappa y_m}. \end{aligned} \quad (\text{I.1})$$

Here we see that the statistics of the energy spacing at different levels are independent from each other and that each of them follows a level dependent exponential distribution.

2. Two level system

For simplicity let us consider a two level system: the ground state + 1st excited state with the energy gap ΔE :

$$Z = 1 + x \quad x \equiv e^{-\beta \Delta E} \quad (\text{I.2})$$

From Eq. (V.24) and Eq. (V.25) we find that the spacing between the ground state and the 1st excited state is given by,

$$p(\Delta E) = \beta_c e^{\beta_c \Delta E} \quad (\text{I.3})$$

We assume that the self-overlap of the two states is 1 and the mutual overlap is 0. Then we find

$$P(q=1) = \frac{1+x^2}{(1+x)^2} = 1 - \frac{2x}{(1+x)^2}. \quad (\text{I.4})$$

so that

$$\begin{aligned} \overline{P(q=0)} = 1 - \overline{P(q=1)} &= \beta_c \int_0^\infty d\Delta E e^{-\beta_c \Delta E} \frac{2x}{(1+x)^2} = \frac{T}{T_K} \int_0^1 dx x^{(T/T_K)-1} \frac{2x}{(1+x)^2} \\ &= \frac{T}{T_K} + O(T/T_K)^2 \end{aligned} \quad (\text{I.5})$$

So we see that this agrees with the result of the replica computation at the lowest order. Now it is possible to show that using three-level model, we find the $O(T/T_K)^2$ becomes canceled. Using 4-level, $O(T/T_K)^3 = 0$, and so on... Replica approach gives the exact result.

Appendix J: Gaussian integrals

$$\int \prod_{i=1}^M dx_i \exp \left(-\frac{1}{2} \sum_{i,j} x_i K_{ij} x_j \right) = \sqrt{2\pi}^M / \sqrt{\det K} \quad (\text{J.1})$$

$$\frac{1}{\sqrt{2\pi}^M / \sqrt{\det K}} \int \prod_{i=1}^M dx_i \exp \left(-\frac{1}{2} \sum_{i,j} x_i K_{ij} x_j + \sum_i h_i x_i \right) = \exp \left(\sum_{ij} h_i K_{ij}^{-1} h_j \right) \quad (\text{J.2})$$

Appendix K: Eigen values of the Hessian matrix

The replica symmetry implies the following matrix structure,

$$M_{a \neq b, c \neq d} = M_1 \frac{\delta_{ac}\delta_{bd} + \delta_{ad}\delta_{bc}}{2} + M_2 \frac{\delta_{ac} + \delta_{ad} + \delta_{bc} + \delta_{bd}}{4} + M_3 \quad (\text{K.1})$$

from which the eigenvalues of the Hessian matrix are obtained as [55, 57],

$$\lambda_R = M_1 \quad (\text{K.2})$$

$$\lambda_L = n(n-1)M_3 + (n-1)M_2 + M_1 \xrightarrow{n \rightarrow 0} M_1 - M_2 \quad (\text{K.3})$$

$$\lambda_A = \frac{1}{2}(n-2)M_2 + M_1 \xrightarrow{n \rightarrow 0} M_1 - M_2 \quad (\text{K.4})$$

$$(\text{K.5})$$

Note: To examine the stability of 1 RSB solution with $q_0 = 0$, replace n by m . In the limit $m \rightarrow 1$, $\lambda_R = \lambda_L$.

Appendix L: Some explicit computations of higher order terms in the Plefka expansion

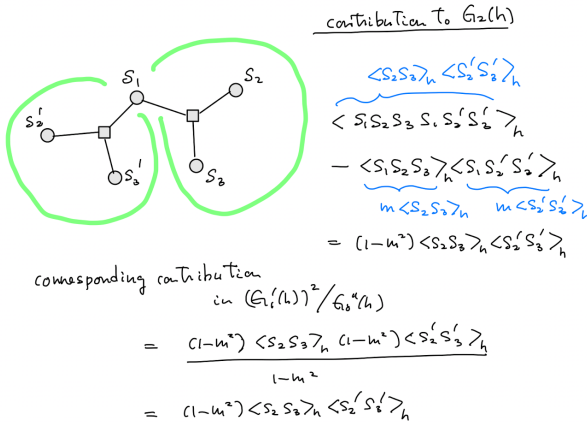


FIG. 52. Cancellation in $F_2(m)$

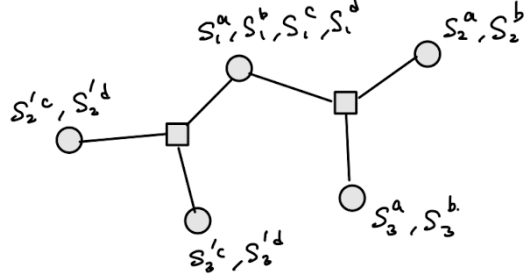


FIG. 53. Contribution to $G_2[\hat{\epsilon}]$ which is canceled in $F_2[\hat{q}]$

Appendix M: Langevin dynamics

For simplicity, let us consider here one-dimensional motion of a particle along x -axis emerged in a viscous fluid. The time evolution of the position of the particle $x(t)$ can be described well by an over-damped Langevin equation,

$$0 = -\gamma \frac{dx}{dt} + f(x) + h(t) + \xi(t) \quad f(x) = -\frac{dU(x)}{dx} \quad (\text{M.1})$$

Here γ is damping constant and $f(x)$ is a deterministic force derived from a potential $U(x)$. We also included an external field $h(t)$ to study linear response. The last term $\xi(t)$ is a random force. We assume it is a white noise,

$$\langle \xi(t) \rangle_\xi = 0 \quad \langle \xi(t) \xi(t') \rangle_\xi = 2\gamma k_B T \delta(t - t') \quad (\text{M.2})$$

1. From Langevin equation to Fokker-Planck equation

Let us consider the probability distribution function of the particle's position x ,

$$P(x, t) = \langle \delta(x - x_\xi(t)) \rangle_\xi \quad (\text{M.3})$$

Here $x_\xi(t)$ represents the actual solution of the Langevin equation with a certain realization of the random force $\xi(t)$. The average $\langle \dots \rangle_\xi$ is the average over different realizations of the noise. One can show that the probability distribution function obeys

$$\frac{\partial P(x, t)}{\partial t} = \mathcal{L}_{\text{FP}} P(x, t) \quad \mathcal{L}_{\text{FP}} = \frac{1}{\gamma} \frac{\partial}{\partial x} \left[\frac{\partial U}{\partial x} - h(t) + k_B T \frac{\partial}{\partial x} \right] \quad (\text{M.4})$$

which is the so called Fokker-Planck equation.

2. Fluctuation dissipation theorems: 1st and 2nd

One can also show that the equilibrium distribution is guaranteed to be stationary (here $h = 0$),

$$\mathcal{L}_{\text{FP}} P_{\text{eq}}(x) = 0 \quad P_{\text{eq}}(x) = Z^{-1} e^{-\beta U(x)} \quad (\text{M.5})$$

where Z is the normalization constant (partition function). For this to hold, it can be seen that the 2nd equation of Eq. (M.2) which is sometimes called as the fluctuation-dissipation theorem (FDT) of the 2nd kind, is crucial.

Now let us introduce a linear-response function (here $h = 0$)

$$R(t, t') = \left. \frac{\delta \langle x(t) \rangle_\xi}{\delta h(t')} \right|_{h=0}. \quad (\text{M.6})$$

The causality implies

$$R(t, t') = 0 \quad \text{for} \quad t < t' \quad (\text{M.7})$$

The response function has a conjugated correlation function,

$$C(t, t') = \langle x(t)x(t') \rangle_\xi. \quad (\text{M.8})$$

One can show that the fluctuation dissipation theorem (FDT) of the 1st kind,

$$R(t, t') = \frac{1}{k_B T} \frac{\partial C(t, t')}{\partial t'} \quad (\text{M.9})$$

holds.

3. MSR generating functional

a. Reminder: functional, functional derivatives and functional integrals (path-integrals)

The trajectory of the particle in the range of time $0 < t < T$. is specified by the function $x(t)$. Let us discretize the time range into N segments of size Δt , i.e. $T = N\Delta t$ as shown in Fig. 54.

Consider a generic physical quantity A which depends on the trajectory. On the discretized time axis, it is just a multivariate function of N variables,

$$A = A(x_0, x_1, \dots, x_{N-1}) \xrightarrow{N \rightarrow \infty} A[x] \quad (\text{M.10})$$

which is said to become a *functional* of function $x(t)$ in $N \rightarrow \infty$ limit.

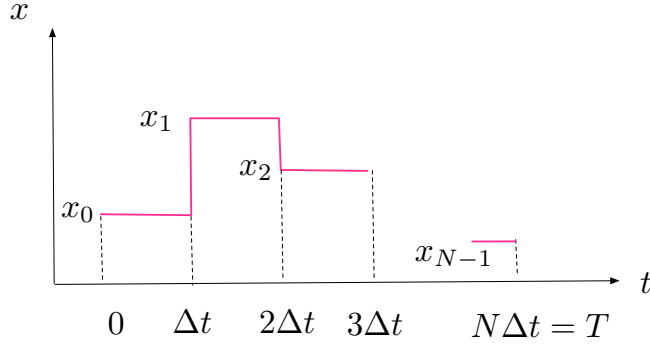


FIG. 54. Discretized path

We can naturally consider partial derivatives as,

$$\frac{\partial A(x_0, x_1, \dots, x_{N-1})}{\partial x_n} \xrightarrow{N \rightarrow \infty} \frac{\delta A[x]}{\delta x(s)} \quad (\text{M.11})$$

which have become a *functional derivative* in the $N \rightarrow \infty$ limit.

Furthermore we can naturally consider integrals. For example,

$$\langle A(x_0, x_1, \dots, x_{N-1}) \rangle = \int dx_0 dx_1 \dots dx_{N-1} P(x_0, x_1, \dots, x_{N-1}) A(x_0, x_1, \dots, x_{N-1}) \rightarrow \int \mathcal{D}[x] P[x] A[x]. \quad (\text{M.12})$$

Here $P(x_0, x_1, \dots, x_{N-1}) \rightarrow N \rightarrow \infty P[x]$ is the probability of the path. Here $\int \mathcal{D}[x] \dots$ is the so called path-integral or functional integral.

b. Discretization of the Langevin dynamics

The Langevin equation Eq. (M.1) may be discretized following Ito's prescription as,

$$\gamma(x_{n+1} - x_n) = (f(x_n) + h_n)\Delta t + \Delta\xi_n \quad (\text{M.13})$$

with

$$\langle\Delta\xi_n\rangle_\xi = 0 \quad \langle\Delta\xi_n\Delta\xi_m\rangle_\xi = \int_{n\Delta t}^{(n+1)\Delta t} dt \int_{m\Delta t}^{(m+1)\Delta t} dt' \langle\xi(t)\xi(t')\rangle_\xi = 2\gamma k_B T \delta_{nm} \Delta t \quad (\text{M.14})$$

where we used Eq. (M.2).

c. Martin-Siggia-Rose (MSR) generating functional

Given the initial point x_0 and a realization of the random forces $\xi(t)$ the trajectory of the particle $x(t)$ for $0 < t < T$ becomes specified so that the value of a generic physical quantity $A[x]$ become specified as well. We can write,

$$\begin{aligned} A &= \int dx_1 dx_2 \dots dx_N A(x_0, x_1, \dots, x_{N-1}) \prod_{n=0}^{N-1} \delta \left[-(x_{n+1} - x_n) + \frac{1}{\gamma} \{(f(x_n) + h_n)\Delta t + \Delta\xi_n\} \right] \\ &= \frac{1}{(2\pi)^N} \int dx_1 dx_2 \dots dx_{N-1} d\hat{x}_1 d\hat{x}_2 \dots d\hat{x}_N A(x_0, x_1, \dots, x_{N-1}) \\ &\quad \exp \left[\sum_{n=0}^{N-1} i\hat{x}_{n+1} \left[-(x_{n+1} - x_n) + \frac{1}{\gamma} \{(f(x_n) + h_n)\Delta t + \Delta\xi_n\} \right] \right] \end{aligned} \quad (\text{M.15})$$

where we introduced integral representations of the delta functions.

Now let us consider the average over different realizations of the random force,

$$\begin{aligned} \langle A \rangle_\xi &= \frac{1}{(2\pi)^N} \int dx_1 dx_2 \dots dx_{N-1} d\hat{x}_1 d\hat{x}_2 \dots d\hat{x}_N A(x_0, x_1, \dots, x_{N-1}) \\ &\quad \exp \left[\sum_{n=0}^{N-1} i\hat{x}_{n+1} \left[-(x_{n+1} - x_n) + \frac{1}{\gamma} \{(f(x_n) + h_n)\Delta t\} \right] \right] \left\langle \prod_{n=0}^{N-1} \exp[i\hat{x}_{n+1}\Delta\xi_n] \right\rangle_\xi \\ &= \frac{1}{(2\pi)^N} \int dx_1 dx_2 \dots dx_{N-1} d\hat{x}_1 d\hat{x}_2 \dots d\hat{x}_N A(x_0, x_1, \dots, x_{N-1}) \\ &\quad \exp \left[\sum_{n=0}^{N-1} i\hat{x}_{n+1} \left[-(x_{n+1} - x_n) + \frac{1}{\gamma} \{(f(x_n) + h_n)\Delta t\} + \gamma k_B T i\hat{x}_{n+1}\Delta t \right] \right] \end{aligned} \quad (\text{M.16})$$

where we evaluated the average over the random force as,

$$\left\langle \prod_{n=0}^{N-1} \exp[i\hat{x}_{n+1}\Delta\xi_n] \right\rangle_\xi = \prod_{n=0}^{N-1} \int_{-\infty}^{\infty} \frac{d\Delta\xi_n}{\sqrt{2\pi\gamma k_B T}} e^{-\frac{(\Delta\xi_{n+1})^2}{4\gamma k_B T\Delta t} + i\hat{x}_{n+1}\Delta\xi_n} = \exp[\gamma k_B T \sum_{n=0}^{N-1} (i\hat{x}_{n+1})^2 \Delta T] \quad (\text{M.17})$$

Taking $N \rightarrow \infty$ ($\Delta T \rightarrow 0$) limit we find,

$$\langle A[x] \rangle_\xi = \int \mathcal{D}[x] \mathcal{D}[\hat{x}] A[x] \exp \left[\int_0^T dt i\hat{x}(t) \left[-\gamma \frac{d}{dt} x - \frac{dU}{dx} + h(t) + \gamma k_B T i\hat{x}(t) \right] \right] \quad (\text{M.18})$$

The above observation motivates us to introduce the Martin-Siggia-Rose (MSR) generating functional[78],

$$Z_{\text{MSR}}[h, \hat{h}] = \int \mathcal{D}[x] \mathcal{D}[\hat{x}] \exp \left[S[x, \hat{x}] + \int_0^T dt [i\hat{x}(t)h(t) + x(t)\hat{h}(t)] \right] \quad (\text{M.19})$$

with

$$\mathcal{S}[x, \hat{x}] = \int_0^T dt i\hat{x}(t) \left[-\gamma \frac{d}{dt} x - \frac{dU}{dx} + \gamma k_B T i\hat{x}(t) \right] \quad (\text{M.20})$$

Note that

$$Z[h, \hat{h} = 0] = 1 \quad (\text{M.21})$$

holds.

From the MSR generating functional we find,

$$\langle x(t) \rangle_\xi = \left. \frac{\partial Z_{\text{MSR}}[h, \hat{h}]}{\partial \hat{h}(t)} \right|_{h=\hat{h}=0} \quad (\text{M.22})$$

the linear-response function,

$$R(t, t') = \left. \frac{\delta \langle x(t) \rangle_\xi}{\delta h(t')} \right|_{h=0} = \langle x(t) i\hat{x}(t') \rangle_\xi == \left. \frac{\delta Z_{\text{MRSB}}[h, \hat{h}]}{\delta \hat{h}(t) \delta h(t')} \right|_{h=\hat{h}=0} \quad (\text{M.23})$$

and the conjugated time auto correlation function,

$$C(t, t') = \langle x(t) x(t') \rangle_\xi = \left. \frac{\delta Z_{\text{MRSB}}[h, \hat{h}]}{\delta \hat{h}(t) \delta \hat{h}(t')} \right|_{h=\hat{h}=0} \quad (\text{M.24})$$

Remarks:

- In the ensemble of paths included in the MSR generating functional introduced above we have assumed a *flat* measure (no bias) for the initial configuration $x(t = 0)$.
- Here we limited ourselves to the simplest case, extension to multi-dimensional, multi-component systems are straightforward.

d. Correlated noise

Finally let us consider the case of correlated noise. Eq. (M.2) is replaced by,

$$\langle \xi(t) \xi(t') \rangle_\xi = D(t, t'). \quad (\text{M.25})$$

which amount to replace Eq. (M.14) by,

$$\langle \Delta \xi_n \rangle_\xi = 0 \quad \langle \Delta \xi_n \Delta \xi_m \rangle_\xi = D_{nm} \Delta t \quad D_{nm} \Delta t = \int_{n \Delta t}^{(n+1) \Delta t} dt \int_{m \Delta t}^{(m+1) \Delta t} dt' D(t, t') \quad (\text{M.26})$$

Now Eq. (M.17) should be replaced by

$$\begin{aligned} \left\langle \prod_{n=0}^{N-1} \exp[i\hat{x}_{n+1} \Delta \xi_n] \right\rangle_\xi &= \int \frac{1}{\sqrt{\det D}} \prod_{n=0}^{N-1} \frac{d \Delta \xi_{n+1}}{\sqrt{2\pi \Delta t}} e^{-\frac{1}{2} \sum_{n,m=0}^{N-1} \Delta \xi_n \frac{D_{nm}^{-1}}{\Delta t} \Delta \xi_m + \sum_{n=0}^{N-1} i\hat{x}_{n+1} \Delta \xi_n} \\ &= \exp \left[\frac{1}{2} \sum_{n,m=0}^{N-1} i\hat{x}_{n+1} D_{nm} i\hat{x}_{m+1} \Delta t \right] \end{aligned} \quad (\text{M.27})$$

This implies Eq. (M.20) is replaced by

$$\mathcal{S}[x, \hat{x}] = \int_0^T dt i\hat{x}(t) \left[-\gamma \frac{d}{dt} x - \frac{dU}{dx} \right] + \int_0^T dt \int_0^T dt' \frac{1}{2} i\hat{x}(t) D(t, t') i\hat{x}(t') \quad (\text{M.28})$$

e. Some useful identities

- In the discretized system we have,

$$\left\langle \frac{\partial x_n}{\partial \Delta \xi_m} \right\rangle_\xi = \langle x_n i \hat{x}_m \rangle_\xi \quad (\text{M.29})$$

which implies in the $N \rightarrow \infty$ limit,

$$\left\langle \frac{\delta x(t)}{\delta \xi(t')} \right\rangle_\xi = \langle x(t) i \hat{x}(t') \rangle_\xi = R(t, t') \quad (\text{M.30})$$

- In the discretized system we have,

$$\frac{\partial x_n}{\partial \Delta \xi_n} = 1 \quad (\text{M.31})$$

which implies in $N \rightarrow \infty$ limit,

$$\lim_{t' \rightarrow t^-} \left\langle \frac{\delta x(t)}{\delta \xi(t')} \right\rangle = \lim_{t' \rightarrow t^-} R(t, t') = 1. \quad (\text{M.32})$$

- In the discretized system we have,

$$\begin{aligned} \langle x_n \Delta \xi_m \rangle_\xi &= \int dx_1 dx_2 \dots dx_N d\hat{x}_1 d\hat{x}_2 \dots d\hat{x}_N \\ &\int \frac{1}{\sqrt{\det D}} \prod_{n=0}^{N-1} \frac{d\Delta \xi_{n+1}}{\sqrt{2\pi \Delta t}} e^{-\frac{1}{2} \sum_{n,m=0}^{N-1} \Delta \xi_n \frac{D_{nm}^{-1}}{\Delta t} \Delta \xi_m + \sum_{n=0}^{N-1} i \hat{x}_{n+1} \Delta \xi_n + \text{noise independent terms}} x_n \Delta \xi_m \\ &= \int dx_1 dx_2 \dots dx_N d\hat{x}_1 d\hat{x}_2 \dots d\hat{x}_N \left(x_n \frac{\partial}{\partial i \hat{x}_{m+1}} \right) e^{-\frac{1}{2} \sum_{n,m=0}^{N-1} i \hat{x}_{n+1} D_{nm} i \hat{x}_{m+1} \Delta t + \text{noise independent terms}} \\ &= \int dx_1 dx_2 \dots dx_N d\hat{x}_1 d\hat{x}_2 \dots d\hat{x}_N \left(x_n \sum_{m'} D_{mm'} i \hat{x}_{m'+1} \Delta t \right) e^{-\frac{1}{2} \sum_{n,m=0}^{N-1} i \hat{x}_{n+1} D_{nm} i \hat{x}_{m+1} + \text{noise independent terms}} \end{aligned} \quad (\text{M.33})$$

which implies in $N \rightarrow \infty$ limit,

$$\langle x(t) \xi(t') \rangle_\xi = \int dt'' R(t, t'') D(t'', t') \quad (\text{M.34})$$

- [1] M. Mézard, G. Parisi, and M. A. Virasoro, *Spin glass theory and beyond* (World Scientific, Singapore, 1987).
- [2] K. Binder and A. P. Young, *Reviews of Modern Physics* **58**, 801 (1986).
- [3] J. A. Mydosh, *Spin glasses: an experimental introduction* (Taylor and Francis, 1993).
- [4] H. Kawamura and T. Taniguchi, in *Handbook of magnetic materials*, Vol. 24 (Elsevier, 2015) pp. 1–137.
- [5] A. Cavagna, *Physics Reports* **476**, 51 (2009).
- [6] T. Castellani and A. Cavagna, *Journal of Statistical Mechanics: Theory and Experiment* **2005**, P05012 (2005).
- [7] L. Berthier and G. Biroli, *Reviews of Modern Physics* **83**, 587 (2011).
- [8] M. Mezard and A. Montanari, *Information, physics, and computation* (Oxford University Press, 2009).
- [9] H. Nishimori, *Statistical physics of spin glasses and information processing: an introduction*, 111 (Clarendon Press, 2001).
- [10] L. Zdeborová and F. Krzakala, *Advances in Physics* **65**, 453 (2016).
- [11] H. Huang, (2022).
- [12] G. Parisi, P. Urbani, and F. Zamponi, *Theory of Simple Glasses: Exact Solutions in Infinite Dimensions* (Cambridge University Press, 2020).
- [13] K. Mitsumoto, C. Hotta, and H. Yoshino, *Physical Review Letters* **124**, 087201 (2020).

- [14] K. Mitsumoto, C. Hotta, and H. Yoshino, *Phys. Rev. Research* **4**, 033157 (2022).
- [15] H. Yoshino, *SciPost Phys.* **4**, 40 (2018).
- [16] L. Zdeborová and F. Krzakala, *Physical Review E* **76**, 031131 (2007).
- [17] X. Zhu, *Discrete mathematics* **229**, 371 (2001).
- [18] Y. Iba, *Journal of Physics A: Mathematical and General* **32**, 3875 (1999).
- [19] H. Nishimori, *Journal of Physics C: Solid State Physics* **13**, 4071 (1980).
- [20] H. Yoshino, *SciPost Phys. Core* **2**, 5 (2020).
- [21] S. F. Edwards and P. W. Anderson, *Journal of Physics F: Metal Physics* **5**, 965 (1975).
- [22] D. Sherrington and S. Kirkpatrick, *Physical review letters* **35**, 1792 (1975).
- [23] H. Nishimori and K. M. Wong, *Physical Review E* **60**, 132 (1999).
- [24] N. Sourlas, *Nature* **339**, 693 (1989).
- [25] Y. Kabashima and D. Saad, *EPL (Europhysics Letters)* **45**, 97 (1999).
- [26] F. Krzakala and L. Zdeborová, *Physical review letters* **102**, 238701 (2009).
- [27] E. Gardner and B. Derrida, *Journal of Physics A: Mathematical and General* **22**, 1983 (1989).
- [28] Y. Kabashima, *Journal of Physics A: Mathematical and General* **36**, 11111 (2003).
- [29] T. Tanaka, *EPL (Europhysics Letters)* **54**, 540 (2001).
- [30] E. J. Candes, J. K. Romberg, and T. Tao, *Communications on Pure and Applied Mathematics: A Journal Issued by the Courant Institute of Mathematical Sciences* **59**, 1207 (2006).
- [31] Y. Kabashima, T. Wadayama, and T. Tanaka, *Journal of Statistical Mechanics: Theory and Experiment* **2009**, L09003 (2009).
- [32] E. Gardner, *Journal of physics A: Mathematical and general* **21**, 257 (1988).
- [33] E. Gardner and B. Derrida, *Journal of Physics A: Mathematical and general* **21**, 271 (1988).
- [34] S. Franz and G. Parisi, *Journal of Physics A: Mathematical and Theoretical* **49**, 145001 (2016).
- [35] J.-P. Hansen and I. R. McDonald, *Theory of simple liquids* (Elsevier, 1990).
- [36] T. Plefka, *Journal of Physics A: Mathematical and general* **15**, 1971 (1982).
- [37] J. Zinn-Justin, *Quantum field theory and critical phenomena*, Vol. 171 (Oxford university press, 2021).
- [38] B. Derrida, *Physical Review Letters* **45**, 79 (1980).
- [39] T. Rizzo and H. Yoshino, *Physical Review B* **73**, 064416 (2006).
- [40] H. Yoshino and T. Rizzo, *Physical Review B* **77**, 104429 (2008).
- [41] J.-P. Bouchaud and M. Mézard, *Journal of Physics A: Mathematical and General* **30**, 7997 (1997).
- [42] H. Yoshino and M. Mézard, *Physical review letters* **105**, 015504 (2010).
- [43] H. Yoshino, *The Journal of Chemical Physics* **136**, 214108 (2012).
- [44] S. Franz, M. Mézard, F. Ricci-Tersenghi, M. Weigt, and R. Zecchina, *EPL (Europhysics Letters)* **55**, 465 (2001).
- [45] G. Parisi and M. A. Virasoro, *Journal de Physique* **50**, 3317 (1989).
- [46] H. Sompolinsky and A. Zippelius, *Physical Review B* **25**, 6860 (1982).
- [47] L. F. Cugliandolo and J. Kurchan, *Physical Review Letters* **71**, 173 (1993).
- [48] S. Franz and M. Mézard, *EPL (Europhysics Letters)* **26**, 209 (1994).
- [49] L. F. Cugliandolo and J. Kurchan, *Journal of Physics A: Mathematical and General* **27**, 5749 (1994).
- [50] S. Franz, M. Mézard, G. Parisi, and L. Peliti, *Physical Review Letters* **81**, 1758 (1998).
- [51] R. Monasson, *Physical review letters* **75**, 2847 (1995).
- [52] I. Kondor, *Journal of Physics A: Mathematical and General* **16**, L127 (1983).
- [53] G. Parisi and T. Rizzo, *Physical review letters* **101**, 117205 (2008).
- [54] G. Parisi, *Physical Review Letters* **43**, 1754 (1979).
- [55] J. De Almeida and D. J. Thouless, *Journal of Physics A: Mathematical and General* **11**, 983 (1978).
- [56] J. Kurchan, G. Parisi, and F. Zamponi, *Journal of Statistical Mechanics: Theory and Experiment* **2012**, P10012 (2012).
- [57] J. Kurchan, G. Parisi, P. Urbani, and F. Zamponi, *The Journal of Physical Chemistry B* **117**, 12979 (2013).
- [58] P. Charbonneau, J. Kurchan, G. Parisi, P. Urbani, and F. Zamponi, *Journal of Statistical Mechanics: Theory and Experiment* **2014**, P10009 (2014).
- [59] A. Engel and C. Van den Broeck, *Statistical mechanics of learning* (Cambridge University Press, 2001).
- [60] T. M. Cover, *IEEE transactions on electronic computers* , 326 (1965).
- [61] E. Gardner, *Nuclear Physics B* **257**, 747 (1985).
- [62] D. Thouless, P. Anderson, and R. Palmer, *Philosophical Magazine* **35**, 593 (1977).
- [63] A. Crisanti, L. Leuzzi, and T. Rizzo, *Physical Review B* **71**, 094202 (2005).
- [64] M. Mézard and G. Parisi, *The Journal of Chemical Physics* **111**, 1076 (1999).
- [65] M. Mézard and G. Parisi, *Phys. Rev. Lett.* **82**, 747 (1999).
- [66] P. Charbonneau, J. Kurchan, G. Parisi, P. Urbani, and F. Zamponi, *Nature communications* **5**, 3725 (2014).
- [67] L. Berthier, G. Biroli, P. Charbonneau, E. I. Corwin, S. Franz, and F. Zamponi, *The Journal of chemical physics* **151**, 010901 (2019).
- [68] T. Rizzo, *Physical Review E* **88**, 032135 (2013).
- [69] A. Crisanti, L. Leuzzi, G. Parisi, and T. Rizzo, *Physical review letters* **92**, 127203 (2004).
- [70] H. Yoshino and F. Zamponi, *Physical Review E* **90**, 022302 (2014).
- [71] S. Nagata and M. Kikuchi, arXiv preprint arXiv:1907.12030 (2019).
- [72] A. Crisanti, H. Horner, and H.-J. Sommers, *Zeitschrift für Physik B Condensed Matter* **92**, 257 (1993).
- [73] S. Franz and G. Parisi, *Journal de Physique I* **5**, 1401 (1995).

- [74] L. Zdeborová and F. Krzakala, [Phys. Rev. B **81**, 224205 \(2010\)](#).
- [75] C. E. Shannon, [The Bell system technical journal **27**, 379 \(1948\)](#).
- [76] K. Nemoto, [Journal of Physics C: Solid State Physics **20**, 1325 \(1987\)](#).
- [77] H. Rieger, [Physical Review B **46**, 14655 \(1992\)](#).
- [78] P. C. Martin, E. Siggia, and H. Rose, [Physical Review A **8**, 423 \(1973\)](#).
- [79] A. Crisanti and H.-J. Sommers, [Zeitschrift für Physik B Condensed Matter **87**, 341 \(1992\)](#).
- [80] L. F. Cugliandolo, J. Kurchan, and L. Peliti, [Physical Review E **55**, 3898 \(1997\)](#).
- [81] L. F. Cugliandolo, [Journal of Physics A: Mathematical and Theoretical **44**, 483001 \(2011\)](#).
- [82] M. Mézard and G. Parisi, [Journal de Physique I **1**, 809 \(1991\)](#).
- [83] C. Rainone, P. Urbani, H. Yoshino, and F. Zamponi, [Physical review letters **114**, 015701 \(2015\)](#).
- [84] G. Parisi and F. Zamponi, [Rev. Mod. Phys. **82**, 789 \(2010\)](#).
- [85] G. Parisi and F. Zamponi, [Reviews of Modern Physics **82**, 789 \(2010\)](#).
- [86] C. Brito and M. Wyart, [Europhysics Letters \(EPL\) **76**, 149 \(2006\)](#).
- [87] M. Wyart, [Physical review letters **109**, 125502 \(2012\)](#).
- [88] E. Bertin, [Physical review letters **95**, 170601 \(2005\)](#).